Mediation of transformation by the *v-fos* oncogene: regulation of the invasive phenotype by histone deacetylases

Thesis

Mediation of transformation by the *v-fos* oncogene: regulation of the invasive phenotype by histone deacetylases

Lynn C. McGarry B.Sc.
The Beatson Institute for Cancer Research,
Cancer Research UK Beatson Laboratories, Glasgow.

Thesis submitted to the Open University
for the degree of Doctor of Philosophy
May 2004

Submission date 20 May 2004
Award date 10 September 2004

ProQuest LLC.
789 East Eisenhower Parkway
P.O. Box 1346
Ann Arbor, MI 48106 – 1346

The work described in this thesis is entirely my own unless otherwise stated.

Lynn McGarry

Acknowledgements

I would like to thank Professor John Wyke, retired director of the Beatson Institute, for allowing me the opportunity to enrol with the Open University and carry out this work within the Institute. I would like to thank Professor Karen Vousden, current director of the Beatson Institute, for allowing me continue the work to completion under her directorship. Thanks, in particular, to Professor Paul Harrison for his efficient dealings with the OU on my behalf, and to Professor Margaret Frame, my advisor, and more recently as my OU contact. Thanks also to all members of R10, past and present. My main debt of gratitude, however, belongs to Professor Brad Ozanne, my supervisor.

Contents

List of Tables

List of Figures

Chapter 1: Introduction

Chapter 2: Materials and Methods

Chapter 3: Results

Abbreviations

AML	acute myeloid leukaemia
APL	acute promyelocytic leukaemia
ATF	activating transcription factor
BCL6	B-cell lymphoma 6
BICR	Beatson Institute for Cancer Research
BMK	big mitogen-activated protein kinase
BSA	bovine serum albumin
CamKIV	calcium/calmodulin-dependent protein kinase 4
CBP	CREB binding protein
ChIP	chromatin immunoprecipitation
CoREST	REST corepressor
CRBP-1	cellular retinol-binding protein-1
CREB	cAMP response element binding protein
CRM1	chromosomal maintenance region 1
CtBP	carboxy terminal binding protein
DAPI	4',6-diamidino-2-phenylindole
dATP	deoxyadenosine triphosphate
dCTP	deoxycytosine triphosphate
dGTP	deoxyguanosine triphosphate
DMAP1	Dnmt1-associated protein 1
DMEM	Dulbecco's minimum essential medium
DMSO	dimethyl sulphoxide
DNA	deoxyribonucleic acid
Dnmt1	DNA methyltransferase 1
dNTPs	deoxyribonucleotides triphosphate

DTT	dithiothreitol
dTTP	deoxythymidine triphosphate
E2F	adenovirus E2 promoter binding factor
E4TF1	adenovirus E4 gene transcription factor 1
ECL	enhanced chemi-luminescence
ECM	extracellular matrix
EDTA	ethylenediamine-tetra-acetic acid
EGF	epidermal growth factor
EGFP	enhanced green fluorescent protein
ERK	extracellular signal-regulated protein kinase
ETO	eight twenty one
FACS	fluorescence-activated cell sorting
FBJ	Finkel Biskis Jinkins
FBR	Finkel Biskis Reilly
FBS	foetal bovine serum
Fos	FBJ-derived osteosarcoma
Fra	fos related antigen
FITC	fluorescein isothiocyanate
Frp4	frizzled-related protein 4
GFP	green fluorescent protein
HDA	histone deacetylase (usually yeast)
HDAC	histone deacetylase (usually mammalian)
HDLP	histone deacetylase-like protein
HDRP	HDAC-related protein
HEPES	4-(2-hydroxyethyl)-1-piperazineethane sulphonic acid
hGABP	human glutaminase binding protein

HOS	HDA1 similar
HP-1	heterochromatin protein 1
HPC	hybrid polar compound
HPLC	high pressure liquid chromatography
HRP	horseradish peroxidase
hr	hour
IL	interleukin
IRF	interferon regulatory transcription factor
Jak	Janus kinase
JNK	c-Jun NH_2-terminal kinase
KAP-1	Krab-associated protein 1
Kb	kilobases
KD	kilodaltons
Krp	kelch-related protein
LAZ3	lymphoma-associated zinc finger protein 3
L-Broth	Luria broth
LTBP	latent TGFβ binding protein
M	molar
MADS	MCM1, amagous deficiens, serum response factor
MAF	musculoaponeurotic fibrosarcoma
MAPK	mitogen-activated protein kinase
MBD	methylated DNA binding domain (protein)
MDM2	mouse double minute 2
MeCP2	methyl-CpG-binding protein 2
MEF2	myocyte enhancer factor 2
MEKK	mitogen-activated protein kinase kinase kinase

MEL	murine erythroleukaemia
min	minute
MITR	MEF2 interacting transcriptional repressor
MKK	mitogen-activated protein kinase kinase
MMP	matrix metalloprotease
MOPS	4-morpholine-propanesulphonic acid
Mr	molecular ratio
mRNA	messenger ribonucleic acid
MTA	metastasis associated
MuSV	murine sarcoma virus
n	nano
NAD	nicotinamide adenine dinucleotide
N-CoR	nuclear receptor co-repressor
NP-40	nonidet (non-ionic detergent) P-40
NuRD	nucleosome remodelling and deacetylase activities
OD	optical density
ORF	open reading frame
PAGE	polyacrylamide gel electrophoresis
PAH	paired amphipathic helix
PBS	phosphate buffered saline
PCDHGC3	protocadherin gamma subfraction C3
pcr	polymerase chain reaction
PDGF	platelet derived growth factor
PE	phosphate buffered ethylenediamine-tetra-acetic acid
PLZF	promyelocytic leukaemia zinc-finger protein
PMSF	phenylmethylsulphonyl fluoride

PVDF	polyvinylidene difluoride
rATP	adenosine triphosphate
RARα	retinoic acid receptor α
Rb	retinoblastoma protein
RbAp46	Rb-associated protein 46
REST	RE1-silencing transcription factor
RNA	ribonucleic acid
Rpd	reduced potassium dependency
RYBP	Ring 1 and YY1 binding protein
SAHA	suberoylanilide hydroxamic acid
SAP18	mSin3-associated polypeptide, molecular ratio 18KD
SAPK	stress-activated protein kinase
sec	second
Sin3	switch independent 3
Sir	silent information regulator
SDS	sodium dodecyl sulphate
SMRT	silencing mediator of retinoic acid and thyroid hormone receptors
SSH	suppressive subtractive hybridisation
STAT6	signal transducer and activator of transcription 6
Swi/Snf	switch/sucrose non-fermenting
TR	thyroid hormone receptor
TCF	ternary complex factor
TE	tris buffered ethylenediamine-tetra-acetic acid
TGFβ1	transforming growth factor β1
TIMP	tissue inhibitor of metalloproteinase
TPA	12-*O*-tetradecanoylphorbol-13-acetate

TRD	transcriptional repression domain
TRE	TPA responsive element
Tris	2-amino-2-(hydroxymethyl) propane-1,3-diol
TSA	trichostatin A
TSC-1	tuberosclerosis complex -1
TSC-36	TGFβ1-stimulated clone 36
Tween 20	polyoxyethylene sorbitan monolaurate
UV	ultraviolet
μ	micro
V	volts
VPA	valproic acid
wt	wild type
YAF1	YY1-associated factor
YEAF1	YY1 and E4TF1/hGABP-associated factor
YY1	Ying-Yang 1
ZNF217	zinc finger protein 217

Abstract

Transformation of fibroblasts with the *v-fos* oncogene produces a highly invasive phenotype. Accordingly, genes up- and down- regulated by v-Fos are of crucial importance in mediating a multigenic invasion programme.

Differential expression studies revealed that components of histone deacetylase (HDAC) transcriptional co-repressor complexes are up-regulated in FBR-v-Fos-transformed (FBR) cells. Since HDACs facilitate gene silencing, we investigated the consequences of inhibiting their activity in terms of gene re-expression and phenotypic changes.

We treated FBR cells with the HDAC inhibitors, trichostatin A (TSA) and valproic acid (VPA), at a range of sub-growth-inhibitory concentrations. At higher concentrations within this range, actin stress-fibres reform, transformed morphology reverts, cells are less motile and invasion is inhibited. Significantly, however, at lower concentrations within this range we inhibit invasion and actin stress-fibres reform but morphology, motility and chemotaxis are unaffected. This demonstrates the involvement of different groups of genes in different aspects of the transformed phenotype.

In a limited study, we found several genes, down-regulated in FBR cells, which are then re-expressed as a consequence of HDAC inhibition. Ectopic re-expression (stable and transient) of three of these genes (RYBP, PCDHGC3 and STAT6) individually, in FBR cells, inhibits invasion without affecting morphology, motility or chemotaxis; nor do actin stress-fibres reform. These results demonstrate that the down-regulation of genes by Fos can be mediated by histone deacetylases and that many of these down-regulated genes, when normally expressed in fibroblasts, function to maintain the non-invasive state, in that their expression is incompatible with the invasive phenotype.

Chapter 1

Introduction

1.1 General introduction

The work detailed in this thesis considers the role of the transforming oncoprotein v-Fos in the invasive cell phenotype. Following a comparative study of genes expressed by normal fibroblasts with those expressed by v-Fos-transformed fibroblasts (Johnston et al. 2000), we sought to provide evidence to support the proposal that the invasive phenotype of these v-Fos transformed cells is not mediated solely by a very small number of up-regulated invasion-specific genes and down-regulated invasion suppressors, but as a consequence of the interplay between the majority (if not all) of those proteins expressed in the transformed cells and importantly, the specific levels at which they are expressed in relation to one another. Thus the status of a cell, for example, non-transformed, transformed, invasive, differentiated, could be considered as a steady-state in terms of gene expression, with each steady-state governed by its own specific multigene programme of expression. This work then, explores the hypothesis that the *v-fos* oncogene regulates a multigenic invasion programme.

Our differential expression results (Johnston et al. 2000), in combination with other published studies (Bakin and Curran 1999), led us to consider the consequences of v-Fos-mediated increased histone deacetylase (HDAC) expression, and consequently, increased histone deacetylation, as a means of achieving wide-scale gene expression changes and adjustments, culminating in the establishment of a new steady-state of protein expression: the invasive state.

Firstly, we sought to investigate the consequences of altering the level of deacetylation in the transformed cells by several mechanisms, but with emphasis on pharmacological HDAC inhibition, and secondly we considered individual genes, down-regulated in the transformed cells as a consequence of increased HDAC expression, with respect to the phenotypic consequences of their re-expression.

In providing a background to these experiments, this introduction begins with a description of Fos and its known functions, with relevance to our study, and therefore, to invasion and cancer in general. It goes on to explain the current understanding of the role of HDACs in transcriptional control against a background of interrelated control mechanisms such as methylation of DNA. There follows an explanation of the strategies we employed to both increase and decrease HDAC activity in our cell system. In addition to studies with HDAC inhibitors, these include over-expressing HDAC4, expressing deacetylase-inactive HDAC4, and altering the level of HDAC4 localised to the nucleus. Finally the introduction is completed with a description of those proteins, down-regulated in response to increased HDAC expression, which we chose to re-express in Fos-transformed cells; these being: Ring 1 and ying yang 1 (YY1) binding protein (RYBP); protocadherin γ subfraction C,3 (PCDHGC3); and, signal transducer and activator of transcription 6 (STAT6).

1.2 Fos

1.2.1 c-Fos and AP-1

C-fos is a nuclear protein. It is a component of the Activator Protein 1 (AP-1) transcription factor, which is the nuclear effector of several signal transduction pathways. Thus, AP-1 activation regulates gene expression in response to a wide range of extracellular stimuli. Its viral counterpart, *v-fos*, is constitutively active and therefore becomes part of a constitutively active AP-1, directly regulating gene expression. It transforms rodent cells, replacing the requirement for the activation of endogenous AP-1 via the signal transduction pathways.

The *c-fos* gene encodes a protein of 381 amino acids which is highly conserved (van Straaten et al. 1983); moreover, the mouse and human genes have a similar intron/exon structure, with the mRNA encoding a 2.2 Kb transcript comprised of four exons from the 3.5 Kb transcription unit (van Straaten et al. 1983). This strong conservation of c-Fos suggests an important role for the protein in normal cellular physiology.

c-Fos is the founding member of a family of transcription factors which also includes, Fos-related antigen 1 (Fra1), Fra2, FosB and FosB2 (also called ΔFosB). As part of AP-1 these proteins heterodimerise with members of the Jun family of transcription factors, which is comprised of c-Jun, JunD, JunB and also includes the retroviral oncoprotein v-Jun. The DNA binding site of AP-1 is the TPA responsive element (TRE). TPA (12-*O*-tetradecanoylphorbol-13-acetate) is a phorbol ester; a tumour promoter, which was found to mediate gene induction through AP-1 (Lamph et al. 1988). In addition to Jun family members, Fos can form heterodimers with several other protein families (Table 1.1), for example, activating transcription factors (ATFs) and musculoaponeurotic fibrosarcoma proteins (MAFs), generally recognising similar,

but distinct DNA binding sites. Fos family members cannot form homodimers, whereas, Jun family members can.

c-Fos can form dimers with	preferred binding site	alternative binding site
c-Jun	TRE	CRE
JunB	TRE	CRE
JunD	TRE	CRE
ATFa	does not bind DNA	-
ATF2	CRE	TRE
ATF4	CRE	-
C-MAF	MARE I/III	-
MAFA	MARE I/III	-
MAFB	MARE I/III	-
MAFF/G/K	MARE I/III	-
NRL	TRE-like	-
NRF2	ARE	-
NFIL6	TRE	-

Table 1.1
The binding partners of c-Fos and their preferred DNA binding sites. Adapted from Eferl and Wagner 2003.

AP-1 has been shown to play a major role in diverse cellular processes such as, embryogenesis, bone formation and organogenesis, cell cycle and proliferation, differentiation, apoptosis, angiogenesis, and T-cell activation. Given that the processes of differentiation, cell cycle, proliferation, angiogenesis and apoptosis, are those which are frequently deregulated in cancer, it is not surprising that AP-1 has been shown to play a central role in the disease.

1.2.2 The v-fos^{FBR} oncogene

The *v-fos* oncogene was initially identified in 1966, when two viral isolates were recovered, one from a spontaneously occurring murine osteosarcoma and one from a ^{90}Sr-induced osteosarcoma. The first of these isolates to be studied yielded the Finkel-Biskis-Jinkins Murine Sarcoma Virus (FBJ-MuSV; Finkel et al. 1966), and the second

yielded the Finkel-Biskis-Reilly Murine Sarcoma Virus (FBR-MuSV; Finkel et al. 1973), which is the more transforming of the two and is the subject of this study.

The FBR-MuSV proviral sequence has a 1662 base pair ORF, encoding a 75KDa protein termed, $p75^{v\text{-}fos}$, which is a fusion of *gag, fos* and *fox* sequences (Figure 1.1) (Van Beveren et al. 1984). The first 310 amino acids of $p75^{v\text{-}fos}$ are part of a viral Gag sequence, which is fused to 236 amino acids of Fos sequence at asp25 of c-Fos, thus there is a 24 amino acid, N-terminal, deletion of the cellular sequence and, in addition, a 98 amino acid truncation of the C-terminus of c-Fos, which is replaced by 8 amino acids of Fox sequence, originating from the murine or rat genome. Within the v-Fos sequence there are also two small internal deletions of 13 and 9 amino acids, and 5 single amino acid substitutions, resulting from 9 point mutations in the nucleotide sequence (Van Beveren et al. 1984). In total, approximately 60% of the *c-fos* nucleotide sequence is retained in $v\text{-}fos^{FBR}$.

The inoculation of newborn mice with FBR-MuSV induced locally invasive tumours (Finkel et al. 1973). V-Fos has been shown to morphologically transform a variety of cell types including fibroblasts, fibroblast-like cells of mesenchymal origin, human keratinocytes and T lymphocytes (Bradbury and Edwards 1988; Appleby et al. 1989; Valge-Archer et al. 1990; Lee et al. 1993). As well as transformation of primary rodent cells in tissue culture, FBR-MuSV is also able to immortalise them (Jenuwein et al. 1985). No other retroviral oncogene is able to induce both these changes.

It was the discovery of *v-fos* which led to the identification of the normal cellular *c-fos* gene (van Straaten et al. 1983), hence the origin of the name Fos: FBJ-derived osteosarcoma.

Comparison of fos genes and proteins

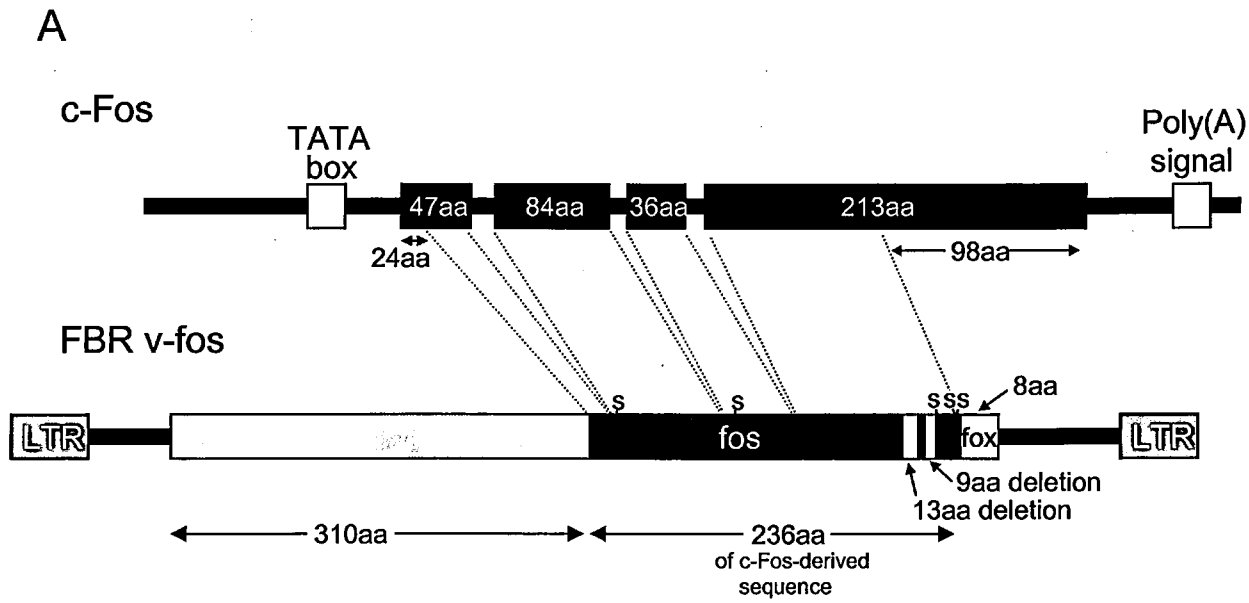

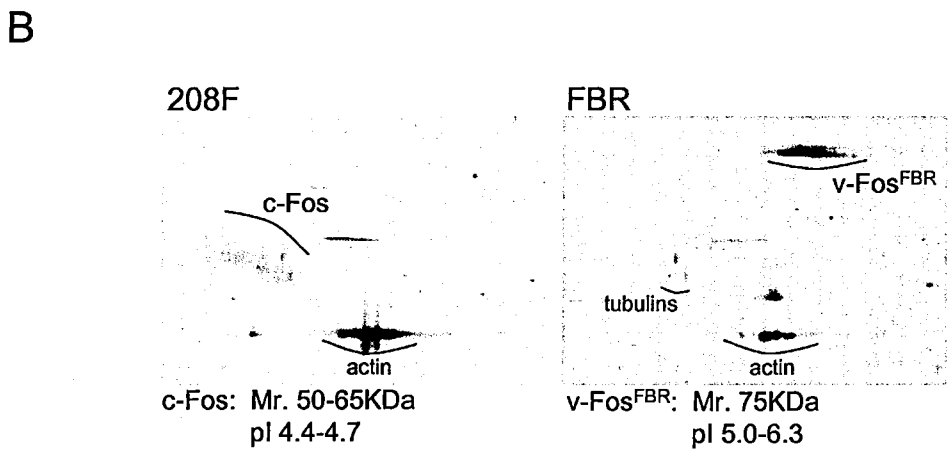

Figure 1.1

A. Comparison of the *c-fos* and *v-fos*^{FBR} genes. s = postion of amino acid substitution.

B. Comparison of immunoprecipitated, ^{35}S-met/cys-labelled c-Fos and v-Fos proteins, separated by 2-dimensional polyacrylamide gel electrophoresis. Cells were serum starved then induced with 10% FCS 1 hour prior to harvest. Actins and tubulins are expected artifacts in these experiments.

1.2.3 Control of Fos activity

1.2.3.1 Introduction

Control of the cellular activity of Fos is complex and occurs at several levels. Firstly, there is the rate of transcription of the *fos* gene itself, and the stability of the *fos* mRNA. Secondly, there is the activity of the Fos protein, its DNA binding affinity, stability, and its efficiency of transactivation. In addition there may be control over the composition of AP-1. Although this is generally agreed to depend largely on the relative amounts of AP-1 component proteins present in the nucleus, phosphorylation of c-Jun at a cluster of sites near its DNA binding domain (Figure 1.2), inhibits homodimer binding, favouring Fos-Jun heterodimer binding. The enzymes primarily responsible for mediating control at all levels are mitogen-activated protein kinases (MAPKs).

1.2.3.2 Signal transduction and MAP kinase pathways

MAP kinases are serine/threonine kinases which mediate signals from a vast array of cell membrane receptors, activated by binding of their specific stimuli, such as: growth factors; cytokines; and proteins involved in cell-cell or cell-matrix interactions. Four main MAP kinase pathways have been characterised (Figure 1.3): The extracellular signal-regulated protein kinase (ERK) pathway; the c-Jun NH_2-terminal kinase/stress-activated protein kinase (JNK/SAPK) pathway; the p38 pathway; and lastly, the ERK5/BMK pathway. The ERK pathway signals through Ras, Raf, Mos, MEK1 and 2, to the MAP kinases, ERK1 and 2. It is stimulated by a large variety of growth factors and cytokines and is central to the up-regulation of transcription from the *c-fos* gene (Figure 1.4) and for the activity of AP-1 (Figure 1.2). JNK/SAPK pathway signalling is via: MEK kinases (MEKKs); to JNK kinases (JNKKs) and SAP kinases (SAPKKs); to

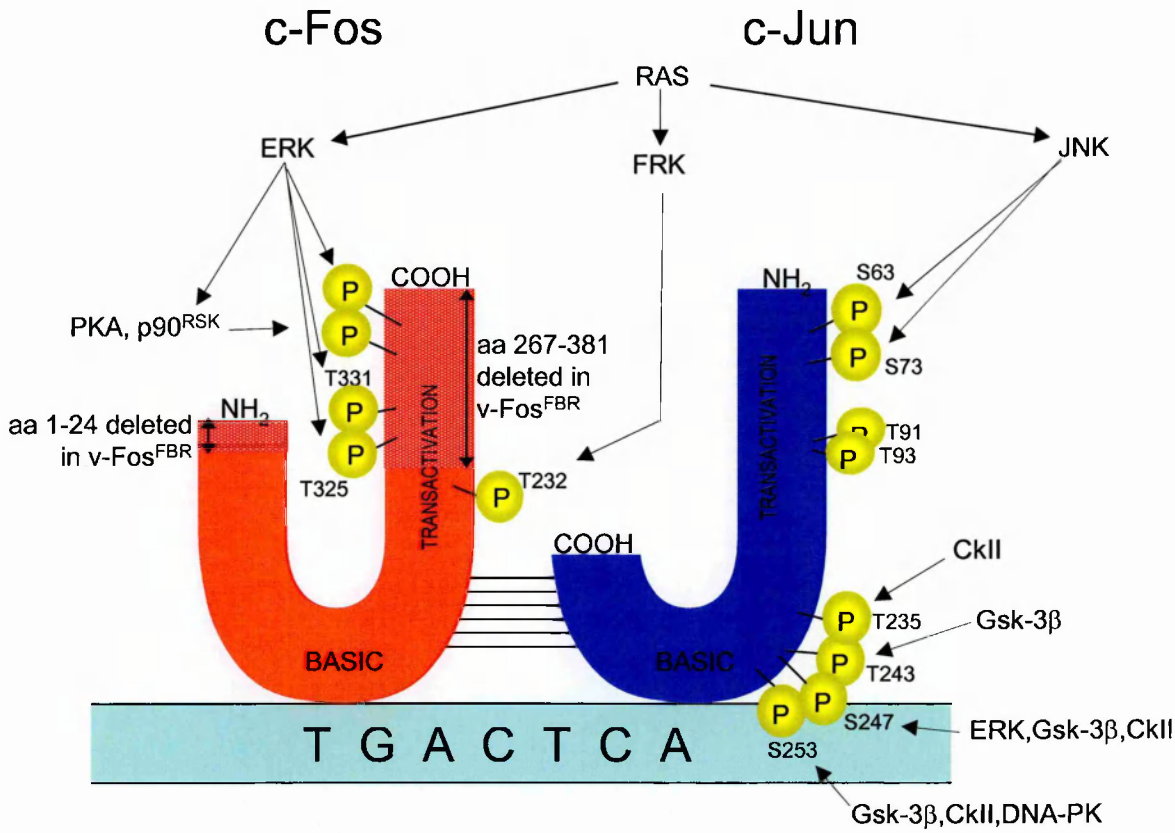

Figure 1.2

Schematic diagram of AP-1 DNA binding, showing the kinases which phosphorylate AP-1 proteins at indicated sites.

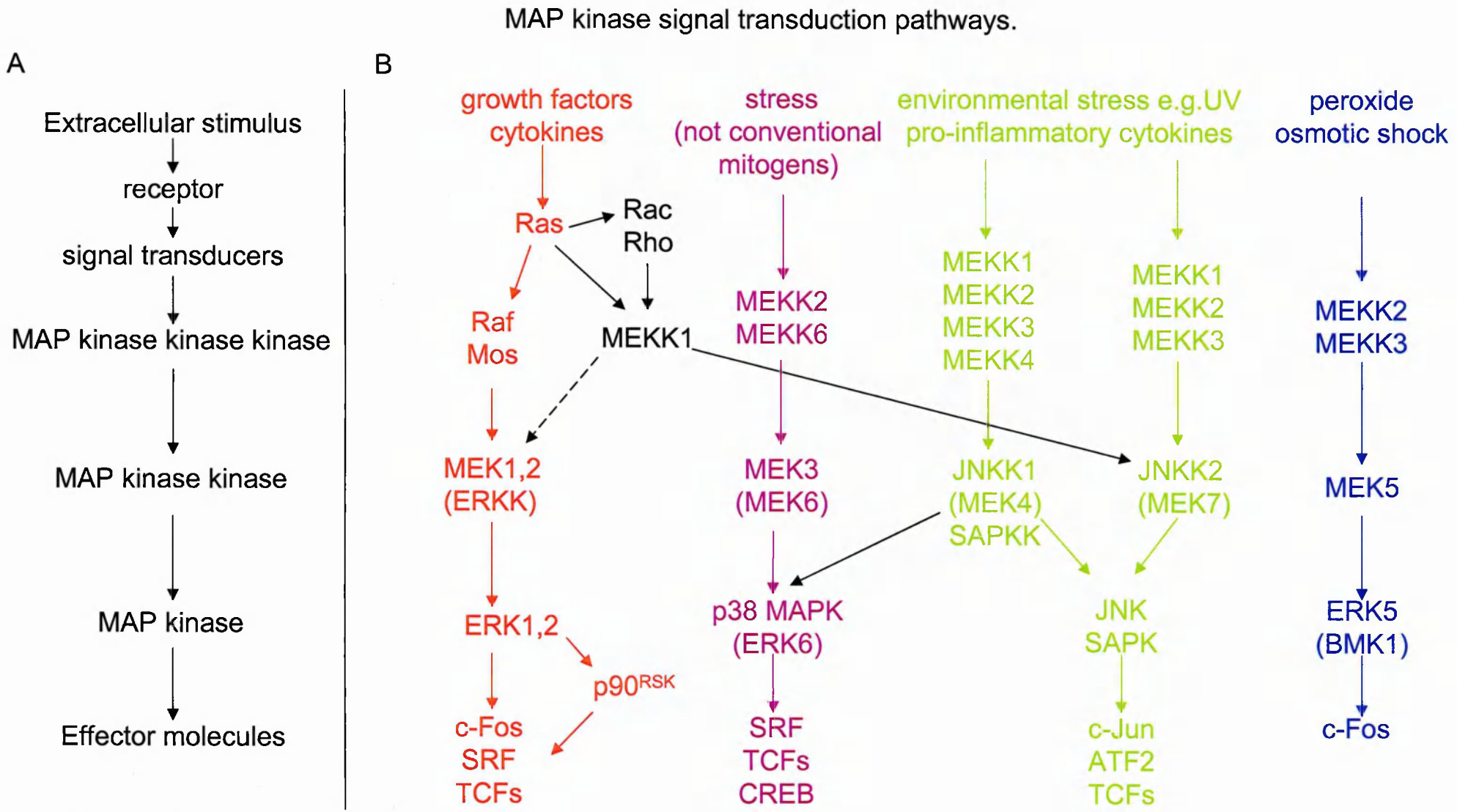

Figure 1.3

A. General characteristics of a MAP kinase pathway.

B. Specific examples of MAP kinase pathways. The ERK pathway is shown in red, the JNK pathway is shown in green, the p38 pathway is shown in purple , and the ERK5/BMK pathway is shown in blue.

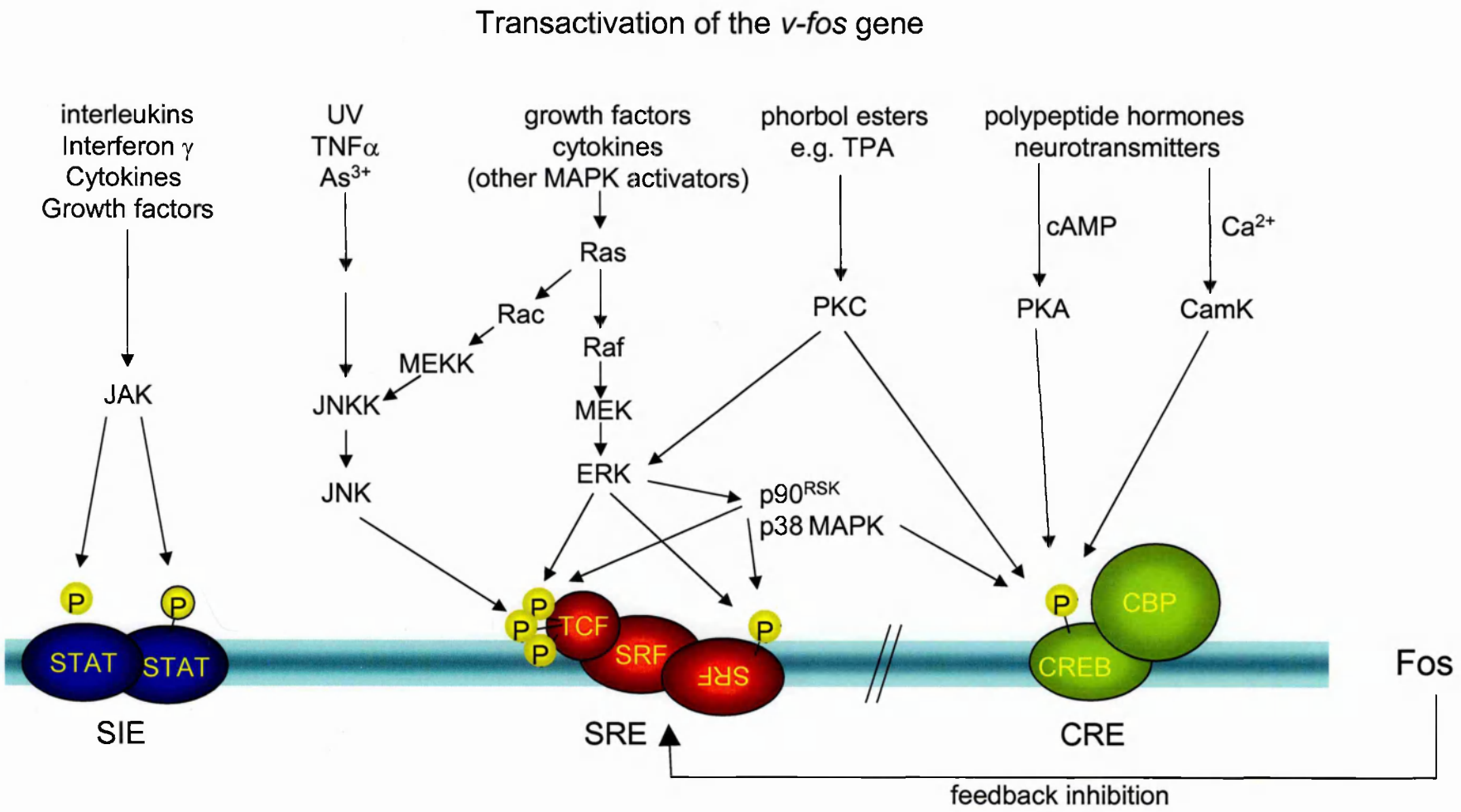

Figure 1.4

Signal transduction from the cell membrane via several pathways to the nucleus can activate transcription of the *c-fos* gene.

JNK and SAPK. This pathway is stimulated by UV and other environmental stress, as well as pro-inflammatory cytokines, however JNK can also be stimulated through Ras, to MEKK1 which phosphorylates JNKK. p38 is closely related to SAPK and JNK, and is activated by similar stimuli, though it is activated by different MEKKs and, unlike JNK, does not phosphorylate c-Jun. Finally, c-Fos can be phosphorylated by ERK5 (Terasawa et al. 2003) in response to stimuli such as peroxide and osmotic shock, which initiate signalling through the ERK5/BMK pathway (Lee et al. 1995; Zhou et al. 1995).

1.2.3.3 Activation of the c-fos gene and the c-Fos protein

Although signal transduction is often discussed in terms of linear pathways, there is a high degree of cross-talk between them, such that they are in fact, highly complex signalling networks, reflecting the complexity of the transcriptional response to each individual extracellular signal; consequently, the signal transduced from any stimulus can be shown to terminate in increased AP-1 expression, however, this is primarily achieved through Ras activation via Raf and MEK to ERKs, which phosphorylate ternary complex factors (TCFs), in this case Elk-1 (Figure 1.4). The TCF binds the serum response factor (SRF) dimer, creating, as the name suggests, a three component (ternary) complex, bound to the serum response element (SRE) in the *c-fos* promoter, activating transcription. TCFs can also be phosphorylated by p38 and by JNK, thus providing a means by which a wide variety of stimuli can activate *fos*. As well as activation via the SRE, transcription from *fos* can also be stimulated via the cyclic AMP response element (CRE) and the sis-inducible enhancer (SIE) (Figure 1.4). Activation at the CRE is in response to signals such as polypeptide hormones and neurotransmitters which use Ca^{2+} or cyclic adenosine monophosphate (cAMP) as second messengers; signalling to Ca^{2+}/calmodulin-dependent kinase (CamK) or

protein kinase A (PKA) respectively. Signal transduction via both these pathways results in the phosphorylation and activation of CRE binding protein (CREB). CREB mediates transactivation of *fos*, at least in part, by recruitment of a histone acetyl transferase (HAT) activity: CREB binding protein (CBP). Finally *fos* can be transactivated by interleukins and interferon as well as growth factors and cytokines, via the JAK/STAT pathway where a STAT homodimer is phosphorylated and transactivates from the SIE (Figure 1.4).

The activity of AP-1 is modulated through phosphorylation of its Fos and Jun family components (Figure 1.2). Many enzymes can phosphorylate AP-1, including, ERK, JNK, p38, ribosomal S6 kinase ($p90^{RSK}$), casein kinase II (CKII), glycogen synthase kinase 3β (GSK-3β), and DNA-dependent protein kinase (DNA-PK) (reviewed in Eferl and Wagner 2003). There are several phosphorylation sites on the c-Fos protein; phosphorylation at any of the four C-terminal sites of c-Fos, results in a protein with a longer half-life as well as increased transactivational activity (Chen et al. 1996; reviewed in Piechaczyk and Blanchard 1994). These sites are deleted in $v\text{-}Fos^{FBR}$, therefore, the protein escapes regulation by kinases at these sites. In addition, phosphorylation by FRK, at threonine 232 (though Ras signalling), increases the transactivation capacity of the protein.

1.2.4 Fos and invasion

In 1992, it was shown that mammary epithelial cells over-expressing an introduced *c-fos* gene become invasive (Reichmann et al. 1992). Now, there is a growing body of evidence that implicates AP-1 in the control of invasion. In this laboratory it was shown that normal rat fibroblasts (208F cells; section 1.2.5) can be induced to invade when treated with epidermal growth factor (EGF) or platelet derived growth factor (PDGF) (Hennigan et al. 1994), stimuli of signal transduction pathways which culminate in the

induction of *c-fos* (Section 1.2.3). These fibroblasts also become invasive in *in vitro* assay when transformed by v-Fos^{FBR} (FBR cells; section 1.2.5; Hennigan et al. 1994), and various Fos target genes implicated in their invasive phenotype have been identified, for example: CD44 (Lamb et al. 1997a); cathepsin L; metastasis-1 (Mts-1; Hennigan et al. 1994); and kelch-related protein (Krp1; Spence et al. 2000); and, ezrin (Jooss and Muller 1995; Lamb et al. 1997b). When expression of CD44, Krp-1 or ezrin was negated the cells were no longer able to invade (Lamb et al. 1997a; Lamb et al. 1997b; Spence et al. 2000). Fos has also been shown to up-regulate tropomyosin 3 and 5b (Jooss and Muller 1995) which are associated with invasion. Recently, in this laboratory, v-Fos$^{FBJ/R}$- and Ha-Ras-transformed human fibroblasts were shown to be invasive and in both of these cell lines, genes relevant to invasion were found to be differentially expressed (Scott et al. 2004).

When a dominant negative form of c-Jun, termed Tam67, is introduced into the FBR cells they lose their ability to invade (Lamb et al. 1997a), and a dominant negative form of c-Fos, called aFos, has a similar effect in HT1080 fibrosarcoma cells (Bahassi et al. 2004). Also in this laboratory, Tam67 was shown to inhibit invasion in human squamous cell carcinoma (A431) cells (Malliri et al. 1998). A431 cells over-express the EGF receptor, and it was also shown that this over-expression, in squamous cell carcinoma-derived cell lines, correlates with invasive ability (Malliri et al. 1998), again demonstrating the link between the induction of *fos*, via growth factor signalling, and invasion. Finally, normal mouse keratinocytes can be induced to invade by TPA (Dong et al. 1997), a phorbol ester which is the initial stimulus in another *fos*-inducing signal transduction pathway (Figure 1.4). Inhibition of Jun activity by Tam67, inhibits this TPA induced invasion (Dong et al. 1997).

The *fos*-family member, Fra-1 is also implicated in promoting invasion. Fra-1 can be a component of AP-1 (Section 1.2.1) and its expression is induced by c-Fos. Mammary

adenocarcinoma-derived cell lines over-expressing Fra-1 have been shown to be more invasive in *in vitro* invasion assays (Kustikova et al. 1998). More recently, it was shown that the invasion of colon carcinoma-derived cell lines, which have activated Ki-Ras, was inhibited when the levels of Fra-1 protein was reduced using siRNA (Vial and Marshall 2003). Fra-1 containing AP-1 has also been shown to preferentially induce expression of those extracellular matrix proteinases of the urokinase plasminogen activator system (Kustikova et al. 1998).

The invasive potential of a tumour is, to a large extent, determined by the balance between expression of matrix metalloproteinases (MMPs), which degrade the extracellular matrix (ECM), and tissue inhibitors of MMPs (TIMPs), secreted by tumour cells. MMPs, then, play a central role in the mechanism of invasion and they can be induced by AP-1. The majority of these genes have at least one conserved AP-1 consensus sequence up-stream of the transcription start site (between -189 and -50) which is required for the induction of MMP expression by growth factors (Kerr et al. 1988; Schonthal et al. 1988; Brenner et al. 1989; Sato et al. 1993; reviewed in Westermarck and Kahari 1999). In c-Fos deficient fibroblasts the induction of MMP-1 and MMP-3 by EGF and PDGF is abrogated (Hu et al. 1994), showing the link between AP-1 and MMPs. In c-Fos deficient cells there was shown to be decreased expression of MMP-1 and MMP-3 (stromelysin) (Hu et al. 1994), and skin tumour progression, in these mice, to invasive squamous cell carcinoma (in the presence of a v-Ha-ras transgene) was impaired (Saez et al. 1995). Increased levels of MMPs have been detected in invasive tumours, for example: MMP-1 (collagenase 1) activity was shown to be necessary for keratinocyte migration on a collagen matrix (Pilcher et al. 1997); AP-1 DNA-binding and transcriptional activation of the MMP-9 (gelatinase) promoter were increased when mouse keratinocytes progressed to invasive spindle cells (Papathoma et al. 2001); and, in human urothelial carcinoma, levels of MMP-9

correlated strongly with tumour invasiveness (Papathoma et al. 2000). Conversely, inhibition of MMPs inhibits invasion or metastasis (Albini et al. 1991; Wang et al. 1997; Valente et al. 1998; Baker et al. 1999).

1.2.5 Transformation of rat fibroblasts with the v-Fos^{FBR} oncogene

In this study we use rat fibroblasts (208F cells) which have previously been infected with the FBR-MuSV and thus stably express the *v-fos*^{FBR} oncogene (FBR cells) (Jenuwein et al. 1985). Western analysis revealed that the constitutive expression of v-Fos^{FBR} in these cells results in the up-regulation of other Fos and Jun family members (Figure 1.5A). In addition, we also see up-regulation of these proteins in 208F cells transformed by the *v-ras* oncogene; though it is perhaps surprising that we see an up-regulation of FosB and FosB2, since this is in contrast to a previous study

	208F	FBR
Expression of AP-1 components	+	+++
Transformed morphology	-	+++
Stress fibres	+++	-
Motility	+	+++
In vitro invasion	-	+++
Focal adhesions	+++	-
Focus formation	-	+++
Growth in soft agar	-	+++
Tumourigenicity	-	+++
Growth in 0.5% FCS	-	-

Table 1.2
Phenotypic differences observed between 208F cells and FBR cells.

of AP-1 compostion in Ras-transformed NIH3T3 cells (Mechta et al. 1997). The Fos-transformed cells differ from the parental, 208F cell line in several important aspects of their phenotype, as a consequence of increased AP-1 activity (Table 1.2). FBR cells

Genotypic and phenotypic differences between normal, transformed and EGF-treated cells

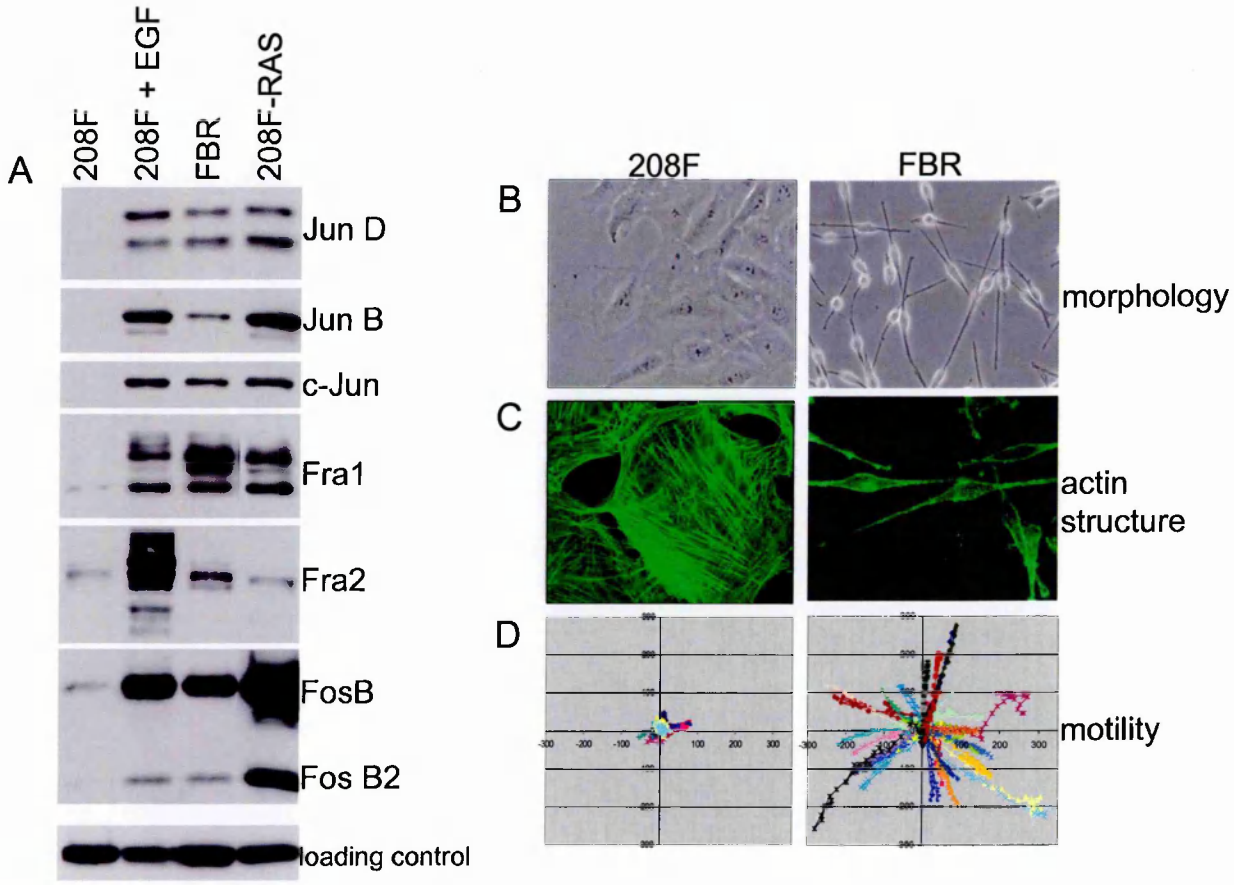

Figure 1.5

A. Western blots showing the up-regulation of Fos and Jun family members in Fos and Ras transformation
(FBR and RAS respectively) and in response to EGF stimulation (100 $ngml^{-1}$ for 24 hrs). An example PCNA loading control is shown.

B. Photographs of phase microscope images showing the difference in morphology between 208F and FBR cells.

C. Confocal microscope images of FITC-phalloidin-stained cells, showing the difference in actin structure between 208F and FBR cells.

D. Windrose diagrams showing the difference in motility between 208F and FBR cells. The tracks of 30 cells are included in each diagram.

have a transformed, bipolar, spindle-cell morphology, with extending pseudopods and a highly light refractile cell body, compared to 208F cells which are flat and polygonal (Figure 1.5B). This shape change is accompanied by a rearrangement of actin stress-fibres such that only cortical F-actin is detectable in FBR cells, in comparison to 208F cells which have a highly defined network of actin stress- fibres (Figure 1.5C). FBR cells are more motile (Figure 1.5D) and can invade in an *in vitro* invasion assay, in growth factor-depleted conditions, unlike 208F cells. In addition FBR cells have considerably less focal adhesions than 208F cells (Neil Carragher, BICR, personal communication). FBR cells also differ in that they form foci on plastic, are anchorage independent for growth, as determined by soft agar assay (Hennigan et al. 1994), and can form locally invasive tumours in nude mice (Finkel et al. 1973). Both cell lines, however, are growth factor dependent for proliferation (Hennigan et al. 1994), showing that Fos, in contrast to Ras, is not sufficient to facilitate cell cycle progression.

1.3 Control of transcription

1.3.1 DNA methylation and histone deacetylation in v-Fos transformation

1.3.1.1 Introduction

Two pieces of work initiated this present study. One was a study from our own laboratory, which identified proteins associated with histone deacetylation, as being up-regulated in v-Fos transformation (Johnston et al., 2000), and the other was a publication by Bakin and Curran (Bakin and Curran 1999), which demonstrated a role for DNA methylation and histone deacetylation, in mediating transformation by v-Fos.

1.3.1.2 Changes in gene expression as a consequence of v-Fos expression

In our laboratory, DNA suppressive subtractive hybridisation (SSH) studies identified sequences differentially expressed between immortalised rat fibroblasts (208F cells; section 1.2.5) and their v-Fos^{FBR}-transformed derivative cell line (FBR cells; section 1.2.5) (Johnston et al., 2000). The technique of SSH (Diatchenko et al. 1996), is a PCR-based approach which selectively amplifies restriction enzyme fragments of cDNAs derived from differentially expressed genes. The technique also suppresses amplification of commonly expressed genes. Two cDNA libraries were created, one comprised of cDNA fragments from genes that are up-regulated in FBR cells, and the other comprised of down-regulated sequences. Random clones were selected from each library and sequenced. Database searches provided names and functions for 55 genes that are up-regulated in FBR cells and 63 genes that are down-regulated. Their differential expression was confirmed by northern analysis. Of the 55 up-regulated genes, 22 had been reported as being associated with tumours or oncogenic transformation and 27 had functions consistent with a role in some aspect of invasion. Twelve of these genes are common to both groups. The remaining 18 genes include 7

associated with protein synthesis, 4 with vesicle transport, and 4 with metabolism. Of the 63 down-regulated genes, 25 had been reported as being associated with tumours or oncogenic transformation and 19 had functions consistent with a role in some aspect of invasion. Fourteen genes are common to both groups. The remaining 33 genes are associated with functions which include, adhesion, vesicle transport, and some are cytoskeletal components or proteases. All of which could be considered consistent with the invasive phenotype.

Two of the up-regulated sequences matched to genes encoding Sin3-associated protein 18KDa (SAP18) and retinoblastoma-associated protein 46KDa (RbAp46). These proteins are known to exist as components of large multiprotein complexes (Section 1.3.4) which are thought to be recruited to methylated DNA or to transcription factors and facilitate gene silencing by deacetylating the lysine residues of the N-terminal "tail" of histone H4 or H3 (Section 1.3.2.1). RbAp46 is thought to tether the complex to the histone (Parthun 1996, Verreault 1996) and SAP18 is thought to direct complex formation (Zhang et al. 1997). Northern analysis confirmed their up-regulation at the RNA level (Figure 1.6) and western analysis of RbAp46/48 expression levels also demonstrated increased protein expression in Fos-transformation (Figure 3.1B).

1.3.1.3 DNA methylation and histone deacetylation in Fos transformation

In 1999 Bakin and Curran first presented evidence that 5-methylcytosine transferase and histone deacetylases have a role in Fos-transformation. They used representational difference analysis to compare mRNA populations present in normal fibroblasts with those present in fibroblasts transformed with inducible *c-fos, or v-fos*$^{FBJ/R}$ (Miller et al. 1985) genes. One of nine up-regulated genes identified was, DNA (cytosine 5) methyltransferase 1 (*dnmt1*) which catalyses the transfer of a methyl

SAP18 and RbAp46/48 are up-regulated in FBR cells

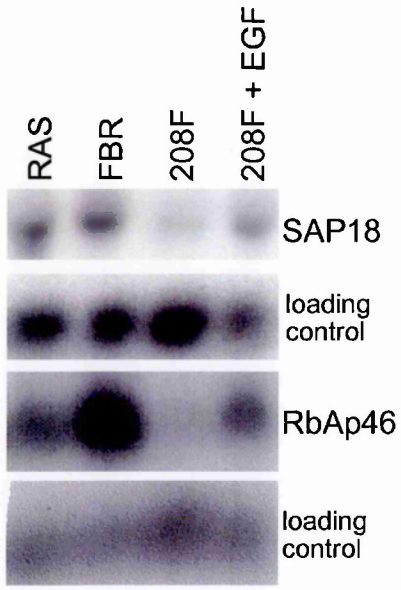

Figure 1.6

Northern blots demonstrating increased expression of SAP18 and RbAp46/48 mRNA in FBR, RAS, and EGF-treated (100 $ngml^{-1}$ for 24 hrs) 208F cells. This experiment was performed by Dr. Joseph Winnie.

group from S-adenosyl methionine to the C-5 position of the cytosine residues of DNA. Dnmt1 is up-regulated 2 to 3-fold in both their c- and v- Fos-transformants. Moreover, high pressure liquid chromatography (HPLC) analyses of nucleosides derived from the DNA present in these cells revealed that the Fos-transformants have 20% more 5-methylcytosine. They went on to show that when recombinant *dnmt1* is expressed in normal fibroblasts these cells became morphologically transformed and that when they inhibited the activity of Dnmt1 in c- and v-Fos transformed cells, with 5-aza-deoxycytosine, their morphology reverted to that of normal fibroblasts. Finally they showed that the transformed morphology is also reverted when histone deacetylases are inhibited by trichostatin A (TSA). The conclusion can then be drawn that Fos-transformation is mediated by increased expression of Dnmt1 which represses gene expression probably by the increased recruitment of histone deacetylases to methylated DNA. Later it was shown that Dnmt1 is directly associated with a deacetylase activity (Fuks et al. 2000).

1.3.2 Methylation and deacetylation

1.3.2.1 Chromatin

The packaging of DNA into chromatin restricts the accessibility of DNA to factors involved in fundamental processes such as DNA replication and transcription. The repeating organising unit of chromatin is the nucleosome (van Holde 1988). Each nucleosome consists of a core built of two copies of histones H2A, H2B, H3, and H4, around which the DNA is tightly wrapped and bound by electrostatic interactions (Luger et al. 1997). Consistent with the repressive effects of chromatin on gene expression, gene activation is often accompanied by nucleosomal rearrangements (Workman and Kingston 1998). Such local or extended structural changes in chromatin are achieved by ATP-driven chromatin remodelling complexes (Wu 1997)

and by methylation, phosphorylation, ubiquitination, and of key importance to our study, acetylation, of histones (Jones and Kadonaga 2000; Wolffe and Guschin 2000).

1.3.2.2 DNA methylation

The correlation between DNA methylation and lack of gene transcription has been well documented since it was initially reported over twenty years ago (Razin and Riggs 1980), however, it was not known whether methylation *mediates* transcriptional silencing or is as a *consequence* of transcriptional silencing. It is only in the last five years that an understanding of the link between methylation and deacetylation of histones has emerged, as a means by which the down-regulatory effects of methylation are mediated.

DNA can be methylated at carbon 5 on those cytosine nucleotides which appear in CpG dinucleotides. In mammalian gene coding sequences, CpG dinucleotides appear at a frequency much lower than one would expect by chance, and these CpGs are generally methylated. In promoter regions CpGs appear at approximately the expected random frequency, however, these CpGs are not methylated in actively transcribed genes. These promoter regions of non-methylated CpGs are termed CpG islands (Antequera and Bird 1993a; Antequera and Bird 1993b). CpG island chromatin contains highly acetylated histones H3 and H4.

Dnmt1 was the first DNA methyltransferase to be cloned (Bestor et al. 1988). This enzyme preferentially methylates hemimethylated CpGs, and is thought to be responsible for the maintenance of methylation patterns post-replication; methylating the daughter strand CpG after replication of a symmetrically methylated locus. It does this without any apparent sequence specificity, other than the CpG itself, suggesting that a hemimethylated CpG sequence is sufficient to guide methylation (Yoder et al. 1997). It is noteworthy, that Dnmt1 is found to be capable of *de novo* methylation *in*

vitro, since presumably it is this ability which facilitates the increase in the total amount of genomic methylation found in human cancer in correlation with up-regulated *dnmt1*. Methyl-CpG-binding protein 2 (MeCP2) was the first methylated-DNA binding protein which binds to a single methyl-CpG pair, to be identified (Lewis et al. 1992; Meehan et al. 1992). It carries an N-terminal methylated DNA binding domain (MBD) and a C-terminal transcriptional repression domain (TRD). The presence of an MBD domain now defines a family of proteins which, along with MeCP2, is comprised of MBD1 to MBD4. Members of this family have been shown to bind large transcriptional co-repressor complexes which have HDAC activity (Section 1.3.4), thereby recruiting HDAC activity to methylated DNA (Jones et al. 1998; Nan et al. 1998). MeCP2 can become part of the switch independent 3 (Sin3) complex, whilst MBD2 and MBD3 can be included in the nucleosome remodelling and deacetylase activities (NuRD/Mi-2) complex.

1.3.2.3 Acetylation and deacetylation of histones

The most widely studied post-translational modification of chromatin is the reversible acetylation of lysine residues in the amino terminal tails of the four core histones. Transcriptionally silenced regions, such as heterochromatin and the inactivated mammalian X chromosome, are associated with hypoacetylated histones (Grunstein 1997). In contrast, transcriptionally active domains in euchromatin are often associated with histone hyperacetylation (Wolffe 1998). Localised changes in histone acetylation levels near the transcriptional start site of certain genes are linked to gene activation or repression (Rundlett et al. 1998). The causal link between histone acetylation and transcriptional regulation is illustrated clearly by the identification and characterisation of transcriptional regulators containing HAT (Cheung et al. 2000) or HDAC activities (Ng and Bird 2000).

1.3.3 Histone deacetylases

1.3.3.1 Introduction

Mammalian HDACs were identified by their homology to yeast histone deacetylases. Yeast cells have at least two distinguishable histone deacetylase activities residing in two multiprotein complexes, termed the histone deacetylase A (Carmen et al. 1996), and histone deacetylase B (Rundlett et al. 1996), complexes, which have molecular weights of 350kD and 600kD respectively. The catalytic subunit of the histone deacetylase A complex is HDA1 and the active component of the histone deacetylase B complex is the reduced potassium dependency 3 (Rpd3) catalytic subunit, or the Rpd3 related proteins HDA one similar (HOS) 1, 2 or 3 (Rundlett et al. 1996). Mammalian HDACs form two homology groups: class I HDACs are more closely related to Rpd3 and class II HDACs are more closely related to HDA1. All HDACs share an approximately 390 amino acid region of homology, termed the deacetylase core (Figure 1.7), which defines the gene superfamily.

1.3.3.2 Class I histone deacetylases

Human HDAC1 was first isolated, along with an associated protein RbAp48, by its binding to an analogue of the HDAC inhibitor, trapoxin, in affinity chromatography (Taunton et al. 1996). Sequence analysis revealed 60% homology to Rpd3, a yeast transcriptional regulator (Section 1.3.3.1; Vidal and Gaber 1991), at the protein level. This then linked transcriptional control and histone deacetylation for the first time. In the same year Yang and colleagues (Yang et al. 1996) identified HDAC2 in yeast two-hybrid studies, as a protein binding to the transcription factor YY1. Human HDAC1 and 2 are 75% identical in DNA sequence and share 85% homology at the protein level. The sequences of HDAC1 and 2 were then used by a number of groups to

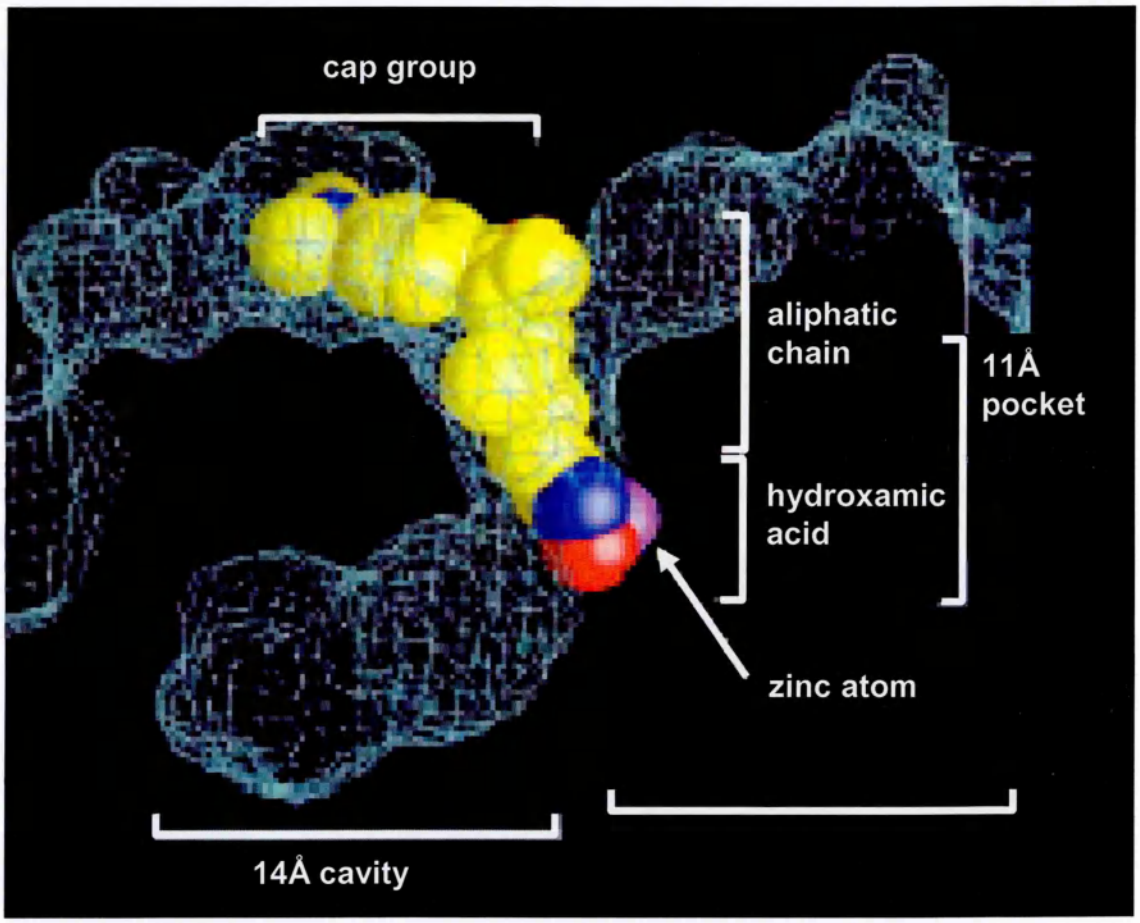

Figure 1.7

The structure of the catalytic core of HDACs, shown complexed to the inhibitor, TSA, as determined by X-ray crystallographic studies. The active catalytic site was shown to be formed by a tubular pocket, a zinc binding site, and two asparagine-histidine charge-relay systems.
Reproduced from Finnin et al., 1999.

identify database sequence homologies and consequently HDAC3 was cloned (Yang et al. 1997; Dangond et al. 1998; Emiliani et al. 1998; Mahlknecht et al. 1999). Finally, two remaining class I HDACs were isolated; HDAC8 (Buggy et al. 2000; Hu et al. 2000; Van den Wyngaert et al. 2000) and HDAC11, which has least homology to other class I HDACs and shows tissue specific expression (Gao et al. 2002).

1.3.3.3 Class II histone deacetylases

Database searches by at least four groups (Fischle et al. 1999; Grozinger et al. 1999; Miska et al. 1999; Wang et al. 1999), for sequence similarity to yeast HDA1 produced several homologies in humans. Collectively these proteins were termed class II histone deacetylases, and, initially this group was comprised of HDAC4, HDAC5 and HDAC6. Following this, HDAC7 (Kao et al. 2000; Fischle et al. 2001), HDAC9 (Zhou et al. 2001b), HDAC10 (Guardiola and Yao 2001; Kao et al. 2001) and HDAC11 (Gao et al. 2002) were identified. Unlike class I, these class II histone deacetylases show a tissue specific pattern of expression. HDAC4 and 5 are reported to be expressed in brain, heart and skeletal muscle. HDAC6 can be detected in heart, liver, kidney and pancreas, and HDAC7 is present in heart, lung and skeletal muscle (Grozinger et al. 1999; Verdel and Khochbin 1999; Kao et al. 2000).

1.3.3.4 The Sir family of histone deacetylases

The silent information regulator (Sir) family of HDACs are now generally considered as the third class of histone deacetylases. In humans, 7 sequences with homology to the yeast Sir2 protein have been identified which, like all Sir HDACs, have NAD^+-dependent activities (Afshar and Murnane 1999; Frye 1999). Class III HDACs appear to have a unique catalytic reaction and are insensitive to inhibition by TSA (Guarente 2000). Interestingly, Sir2 can interact with, and deacetylate p53, reducing its

transcriptional activity (Luo et al. 2001; Vaziri et al. 2001). This is an example of direct deacetylation of a transcription factor to suppress transcription and is probably demonstrates one of multiple mechanisms of repression, which are beginning to emerge for HDACs.

1.3.4 Protein complexes with histone deacetylase activity

1.3.4.1 Sin3 complex

In 1997 two groups published in the same issue of Cell (Laherty et al. 1997; Zhang et al. 1997) providing the first evidence that HDACs exist in the mammalian cell as part of multiprotein complexes. Studies in yeast had previously made the functional link between the Sin3 protein and the yeast Class I HDAC homologue, Rpd3, since they function in the same pathway. This gave rise to these studies, which both showed mSin3A associates with HDAC1 and HDAC2 *in vivo.* In addition, the study by Zhang and co-workers identified other mSin3 associated proteins, two of which were novel. They called these, SAP18 and SAP30. They also identified, RbAp46 and RbAp48 as being part of the complex. Previous evidence suggests these proteins act as a molecular bridge between the complex and the histone (Parthun et al. 1996; Verreault et al. 1996). The study by Laherty and co-workers also demonstrated that these mSin3-associated HDACs mediate transcriptional repression by the DNA-binding protein, Mad. Previously, it had been shown that the Mad-Max heterodimer represses genes which are activated by Myc-Max (Ayer et al. 1993) and that this repression is dependent on binding of Mad to mSin3 (Ayer et al. 1995). This provided the first evidence that the Sin3 complex can be recruited to promoter sites through interaction with transcription factors. Mad interacts with mSin3 at the second of its four paired amphipathic helix (PAH) domains (Ayer et al. 1995). These protein-protein interaction

domains can mediate associations with other complex components as well as with several transcription factors and transcriptional repressors (Table 1.3).

In 1998, Nan and co-workers demonstrated the link between methylation and the HDAC-containing, Sin3 complex. They found that the methylated-DNA binding protein, MeCP2, was able to bind HDAC1 and 2 and mSin3A, and that its transcriptional repression was relieved by the HDAC inhibitor TSA. Thus methylated DNA binding proteins are part of the Sin3 complex.

Protein	Example of cellular role	Reference
NCoR / SMRT	transcriptional repressor complex components	Heinzel et al. 1997
RAR (via N-CoR/SMRT)	retinoic acid receptor / transcription factor	Chen et al. 1995
TR	thyroid hormone receptor / transcription factor	Chen et al. 1995
ETO	transcriptional repressor	Wang et al. 1998
MeCP2	methylated DNA binding protein	Nan et al. 1998
Mad / Mxi	transcriptional repressors	Ayer et al. 1995
c-Ski / Sno	transcriptional co-repressor	Nomura et al. 1999
REST	transcriptional repressor	Grimes et al. 2000
p53	transcription factor	Murphy et al. 1999
Ikaros / Aiolos	transcriptional repressors	Koipally et al. 1999

Table 1.3
Examples of proteins which interact with components of the Sin3 complex.

1.3.4.2 NuRD/Mi-2 complex

Like the Sin3 complex, the NuRD/Mi-2 complex (Tong et al. 1998; Xue et al. 1998; Zhang et al. 1998) is also capable of connecting methylated DNA and HDAC activity, however, it differs in that it also has nucleosome remodelling activity. The core NuRD complex contains Mi-2, HDAC1 and 2, and, RbAp46 and RbAp48, but also in the complex are metastasis associated protein 2 (MTA2), which modulates the HDAC enzymatic activity, MBD3 which, unlike its close relative MBD2, doesn't bind methylated DNA directly but appears to mediate association of MTA2 with the core complex (Zhang et al. 1999).

1.3.4.3 N-CoR and SMRT

Although cloned on the basis of their interaction with unliganded retinoic acid receptor (RAR) and thyroid hormone receptor (TR), nuclear receptor co-repressor (N-CoR) and silencing mediator of retinoic acid and thyroid hormone receptors (SMRT) appear to confer transcriptional repression on many transcription factors. The current majority of these are members of the nuclear receptor superfamily, however, they are also co-repressors for a variety of other transcription factors which regulate diverse cellular processes (Table 1.4). AP-1 can bind to the co-repressor at a C-terminal region which overlaps the binding site for nuclear receptors. Several binding sites overlap on the N-CoR/SMRT protein, suggesting a possible control mechanism whereby transcription factors compete to recruit the co-repressor complex to DNA.

Protein	Examples of cellular roles	Reference
AP-1	regulates many diverse cellular processes	Lee et al. 2000
SRF	activates c-Fos, growth, differentiation, neuronal transmission, muscle development and function	Lee et al. 2000
STAT5	induced by cytokine signalling	Nakajima et al. 2001
Myo-D	mediates muscle differentiation	Bailey et al. 1999
NFκB	immune and inflammatory response, cell survival	Lee et al. 2000
BCL-6	apoptosis	Dhordain et al. 1998
Oct-1	development	Kakizawa et al. 2001
Pit-1	development	Xu et al. 1998
PBX	homeobox factor	Saleh et al. 2000
HERPs	stress-responsive endoplasmic reticulum protein	Iso et al. 2001
Su(H)/RBP-J/CBF1	transcriptional repressor	Zhou and Hayward 2001a

Table 1.4
Examples of transcription factors known to bind N-CoR/SMRT.

The HDACs 3, 4, 5 and 7 have been shown to bind N-CoR and SMRT directly. HDACs 4, 5 and 7 share a common binding site within the region required for repression, whereas HDAC3 has two separate binding sites only one of which overlaps a repressor domain. The fact that class I and class II HDACs have separate

binding sites may suggest differential control by these two classes of enzymes. SMRT and N-CoR can also bind the Sin3 complex proteins, therefore HDAC1 and 2 are also found in association with SMRT and N-CoR.

One study has shown that the SMRT/N-CoR complex has nucleosome remodelling activity: it was found that an N-CoR-SMRT-HDAC3 complex can also contain Krab-associated protein 1 (KAP-1), a TSA-sensitive co-repressor that interacts with members of the heterochromatin 1 (HP-1) family, which has homology to the switch/ sucrose non-fermenting (Swi/Snf), ATP-dependent chromatin remodelling complex proteins found in NuRD/Mi-2 (Underhill et al. 2000).

1.3.4.4 CoREST

Studies purifying HDAC1- and HDAC2-associated proteins, identified a novel protein found to be a co-repressor of the RE1 silencing transcription factor/neural restrictive silencing factor (REST) protein (Andres et al. 1999), and so was called Co-REST (You et al. 2001). REST has been shown to have two repression domains: the N-terminal domain recruits the Sin3 complex and the C-terminal domain recruits Co-REST. The Co-REST complex, which recruits HDAC activity, was found to be distinct from Sin3 in composition (You et al. 2001), for example, it lacks RbAp46/48 present in both the Sin3 and NuRD/Mi-2 core complex, and includes a 110KDa protein not found in the other complexes. Thus REST has the potential to mediate transcriptional repression via two distinct HDAC complexes. Although CoREST was identified as a REST associated protein it has emerged that CoREST interacts with other transcription factors, for example, zinc finger protein 217 (ZNF217), which is a transcription factor and candidate oncogene, by virtue of its up-regulation in several human cancers (Bar-Shira et al. 2002; Peiro et al. 2002; Freier et al. 2003; Weiss et al. 2003).

1.3.5 Deacetylase independent transcriptional repression by HDACs

MeCP2 has been found to repress transcription by a histone deacetylase-independent pathway (Yu et al. 2000). In colorectal carcinoma and in leukaemic cell lines, hypermethylated, transcriptionally silent genes can be reactivated by simultaneous treatment with the HDAC inhibitor, TSA, and the demethylating agent, 5-Aza-dC but not by TSA alone (Cameron et al. 1999). These findings suggest either that DNA methylation has additional repressive effects that are independent of histone deacetylation, or that unknown TSA-insensitive HDACs are also involved. Interestingly, Dnmt1 associates with Dnmt1-associated protein 1 (DMAP1), which is a putative HDAC-independent transcriptional repressor (Rountree et al. 2000).

Several of the class II histone deacetylases have a second transcriptional repression domain. HDAC4 and 5 posses two independent repression domains, the first of which is able to repress transcription independently of deacetylase activity (Wang et al. 1999). HDAC6 has two active deacetylase domains, however, in HDAC10, which is closely related, the second domain is catalytically inactive. Both HDAC6 and 10 are resistant to trapoxin B and butyrate and this resistance is reported to be dependent on the presence of the second putative deacetylase domain (Guardiola and Yao 2001). HDAC9 (Zhou et al. 2001b) was found to have several alternatively spliced isoforms (as has HDAC10; Kao et al. 2001) including the previously discovered HDAC-related protein/myocyte enhancer factor 2-interacting transcriptional repressor (HDRP/MITR; Sparrow et al. 1999; Zhou et al. 2000) which has 50% homology to the N-terminus of HDAC4 which includes the deacetylase-independent repression domain and can repress transcription by a deacetylation independent mechanism. Although HDRP/MITR was not found to possess intrinsic HDAC activity it does form complexes with both HDAC1 and HDAC3 and is therefore able to recruit deacetylase activity. HDAC7 has just one catalytic domain, however, it is found to be inactive with its

activity dependent on HDAC7 binding to HDAC3 in the nucleus (Kao et al. 2000; Fischle et al. 2001).

1.3.6 Subcellular localisation of class II HDACs regulates their activity

Although most class II HDACs can be detected in both the nucleus and the cytoplasm they differ in their relative distribution. HDACs 4, 5 and 6 are predominantly cytoplasmic (Miska et al. 1999; Grozinger and Schreiber 2000; McKinsey et al. 2000b; Verdel et al. 2000; Wang et al. 2000), HDAC7 and HDAC11 localise predominantly to the nucleus (Dressel et al. 2001; Fischle et al. 2001; Gao et al. 2002) though they can be detected in the cytoplasm, and HDAC10 can be found in equal nuclear/cytoplasmic amounts (Guardiola and Yao 2001; Kao et al. 2001). This differential distribution coupled with the tissue specific pattern of expression of class II HDACs strongly suggests different molecular roles for each protein.

The active transport of class II HDACs from the nucleus is a major mechanism controlling their activity. Nucleocytoplasmic shuttling has been demonstrated or implied for all class II HDACs. Surprisingly, the class I histone deacetylase, HDAC3, has also been found to carry a nuclear export signal and associates with chromosomal maintenance region 1 protein (CRM1), a nuclear export factor, in co-transfections (Yang et al. 2002). Endogenous HDAC3 has been detected in both the cytoplasm and nucleus of DT40 cells (Takami and Nakayama 2000; Yang et al. 2002) though other studies maintain that HDAC3 is an exclusively nuclear protein (Emiliani et al. 1998; Grozinger and Schreiber 2000).

A large part of the research on this subject has been concentrated on HDACs 4 and 5. These deacetylases are seen to localise exclusively to either the cytoplasm or the nucleus within the same cell culture (Miska et al. 1999; Grozinger and Schreiber 2000), a phenomenon which we have observed in both 208F and FBR cells stably

transfected with GFP-tagged HDAC4 (Figure 5.4), where the larger proportion of cells have HDAC4 in the cytoplasm, though it can also be observed exclusively in the nucleus. This nuclear localisation is dynamic and translocation can occur under normal conditions of cell growth (Grozinger and Schreiber 2000). Immunoprecipitation and yeast two-hybrid experiments identified 14-3-3 proteins as HDAC 4 and 5 interacting factors (Grozinger and Schreiber 2000; McKinsey et al. 2000b; Wang et al. 2000) and later this was also shown for HDAC7 (Dequiedt et al. 2003) and implied for HDAC9 based on homologies. The 14-3-3 family of proteins function as signal-dependent intracellular chaperones, which bind proteins, allowing them to be transported across the nuclear membrane by the nuclear export receptor, CRM1/exportin1 (Adachi and Yanagida 1989; Stade et al. 1997), in a trimeric complex, and sequester them in the cytoplasm (Fu et al. 2000) preventing them from performing their nuclear function. They are known to bind specifically to conserved phosphoserine-containing motifs which act as docking sites. Deletion analyses indicated that S246, S467, and S632 of HDAC4 mediate this interaction [S259 and S498 in HDAC5 (McKinsey et al. 2000a), and S155, S318 and S448 in HDAC7 (Dequiedt et al. 2003)], and alanine substitutions of these serine residues abrogated 14-3-3 binding, with very minimal effects on the deacetylase activity of HDAC4 (Grozinger and Schreiber 2000; Wang et al. 2000). In transient transfections this triple mutant HDAC4 (TMHDAC4) showed increased nuclear localisation compared to transiently expressed wild type HDAC4 (Wang et al. 2000) and when wild type HDAC4 is co-expressed transiently with 14-3-3 it showed increased cytoplasmic localization (Grozinger and Schreiber 2000). The association of 14-3-3 with HDAC4, 5 and 7 then, results in the sequestration of these proteins in the cytoplasm and loss of this interaction allows HDAC4 and HDAC5 to translocate to the nucleus.

In muscle myogenesis, calcium/calmodulin-dependent protein kinase IV (CamKIV) has been demonstrated to phosphorylate those serines in HDAC4 and 5, which subsequently serve as docking sites for 14-3-3 (McKinsey et al. 2000a; McKinsey et al. 2000b).

Since class II HDACs can be found in the cytoplasm, the possibility of their having a cytoplasmic role cannot be ruled out. Indeed HDAC6 has a known cytoplasmic role. It has been shown to reverse the post-translational acetylation of tubulin, which is reported to destabilise the microtubules and enhance microtubule dependent cell motility (Hubbert et al. 2002; Matsuyama et al. 2002). Very recently it has also been shown that HDAC6 is involved in the removal of cytotoxic aggregates of misfolded proteins, via the microtubule network, to a processing organelle called the aggresome (Kawaguchi et al. 2003). In this role HDAC6 is considered to be a linker protein.

1.3.7 Histone deacetylases and cancer

A wealth of evidence is now appearing in the literature implicating histone deacetylases in cancers, particularly of the blood and lymphoid systems. The current evidence points mainly to the aberrant recruitment of histone deacetylases by mutated transcription factors or to the recruitment of deacetylases by transcription factors which are ectopically expressed, rather than to deregulated or ectopic expression of the HDACs themselves.

Several transcription factors implicated in leukaemias repress expression of specific genes because of aberrant recruitment of HDACs. In acute promyelocytic leukaemia (APL) the transforming proteins are fusions of the promyelocytic leukaemia (PML) or the promyelocytic leukaemia zinc-finger (PLZF) proteins with the retinoic acid receptor-α (RAR-α). The ability of the RAR-α protein to block haematopoietic differentiation depends on its DNA binding domain which is retained by the fusion

protein; however, the retinoic acid binding ability of the RAR is also retained which provides the opportunity for therapy with retinoic acid.

In cell lines derived from patients with APL, the oncoprotein encoded by the translocation-generated fusion gene (PML-RAR-α) represses transcription by recruitment of HDAC1 (Grignani et al. 1998; He et al. 1998; Lin et al. 1998). APL patients can be treated with retinoic acid but often become resistant. In one patient this resistance was overcome by co-treatment with an inhibitor of histone deacetylases (Warrell et al. 1998), though no other studies, to date, have shown this.

HDAC-dependent aberrant transcriptional repression is implicated as the main oncogenic mechanism in specific types of myeloid leukaemia and lymphomas. In non-Hodgkin's lymphoma, the transcriptional repressor, B-cell lymphoma gene 6 (BCL6) [also called lymphoma-associated zinc finger protein 3 (LAZ3)] is inappropriately expressed within the lymphoid compartment, resulting in aberrant transcriptional repression (Kerckaert et al. 1993). BCL6 has been found to co-immunoprecipitate with SMRT, mSin3 and an HDAC activity (Dhordain et al. 1998). In addition HDAC inhibitors significantly reduce BCL6-mediated repression. It is therefore concluded that oncogenic transcriptional repression by BCL6 is mediated, largely, by an associated histone deacetylase activity.

In acute myeloid leukaemia (AML), 12-15% of cases have a t(8;21) chromosomal translocation. This is the second most common genetic lesion in AMLs where the N-terminus of the AML1 gene is fused to the C-terminus of the eight twenty one (ETO) gene (Erickson et al. 1992). In the normal cell, the AML-1 protein is a transcriptional activator of a number of genes involved in haematopoiesis, however, fused to ETO, is becomes a potent dominant transcriptional repressor. Experiments showed that ETO is able to co-immunoprecipitate N-CoR (Section 1.3.4.3) mSin3 and HDAC1. The binding to N-CoR was found to be direct and hence it was concluded that ETO recruits

the N-CoR/Sin3/histone deacetylase complex by binding to N-CoR, resulting in a fusion protein which is a transcriptional repressor by virtue of its associated deacetylase activity (Wang et al. 1998). Significantly, the AML1 ETO fusion protein represses transcription of the $p14^{ARF}$ tumour suppressor (Linggi et al. 2002) and does so by binding co-repressors and HDACs (Hiebert et al. 2003).

1.4 Histone deacetylase inhibitors

1.4.1 Introduction

In our study we used chemical inhibitors to HDACs to investigate the consequences of reducing HDAC activity in our Fos-transformed cells (FBR), remembering that HDACs are up-regulated in these cells, compared to levels in their non-transformed parental cell line (208F). We chose the inhibitors, TSA and valproic acid (VPA), on the basis that since they come from structurally distinct inhibitor families their inhibition is mechanistically different and, because they are both currently prime candidate drugs in anticancer therapy.

1.4.2 Classes of histone deacetylase inhibitors

1.4.2.1 Introduction

There are four main classes of known histone deactetylase inhibitors. These are: hydroxamic acid-related hybrid polar compounds (HPCs); short chain fatty acids; benzamidines; and cyclic tetrapeptides. TSA is a member of the family of hydroxamic acid-related HPCs whilst VPA is a short chain fatty acid.

1.4.2.2 TSA: a hydroxamic acid-related hybrid polar compound

TSA is an HPC (Tsuji et al. 1976; Yoshida et al. 1990). The essential characteristics of HPCs are: a polar site, the hydroxamic group, a six-carbon hydrophobic methylene spacer, a second polar site and a terminal hydrophobic group (Figure 1.8). Another HPC which is currently in clinical trials is suberoylanilide hydroxamic acid (SAHA) (Richon et al. 1998).

TSA was originally isolated (along with its glucopyranosyl derivative, trichostatin C) in 1976 as an antibiotic against trichophytons and some fungi (Tsuji et al. 1976). It was

not until about 10 years later it was found that these trichostatins were able to strongly induce the differentiation in two types of murine erythroleukaemia (MEL) cells such that they became haemoglobin-positive after 5 days in 15nM TSA and to inhibit proliferation in mammalian cells (Yoshida et al. 1987).

TSA was initially found to cause an accumulation of acetylated histones, and pulse-chase experiments subsequently revealed that histone hyperacetylation induced by TSA is due, not to increased acetylation but to decreased deacetylation of histones (Yoshida et al. 1990). *In vitro* experiments using partially purified histone deacetylase from mouse mammary tumour cells have shown that TSA is a potent inhibitor with a Ki value of 3.4nM. A TSA resistant cell line derived from these tumour cells was found to have a markedly increased Ki value of 31nM, indicating that the enzyme itself had become resistant to TSA. This confirmed that histone deacetylase is the primary intracellular target of TSA. Figure 1.6 shows the catalytic core of an HDAC complexed to TSA. The hydroxamic acid moiety of TSA bind to the zinc at the bottom of the tubular pocket and the benzene-ring group projects out of the pocket on the surface of the protein.

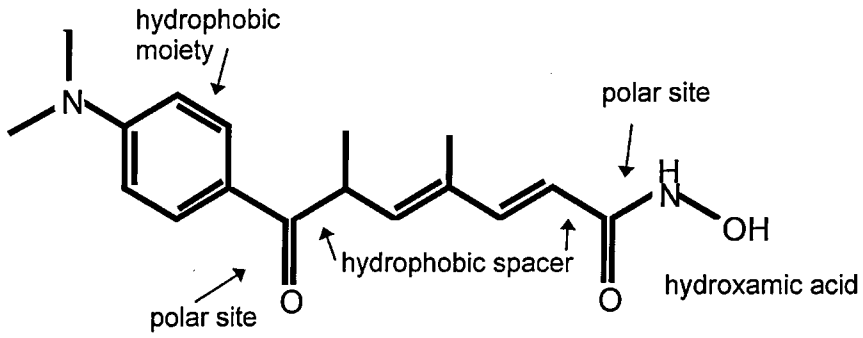

Figure 1.8

The structure of TSA, showing the essential characteristics of all hydroxamic acid-related hybrid polar compounds.

1.4.2.3 VPA: a short chain fatty acid.

Until recently butyrate and phenylbutyrate (Newmark et al. 1994; Carducci et al. 1996) were the only class of HDAC inhibitors approved for use in the treatment of cancer, with mixed results. They have, however, the limitation that they must be used at very high concentrations to inhibit HDAC activity, particularly *in vivo* since they are degraded rapidly after intravenous administration (Warrell et al. 1998), furthermore they are not specific for HDACs as they also inhibit phosphorylation and methylation of proteins as well as DNA methylation (Newmark and Young 1995).

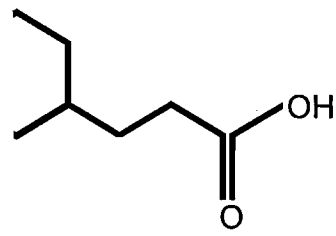

Figure 1.9
The simple structure of VPA: 2-propylpentanoic acid.

VPA is one of the more recent short chain fatty acid, anti-cancer drugs to be studied. In the clinic it has several names, for example; depakene, depakote and divalproex sodium. It has the simple chemical structure: 2-propylpentanoic acid (Figure 1.9). VPA was used, historically, as a treatment for epilepsy and is without major side effects, though during early pregnancy it has been seen to cause serious birth defects such as non-closure of the neural tube (Nau et al. 1991). Interestingly its antiepileptic function and its teratogenic function are mechanistically distinct since modification of the molecule has been shown to generate compounds which may be antiepileptic or teratogenic but not both (Nau et al. 1991; Vorhees et al. 1991). The ability of VPA to inhibit HDACs was discovered almost 20 years ago (Horie and Suga 1985), but only

recently has it been demonstrated to be a potent HDAC inhibitor which relieves HDAC-dependent transcriptional repression and causes hyperacetylation of histones both in cultured cells and *in vivo* (Gottlicher et al. 2001). VPA has been shown to induce differentiation in carcinoma cells (Werling et al. 2001), transformed haematopoietic progenitor cells and leukaemic blasts from acute myeloid leukaemia patients (Gottlicher et al. 2001). Most interestingly, tumour growth and metastasis formation are significantly reduced in animal experiments (Gottlicher et al. 2001).

1.5 Re-expressed genes

1.5.1 Introduction

We show in this study that the following three proteins (with others) are down-regulated in v-Fos^{FBR}-transformed cells and that their expression can be restored by treatment with HDAC inhibitors. We go on to re-express these genes ectopically in FBR cells, and show that their expression inhibits invasion.

1.5.2 STAT 6

Signal transducer and activator of transcription (STAT) 6, is a transcription factor. It is activated at the cell membrane by phosphorylation at Tyr-641 (Mikita et al. 1996; Mikita et al. 1998). This happens when, for example, the activating cytokine, IL (interleukin) -4 or IL-13 binds to its cell surface receptor, leading to receptor clustering and transphosphorylation of receptor-associated Janus kinases (Jaks), which then mediate phosphorylation of STAT6 (Shimoda et al. 1996; Takeda et al. 1996). This tyrosine phosphorylation is essential for dimerisation of STAT6 preceding translocation of the dimer to the nucleus. STATs, however, can also undergo serine phosphorylation (Decker and Kovarik 2000) and are therefore potential substrates for MAP kinases. This would provide a mechanism for cross-talk between the JAK-STAT and MAP kinase signal transduction pathways.

Generally, the deregulation of STAT signalling pathways is considered to contribute to cellular transformation *in vivo* particularly leukaemogenesis (Benekli et al. 2003), but this is associated with *increased* STAT activity particularly STAT3 and STAT5. *In vitro*, STAT3 is constitutively active in Src-transformed NIH3T3 cells. It is thought that STATs exert their transforming activity through the induction of an anti-apoptotic

pathway (Barton et al. 2004), however, there is also evidence of the opposite effect. STAT1-deficient mice develop spontaneous tumours and STAT1-deficient cells are more resistant to agents which induce apoptosis (Stephanou and Latchman 2003). In addition STAT1-deficient cells have increased MDM2 (a p53 inhibitor) and decreased p53 expression (Townsend et al. 2004).

Interestingly, in addition to a role in activating transcription of tissue inhibitor of matrix metalloproteinase (TIMP) genes (Gatsios et al. 1996; Bugno et al. 1995), STAT6 has recently been shown to have a role in activating extracellular matrix genes. It has been demonstrated by two groups that IL-4 can up-regulate type I collagen and that this up-regulation is mediated through STAT6 (McGaha et al. 2003; Buttner et al. 2004).

1.5.3 RYBP

Ring1 and YY1 binding protein (RYBP), a zinc finger protein, was first identified, by virtue of its binding, in a yeast two-hybrid screen (Garcia et al. 1999), to Ring1A, a member of the mammalian polycomb complex. The same study also showed that RYBP binds Ring1B and M33, the mammalian homologue of the Drosophila Polycomb (PC) protein, and also to the transcription factor YY1. It was found initially to have homology to YY1 associated factor 1 (YAF1) and later acquired the alternative name of YY1 and E4TF1/hGABP associated factor 1 (YEAF1), which reflects this homology (Sawa et al. 2002) and its binding to both adenovirus early 4 transcription factor 1 / human GA binding protein (E4TF1/hGABP) and YY1. RYBP was also later recognised by yeast two-hybrid screen as interacting with the E2 promoter binding factor 2 (E2F2) and E2F3 proteins (Schlisio et al. 2002) and with E2F6 (Trimarchi et al. 2001).

From all of these studies, comes the idea that RYBP functions as a molecular bridge. Interactions between transcription factors to which it binds, occur only in the presence of RYBP. Thus, it is thought to mediate interactions between transcription factors

which bind to a promoter at neighbouring response elements; such that the transcription factors act synergistically, in activating (or repressing) transcription. This is also thought to provide a basis for specificity within the E2F protein family (Schlisio et al. 2002), where E2F binding in combination with YY1, and their interaction, is required to control promoter activity correctly.

RYBP was initially considered to be a transcriptional co-repressor, by virtue of its associations with polycomb group proteins, which maintain the repressed state of genes, particularly during development, and also by its binding to the repressor domain of E2F6, which is also a component of the Bmi-containing polycomb complex (Trimarchi et al. 2001). It now seems though, that RYBP can act as either repressor or activator (Schlisio et al. 2002) depending on the combination of transcription factors to which it binds.

1.5.4 PCDHGC3

Protocadherin γ subfraction C3 (PCDHGC3) first appears in the literature as pc43, which was originally identified along with pc42 as founding members of the protocadherin subfamily of the cadherin super family (Sano et al. 1993; Suzuki 2000) characterised by their extracellular cadherin repeat motif. More than 70 protocadherins have now been identified in mammals, and they are also present in a wide range of species, including invertebrates. Cadherins, however, are not found in lower order species and for this reason protocadherins are thought to have preceded cadherins in evolution. They are integral membrane proteins. Their extracellular domains consist of five or more cadherin repeats and their cytoplasmic domains have no homology to cadherins, nor any other databased protein sequences. Little homology exists between these domains in protocadherins themselves, though some sequence homology has been demonstrated between the cytoplasmic domain of PCDHGC3 and

two other protocadherin-like molecules (Obata et al. 1998). PCDHGC3 (which has also been called PCDH2) has six extracellular cadherin repeats and participates in calcium-dependent homophilic cell-cell adhesions, as do all cadherins. It is known to be highly expressed in the central nervous system, where levels are developmentally regulated, and it is thought to be involved in the formation of neuronal circuits (Sano et al. 1993; Suzuki 2000; Kallenbach et al. 2003). Its expression is also high in adult brain, however, where it is thought to be involved in the formation of synaptic contacts and in transmission of signals across the synapse (Sano et al. 1993; Suzuki 2000). Its expression has also been demonstrated in fibroblasts and keratinocytes (Matsuyoshi and Imamura 1997) and we show here that the mRNA is relatively abundant in 208F cells. The homophilic interaction of protocadherin molecules is weak in comparison to that between classical cadherins (Obata et al. 1995). This is thought to be a function of the intracellular domain. Classical cadherins are known to be linked intracellularly to the actin cytoskeleton through binding to β, γ, (directly) and α (indirectly) catenins (Ozawa et al. 1989; Ozawa et al. 1990; Ozawa and Kemler 1992), however, PCDHGC3 does not bind catenins (Obata et al. 1995). When the interacellular domain of PCDHGC3 is replaced with that of E-cadherin, PCDHGC3 becomes capable of strong homophilic interaction, and co-immunoprecipitates with α and β catenins (Obata et al. 1995).

The developmental role PCDHGC3 in the central nervous and the capability of protocadherins for only weak interaction has led to the suggestion that they may be more concerned with cell-cell recognition rather that cell-cell adhesion (Dunne et al. 1995). It is also thought possible that these proteins may be capable of heterophilic interaction since localisation studies have shown that, at cell-cell contacts, PCDHGC3 can be present only in one cell membrane (Obata et al. 1995).

1.6 Summary of experiments

Initially here, we demonstrate HDACs to be up-regulated in FBR cells. The following three chapters examine the role of HDACs in the Fos-transformed phenotype. Firstly, we use pharmacological inhibition of HDACs in FBR cells to determine the contribution of these enzymes to specific phenotypic aspects. Secondly, we identify genes which are down-regulated as a consequence of v-Fos expression but which are re-expressed on inhibition of HDACs; the implication being, that HDAC activity mediates their down-regulation. We re-express three of these proteins, from cDNAs, and examine the consequence to the transformed phenotype. Thirdly, we employ several stategies to modulate the activity of, specifically, HDAC4, in our cell system. Theoretically we anticipated that increasing HDAC4 activity in 208F cells may confer some aspect of transformation on them, and that decreasing HDAC activity in FBR cells may revert some aspect of their transformed phenotype. With the intention of increasing HDAC4 activity, we ectopically express wild type HDAC4 or a mutant of HDAC4 which cannot be exported from the nucleus. With the intention of decreasing HDAC4 activity we ectopically express a deacetylase-inactive HDAC4 mutant, or those proteins involved in the nuclear export of HDAC4: 14-3-3β and/or constitutively active CamKIV.

Chapter 2

Materials and Methods

2.1 Materials

Materials are listed by "technique" in, essentially, chronological order. The same order is used in the "Methods" and "Results" sections.

2.1.1 Cells

2.1.1.1 Cell lines

208F cells are a subclone of the Rat-1 fibroblast cell line and were obtained from Dr. Kristine Quade, Cancer Research UK., London Research Institute, London, UK.

FBR cells are 208F cells infected with FBR-MuSV (Sections 1.2.2 and 1.2.5). 208F cells are non-producer cells and FBR-MuSV is replication defective. FBR cells were obtained from Prof. Tom Curran, St. Jude Children's Research Hospital, Memphis, Tennessee, USA.

Cos-7 cells were supplied by Dr. Joseph Winnie, BICR.

2.1.1.2 Tissue culture

Sterile glass pipettes and plastic Gilson tips and sterile solutions: PE, PBS, MilliQ H_2O were prepared by central services personnel, BICR.

•Cell culture plastic dishes (all sizes)	Becton-Dickinson Labware, Cowley, Oxfordshire, UK.
•Cell scraper (plastic)	Corning UK Ltd., High Wycombe, Buckinghamshire, UK.
•DMEM	Invitrogen, Paisley, UK.
•DMSO	Fisher Scientific (UK) Ltd., Loughborough, Leicestershire, UK.

•FCS	Sigma, Gillingham, Dorset, UK.
•Freezing "Nunc" vials	Nalge Nunc International, Roskilde, Denmark.
•G418 (Geneticin)	Invitrogen, Paisley, UK.
•HEPES	Invitrogen, Paisley, UK.
•L-glutamine	Invitrogen, Paisley, UK.
•Liquid Nitrogen	Cryoservice Ltd., Worcester, UK.
•Sodium bicarbonate	Sigma, Gillingham, Dorset, UK.
•Sodium pyruvate	Sigma, Gillingham, Dorset, UK.
•Sodium valproate	Sigma, Gillingham, Dorset, UK.
•Trichostatin A	Sigma, Gillingham, Dorset, UK.
•Trypsin (2.5%)	Sigma, Gillingham, Dorset, UK.

2.1.2 Northern analysis

•EcoscintA	National Diagnostics, Atlanta, Georgia, USA.
•Expresshyb	Clontech Laboratories, Basingstoke, Hampshire, UK.
•Formaldehyde	Fisher Scientific, Loughborough, Leicestershire, UK.
•Formamide	Fluka Chemika-Biochemika AG, Buchs, Switzerland.
•Hybond N+ nylon membrane	Amersham Pharmacia, Little Chalfont, Buckinghamshire, UK.
•MOPS	Roche Diagnostics, Lewes, East Sussex, UK.
•Oligolabelling Kit	Amersham Pharmacia Biotech UK Ltd.,

	Little Chalfont, Buckinghamshire, UK.
•RNAzol B	Tel-Test Inc., Friendswood, Texas, USA.
•Sephacryl S-400 HR Microspin columns	Amersham Pharmacia Biotech UK Ltd., Little Chalfont, Buckinghamshire, UK.
•Sodium acetate	Fisons Scientific (UK) Ltd., Loughborough, Leicestershire, UK.
•Sodium citrate	Fisher Scientific (UK) Ltd., Loughborough, Leicestershire, UK.
•Super RX medical X-ray film	Fuji Photofilm Co. Ltd.,Tokyo, Japan.
•7S ribosomal RNA, cDNA probe	Dr. Fiona McGregor, BICR.
•[α^{32}P]-dCTP 3000 Cimmol^{-1}	Amersham Pharmacia Biotech UK Ltd., Little Chalfont, Buckinghamshire, UK.

2.1.3 Western analysis

2.1.3.1 Protein extraction

•Aprotinin	Sigma, Gillingham, Dorset, UK.
•Leupeptin	Sigma, Gillingham, Dorset, UK.
•Nonidet P-40 (NP-40)	Sigma, Gillingham, Dorset, UK.
•PMSF	Sigma, Gillingham, Dorset, UK.
•Sodium fluoride	Sigma, Gillingham, Dorset, UK.
•96 well assay plate	Corning UK Ltd., High Wycombe, Buckinghamshire, UK.

2.1.3.2 SDS-PAGE

•Benchmark prestained protein ladder (PAGE molecular weight markers)	Invitrogen, Paisley, UK.
•Precast 10% Tris-glycine gels, 10 well, 1.0 mm	Invitrogen, Paisley, UK.

2.1.3.3 Blotting and detection

•ECl Western Blotting Detection Kit	Amersham Pharmacia, Little Chalfont, Buckinghamshire, UK.
•Immobilon-P	Millipore (UK) Ltd., Watford, Hertfordshire, UK.
•Marvel dried milk powder	Premier Brands UK Ltd., Spalding, Lincolnshire, UK.
•Saranwrap	Dow Chemical Company, USA.
•Super RX medical X-ray film	Fuji Photofilm Co. Ltd., Tokyo, Japan.
•3MM filter paper	Whatmann International Ltd., Maidstone, Kent, UK.

2.1.3.4 Antibodies

•anti-(human)HDAC4 rabbit polyclonal antibody was a gift from Dr. Eric Miska, Wellcome/ Cancer Research UK Institute, University of Cambridge, Cambridge, UK. This antibody could be used in western analysis to visualise wtHDAC4, HDAC4-H803A, HDAC4-D840N and TMHDAC4, though was not suitable for use in immunocytochemistry.

•anti-14-3-3 β and ζ, rabbit polyclonal antibody, 06-351	Upstate Biotechnology, Lake Placid, New York, USA.
•anti-(human)CamKIV, mouse monoclonal antibody, C28420	Transduction Laboratories, Lexington, Kentucky, USA.
•anti-flag M2 mouse monoclonal antibody	Sigma, Gillingham, Dorset, UK.
•Living colours A.v. (JL-8), anti- EGFP mouse monoclonal antibody	Clontech Laboratories, Basingstoke, Hampshire, UK.
•HRP- conjugated anti-mouse IgG, $F(ab')_2$ fragment (from sheep)	Amersham Pharmacia Biotech UK Ltd., Little Chalfont,Buckinghamshire, UK.
•HRP-conjugated anti-rabbit IgG, whole molecule (from donkey)	Amersham Pharmacia Biotech UK Ltd., Little Chalfont, Buckinghamshire, UK.

2.1.4 Invasion assays

•Calcein, AM	Molecular Probes, Leiden, The Netherlands.
•Complete Matrigel™	Becton-Dickinson Labware, Cowley, Oxfordshire, UK.
•Epidermal growth factor	Sigma, Gillingham, Dorset, UK.
•Propidium Iodide	Sigma, Gillingham, Dorset, UK.
•Reduced growth factor matrigel	Becton-Dickinson Labware, Cowley, Oxfordshire, UK.
•6.5mm Transwell™, 8.0μm pore size	Corning UK Ltd., High Wycombe, Buckinghamshire, UK.

2.1.5 Genetic manipulation

2.1.5.1 cDNAs

RYBP full-length cDNA (Garcia et al. 1999) was a kind gift from Dr. Miguel Vidal, Centro De Investigaciones Biologicas, Madrid, Spain.

STAT6 full-length cDNA (Quelle et al. 1995) was a kind gift from Prof. James Ihle, St. Jude Children's Research Hospital. Memphis, USA.

Protocadherin 43 (PCDHGC3) (Sano et al. 1993) full-length cDNA was a kind gift from Dr. Shintaro T. Suzuki, Kwanseigakuin University, Hyogo, Japan.

The human HDAC4 wild type gene, Genbank accession number AF132607 was provided by Dr. Eric Miska, Wellcome/Cancer Research UK Institute, University of Cambridge, Cambridge, UK. I have referred to this as wtHDAC4.

Mutant human HDAC4, which has three serine residues (S246, S467, and S632) mutated to alanines was a gift from Dr. Xiang-Jiao Yang. I have referred to this as TMHDAC4.

Two mutant human HDAC4 genes: HDAC4-H803A, which has histidine 803 mutated to alanine; and HDAC4-D840N which has aspartic acid 840 mutated to asparagine; were supplied by Dr. Eric Miska, Wellcome/Cancer Research UK Institute, University of Cambridge, Cambridge, UK, in pcDNA3.1.

$CamKIV_{1-313}$, a constitutively active mouse CamKIV gene, Genbank accession number NM_009793 (full length sequence), in an RSV vector was made by Dr. Peiqing Sun, Oregon Health Sciences University, Oregon, USA.

The human 14-3-3β wild type gene, Genbank accession number X57346, was provided in the pcDNA3 vector, by Prof. Walter Kolch, BICR, Glasgow, UK., in collaboration with Dr. John Sedivy, Yale University, Connecticut, USA.

2.1.5.2 Vectors

•pCR-Script	Stratagene Europe, Amsterdam Zuidoost, The Netherlands.
•pEGFP-N1	Clontech Laboratories (UK) Ltd., Basingstoke, Hampshire, UK.
•pLPCX2	Clontech Laboratories (UK) Ltd., Basingstoke, Hampshire, UK.

2.1.5.3 PCR

•BIOTAQ™ DNA polymerase	Bioline UK Ltd., London, UK.
•dNTPs	Promega Corporation, Madison, Wisconsin, USA.
•Glycerol	Fisher Scientific (UK) Ltd., Loughborough, Leicestershire, UK.
•Magnesium chloride (supplied with BIOTAQ)	Bioline UK Ltd., London, UK
•NH_4 reaction buffer (supplied with BIOTAQ)	Bioline UK Ltd., London, UK.
•pfu reaction buffer (supplied with pfu)	Stratagene Europe, Amsterdam Zuidoost, The Netherlands.
•PTC-100 Programmable Thermal Controller	M.J. Research Inc., Watertown, Massachusetts, USA.
•Turbo pfu DNA polymerase	Stratagene Europe, Amsterdam, Zuidoost, The Netherlands.

2.1.5.4 Kits

•PCR-Script Cloning Kit	Stratagene Europe, Amsterdam Zuidoost, The Netherlands.
•Qiafilter Plasmid Maxi Kit	Qiagen Ltd., Crawley, West Sussex, UK.
•Qiagen Mini Plasmid Kit	Qiagen Ltd., Crawley, West Sussex, UK.
•QIAquick Gel Extraction Kit	Qiagen Ltd., Crawley, West Sussex, UK.
•Rapid DNA Ligation Kit	Roche Diagnostics, Lewes, East Sussex, UK.

2.1.5.5 Agarose gel electrophoresis

•Bioline Hyperladder I	Bioline UK Ltd., London, UK.
•Boric acid	Fisher Scientific (UK) Ltd., Loughborough, Leicestershire, UK.
•Ficoll	Sigma, Gillingham, Dorset, UK.

2.1.5.6 Manipulations in bacteria

•Ampicillin	Sigma, Gillingham, Dorset, UK.
•Kanamycin	Sigma, Gillingham, Dorset, UK.
•Chloramphenicol	Sigma, Gillingham, Dorset, UK.
•X-gal	Melford Laboratories Ltd., Ipswich, Suffolk, UK.
•IPTG	Melford Laboratories Ltd., Ipswich, Suffolk, UK.
•BactoAgar	Becton-Dickinson, Cowley, Oxfordshire, UK. Anachem, Luton, Bedfordshire, UK.
•DH5α competent cells	Invitrogen, Paisley, UK.

2.1.5.7 Restriction digestion

•Restriction enzymes (except SacII)	Invitrogen, Paisley, UK.
•React buffers (supplied with restriction enzymes)	Invitrogen, Paisley, UK.
•SacII	Promega Corporation, Madison, Wisconsin, USA.
•Reaction buffer C (supplied with SacII)	Promega Corporation, Madison, Wisconsin, USA.
•Acetylated BSA (supplied with SacII)	Promega Corporation, Madison, Wisconsin, USA.
•Alkaline phosphatase (calf intestinal)	Transgenomic, Crewe, Cheshire, UK.

2.1.5.8 DNA Sequencing

•Dextran blue	Sigma, Gillingham, Dorset, UK.
•"DyeDeoxy" reaction mix	Perkin Elmer, Roche Molecular Systems Inc., Branchburg, New Jersey, USA.

2.1.6 Transfection / nucleofection

•FuGene6	Roche Diagnostics, Lewes, East Sussex, UK.
•Nucleofection cuvettes	Amaxa, Nattermannallee, Germany.
•Nucleofection solution R, plus supplement	Amaxa, Nattermannallee, Germany.
•Nucleofector	Amaxa, Nattermannallee, Germany.
•RPMI medium	Invitrogen, Paisley, UK.

2.1.7 Immunohistochemistry / actin staining

Confocal microscope images were taken using a BioRad MRC 600 confocal illumination unit attached to a Nikon Diaphot inverted microscope at stated magnifications.

2.1.7.1 Antibodies and stains

•FITC-conjugated phalloidin	Sigma, Gillingham, Dorset, UK.
•TRITC-conjugated phalloidin	Sigma, Gillingham, Dorset, UK.
•anti-myc 9E10 mouse monoclonal antibody	Invitrogen, Paisley, UK.
•anti-flag M2 mouse monoclonal antibody.	Sigma, Gillingham, Dorset, UK.
•Vectashield containing DAPI stain	Vector Laboratories Ltd., Peterborough, Cambridgeshire, UK.
•FITC-conjugated anti-mouse antibody ($F(ab')_2$ fragment, from sheep)	Sigma, Gilligham, Dorset, UK.
•TRITC-conjugated anti-mouse antibody (Fab specific, from goat)	Sigma, Gilligham, Dorset, UK.

2.1.7.2 Preparation of coverslips

•Paraformaldehyde	Sigma, Gilligham, Dorset, UK.
•Bovine albumin fraction V	Sigma, Gilligham, Dorset, UK.
•Coverslips (glass)	BDH Chemicals Ltd., Poole, Dorset, UK.
•Vectashield	Vector Laboratories Ltd., Peterborough, Cambridgeshire, UK.

2.1.8 General

2.1.8.1 Water

MilliRO H_20, which is purified by reverse osmosis, was obtained from a MilliRO 10, Water Purification System from Millipore UK Ltd., Watford, Hertfordshire, UK.

MilliQ H_20, which is MilliRO H_20 further purified by fine filtration, was obtained from a Millipore MilliQplus Ultrapure Water System from Millipore UK Ltd., Watford, Hertfordshire, UK.

2.1.8.2 Chemicals and Reagents

Solutions and buffers were prepared using MilliRO H_2O.

•Agarose	Invitrogen, Paisley, UK.
•Bicinchoninic acid solution	Sigma, Gillingham, Dorset, UK.
•β-mercaptoethanol	Sigma, Gillingham, Dorset, UK.
•Bromophenol blue	Sigma, Gillingham, Dorset, UK.
•Copper II sulphate	Sigma, Gillingham, Dorset, UK.
•Dithiothreitol (DTT)	Millipore UK Ltd.,Watford, Hertfordshire, UK.
•EDTA	Fisher Scientific UK., Loughborough, Leicestershire, UK.
•Ethanol	James Burrough Ltd., Witham, Essex, UK.
•Ethidium bromide	Sigma, Gillingham, Dorset, UK.
•Glycine	BDH Chemicals Ltd., Poole, Dorset, UK.
•Methanol	Fisher Scientific, Loughborough, Leicestershire, UK.
•Nonidet-P40	BDH Laboratory Supplies, Poole, Dorset, UK.

•Parafilm 'M'	American National Can, Chicago, Ilanois, USA.
•Paraformaldehyde	Sigma, Gillingham, Dorset, UK.
•PBS tablets	Oxoid Ltd., Basingstoke, Hampshire, UK
•Propan-2-ol (isopropanol)	Fisher Scientific (UK) Ltd.,Loughborough, Leicestershire, UK.
•Sodium Chloride	Fisher Scientific (UK) Ltd., Loughborough, Leicestershire, UK.
•Sodium dodecyl sulphate	Fisher Scientific (UK) Ltd., Loughborough, Leicestershire, UK.
•Sodium hydroxide	Fisher Scientific (UK) Ltd.,Loughborough, Leicestershire, UK.
•Sodium orthovanadate	BDH Chemicals Ltd., Poole, Dorset, UK.
•Sucrose	Fisher Scientific (UK) Ltd., Loughborough, Leicestershire, UK.
•Tris	Melford Laboratories Ltd.,Ipswich, Suffolk.
•Triton X-100	Sigma, Gillingham, Dorset, UK.
•Tween 20	Sigma, Gillingham, Dorset, UK.

2.1.8.3 Plasticware

•Bijou bottles (sterile)	Bibby Sterilin, Stone, Staffordshire, UK.
•Falcon tubes 15ml and 50ml	Becton-Dickinson Labware, Cowley, Oxfordshire, UK.

•Filter pipette tips	Greiner Labortechnik Ltd., Gloucestershire, UK.
•Glass microscope slides	BDH Laboratory Supplies, Poole, Dorset, UK.
•Microfuge tubes 1.5ml	Eppendorf-Netheler-Hinz GmbH., Cambridge, Cambridgeshire, UK.
•Pipette tips	Elkay Laboratory Products UK Ltd., Basingstoke, Hampshire, UK.
•Universal bottles (sterile)	Bibby Sterilin, Stone, Staffordshire, UK.

2.2 Methods

Methods are listed in the order in which they appear in the results sections, i.e., essentially, in chronological order.

2.2.1 Tissue culture

2.2.1.1 Maintenance of cell lines

Cells were maintained in DMEM supplemented with 0.3% sodium bicarbonate, 1 mM sodium pyruvate, 2 mM glutamine, 10 mM HEPES and, 10% FCS. G418 (Geneticin), to a final concentration of 700 $\mu g ml^{-1}$, was also added to DMEM used to maintain those cell lines carrying stably transfected genes. Cells were passaged every 3 to 4 days with a 1:10 split ratio. For all cell lines, other than FBR, the DMEM was removed and the cells rinsed once in 0.25% trypsin. After a short incubation in the residual trypsin (approximately 2 mins depending on the cell line) 10ml of DMEM with 10% FCS (and other supplements discussed above) was sprayed onto the plate from a 10 ml glass pipette and the cells resuspended. 1 ml of this suspension was added to each new 10 cm plate and the volume of DMEM made up to 10 ml. Cells were then incubated at 37°C in a humidified atmosphere also containing 5% CO_2. Passage of FBR cells differed only in that cells were not incubated in trypsin prior to being sprayed from the plate.

2.2.1.2 Storage of cells

Long-term storage of cells was in liquid nitrogen. Cells were trypsinised or sprayed from a subconfluent 10 cm plate (as described above) and centrifuged at 1000 rpm in a Beckman GP bench top centrifuge for 5 mins. The resulting pellet was then resuspended in 1 ml DMEM plus supplements (as described above) but, in this

instance, containing 50% FCS and 10% DMSO. This 1 ml was then transferred to a "nunc" vial, which was then wrapped in cotton wool transferred to a small plastic box and placed at -70°C for at least 4 hours to allow the cells to freeze slowly. After this time vials were transferred to liquid nitrogen.

Vials were defrosted quickly by transfer from liquid nitrogen immediately into water at 37°C. Their contents were then transferred to a plastic universal containing 20 ml of DMEM and centrifuged as described above. The resultant pellet was resuspended in 10 ml DMEM (plus supplements) and transferred to a 10 cm dish.

2.2.2 Northern analysis

2.2.2.1 Isolation of total cellular RNA

The method of total cellular RNA isolation was that supplied with RNAzol B. Cells were grown to sub-confluence in 10cm tissue culture dishes. Growth medium was aspirated and 1 ml of RNAzol B added to each dish. The cell lysate was scraped into the RNAzol using a cell scraper and pipetted 3 times into a 1 ml Gilson tip, before being transferred into a 1 ml Eppendorf. For convenience the lysates were then stored at -70°C until required. On defrosting 100 μl of chloroform was added to each lysate which was then shaken vigorously and left on ice for 5 mins to allow the phase separation to establish. Samples were then centrifuged at 12,000 x g for 10 mins in a refrigerated centrifuge at 4°C. The upper, aqueous phase was then removed into a new Eppendorf and an equal volume (approximately 500 μl) of propan-2-ol added. The tubes were shaken vigorously and left on ice for 15 mins, followed by centrifugation at 12,000 x g for 15 mins at 4°C. The liquid was then removed leaving an RNA pellet which was washed once in 75% ethanol. The pellet was then dried for 15 mins by centrifugation under vacuum and resuspended in 50 μl DEPC treated

water. 5 μl of the RNA preparation was then diluted 1:100 in dH_20 and quantified by UV-spectrophotometry at 260 nm.

2.2.2.2 Denaturing gel electrophoresis and electroblotting of RNA

Total cellular RNA samples were separated on both small (50 ml) and large (300 ml) agarose gels. 10 μg and 30 μg of total cellular RNA was loaded respectively, both having been aliquoted then dried down by centrifugation under vacuum for approximately 1 hour and resuspended in 12 μl RNA sample loading buffer (50% formamide; 33.3% formaldehyde, from a 37% solution; 0.5X MOPS buffer (see below); 5 μgml^{-1} ethidium bromide; and, 13.3% RNA loading dye, which comprises, 50% glycerol, 1 mM EDTA, 0.4% bromophenol blue. Prior to loading, samples were heated in a heating block to 68°C for 5 mins then placed immediately on ice. To make a small agarose gel, 0.5 g of agarose was dissolved in 31.1 ml sterile dH_20 by microwaving. 10 ml of 5X MOPS buffer (0.1 M MOPS; 50 mM sodium acetate; 5 mM EDTA; pH to 7.0 with NaOH pellets) was then added and the solution allowed to cool to approximately 60°C before the addition of 8.9 ml of formaldehyde (from a 37% stock solution), immediately prior to pouring. After loading, samples were run at 100 V for approximately 3.5 hours, under 1X MOPS running buffer. The RNA was then visualised by UV transillumination and the gel photographed. The RNA was then transferred to Hybond N+ nylon membrane overnight by upward capillary blotting by the method of Maniatis (Sambrook et al. 1989), using 1X SSC (150 mM NaCl, 15 mM sodium citrate, pH 7.0) as transfer buffer. The blot was then allowed to dry before UV-crosslinking of the nucleic acid to the membrane using a UV Stratalinker™ 1800 (Stratagene).

2.2.2.3 Random priming and hybridisation

DNA probes were radiolabelled by random priming using an oligolabelling kit. Approximately 50 ng of DNA in a total volume of 34 µl was denatured by heating to 100°C in a heating block and transferred immediately to ice. 10 µl of reagent mix (a buffered solution containing dATP, dGTP, dTTP and random hexadeoxyribo-nucleotides) was added, then 1.85 MBq (5 µl) of [α-^{32}P] dCTP and 1 µl Klenow fragment. This solution was incubated at 37°C for 1 hour. Unincorporated nucleotides were then removed by passing the reaction mix through a Sephacryl S-400 HR microspin column (previously centrifuged at 3 K for 2 mins) by centrifugation at 3,000 rpm in an Eppendorf 5415c microfuge for 2 mins. The eluted probe was then heated to 100°C in a heating block for 5 mins and immediately transferred to ice for 2 mins. 1 µl was removed into a scintillation vial containing 10 ml of scintillation fluid (Ecoscint A). The counts per minute (cpm) were then determined by counting in a Beckman LS5000CE scintillation counter and those samples with values greater than 10^5 considered acceptable for hybridisation. The labelled probe was then transferred to a plastic universal containing the Hybond N+ nylon membrane which had immediately previously been incubated at 68°C for 30-60 mins with 5 ml of Expresshyb. Care was taken to add the probe directly into the Expresshyb at 68°C and to disperse it immediately. The membrane and probe were then incubated at 68°C for at least 1 hour, rotating slowly. The membrane was then removed into wash buffer 1 (1X SSC, 0.1% SDS) which had been preheated to 50°C. After a few seconds the membrane was transferred to fresh wash buffer 1 at 50°C and the container allowed to shake gently in a 50°C water bath for 30 mins. A Geiger-Muller tube was then used to monitor the cpm present on the membrane. If these were low then the membrane was removed for autoradiography. If they were still high the membrane was transferred to wash buffer 2 (0.1X SSC, 0.1% SDS) and incubated at 50°C with gentle agitation for

30mins. If counts were still high this wash was repeated with fresh wash buffer and finally the temperature of the wash could be raised to 68°C if necessary. The membrane was then wrapped in Saranwrap, placed in a medical X-ray cassette with two intensifying screens, and overlayed with Fuji Super RX medical X-ray film. Exposure, at -70°C, was initially overnight. The autoradiograph was developed using a Kodak X-Omat 480 RA, X-ray processor. To control for loading, membranes were later stripped of hybridised probe and reprobed for 7S RNA following the protocol described above. To strip the membrane a 0.1% SDS solution was heated to boiling in a microwave oven. The membrane was immediately immersed and rocked gently in the solution which was allowed to cool to room temperature before the membrane was removed and rinsed in 2X SSC.

2.2.3 Western analysis

2.2.3.1 Protein extraction

Cells were grown to approximately 70% confluence in 10 cm dishes. They were washed 3 times in ice cold PBS then drained well before the addition of 300 μl of EBC (50 mM Tris-HCl pH 8.0, 120 mM NaCl, 0.5% Nonidet P-40, 1 mM EDTA) supplemented with the protease inhibitors, aprotinin (10 μgml^{-1}), leupeptin (10 μgml^{-1}), and PMSF (1 mM), and the phosphatase inhibitors $Na_3(V0)_4$ (50 μM), and NaF (50 mM). Cells were scraped into the buffer and transferred to a 1.5 ml microfuge tube. They were kept on ice for 30 mins then centrifuged at 12,000 x g for 5 mins at 4°C. The supernate was then decanted into a fresh microfuge tube and the protein concentration determined.

2.2.3.2 Nuclear protein extraction

Cells were grown to approximately 70% confluence in 10 cm dishes. They were washed 3 times in ice cold PBS then drained well before being scraped into 1.5 ml ice cold PBS and centrifuged at 1,500 x g for 2 mins. The cell pellet was resuspended in 400μl ice cold nuclear extract buffer A (10 mM HEPES, 10 mM KCl, 0.1 mM EDTA) supplemented with 1 mM DTT and 0.5 mM PMSF immediately before use. Samples were then incubated on ice for 15 mins, following which, 25 μl of 10% NP-40 was added and the samples vortexed for 30 secs. They were then centrifuged at 12,000 x g for 30 secs. The nuclear pellet is resuspended in 50 μl ice cold nuclear extract buffer C (20 mM HEPES pH 7.9, 0.4 M NaCl, 1 mM EDTA, 25% glycerol) supplemented with 1 mM DTT and 0.5 mM PMSF immediately before use, and the samples are rocked vigorously for 15 mins at 4°C. Samples are then centrifuged at 12,000 x g for 5 mins at 4°C and the resulting supernate of nuclear proteins transferred to a fresh Eppendorf tube.

2.2.3.3 Determination of protein concentration

The protein concentration of the whole cell and nuclear extracts was determined by a bicinchoninic acid colourimetric assay based on the method by Lowry (Lowry et al. 1951). The extracts were incubated at 37°C for 30 mins in a 50:1 solution of bicinchoninic acid: copper II sulphate solution, in 96 well assay plate and the resulting optical density at 580 nm was measured using a Dynatech MR7000 spectrophotometer. The standard curve was drawn from six BSA standards at 80, 100, 200, 400, 1000 and 2000 $\mu g ml^{-1}$ in the same buffer as the protein samples being measured.

2.2.3.4 Polyacrylamide gel electrophoresis of proteins

Proteins were resolved by polyacrylamide gel electrophoresis through a precast 10% polyacrylamide gel measuring 8 cm x 6.5 cm x 0.1 cm, electrophoresed in SDS-PAGE running buffer (50 mM Tris-HCl; 1% glycine; 0.1% SDS) for 1 hour 45 mins at 125 volts. 25 μg of protein extract in a volume adjusted to 20 μl with dH_20 was combined with 5 μl of 5X sample loading buffer (final concentration: 60 mM Tris-HCl, pH 6.8; 2% SDS; 0.1% bromophenol blue; 25% glycerol; 100 mM β-mercaptoethanol) and loaded per lane.

2.2.3.5 Blotting and hybridisation to antibody

After separation by polyacrylamide gel electrophoresis, proteins were then transferred to Immobilon-P (Millipore) by semi-dry blotting in buffer containing: 60 mM Tris-HCl, 50 mM glycine, 1.6 mM SDS, 20% (v/v) methanol. Blots were incubated in blocking solution (PBS containing 5% Marvel and 0.1% Tween-20). Then in blocking solution containing the appropriate antibody at dilution as directed by the manufacturer for each individual antibody. Blots were washed three times in blocking solution then incubated in blocking solution containing anti-rabbit or anti-mouse immunoglobulin horseradish peroxidase-linked whole antibody, diluted as directed by the manufacturer. All incubations were for 1 hour at room temperature with gentle agitation. Blots were washed three times in PBS containing 0.1% Tween-20 and proteins visualised using ECL western blotting chemilluminescent detection reagent followed by autoradiography, where the membrane was then wrapped in Saranwrap, placed in a medical X-ray cassette, and overlayed with Fuji Super RX medical X-ray film. Exposure was initially for 30 secs to determine optimal exposure times. The autoradiograph was developed using a Kodak X-Omat 480 RA, X-ray processor.

2.2.4 Growth curves

Cells were seeded in multiple wells of 3.6 cm diameter tissue culture (6 well) plates at 2×10^4 or 4×10^4 per well, medium was changed every 2 days and cells from 3 wells per sample counted on indicated days using a Sharfe Casy1 TT cell counter.

2.2.5 F-actin staining

Cells were seeded at 5×10^3 per well on sterile glass coverslips (19 mm) in 2.1 cm diameter tissue culture wells. At stated times and concentrations, VPA or TSA was added to the growth medium (and replaced every 48 hrs), so that cells were fixed at equivalent confluence on day 5, irrespective of length of treatment. To fix cells to coverslips, the medium (plus VPA or TSA if present) was removed and replaced with 400 µl of fix solution (4% paraformaldehyde; 2% sucrose in PBS) for 15 mins. The paraformaldehyde was removed and the cells washed three times in PBS. They were then permeabilised with 400 µl of PBS containing 20 mM glycine and 0.05% Triton X-100, for 5 mins and again washed 3 times in PBS. Coverslips were then transferred to a light-tight container which was lined with parafilm to ease handling of coverslips with forceps. FITC-conjugated-phalloidin was diluted to 100 $ngml^{-1}$ in blocking buffer (0.5% BSA, 10% FCS in PBS), and 100 µl was added to each coverslip. After 15 mins incubation in the dark (lid on), the coverslips were dipped sequentially in three beakers of dH_2O, blotted onto a paper towel and placed face-down slowly onto a drop of Vectashield on a glass microscope slide. Excess Vectashield was aspirated and the edge of the coverslip was then sealed with clear nail varnish. Confocal microscope (Section 2.1.7) images were taken using a 63X or 40X objective for display purposes, and a 20X objective for quantitation purposes, to obtain a larger sample size per field. For quantitation, an average of 28 cells were counted per field and 12 fields were counted per treatment.

2.2.6 Motility assays

2.2.6.1 Wounding assays

Cells were seeded at 7 x 10^4 in the 3.6 cm diameter wells of a 6 well tissue culture plate, approximately 3.5 days prior to wounding, in the absence or presence of VPA or TSA at the required concentration. For 1 day treatments inhibitor was added 14 hours before wounding. A single wound was made down the centre of each well with the 200 μl tip of a Gilson pipetman. The growth medium, plus VPA or TSA if required, was then replaced. Phase contrast timelapse images were captured at 20 min intervals over a 24 hour period, on a Zeiss Axiovert 200m microscope with a Hamamatsu Orca camera. Images were captured from 6 wells per time point, by this method. During this time the plate was incubated in a Solent CO_2 incubator designed around a Ludl microscope stage. The timelapse stage manipulation and captured images were handled using "AQM" software by Kinetic Imaging. For each assay, we chose the time point immediately before the cells in the wound edge make contact with the other edge. This avoids cell-cell contact effects which may be differential between wounds, given that, although wound sizes are comparable, it is impossible to make them absolutely exact. At the chosen time point we measured the width of the wound in the centre of the field and compared it to the measurement taken at t=0. This determined the rate of movement of cells into the wound.

2.2.6.2 Free motility assays

Early motility assays were carried out on cells grown to low density in 10 cm diameter tissue culture plates, having been seeded at 10^4 cells per plate 4 days prior to wounding. For 4 day TSA treatments, TSA was added four hours after seeding, for 2 day treatments, DMEM (10% FCS) was replaced with DMEM (10% FCS) plus TSA, 2 days prior to imaging, and for 1 day treatments, this was done 1 day prior to imaging.

Images were captured with a Zeiss, Axiovert S 100 microscope using "Openlab" software by Improvision. Measurements of cell nucleus displacement were made by hand on still images from the timelapse sequence, and results expressed in comparative, not absolute values.

In later assays imaging and VPA treatment was carried out as described for wounding assays above (Section 2.2.6.1), except that cells were seeded at 10^3 cells per well and grown to low density, and that images were captured at 10 min intervals over a 10 hour period. Using "Tracker" software, by Kinetic Imaging, a track was drawn following the displacement of an individual cell nucleus over a 5 hour period within the 10 hours of timelapse sequence; this was to avoid periods of cell division. The co-ordinates of each of the 30 points per track were then exported to Microsoft Excel XP software, and tracks depicted in graph form, such that each had same origin, thus Windrose diagrams were constructed, of 30 overlayed tracks.

2.2.7 Inverse Invasion assays

2.2.7.1 Inverse invasion assay

The method used was a modified version of that devised previously in our laboratory (Hennigan et al. 1994). An aliquot of Matrigel was thawed slowly on ice then diluted 1:1 in ice cold PBS (containing 2X concentration TSA or VPA, if required). 100 µl of this was then pipetted carefully into each Transwell (inserted into a well of a 24 well tissue culture plate) and incubated for 2 hours at 37°C to allow it to set. During this time, cell suspensions of 2 x 10^5 cells per ml were prepared in DMEM containing 10% FCS. The Transwells were inverted and 100 µl of the cell suspension (2 x 10^4 cells) was pipetted onto the underside of the filter. If the cells are to be nucleofected prior to the invasion assay refer to section 2.2.10.4. The Transwells were covered carefully with the base of the 24 well tissue culture plate such that it contacts the droplet of cell

suspension. The plate was incubated, inverted, for 2 hours to allow the cells to attach. It was then turned right-side-up and each Transwell removed and dipped sequentially into 2 x 1 ml serum free DMEM (containing TSA or VPA, if required) to wash, and finally placed into 1ml of serum free DMEM (containing TSA or VPA, if required). Then 100 μl of DMEM plus 10% FBS (containing TSA or VPA or EGF, if required) was pipetted gently into the Transwell on top of the matrigel/PBS. The lid was replaced and the plate incubated at 37°C for 3 days.

2.2.7.2 Fixation and staining of inverse invasion assays

To fix and/or stain the assays, one of two methods was used.

Propidium iodine staining: 2 ml of methanol was pipetted into the wells of a 24 well plate and placed at -20°C for 1 hour. The Transwells were then placed in these wells for 20 mins after which they were transferred to wells containing 2 ml propidium iodide at 10 $\mu g ml^{-1}$ in PBS. Each Transwell was then washed 3 times by placing sequentially into wells containing 2 ml PBS for 5 mins per well. This method fixes the cells, stains only the nucleus (fluorescent red) and can be kept at 4°C for up to 5 days prior to confocal microscopy (Section 2.2.7.3).

Calcein staining: Transwells were transferred to wells containing 0.5 ml calcein AM (acetoxymethylester of calcein) diluted to 4 μM in serum free DMEM and 0.5 ml of the same calcein solution was pipetted into the Transwell. After 1 hour incubation at 37°C, assays were ready for confocal microscopy (Section 2.2.7.3). This method uses a living dye, stains the whole cell (fluorescent green) and should not be stored for more than 1 hour prior to confocal microscopy.

2.2.7.3 Imaging and quantitation of inverse invasion assays

Stained nuclei or whole cells were visualised by confocal microscope (Section 2.1.7) using a 20X objective. Optical sections (Z-sections) were scanned at 3 μm intervals (Z-steps) moving up from the underside of the filter into the matrigel, producing a series of up to 10 grey-scale images (Figure 2.1). To quantify these Z-sections a computer programme, designed "in house" (by Mr. Peter McHardy and Dr. Robert Hennigan), was used. Essentially, this programme gives each on-screen pixel an intensity value from 0 (black) through to 255 (white). The background pixel value is then operator-defined as the point (pixel value) on the 0-255 scale at which only cells from that individual section are visible with no bleed-through from bordering sections. Only pixels with an intensity value greater than background are then counted by the computer and expressed as a percentage of the total pixels. For quantitation purposes, only cells in the 4th (9 μm) section or above were considered invasive. A compound image of these sections (Figure 2.2) was created using "Confocal Assistant" computer software (by Todd Clarke, Berlje), quantified as described, then normalised to the value obtained from the corresponding 0μm section as a "loading" control. Overall results were determined from at least three separate assays with duplicate samples in each and a total of at least three Z-series were taken for each sample per assay.

2.2.8 Chemotaxis assay

Chemotaxis was measured using the results from the invasion assay. In this case the 0 μm and 3 μm sections were used in quantitation as described for the inverse invasion assay (Section 2.2.7.3), with the exception that a higher background

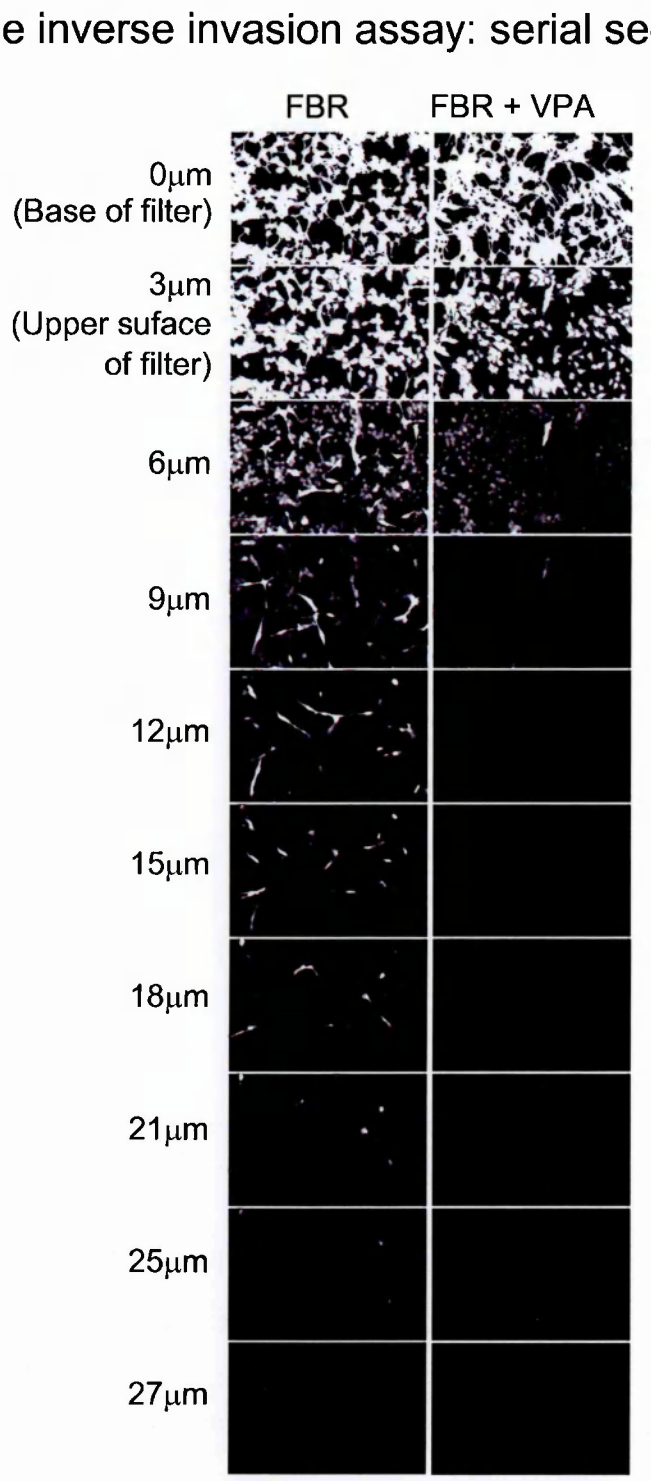

Figure 2.1

Raw data from a 3 day, Calcein-stained, inverse invasion assay, showing 2 series of 10, Z-sections taken (by confocal microscope) through the Matrigel. The 0μm section corresponds to the underside of the filter where the cells were seeded and the 3μm section corresponds to the top of the filter; cells which are motile and respond to chemotaxis can reach this point, they do not require the ability to invade. Cells which have reached the next Z-section at 6μm are invasive. For the purpose of quantitation of invasion, only cells in the 9μm section and above were counted, this reduces the error of including cells which have only reached the top of the filter but can still be seen (due to bleed-through) in the 6μm section. At least three of these Z-series were taken for each sample per assay.

Example inverse invasion assay: quantitation

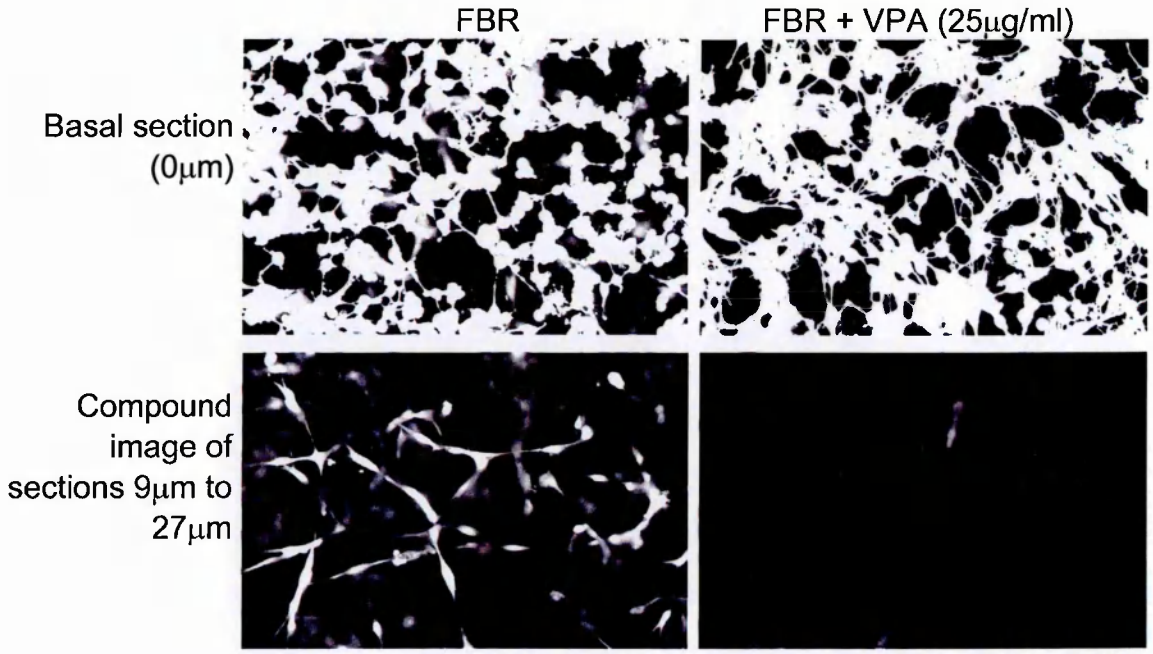

Figure 2.2

These are the images used to quantify the inverse invasion assay shown in Figure 2.1: The basal 0µm section shows those cells which have remained on the filter where they were seeded. The compound image of sections 9µm to 27µm, shows cells which have invaded 9µm or more into the Matrigel.The number of positive pixels per image is expressed as a percentage of the total number of pixels. The values calculated for the basal section are used to normalise the values for the compound image. Overall results were determined from at least three separate assays with duplicate samples in each and a total of at least three Z-series were taken for each sample per assay.

subtraction threshold was set for the 3 μm section to minimise the interference from the bright basal section. The 3 μm section shows cells that have migrated only to the upper surface of the filter but not into the matrigel. They have moved in response to *chemotactic* signals but have not *invaded* into the matrigel.

2.2.9 Genetic manipulation

2.2.9.1 Summary

Using established PCR and molecular cloning methods each cDNA was amplified from its original vector using primers to the 5' and 3' sequences of the cDNA which were flanked by restriction enzyme sites (Figures 2.3 and 2.4). The PCR products were blunt-end ligated into the PCR-Script vector, excised using the appropriate restriction enzyme, then ligated into pEGFP-N1, which provides a C-terminal EGFP tag. Where co-transfection of cDNAs was intended (as with $CamKIV_{1-313}$ and 14-3-3β), the cDNAs were also myc-tagged in the original PCR step. In this case the 3' PCR primer, was synthesised with the myc-tag sequence preceding the restriction enzyme site and the 5' PCR primer was either the same as that used for cloning into pEGFP-N1 or differed only in the restriction site, if the initial enzyme was incompatible with the pLPCX2 vector, into which the cDNAs were ultimately cloned (Figures 2.3 and 2.4).

2.2.9.2 Synthesis of oligonucleotides

Synthetic oligonucleotides, used as PCR or sequencing primers, were synthesised by Robert McFarlane or Christine Lang, Technical Services, BICR, on an Applied Biosystems RNA/DNA synthesiser model 392 or 394, using phosphoramidite chemistry, using the protocol supplied by Applied Biosystems. Lyophilised oligonucleotides were resuspended in 1 ml sterile MilliQ H_2O. For quantification 10 μl

PCR primers: RYBP, PCDHGC3 and STAT6

A. Murine RYBP

5' sequence of RYBP

Primer 1: 5' act cca gaa ttc gat atg ggc gac aag aag agc ccg acc agg cca
Primer 2: 5' taa acc gaa ttc cga aag att cat cat tca ctg ctg aca tgt ccg

3' sequence of RYBP

gcgacatgtcagcagtgaatgatgaatctttcg gaattc ggttta
taaacc gaattc cgaaagattcatcattcactgctgacatgtccg

B. Human PCDHGC3

5' sequence of PCDHGC3

Primer 1: 5' act cca gaa ttc gat atg gtc cca gag gcc tgg agg agc gga ctg
Primer 2: 5' taa acc gaa ttc cgt gtg cat tgc tgc ctg gga tgt aga cat tct

3' sequence of PCDHGC3

agaatgtctacatcccaggcagcaatgcacacg gaattc ggttta
taaacc gaattc cgtgtgcattgctgcctgggatgtagacattct

C. Murine STAT6

5' sequence of STAT6

Primer 1: 5' act cca gaa ttc gat atg tct ctg tgg ggc cta att tcc aag atg
Primer 2: 5' taa acc gaa ttc ccc agc tgg ggt tgg tcc tta ggt cca ggt ggg

3' sequence of STAT6

cccacctggacctaaggaccaaccccagctggg gaattc ggttta
taaacc gaattc ccccagctggggttggtccttaggtccaggtggg

KEY
red = restriction enzyme site
blue = spacer bases
green = Kozak base
grey = frame shift base
black = cDNA sequence

Figure 2.3

PCR primers used for: A. Murine RYBP; B. Human PCDHGC3; C. Murine STAT6. Colours depict the purpose or function or each base: refer to key above. Also shown for each set of primers is the 3' sequence of the cDNA, in relation to the restriction enzyme site etc. Primer 2 is the compliment to this strand drawn 5' to 3'.

PCR primers: HDAC4, HDAC4-H803A, HDAC4-D840N, CamKIV$_{1-313}$ and 14-3-3β

A. HDAC4, HDAC4-H803A, HDAC4-D840N (human) for cloning into pEGFP-N1

primer 1: 5' act cca gaa ttc gat atg agc tcc caa agc cat cca gat gga ctt
primer 2: 5' tca acc gaa ttc cca ggg gcg gct cct ctt cca tgg gct cct cat

B. CamKIV$_{1-313}$ (murine)

(i) for cloning into pEGFP-N1

primer 1: 5' act cca ccg ccg agc atg ctc aaa gtc acg gtg ccc tcc tgt ccc
primer 2: 5' tca acc ccg cgg aag ttt ctt ctg agc agt gtc cat gtg aac aaa

(ii) for cloning into pLPCX$_2$

primer 1: 5' act cca gcg gcc gca atg ctc aaa gtc acg gtg ccc tcc tgt ccc
primer 2: 5' tca aac gcg gcc gct cac aga tcc tct tct gag atg agt ttt tgt
tca agt ttc ttc tga gca gtg tcc atg

C. 14-3-3β (human)

(i) for cloning into pEGFP-N1

primer 1: 5' act cca gaa ttc ata atg gac aaa agt gag ctg gta cag aaa gcc
primer 2: 5' tca acc gaa ttc cgt tct ctc cct ctc cag cat ctc ctt cgt ccc

(ii) for cloning into pLPCX$_2$

primer 1: 5' act cca gaa ttc ata atg gac aaa agt gag ctg gta cag aaa gcc
primer 2: 5' tca acc gaa ttc tca cag atc ctc ttc tga gat gag ttt ttg ttc
gtt ctc tcc ctc tcc agc atc tcc ttc

KEY
red = restriction enzyme site
blue = spacer bases
green = Kozak base
grey = frame shift base
black = cDNA sequence
purple = stop codon
orange = myc-tag

Figure 2.4

PCR primers used to amplify and tag: A. Human HDAC4, HDAC4-H803A and HDAC4-D840N, for cloning into pEGFP-N1; B. Murine CamKIV$_{1-313}$, for cloning into (i) pEGFP-N1 or (ii) pLPCX2; C. Human 14-3-3β, for cloning into (i) pEGFP-N1 or (ii) pLPCX2. Colours depict the purpose or function or each base: refer to key above.

was removed into 490 μl MilliRO H_2O and the OD at 260 nm determined by UV spectrophotometry. The concentration of DNA was then adjusted to 50 μM.

2.2.9.3 PCR amplification

Each 50 μl PCR reaction contained: 1X pfu reaction buffer; all 4 dNTPs, each at 100 μM; 1.25 U of turbo pfu; 5% glycerol; 10% DMSO; both primers at a final concentration of 0.4 μM; and, 20 ng of template (plasmid) DNA. The volume of each reaction was adjusted to 50 μl with sterile MilliQ H_2O. Using a PTC-100 Programmable Thermal Controller, PCR conditions were as follows: Initial denaturation for 2 min at 95°C; then 30 cycles comprising, denaturation for 30 secs at 95°C, annealing for 1 min at 63°C, extension for 5 mins at 72°C; and, finally a further extension for 5 mins at 72°C.

2.2.9.4 Agarose gel electrophoresis

PCR reactions and restriction enzyme digests were separated by agarose gel electrophoresis. 10 μl of DNA loading dye (15% ficoll, 0.25% bromophenol blue) was added to each 50 μl PCR reaction and the total volume loaded onto an agarose gel. The gel was made by melting 3 g of electrophoresis grade agarose in 300 ml 1XTBE (90 mM Tris, 90 mM borate, 3 mM EDTA) by heating in a microwave oven. When the solution had cooled (but not set), ethidium bromide was added to a final concentration of 0.2 $\mu g ml^{-1}$, and the gel poured. The Bioline Hyperladder I was used as molecular size markers. Electrophoresis was carried out in a horizontal electrophoresis tank containing 1XTBE, for approximately 1 hr 30 mins at 100 V. The separated DNA was visualised by UV-transillumination of the gel.

2.2.9.5 Purification of DNA from agarose gels

After separation of the PCR reaction product, or restriction enzyme digest, on a TBE/agarose gel, the single band of the correct size was excised using a scalpel. The DNA was purified from the gel fragment using the Qiagen QIAquick Gel Extraction Kit according to the manufacturer's protocol. The fragment was weighed and 3 times the volume (assuming weight in μg is equivalent to volume in μl) of QG buffer added followed by incubation at 50°C, with occasional agitation, until the gel slice dissolved. One gel volume of isopropanol was then added, and following mixing, the solution was applied to a QIAquick spin column and centrifuged at 12,000 x g for 1 min. The DNA now bound to the column was washed by applying 750 μl PE buffer to the column and centrifuging, at 12,000 x g, for 1 min. The flow-through was discarded and the column centrifuged again at 12,000 x g for 1 min. The bound DNA was then eluted by applying 50 μl of EB buffer (10 mM Tris-HCl, pH 8.5), leaving the column to stand for 2 mins and centrifuging at 12,000 x g for 1 min.

2.2.9.6 Cloning PCR products into the PCR-Script vector

The blunt ended PCR products were ligated into the PCR-Script Cam SK+ cloning vector using the PCR-Script Cam Cloning Kit with the protocol provided by Stratagene. The reaction mix for the blunt end ligation contains: 10 ng of the cloning vector, pre-digested with *Srf* I; 1X PCR-Script reaction buffer; 0.5 mM rATP; PCR product, at a concentration which is 100 times the molarity of the PCR-Script vector; 5 U *Srf* I; and, 4 U T4 DNA ligase, in a final volume of 10 μl. After mixing, the reaction was incubated for 1 hour at room temperature, then the enzymes were inactivated by incubation at 65°C for 10 mins. After brief cooling on ice, the reaction mix was ready for transformation into Epicurian Coli XL10-Gold Kan ultracompetent cells (provided

as part of the cloning kit). 40 μl of the ultracompetent cells, in a 15 ml Falcon tube was thawed on ice and 1.6 μl β-mercaptoethanol (provided in cloning kit) added. This was incubated on ice for 10 mins with occasional gentle agitation. 2 μl of the cloning reaction was added, mixed gently and incubated for 30 mins on ice. The bacteria were then heat-shocked at 42°C for exactly 30 secs, before being cooled on ice for 2 mins. 450 μl of L-broth, pre-heated to 42°C, was added and the tubes incubated at 37°C, shaking at 225 rpm, for 1 hour. The whole reaction was spread onto an L-broth-agar petri dish containing chloramphenicol at 30 $\mu g ml^{-1}$, which had previously been spread with 100 μl L-broth containing 2% X-gal and 10 mM IPTG to facilitate blue/white colour selection. Incubation was for a minimum of 17 hours at 37°C after which time, white (and therefore probably insert-positive) colonies were picked, and used to inoculate 5 ml L-broth, containing chloramphenicol at 30 $\mu g ml^{-1}$, and incubated overnight, shaking, at 37°C.

2.2.9.7 Preparation of agar plates

10 g Bactoagar was added to a 500 ml bottle of L-broth, and autoclaved. The bottle was allowed to cool to 55°C in a water bath, then the required antibiotic was added using sterile technique. Ampicillin was added to a final concentration of 100 $\mu g ml^{-1}$, for selection of pLPCX2 carrying bacteria; or kanamycin to 40 $\mu g ml^{-1}$, for selection of pEGFP-N1 carrying bacteria; or chloramphenicol to 30 $\mu g ml^{-1}$, for selection of pCR-Script carrying bacteria. The L-broth-agar was then poured into 10 cm diameter petri dishes, approximately 10 ml per dish, and allowed to cool before the lids were replaced. The plates were stored at 4°C.

2.2.9.8 "Wiggle" PCR

After overnight incubation of the 5 ml L-broth cultures, "wiggle" PCR was used to confirm the presence of insert-positive PCR-Script vector. 5 μl of L-broth culture was used as the template in a 50 μl PCR reaction which also included: 1X Taq polymerase reaction buffer; all 4 dNTPs, each at 100 μM; 1.25 U of Taq polymerase; 1.5 mM $MgCl_2$; and, both primers at a final concentration of 0.4 μM. The volume of each reaction was adjusted to 50 μl with sterile MilliQ H_2O. Using a PTC-100 Programmable Thermal Controller, PCR conditions were as follows: Initial denaturation for 2 mins at 95°C; then 30 cycles comprising, denaturation for 30 secs at 95°C, annealing for 1 min at 55°C, extension for 3 mins 30 secs at 72°C; and, finally a further extension for 5 mins at 72°C. PCR products were separated by agarose gel electrophoresis, as described (Section 2.2.9.4).

2.2.9.9 Small scale "miniprep" plasmid preparation

After wiggle PCR confirmed the presence of insert in the PCR-Script cloning vector, small scale plasmid preparations ("minipreps") were carried out on up to three of the insert-positive, 5 ml overnight L-broth cultures (Section 2.2.9.6) using a Qiagen plasmid mini-purification kit, as directed by the supplied protocol. From these cultures 3ml was removed and the bacteria were pelleted by centrifugation for 1 min at 12,000 x g then resuspended in 250 μl of P1 buffer (50 mM Tris-HCl, 10 mM, EDTA, 100 $\mu g ml^{-1}$ RNase A), then lysed by the addition of 250 μl of P2 buffer (0.2 M NaOH, 1% SDS), and thorough mixing by inversion. Proteins and detergent were precipitated by addition of 350 μl of cold P3 buffer (3 M potassium acetate, pH 5.5) and again, thorough mixing. A thick white precipitate forms which was pelleted by centrifugation at 12,000 x g for 10 mins. The supernate was decanted into a Qiaprep spin column,

which was then centrifuged at 12,000 x g for 1 min. At this point the plasmid DNA is bound to the column, which was then washed with 750 µl PE buffer (1 mM EDTA buffered in PBS). After the flow-through was discarded the column was centrifuged for a further 1 min to remove remaining traces of PE. The DNA was then eluted from the column by addition of 50 µl EB buffer (10 mM Tris-HCl, pH 8.5).

2.2.9.10 Restriction enzyme digestion

Following the purification of insert-positive pCR-Script (Section 2.2.9.9), the cDNA insert was removed from pCR-Script by restriction enzyme digestion. Each reaction contained 45 µl "miniprep" DNA and other components as detailed (Table 2.1).

cDNA	Enzyme 1 (2 µl)	Enzyme 2 (2 µl)	Ac BSA (0.6 µl)	Buffer (5.5 µl)	H_2O (µl)
RYBP	EcoRI	-	-	React 1	0.5
PCDHGC3	EcoRI	-	-	React 1	0.5
STAT6	EcoRI	-	-	React 1	0.5
HDAC4	EcoRI	SspI	-	React 1	0.5
HDAC4 H803	EcoRI	SspI	-	React 1	0.5
HDAC4 D840	EcoRI	SspI	-	React 1	0.5
$CamKIV_{1-313}$	NotI	-	-	React 3	2.5
$CamKIV_{1-313}$	SacII	-	+	SacII buffer	1.9
14-3-3β	EcoRI	-	-	React 3	2.5
14-3-3β	EcoRI	-	-	React 3	2.5

Table 2.1
Restriction enzyme digestion of cDNAs from PCR-Script.

HDAC4 is approximately the same size as the PCR-Script vector, which means that the two could not be distinguished by agarose gel electrophoresis. SspI was added to those reactions containing the wt, or deacetylases inactive, HDAC4 cDNAs, to cut PCR-Script, making it smaller than HDAC4 and therefore distinguishable from it. Digestion was carried out at 37°C for 1 hour, after which, the whole reaction, plus 1X DNA loading buffer, was run on an agarose gel (Section 2.2.9.4), and the fragments

of the correct size excised and purified as described (Section 2.2.9.5). The pEGFP-N1 and pLPCX2 vectors, which were to receive the inserts removed from PCR-Script, were also digested with the appropriate restriction enzyme, and, to prevent religation of vector in the subsequent ligation reaction, the vectors were also dephosphorylated. 1 μg of pEGFP-N1 was digested with EcoR1 or SacII and 1μg of pLNCX$_2$ was digested with either NotI or EcoRI, in reactions similar to those detailed above but with a total volume of 20 μl as the substrate volumes were smaller and including 1 unit of calf intestinal alkaline phosphatase (CIAP). The linearised vectors were then separated from the other reaction components on the same agarose gel used to separate the fragments to be ligated into them. The relevant bands were excised from the gel and purified as described (Sections 2.2.9.4 and 2.2.9.5).

2.2.9.11 Ligation of cDNA into vector

Ligation of genes into vectors was achieved using a Rapid DNA Ligation Kit, following the recommended procedure. Vector and insert DNA, in a molar ratio of 1:3 to 1:5, were diluted in the DNA dilution buffer supplied, to a volume of 10 μl, then further diluted in T4 DNA ligation buffer (supplied) to a volume of 20 μl. After thorough mixing, 1 μl of DNA ligase (supplied) was added, and mixed again. Incubation was for 5 mins at room temperature before immediate transformation of 5 μl of the reaction into E.coli DH5α competent cells (Section 2.2.9.12).

2.2.9.12 Transformation of E.coli DH5α competent cells

E.coli DH5α competent cells were thawed on ice and a 100 μl aliquot removed per transformation. 5 μl (approximately 100 ng) of plasmid DNA, or 5 μl of ligation reaction was added to the aliquot on ice for 30 mins. The bacteria were then heat shocked for

45 secs at 42°C and returned to the ice. 400 µl of L-broth was then added and the tubes incubated at 37°C in an orbital shaker at 225 rpm for 45 mins. If the transformation was simply to amplify a plasmid, 40 µl of bacteria was pipetted onto the surface of an L-broth-agar petri dish, containing the appropriate antibiotic (Section 2.2.9.7), spread and allowed to dry. If the transformation was using the product of a ligation reaction then the whole 500 µl was pipetted onto the dish, spread and allowed to dry with the lid off. Petri dishes were then incubated, inverted, overnight at 37°C.

2.2.9.13 Selection of cDNA-positive clones

Up to 8 bacterial colonies, which had been transformed with the ligation mix (Section 2.2.9.11) were picked and used to inoculate 5ml of L-broth containing the appropriate antibiotic: ampicillin was added to a final concentration of 100 $\mu g ml^{-1}$, for selection of pLPCX2 carrying bacteria; or kanamycin to a final concentration of 40 $\mu g ml^{-1}$, for selection of pEGFP-N1 carrying bacteria. After overnight incubation, shaking, at 37°C, the plasmid was purified from 2ml of bacterial culture using a Qiagen plasmid mini-purification kit as described (Section 2.2.9.9).

Each "miniprep"-purified plasmid was digested separately with two restriction enzymes (Table 2.2). The first is the enzyme which initially produced the sticky ends used to facilitate the ligation. This cuts out the insert, confirming its presence and size. The second enzyme is selected to determine orientation of the inserted gene. It cuts the insert at one eccentric site and cuts the vector at one eccentric site, thereby generating fragments of sizes specific to the orientation of the gene. Reactions are similar to those described (Section 2.2.9.10). The resultant fragments were separated by agarose gel electrophoresis (Section 2.2.9.4) and visualised by UV-transillumination.

Plasmid	Insert	Restriction enzymes	
pEGFP-N1	RYBP	EcoRI	HaeII
pEGFP-N1	PCDHGC3	EcoRI	ApaI
pEGFP-N1	STAT6	EcoRI	HindIII
pEGFP-N1	HDAC4	EcoRI	HindIII
pEGFP-N1	HDAC4 H803	EcoRI	HindIII
pEGFP-N1	HDAC4 D840	EcoRI	HindIII
pEGFP-N1	$CamKIV_{1-313}$	SacII	EcoRI
pEGFP-N1	14-3-3β	EcoRI	HindIII
pLPCX2	$CamKIV_{1-313}$	NotI	EcoRI
pLPCX2	14-3-3β	EcoR1	HindIII

Table 2.2

Restriction enzymes used to digest each cDNA-positive vector to establish size and orientation are correct.

2.2.9.14 DNA sequencing

Two plasmids were selected, per cDNA, for sequencing. These had been determined, by restriction enzyme digestion of "minipreps" DNA, to carry a correctly orientated insert of the correct size. The DNA sequence of the insert and insert/vector junctions was determined. Sequencing primers (15 bases long) were designed in both the 5' and 3' directions every 300 base pairs within the appropriate cDNAs and were synthesised as described (Section 2.2.9.2). In addition the sequencing primers supplied by the manufacturers of pLPCX2 and pEGFP-N1 were used to sequence vector/insert junctions. The method of sequencing was based on the method of Sanger (Sanger et al. 1977). 20 ng "miniprep" plasmid DNA, 3.2 pmols sequencing primer, and 8 μl of "Dyedeoxy" reaction mix, were combined in a total volume of 20 μl. This was subject to "cycle sequencing" in a PTC-100 Programmable Thermal Controller for 25 cycles. Each cycle comprised, 15 secs at 96°C to denature DNA, 1 sec at 50°C to anneal, and 4 mins at 60°C to extend. The product was ethanol precipitated, washed in 70% ethanol and dried by centrifugation under vacuum in a Jouan RC10.10. "speedivac", prior to resuspension in loading buffer (95% formamide; 25 mM EDTA, pH 8.0; 1.5 $mgml^{-1}$ detran blue). Samples were then denatured at 94°C

for 5 mins and transferred immediately to ice. Sequencing was then carried out by Mr. Robert McFarlane, BICR Technology Services, using a Biosystems ABI 373A automated DNA sequencer, according to the manufacturer's instructions.

2.2.9.15 Large scale "maxiprep" plasmid preparations

The remaining 3 ml of the 5 ml overnight L-broth cultures carrying plasmid with correctly orientated insert, was used to inoculate 300 ml L-broth, containing the appropriate antibiotic (Section 2.2.9.13), in 1 litre flasks. Cultures were incubated at 37°C in an orbital shaker at 225 rpm overnight Large scale plasmid preparations, "maxipreps", were performed, to prepare DNA for transfection into mammalian cells (Section 2.2.10). This was done using a QIAfilter plasmid maxi-purification kit as directed by the protocol supplied by Qiagen. Bacteria were pelleted from the overnight culture by centrifugation at 6,000 x g for 15 mins, and the pellet resuspended in 10 ml P1 buffer (50 mM Tris-HCl, 10 mM EDTA, 100 $mgml^{-1}$ RNase A). Bacteria were then lysed by the addition of 10 ml buffer P2 (0.2 M NaOH, 1% SDS), with thorough mixing. Then 10 ml of cold P3 buffer (3 M potassium acetate, pH 5.5) was added, mixed thoroughly and decanted immediately into a QIAfilter Cartridge, where it was allowed to stand undisturbed at room temperature for 15 mins. A thick white precipitate forms in the lysate which is removed when the contents of the cartridge are passed over the QIAfilter as they are expelled, using a plunger, into a QIAGEN-tip 500, which had previously been equilibrated using 10 ml QBT buffer (750 mM NaCl, 50 mM MOPS pH 7.0, 15% isopropanol, 0.15% Triton X-100). The cleared lysate drips through the QIAGEN Resin at the base of the QIAGEN-tip 500, so that at this point the plasmid DNA becomes bound within the resin. The tip was washed twice with 30 ml QC buffer (1 mM NaCl, 50 mM MOPS pH 7.0, 15% isopropanol) and the plasmid DNA then eluted with 15 ml QF buffer (1.25 M NaCl, 50 mM Tris-HCl pH 8.5, 15% isopropanol).

The DNA was precipitated by the addition of 10.5 ml isopropanol and immediately centrifuged at 15,000 x g for 30 mins. The precipitate was then washed with 70% ethanol and the air-dried pellet resuspended in sterile MilliQ H_2O.

2.2.10 Transfection / nucleofection

2.2.10.1 Transfection of cells using "FuGene6"

Following the protocol supplied with FuGene transfection reagent, cells were grown to 70% confluence in 6 well plates (3.6 cm diameter wells). For each well, 3 μl of FuGene transfection reagent was added to 97 μl of serum free DMEM and incubated at room temperature for 5 mins. This mixture was then added dropwise to 1μg of plasmid maxiprep DNA carrying the gene to be transfected. This was then further incubated for 15 mins at room temperature, prior to dropwise addition to the 2 ml DMEM, with 10% FCS, already covering the cell monolayer in each well. The transfection reagents were left on the cells overnight after which time the cells were washed with PBS, fresh DMEM plus 10% FCS was added and the cells were incubated for a further 24 hours.

2.2.10.2 Stable expression of cDNAs from "FuGene" transfections

Transfections using FuGene were carried out to achieve stable expression of HDAC4, HDAC4-H803A, HDAC4-D840, $CamKIV_{1-313}$ and 14-3-3β. Following on from the above (Section 2.2.10.1), transfected cells were then trypsinised from the dish (Section 2.2.1.1) and four 10 cm dishes were each seeded with 1/40th of the total number of cells in DMEM plus 10% FCS. These were incubated for 24 hours before the medium was replaced with DMEM plus 10% FCS, this time containing G418 at 700 μgml^{-1}. Cells were then incubated for 2-3 weeks during which time medium was

replaced mainly every two days, increasing to daily between approximately 5 to 10 days, during which time there is a high degree of cell death as the G418 selection proceeds. When cells were approaching confluence they were harvested (Section 2.2.1.1) and selected for green fluorescence by fluorescent activated cell sorting (FACS) using a FACS Vantage SE (BD Biosciences, Cowley, Oxfordshire, UK.). In the case of HDAC4 cells were sorted into individual wells of a 96 well tissue culture plate, at 5 cells per well, and grown as normal. Within a few days, wells which had only one colony growing were identified and from these clonal populations of HDAC4-expressing cells were obtained. For all other cDNAs, FACS-sorted cells were pooled into a single polyclonal population. However, four of these polyclonal populations were created for each cDNA.

2.2.10.3 Cos-7 cells

Transfections using FuGene were carried out to introduce expression vectors into Cos-7 cells to confirm that the vector expresses a protein of the correct molecular weight. In this case the cells transiently express the cDNA. Between 24 and 48 hours post-transfection (Section 2.2.10.1), the cells were harvested and prepared for western analysis as described (Section 2.2.3).

2.2.10.4 Nucleofection

Nucleofector technology is a more efficient way of introducing expression vectors into cells and superseded FuGene transfection during this project. Nucleofection was carried out using an Amaxa nucleofector, according to the manufacturers protocol. Briefly, 5 x 10^5 FBR cells were resuspended in 100 µl nucleofection solution R, and this suspension was then added to 5 µg of plasmid DNA (usually approximately 3 µl). The suspension was immediately transferred to a nucleofection cuvette, which

contains electrodes, and nucleofected using programme T-20. Immediately post-nucleofection, 500 µl of RPMI tissue culture medium, at 37°C, was added to the contents of the cuvette, and the suspension removed.

2.2.10.5 Stable expression of cDNAs from nucleofection

Nucleofector technology was used to achieve stable expression of RYBP, STAT6 or RYBP. Following nucleofection (Section 2.2.10.3) the content of the cuvette was removed and 1/10th was added to each of two 10 cm dishes containing DMEM plus 10% FCS, at 37°C. These were incubated for 24 hours before the medium was replaced with DMEM plus 10% FCS, containing G418 at 700 $\mu g ml^{-1}$. The procedure then follows that used to obtain stable expression after transfection using FuGene (Section 2.2.10.2). A small amount of the nucleofected cell suspension was also added to coverslips to determine the efficiency of nucleofection, though this was not necessary for EGFP-tagged cDNAs which could be viewed directly by fluorescent microscopy.

2.2.10.6 Nucleofection prior to invasion assays

Cells were transiently nucleofected, primarily for assessment in the invasion assay. In this case, following nucleofection (2.2.10.4), the content of the cuvette was removed into 10ml DMEM and centrifuged at 400 x g for 5 mins. The cell pellet was carefully resuspended in 250 µl DMEM plus 10% FCS and 100 µl was added to the underside of the filter on each of two Transwells. The invasion assay then proceeded as described (Section 2.2.7.1). The remaining 50µl of nucleofected cell suspension was divided between two coverslips for immunohistochemistry or actin staining, as described (Sections 2.2.11 and 2.2.5), to confirm that a high enough proportion of the

cells are expressing the transgene. Immunohistochemistry and/or actin staining was carried out 48 hours post-nucleofection.

2.2.11 Immunohistochemistry

19 mm glass coverslips were sterilised in ethanol, allowed to air dry, placed in 2.1 cm tissue culture wells (12 well plates), covered with 1.5 ml DMEM and incubated at 37°C. Nucleofections were carried out as described (Section 2.2.10.3) and 1/10th of the total 100 µl nucleofection reaction was added to each pre-incubated well. After 48 hours, the medium was removed and fixing and permeabilisation of cells was carried out as described (Section 2.2.5). Blocking of non-specific binding was then carried out, in 400 µl of blocking buffer (0.5% BSA, 10% FCS in PBS) for 20 mins. Coverslips were then transferred to a light-tight container which was lined with parafilm to ease handling of coverslips with forceps. Primary antibody, diluted as directed by the manufacturers protocol, in 50 µl of blocking buffer, was added to the surface of the coverslips and left at room temperature in the dark for 45 mins after which the coverslips were washed 3 times with blocking buffer. Then FITC-conjugated secondary antibody, diluted as recommended, in 50 µl blocking buffer also containing 100 $ngml^{-1}$ TRIC-conjugated phalloidin (to stain actin) was added for 45 mins, after which the coverslips were immersed in dH_20, 3 times sequentially, drained, and placed inverted on a drop of Vectashield on a glass microscope slide. Where nuclear staining was required, Vectashield containing DAPI stain was used. Excess Vectashield was aspirated and the edge of the coverslip sealed with clear nail varnish. In experiments where only phalloidin-staining of actin is required, the protocol described in section 2.2.5 was followed. Red/green fluorescent images were captured by confocal microscope (Section 2.1.7) using a 63X objective.

Chapter 3

Studies with histone deacetylase inhibitors

3.1 Expression levels of histone deacetylases and associated proteins in Fos-transformed fibroblasts relative to non-transformed cells

3.1.1 Introduction

Since we had shown in differential gene expression studies (Johnston et al. 2000) (Section 1.3.1.2) that two components of the Sin3 complex, SAP18 and RbAp46, are up-regulated in Fos-transformed cells (Figure 1.6), and because this complex is implicated in the silencing of gene transcription by histone deacetylation, we further investigated the comparative expression levels of other genes with products known to be components of the complex, and of other HDACs. If HDACs are also up-regulated, then increased histone deacetylation may be a mechanism by which genes are down-regulated in Fos-transformation. This would be consistent with previous work (Bakin and Curran 1999; section 1.3.1.3) implicating histone deacetylation in transformation by the chimaeric, recombinant $Fos^{FBJ/R}$ protein and by sustained expression of c-Fos. Thus we investigated the expression of HDACs and HDAC complex components at the RNA and protein level in FBR cells, compared to that in 208F cells; and to extend this to transformation by other oncogenes we made a similar comparison of Ha-Ras-transformed 208F cells. Ras being of particular importance since it is frequently mutated in human cancer, and because AP-1, being a target of the Ras/Raf/MEK/ERK signal transduction pathway, is a downstream effector of Ras (Section 1.2.3).

3.1.2 Expression levels of HDACs and related proteins

Firstly, the up-regulation of RbAp46/48 was confirmed by western analysis (Figure 3.1A), though this was not done for SAP18, since antibodies were unavailable, however, previously northern analysis had validated the differential expression of all genes identified by the suppressive subtractive hybridisation study (Johnston et al. 2000; Section 1.3.1.2).

Many histone deacetylases and associated proteins are up-regulated in Fos-transformants

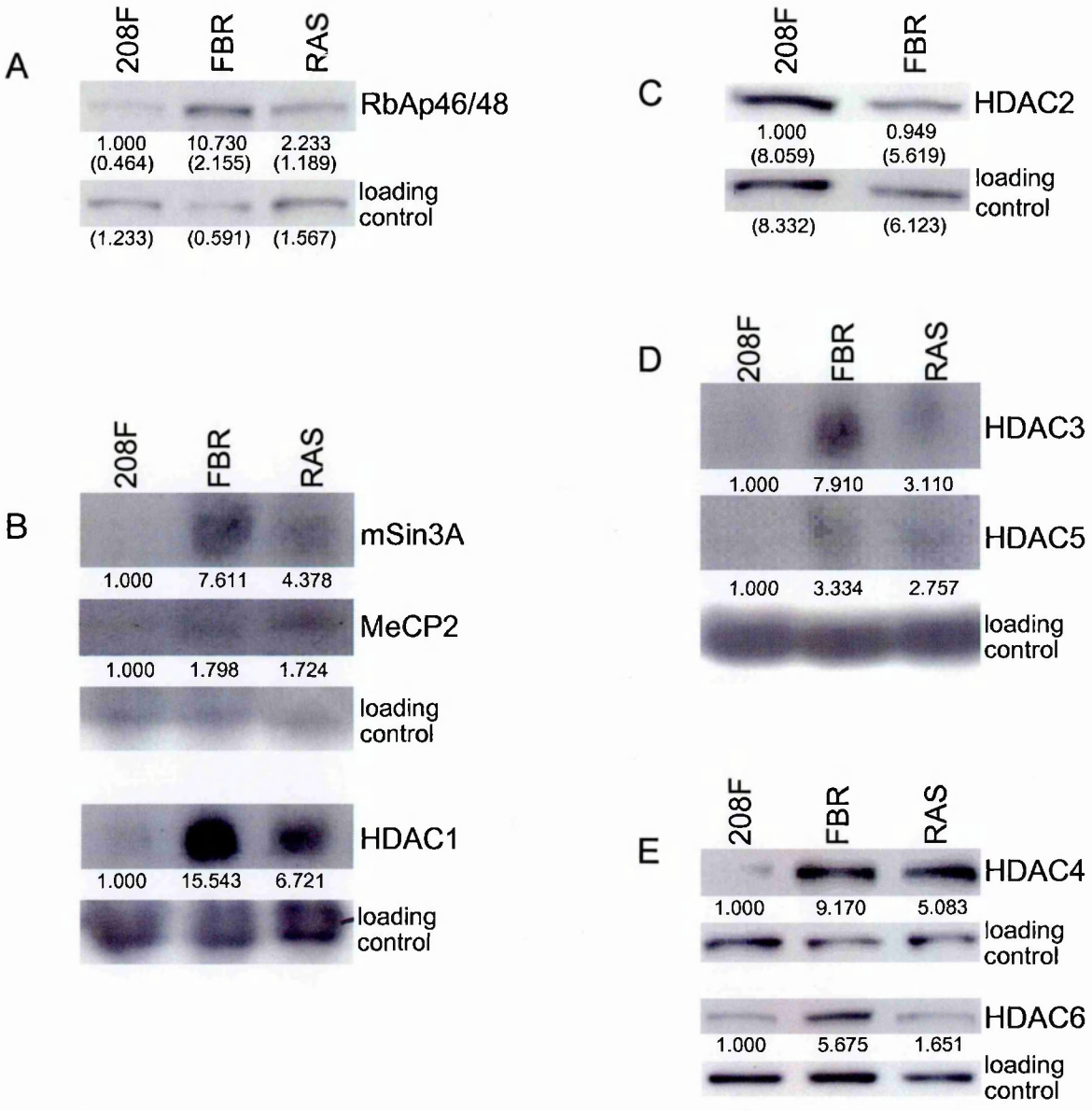

Figure 3.1

Northern and western analyses, showing expression levels of HDACs and related proteins in Fos- and Ras-transformed 208F cells. Loading controls are 7s rRNA for all northern blots and ERK2 for all western blots. Printed values are in units of OD X mm^2, i.e., optical density of a band x the area it covers; and have been normalised to the values obtained for the loading control. Additional figures in brackets are *actual* densitometric values prior to normalisation to the loading control shown.

A. Western blot confirming increased expression of RbAp46/48 protein in both FBR and RAS cells.

B. Northern blot demonstrating the up-regulation of Sin3A, HDAC1 and MeCP2, in both FBR and RAS cells. The experiment shown (excluding quantitation) was performed by Mr. Liam Meagher.

C. Western blot showing that HDAC2 is not up-regulated in FBR cells.

D. Northern blot demonstrating the up-regulation of HDAC3 and HDAC5 in both FBR and RAS cells.

E. Western blots demonstrating increased expression of HDAC4 and HDAC6 in both FBR and RAS cells.

To investigate the relative expression levels of Sin3 complex components and related proteins we used northern analysis or western analysis (where antibodies were available). Sin3A itself was found to be up-regulated 7.6-fold and HDAC1 15.5-fold in FBR cells, and in Ha-ras transformed 208F (RAS) cells, these figures were 4.4- and 6.7-fold respectively (Figure 3.1B). In addition the methyl transferase, MeCP2 was also up-regulated in FBR and RAS cells (Figure 3.1B). At the protein level, HDAC2 expression was, however, found to be equivalent in 208F and FBR (Figure 3.1C). In addition, other HDACs, not known to be part of the core complex, but which can associate with known complex components, were also found to be up-regulated (Figure 3.1D and E). The class I, HDAC3 RNA is up-regulated 7.9-fold in FBRs and 3.1-fold in RAS cells and expression of the class II, HDACs 4, 5 and 6 is also increased. By northern analysis HDAC5 mRNA is 3.3-times more abundant in FBR cells and 2.8-times in RAS cells (Figure 3.1D) and by western analysis, the expression of HDAC4 is up-regulated 9.2-fold in FBRs and 5.1-fold in RAS cells, and HDAC6 is up-regulated 5.7-fold in FBR cells and, to a lesser extent, 1.7-fold in RAS cells (Figure 3.1E). Thus we have demonstrated that in 208F cells transformed by v-Fos^{FBR} or by Ha-Ras there is increased expression of HDACs and of components of HDAC repressor complex components.

3.2 Inhibition of histone deacetylases in Fos-transformed cells

3.2.1 Introduction

Since the expression of all the HDACs investigated, with the exception of HDAC2, was found to be up-regulated in FBR cells, we investigated the consequences of inhibiting HDAC activity, with regard to the transformed phenotype and its possible reversion, by treating FBR cells with the histone deacetylase inhibitors, trichostatin A (TSA) and valproic acid (VPA).

3.2.2 Effect on proliferation

Firstly, we measured the effect the inhibitors have on the proliferation rate of FBR cells to determine the optimal experimental concentrations which ensure growth inhibition is not a factor affecting results (Figure 3.2). We found that treatment with up to 12 nM TSA does not affect proliferation, however, when grown in 20 nM TSA, there was approximately, 75% less cells counted after 4 days growth compared to untreated FBR cells. VPA does not affect the rate of proliferation at concentrations of up to 50 μgml^{-1}, but by 100 μgml^{-1} there were 68% fewer cells counted at 4 days.

3.2.3 Effect on morphology and actin stress-fibres

We then proceeded to treat FBR cells with TSA and VPA, at concentrations below those which affect their proliferation rate (12 nM and 50 μgml^{-1} respectively), for 4 days. Both inhibitors induced reversion of the bipolar morphology, to a less refractile, more flattened, morphology similar to that of the parental 208F cells (Figure 3.3). This shape change is accompanied by a structural rearrangement of the actin cytoskeleton (Figure 3.4). Bipolar FBR cells have lost the actin stress-fibres which are clearly visible in the parental 208F cells. Treatment with either TSA or VPA induces their reassembly. This implies that increased HDAC expression in Fos-transformed cells is responsible for transformed morphology and loss of actin stress-fibres.

Both these morphological and cytoskeletal rearrangements are reversible; by 4 days after the removal of inhibitors, FBR cells have almost completely regained their bipolar morphology (Figure 3.3) differing only in that they appear to retain a small number of short lateral extensions along the lengths of their pseudopods, giving the cells a ragged appearance, and in that a small proportion of the cell bodies retain a slightly more flattened appearance; however, if the cells are passaged 2 days after the

FBR cell proliferation is unaffected by concentrations of HDAC inhibitors used in subsequent experiments

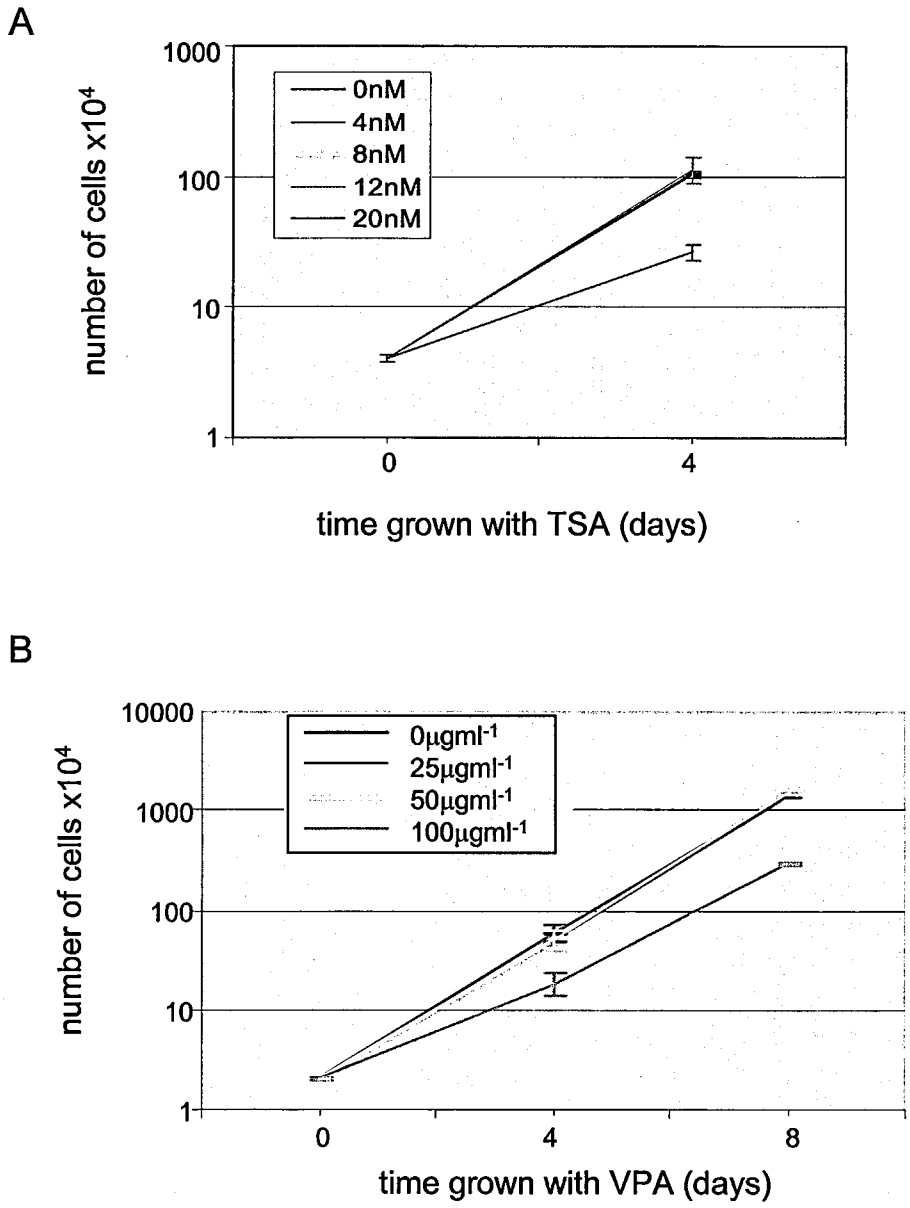

Figure 3.2

FBR cell growth in the presence of HDAC inhibitors

A. Graph showing how the growth of FBR cells is affected by increasing concentrations of TSA. Cell numbers, and therefore, rate of proliferation, is unaffected by concentrations of TSA lower than, or equal to, 12 nM. Growth medium plus TSA was replaced every 2 days.

B. Graph showing how the growth of FBR cells is affected by increasing concentrations of VPA. Cell numbers, and therefore, rate of proliferation, is unaffected by concentrations of VPA lower than, or equal to, 50 μgml^{-1}. Growth medium plus VPA was replaced every 2 days.

Results shown are derived from 2 separate experiments with triplicate sample in each.

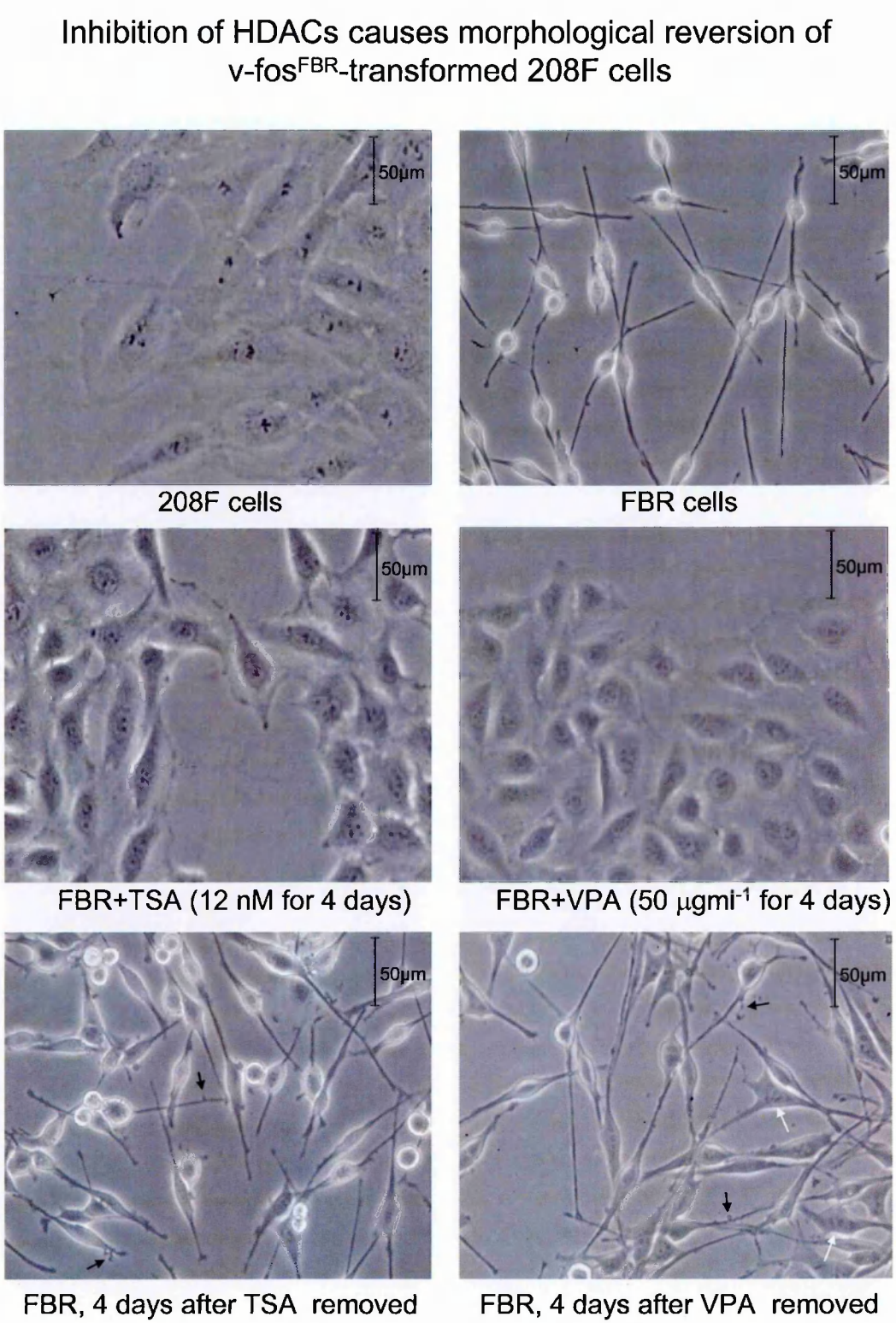

Figure 3.3

Digital photographs of phase microscopy.

208F cells are flat and contact inhibited. FBR cells are more light refractile, bipolar in shape, and not contact inhibited. On treatment with the HDAC inhibitors, FBR cell morphology reverts to a more 208F-like appearance: flat and contact inhibited. Removal of HDAC inhibitors allows the FBR cells to return almost completely to their previous transformed morphology, differing only in that they appear to retain small lateral extensions on the pseudopods (indicated by black arrows) and a small number of cell bodies have a slightly more flattened appearance (indicated by white arrows). These differences compared to FBR cells are lost on passage. In this experiment cells were grown in plastic tissue culture dishes.

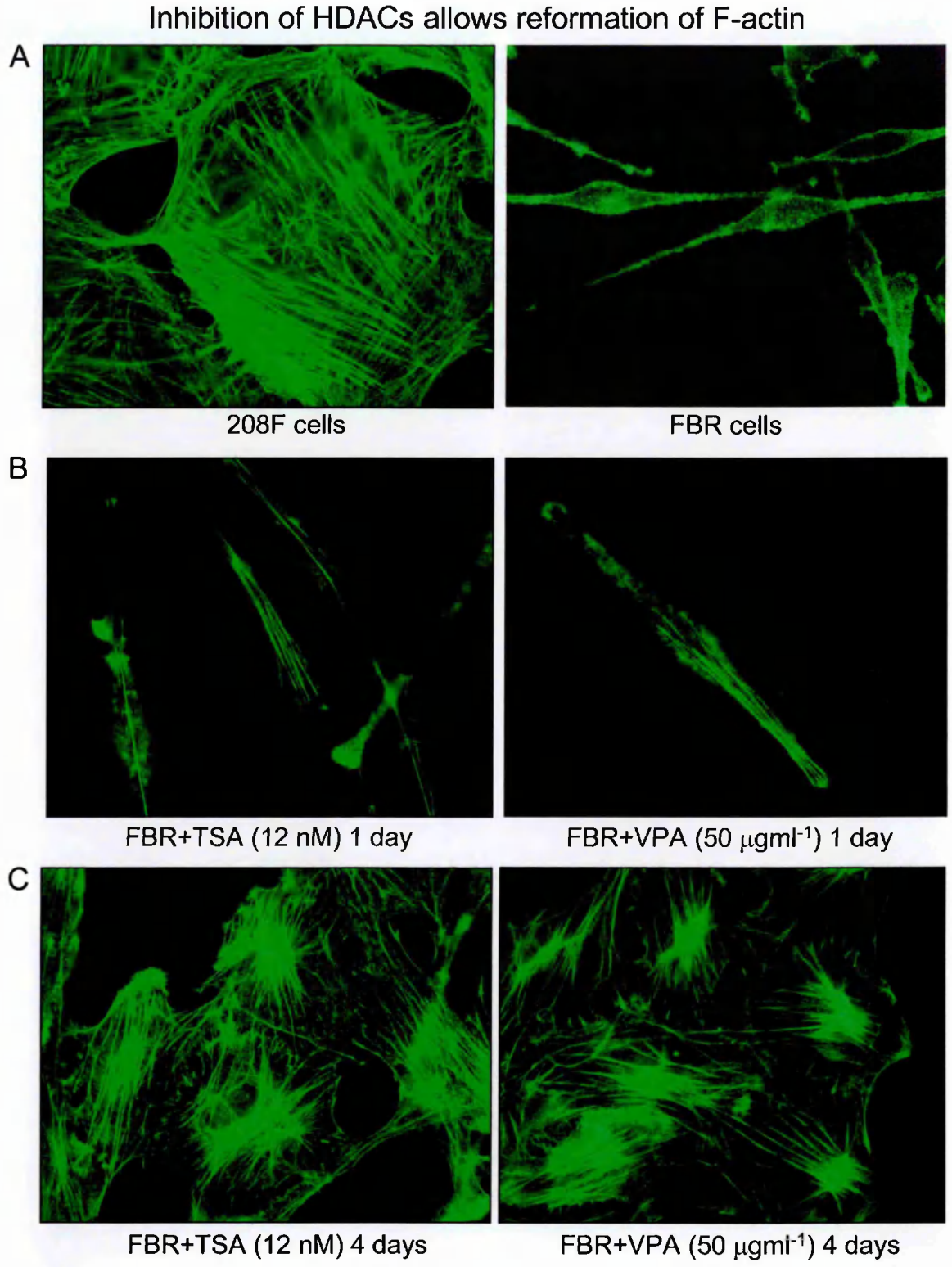

Figure 3.4

Fluorescent microscopy of cells stained for F-actin with FITC-conjugated phalloidin.

A. Actin stress-fibres are clearly visible in 208F cells, whereas FBR cells have no filamentous actin, other than cortical actin.

B. On treatment with TSA or VPA, stress-fibres can be seen in FBR cells within 24 hours.

C. By 4 days, FBRs have a similar amount of F-actin to 208F and have assumed a flat, polygonal morphology.

removal of inhibitors the re-seeded cells become bipolar on attachment to the plastic and are indistinguishable from untreated FBR cells (data not shown).

Both inhibitors achieve these results, however we observed VPA to be slightly more efficient in effecting reversion in cells grown either on plastic or on glass. VPA (50 μgml^{-1} for 4 days) treated FBR cells are closer than TSA (12 nM for 4 days) treated FBR cells, in appearance to 208F cells (Figure 3.3). In quantitation of cells grown on plastic, optimally, less than 8% of VPA treated cells (50 μgml^{-1} for 4 days) remain bipolar, compared to approximately 15% of TSA treated cells (12 nM for 4 days) These figures are based on the classification of an average of 28 cells in each of 12 separate, random fields of view, done on two separate occasions (data not shown). In quantitation of cells grown on glass coverslips, 17% of VPA treated cells (50 μgml^{-1} for 4 days) remain bipolar (Figure 3.5A), compared to approximately 22% of TSA treated cells (12 nM for 4 days; data not shown), however, after 8 days of treatment, with either inhibitor, these figures drop further to 7% of VPA treated cells (Figure 3.5A) and 15% of TSA treated cells (data not shown). Again, these figures are based on the classification of an average of 28 cells in each of 12 separate, random fields of view, done on two separate occasions.

In a time-course to track the reappearance of actin stress-fibres in FBR cells, grown on glass coverslips, at increasing concentrations of inhibitors, we found that the reappearance of stress-fibres precedes morphological reversion, actually re-appearing within 24 hours (Figure 3.5B), with little increase, after 24 hrs, in the proportion of cells with stress-fibres (Figure 3.5B and C). Surprisingly, this re-appearance of stress-fibres even occurs at the lower concentration of 25 μgml^{-1} VPA (Figure 3.5B), which does not induce morphological reversion (Figure 3.5A), in contrast to treatment with 50 μgml^{-1} VPA, which does induce reversion (Figure 3.5A). In addition, there is a

Reformation of F-actin, in response to HDAC inhibition, occurs before morphological reversion and at a lower concentration of HDAC inhibitor

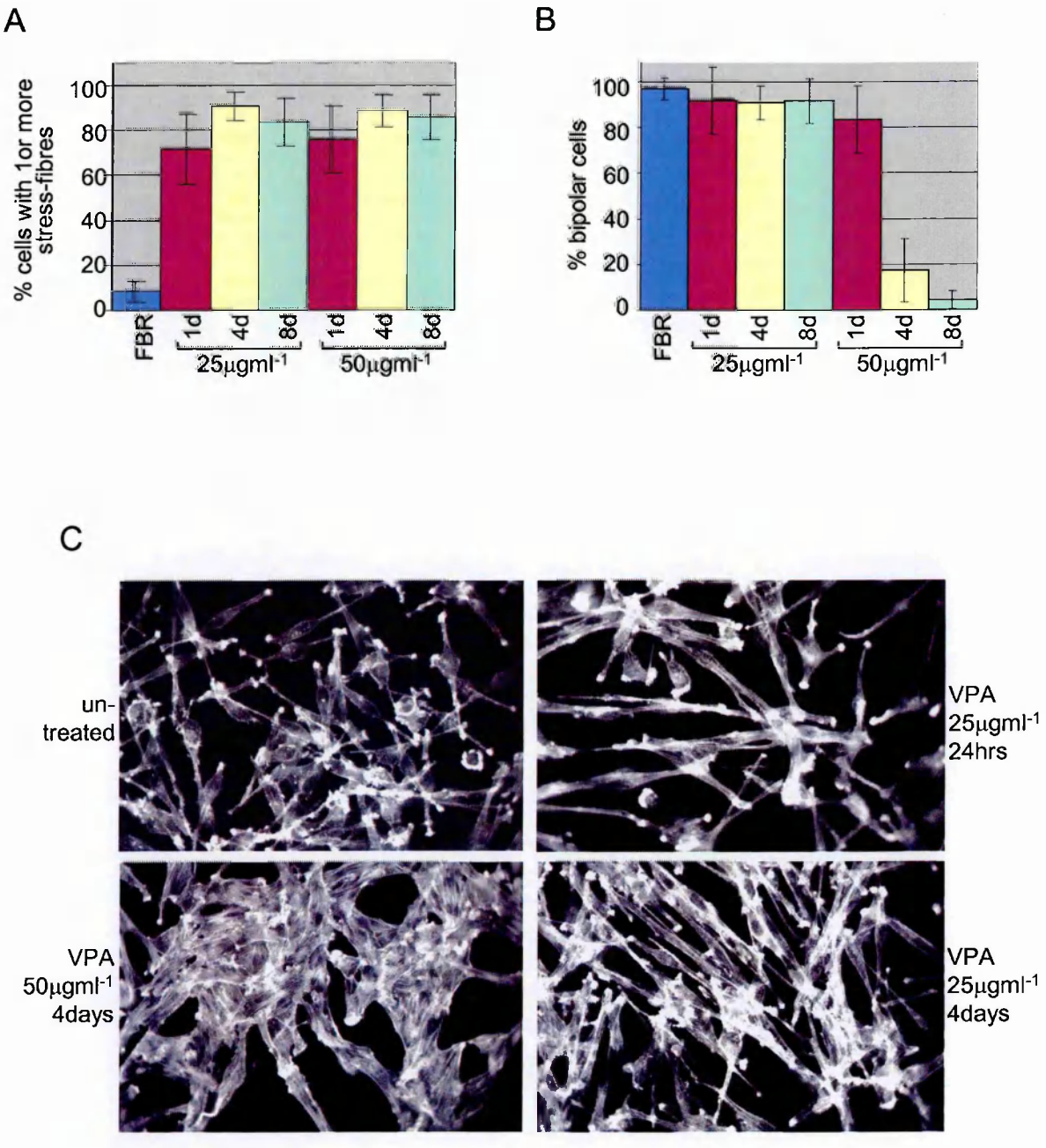

Figure 3.5

A. Histogram showing a time-course of stress-fibre reformation in FBR cells in response to 25 μgml^{-1} VPA or 50 μgml^{-1} VPA treatment. At both concentrations of VPA, stress-fibres reform within 24 hours and there is only a small increase in the number of cells containing fibres with time.
B. Histogram showing that there is no significant drop in the number of bipolar cells present in FBR cells treated with 25 μgml^{-1} VPA, in up to 8 days. This is in contrast to FBR cells treated with 50 μgml^{-1} VPA in which there is a 83% drop in number of bipolar cells by 4 days of treatment.
C. Fluorescent microscopy of cells stained for F-actin with FITC-conjugated phalloidin, showing there are stress-fibres present in bipolar FBR cells treated with 25 μgml^{-1} VPA for 24 hours and 4 days, compared to parental cells, and showing stress-fibres present after 4 days in 50 μgml^{-1} VPA in FBR cells which show revertant morphology.

difference in the structure of stress-fibres in cells treated for 4 days with 25 μgml^{-1} VPA compared to 50 μgml^{-1} VPA, we see that at 25 μgml^{-1} VPA the fibres align in parallel with the long axis of the cell but at 50 μgml^{-1} VPA the fibres are less parallel and begin more to radiate from the cell centre (Figures 3.5C and 3.4). Thus the difference in the morphologically reverted cell is not in the quantity of stress-fibres but in their organisation.

These results suggest that 25 μgml^{-1} VPA is sufficient to facilitate F-actin formation, but that the rearrangement of stress-fibres which accompanies morphological reversion occurs only at the higher concentration of VPA (50 μgml^{-1}). This demonstrates that the formation of stress-fibres *per se* is not sufficient to facilitate morphological reversion.

3.2.4 Effect on motility

To investigate whether increased HDAC expression in FBR cells is a contributory factor in their increased motility, we carried out scrape wound assays in inhibitor treated FBR cells (Section 2.2.6). Here we measured the rate of closure of a wound, of between 0.5 and 0.7 mm, scraped in a cell monolayer. We found that 8 nM TSA and 25 μgml^{-1} VPA had no effect on rate of wound closure even after pre-treatment of the cells with inhibitor for 4 days (Figure 3.6). When we increased these concentrations to 12 nM and 50 μgml^{-1} respectively, there was a significant drop in the rate of closure after 4 day (i.e. 3.5 days pre-treatment) treatments with both inhibitors. With TSA treatment this drop in motility is 21% and with VPA treatment the drop is 39% (Figure 3.7).

As an alternative method of assessing 2-D motility, to substantiate the wound assay data, we tracked the movement of HDAC inhibitor treated FBR cells, in low density

Rate of wound closure, and therefore motility, is unaffected by HDAC inhibitors at concentrations and durations used to inhibit invasion

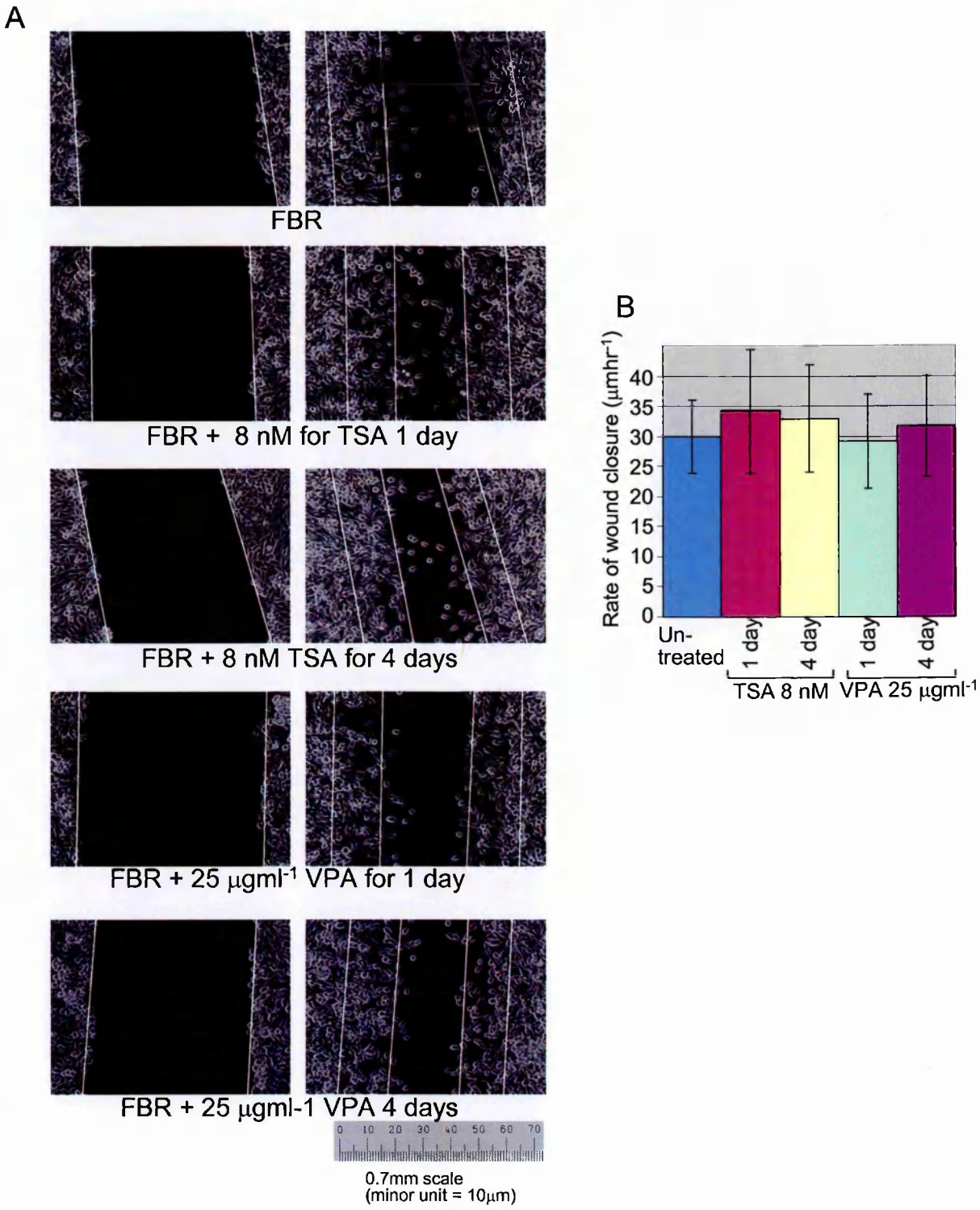

Figure 3.6

Motility of FBR cells treated with HDAC inhibitors

A. Phase microscopy of an example wounding assay with photographs taken from a time-lapse series, where images were captured concurrently at each time point.

"24 hour" treatment of FBR cells is, more exactly, 14 hours pre-treatment plus treatment for the duration of the assay. "4 day" treatment is, more exactly, 3.5 days pre-treatment plus treatment for the duration of the assay.

The left-hand column shows the wounds at t=0 and the right-hand column shows the wounds at t=13 hrs.

The scale bar shows that the initial wounds were on average 0.6mm.

White lines show the positions at which the measurements were taken.

B. Graph showing the rate of wound closure (μm per hour) in each case. Results depicted represent the average of 3 separate time-lapse experiments with single samples in each.

Higher concentrations of HDAC inhibitors inhibit motility of FBR cells

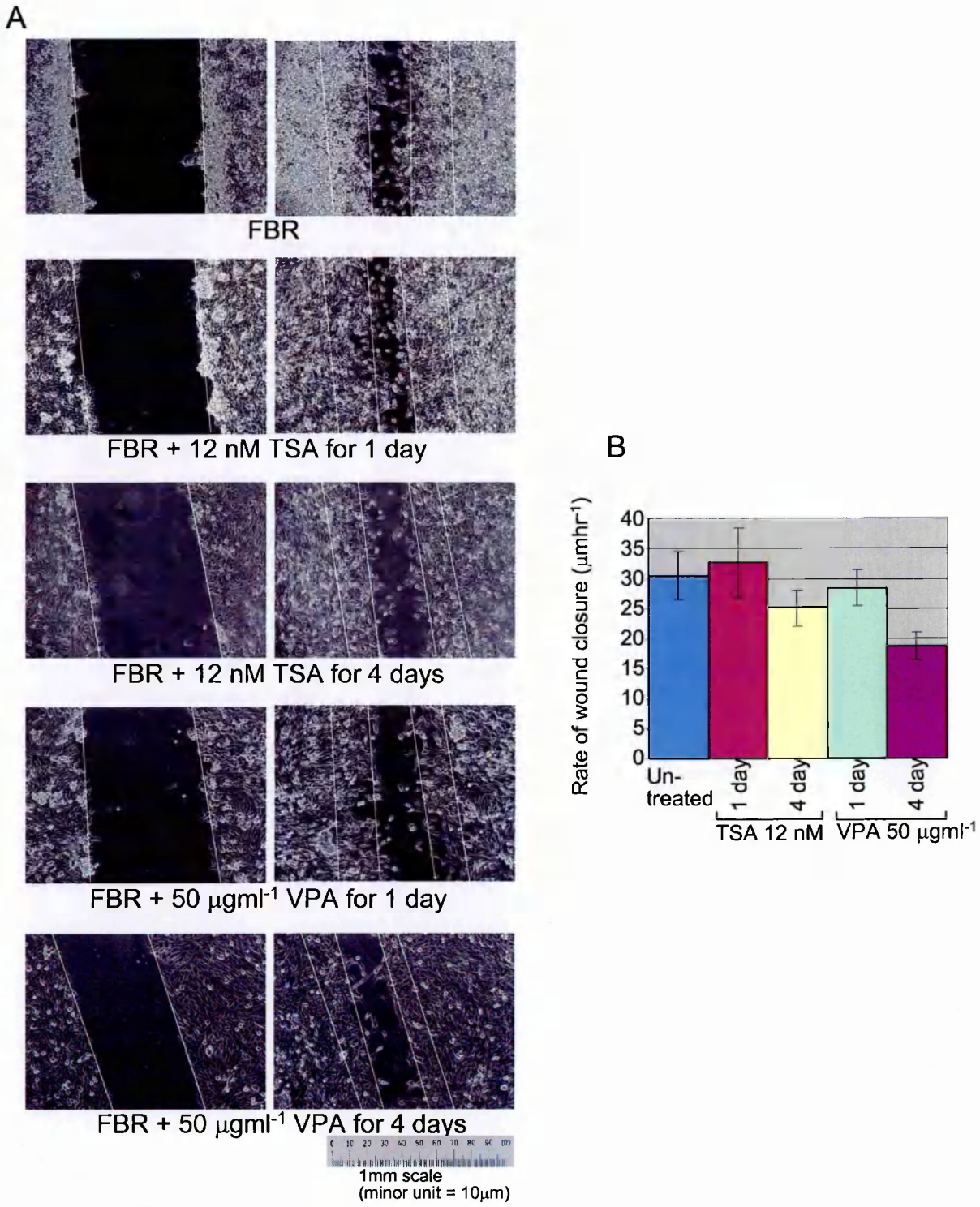

Figure 3.7

Motility of FBR cells treated with HDAC inhibitors.

A. Phase microscopy of an example wounding assay with photographs taken from a time-lapse series, where images were captured concurrently at each time point.

"24 hour" treatment of FBR cells is, more exactly, 14 hours pre-treatment plus treatment for the duration of the assay. "4 day" treatment is, more exactly, 3.5 days pre-treatment plus treatment for the duration of the assay.

The left-hand column shows the wounds at t=0 and the right-hand column shows the wounds at t=13 hrs.

The scale bar shows that the initial wounds ranged in width from 0.5 to 0.7mm.

White lines show the positions at which the measurements were taken.

B. Graph showing the rate of wound closure (μm per hour) in each case. Results depicted represent the average of 3 separate time-lapse experiments with single samples in each.

culture, to minimise any directional or chemotactic effects that could be present in the wound assay experiments. Cells were treated for 1, 2 and 4 days with TSA then their motility, over a three hour period, was monitored by time-lapse photography (Figure 3.8). We found that, when FBR cells are treated with 12 nM TSA, at 24 hrs there was no significant effect on cell motility, at 2 days, only cells which had flattened in response to TSA had reduced motility (cells with an intermediate morphology had an intermediate rate of movement; data not shown), and at 4 days, motility was significantly inhibited. At 8 nM TSA for 4 days, where, as we have shown, morphological reversion does not occur there is no measured effect on motility. We concluded that the cells became less motile only when morphologically reverted in response to TSA.

Later in this project, the advent of a more sophisticated technology in timelapse imaging (Section 2.2.6.2) and in the analysis and quantitation of motility ("Tracker" software by Kinetic Imaging) allowed us to repeat this experiment under more exacting conditions and such that the results are more easily quantified and presented. In these experiments we treated the FBR cells with VPA, but achieved similar results to those obtained earlier for TSA. Windrose diagrams (Figure 3.9) illustrate that there is little effect on motility with 25 μgml^{-1} VPA treatment. This shows, that the concentration of inhibitor, at which actin stress-fibres reform, and at which FBR cell invasion is inhibited, but at which morphological reversion does not occur, there is no effect on motility. When FBR cells are treated with 50 μgml^{-1} VPA for 4 days, and therefore have reverted morphology, motility is significantly inhibited. This shows that motility is inhibited at the concentration of inhibitor which causes reversion of FBR cell morphology.

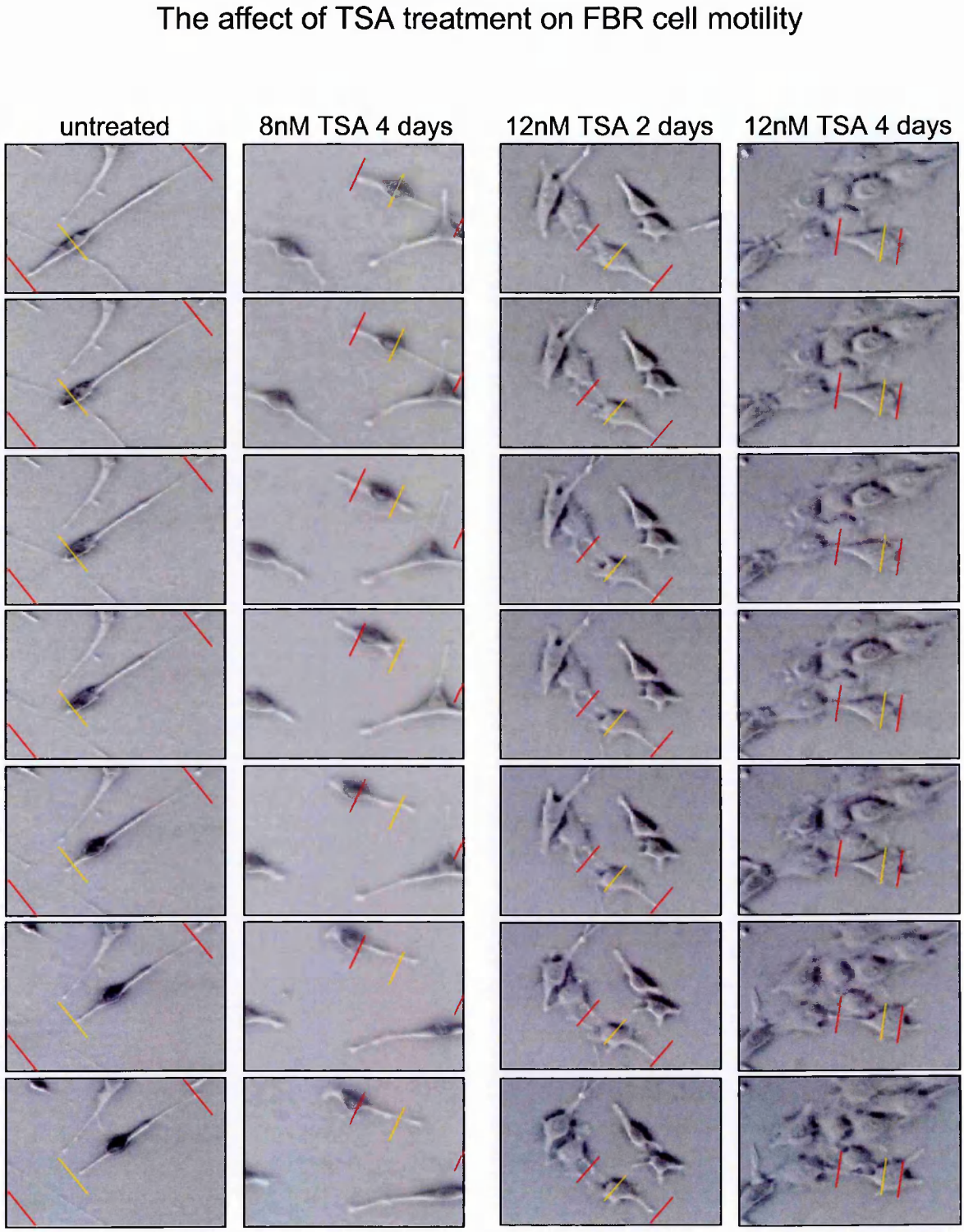

Figure 3.8

Digital phase contrast microscope images from timelapse sequences, taken of FBR cells which have been treated with TSA at indicated concentrations and durations. Yellow lines mark the starting positions of the nucleus, and red lines indicate the starting positions of the extremes of the pseudopods.
These images show that when FBR cells are treated with 12 nM TSA, at 24 hrs there is no significant affect on cell motility, at 2 days cells which have flattened in response to TSA have reduced motility and at 4 days motility was significantly inhibited. Motility is unaffected when FBR cells are treated with 8 nM TSA for 4 days.

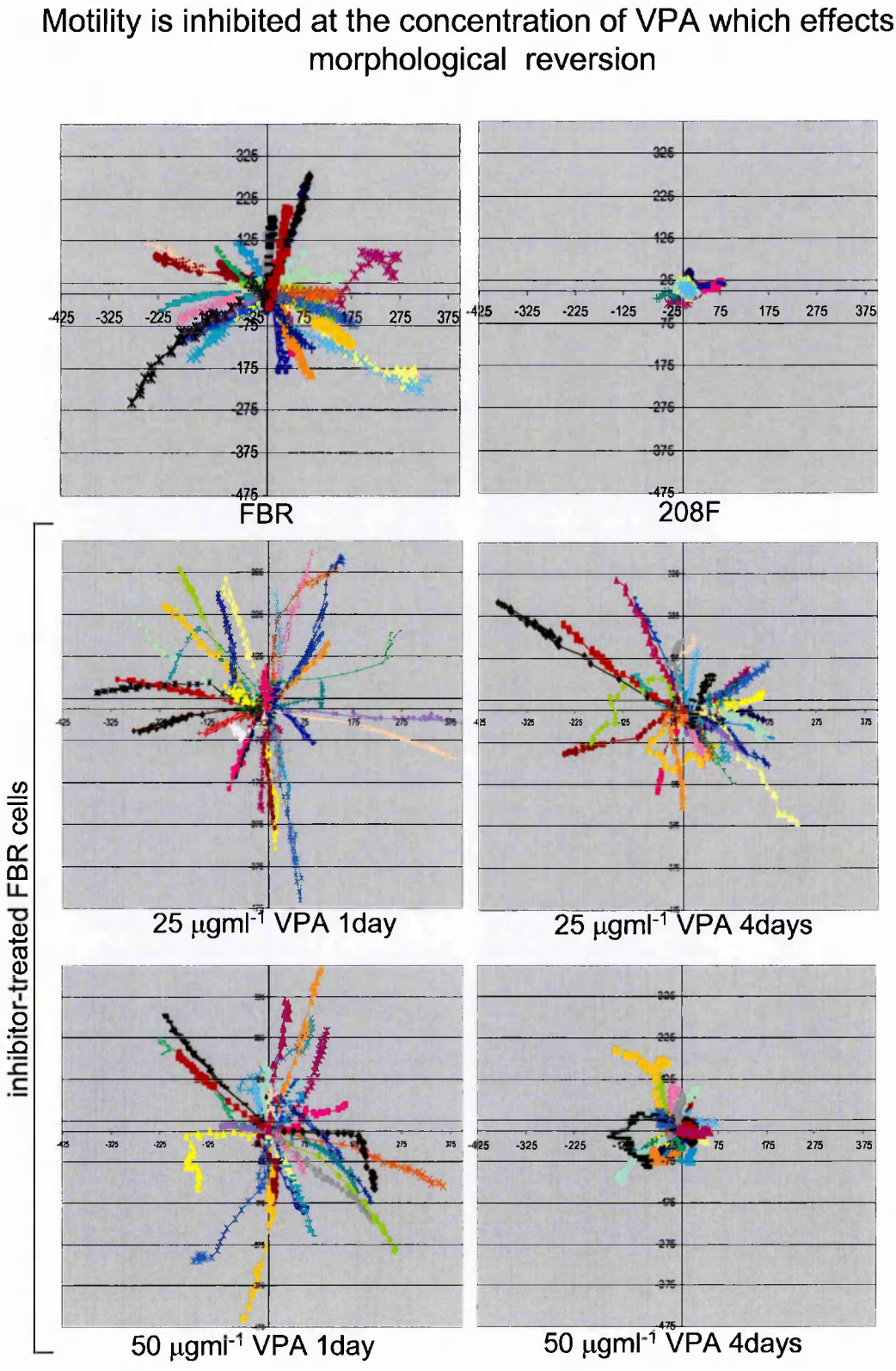

Figure 3.9

Windrose diagrams which show that treatment with 25 μgml^{-1} VPA for up to 4 days, or with 50 μgml^{-1} for 1 day, does not affect the motility of FBR cells; but that treatment with, 50 μgml^{-1} VPA for 4 days, significantly inhibits motility. Each diagram shows the tracks of 30 cells overlayed with the same origin. Tracks were taken from timelapse sequences, with images (at 64X magnification) captured every 10 mins for 5 hours.

3.2.5 Effect on invasion

By *in vitro* inverse invasion assay, FBR cells are invasive compared with 208F cells (Hennigan et al. 1994). To determine whether the up-regulated histone deacetylases in FBR cells, contribute to their ability to invade, we performed this invasion assay (Section 2.2.7). The FBR cells were treated with HDAC inhibitors to determine whether inhibiting histone deacetylases also inhibits invasion. TSA and VPA were used at concentrations which, as we had previously determined, do not affect the proliferation rate of the cells (Section 3.2.2), and which do not affect the motility of the cells within a time period equivalent to the duration of the assay. Our results showed that both HDAC inhibitors were able to inhibit invasion of FBR cells at these concentrations (Figure 3.10A). The extent of inhibition is dose dependent, and inhibition by can be measured even at concentrations of inhibitor lower than that required to revert their morphology (Figure 3.10B). This provides evidence then, that histone deacetylases have a role in effecting invasion.

3.2.6 Effect on chemotaxis

It could, however, be argued that impaired invasive ability may actually be a product of impaired chemotaxis, since it was previously shown in this laboratory, that in the absence of Matrigel (which provides chemotactic factors), FBR cells do not migrate to the upper surface of the filter in an inverse invasion assay (Hennigan et al. 1994). To discount this possibility we further quantified the original invasion assays, determining the number of cells which had migrated to the upper surface of the filter and expressing them as a proportion of those cells remaining on the underside. We found that there is no significant difference in migration between untreated FBR cells and those treated with TSA or VPA, at the concentrations used (Figure 3.11). Therefore,

Histone deacetylase inhibitors inhibit invasion in FBR cells

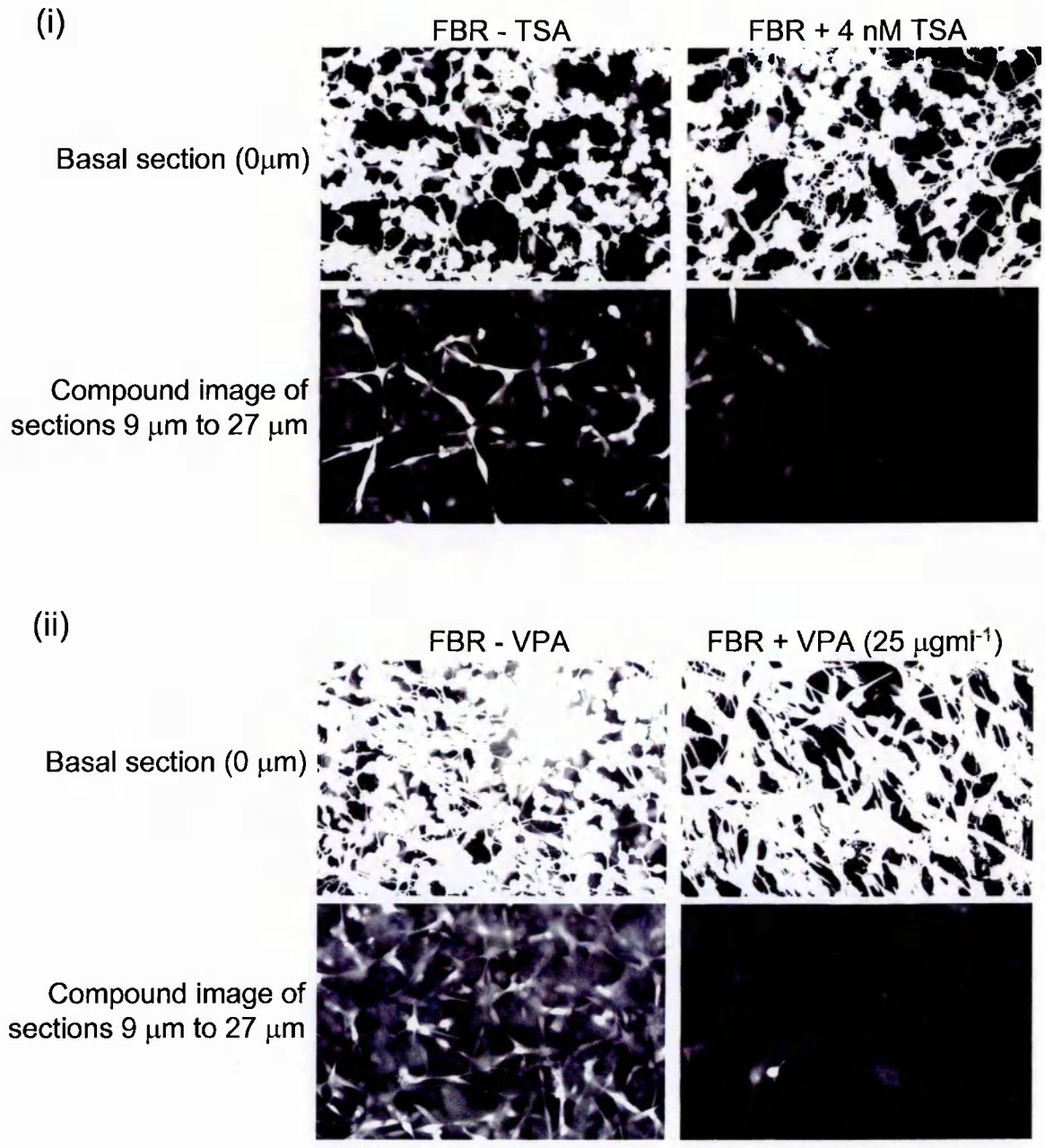

Figure 3.10A

Invasion assays showing FBR cell invasion is inhibited by histone deacetylase inhibitors. The protocol and quantitation of invasion assays is fully described in Section 2.2.7. Briefly, basal sections show those cells which have remained on the filter and have, therefore, not invaded. The compound images show all cells which have travelled 9 μm or more into the Matrigel and are therefore invasive.

(i) 4 nM TSA inhibits invasion of FBR cells.

(ii) 25 $\mu g ml^{-1}$ VPA inhibits invasion of FBR cells.

Invasion in FBR cells is inhibited by histone deacetylase inhibitors at concentrations which do not alter morphology, motility or growth rate

(i)

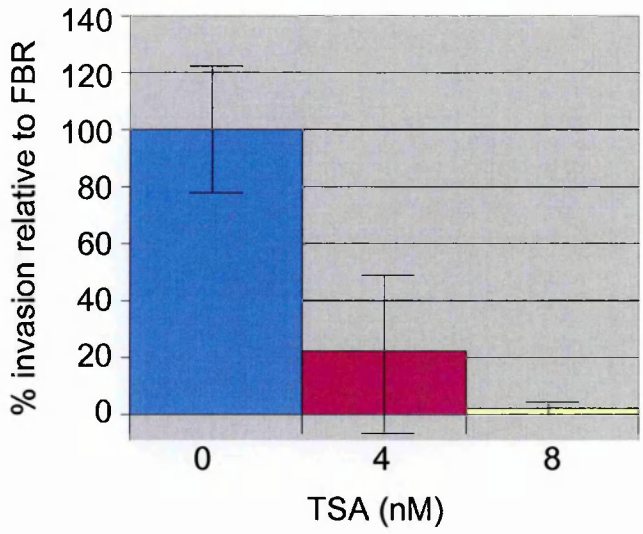

(ii)

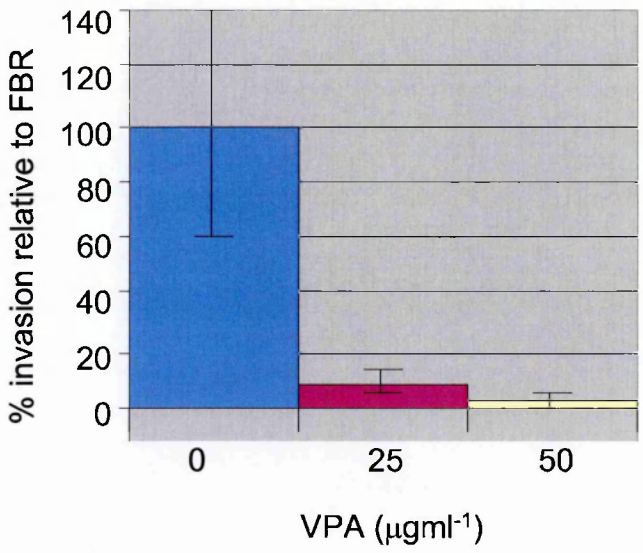

Figure 3.10B

Histograms of quantified results from invasion assays (Figure 3.10A).

(i) Invasion of FBR cells is inhibited by 4 nM and 8 nM TSA.

(ii) Invasion of FBR cells is inhibited by 25 μgml^{-1} and 50 μgml^{-1} VPA.

Overall results were determined from at least three separate assays with at least duplicate samples within each.

The chemotaxis of FBR cells is unaffected by HDAC inhibitors at concentrations which inhibit invasion

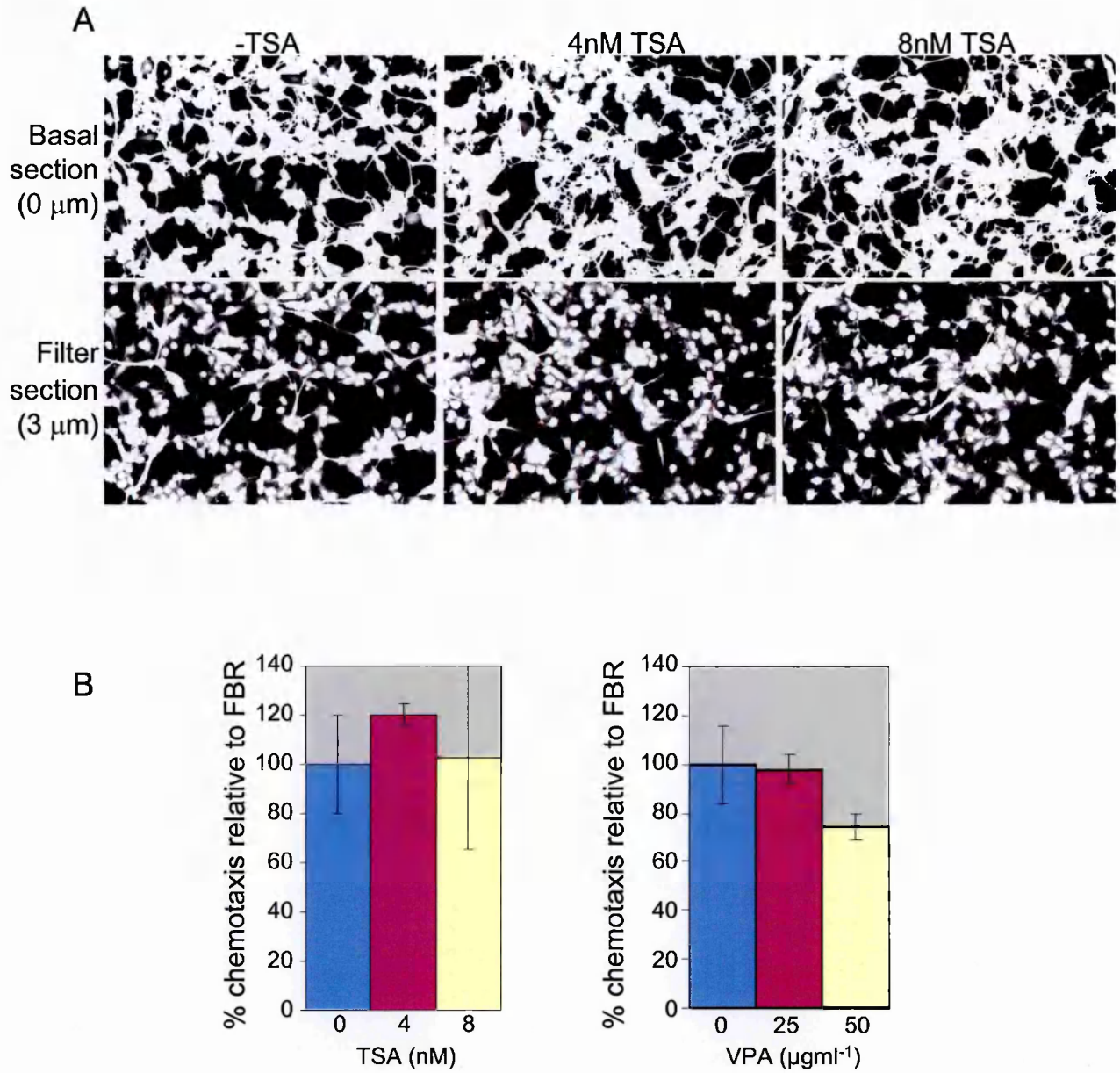

Figure 3.11

A. Example sections used to quantify chemotaxis. The upper row shows those cells remaining on the underside of the filter and the lower row shows those cells which have moved through the filter pores to the upper surface of the filter. In quantitation a high background value must be subtracted to avoid bleed-through from the basal section, to the filter section, affecting the result; also the chemotactic cells were counted by eye to verify and validated the computer quantitation.

B. Histograms showing that the chemotactic response in FBR cells treated with 8nM TSA or 25 μgml^{-1} VPA for 4 days is equivalent to that of untreated cells. Each graph is produced from the combined quantitation of three assays with duplicate samples in each.

HDAC inhibitors, at these concentrations do not affect the chemotactic response of the cells.

3.2.7 The effect of histone deacetylase inhibition on EGF-stimulated invasion of 208F cells

In a supplementary experiment we also showed that TSA inhibits EGF-induced invasion of 208F cells (Figure 3.12). EGF binding at the cell surface signals through the Ras/Raf/MEK/ERK transduction pathway to Fos. Thus EGF treatment of 208F cells is an alternative way of up-regulating AP-1. This experiment, therefore, supports our proposal that invasion, as a consequence of increased Fos activity, is facilitated by histone deacetylases.

3.3 Conclusions

In this chapter we have shown that HDACs are up-regulated in Fos-transformed cells and that HDAC activity is required for Fos-transformed morphology, actin structure, motility and invasion. We have also seen that the different aspects of the transformed phenotype are reverted at different concentrations of HDAC inhibitor. Table 3.1 shows that invasion is inhibited and stress-fibres reform at 25 $\mu g ml^{-1}$ VPA or 8 nM TSA; transformed morphology reverts and motility is inhibited at 50 $\mu g ml^{-1}$ VPA or 12 nM TSA; and finally, cell proliferation is inhibited at 100 $\mu g ml^{-1}$ VPA or 20 nM TSA. These results suggest that individual aspects of transformation are controlled by specific groups of genes.

Inhibition of histone deacetylases inhibits EGF-induced invasion in non-transformed cells

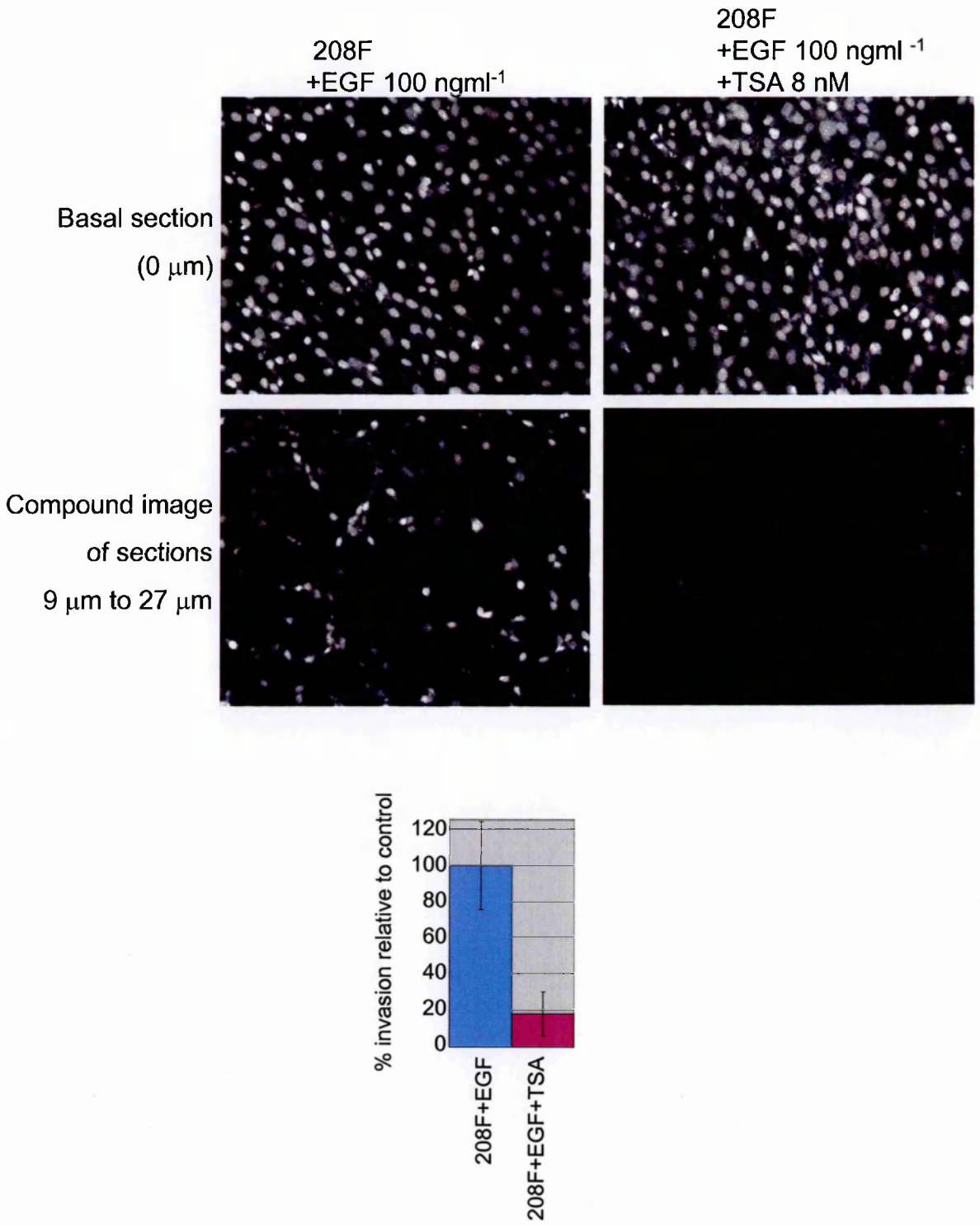

Figure 3.12

Inhibition of HDACs inhibits EGF-induced invasion of 208F cells. 208F cells can be induced to invade by treatment with EGF at 100 ngml^{-1}. This invasion is inhibited by 8 nM TSA.

The protocol and quantitation of invasion assays is fully described in Section 2.2.7. Briefly, basal sections show those cells which have remained on the filter and have, therefore, not invaded. The compound images show all cells which have travelled 9 μm or more into the Matrigel and are therefore invasive. The cells were stained using the nuclear stain propidium iodide which accounts for the apparent difference in appearance between this and previous assays.

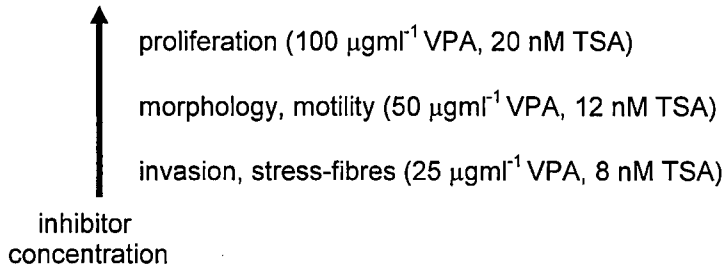

Table 3.1

Summary of the effects of HDAC inhibitor treatment on FBR cells, showing the relationship between concentration of inhibitor used and the aspect of the FBR phenotype which is affected.

Chapter 4

Genes down-regulated by histone deacetylation

4.1 Genes down-regulated in Fos-transformed cells: their expression levels in response to inhibition of histone deacetylases

4.1.1 Introduction

HDACs are involved in gene silencing (Section 1.2.2.3). For this reason we asked whether the increased HDAC expression we find in FBR cells, relative to 208F cells, facilitates silencing of those genes found, previously, to be *down*-regulated in FBR cells (Johnston et al., 2000). Thus, if we inhibit HDAC activity, by treatment with VPA or TSA, are these down-regulated genes re-expressed?

4.1.2 Expression levels of RYBP, PCDHGC3 and STAT6

Northern analyses demonstrated that a proportion of those genes down-regulated (at the level of transcription) in Fos-transformation are indeed re-expressed in FBR cells when HDAC activity is inhibited by treatment with either VPA or TSA. Of the 11 genes investigated, those genes found to be re-expressed are: RYBP; STAT6; PCDHGC3; fibronectin; and annexin IVA (Figure 4.1; section 1.5). In fact, in an initial experiment to determine optimal TSA concentration and treatment duration, for re-expression of STAT6, we also showed that this re-expression is time and dose dependent (Figure 4.1B). Those genes not found to be re-expressed are: cellular retinol binding protein 1 (CRBP-1); TSC36; frizzled related protein 4 (Frp4); latent transforming growth factor β binding protein (LTBP); caspase II; plus a mRNA identified by a novel cDNA sequence (clone PD18) from the initial differential screen (Figure 4.2A and B). In addition, western analysis of tuberosclerosis complex 1 (TSC1) expression showed that this tumour suppressor protein was also not re-expressed (at the protein level) on inhibition of HDACs (Figure 4.2C).

Inhibition of HDAC activity facilitates re-expression of genes down-regulated in v-Fos^{FBR}-transformed cells

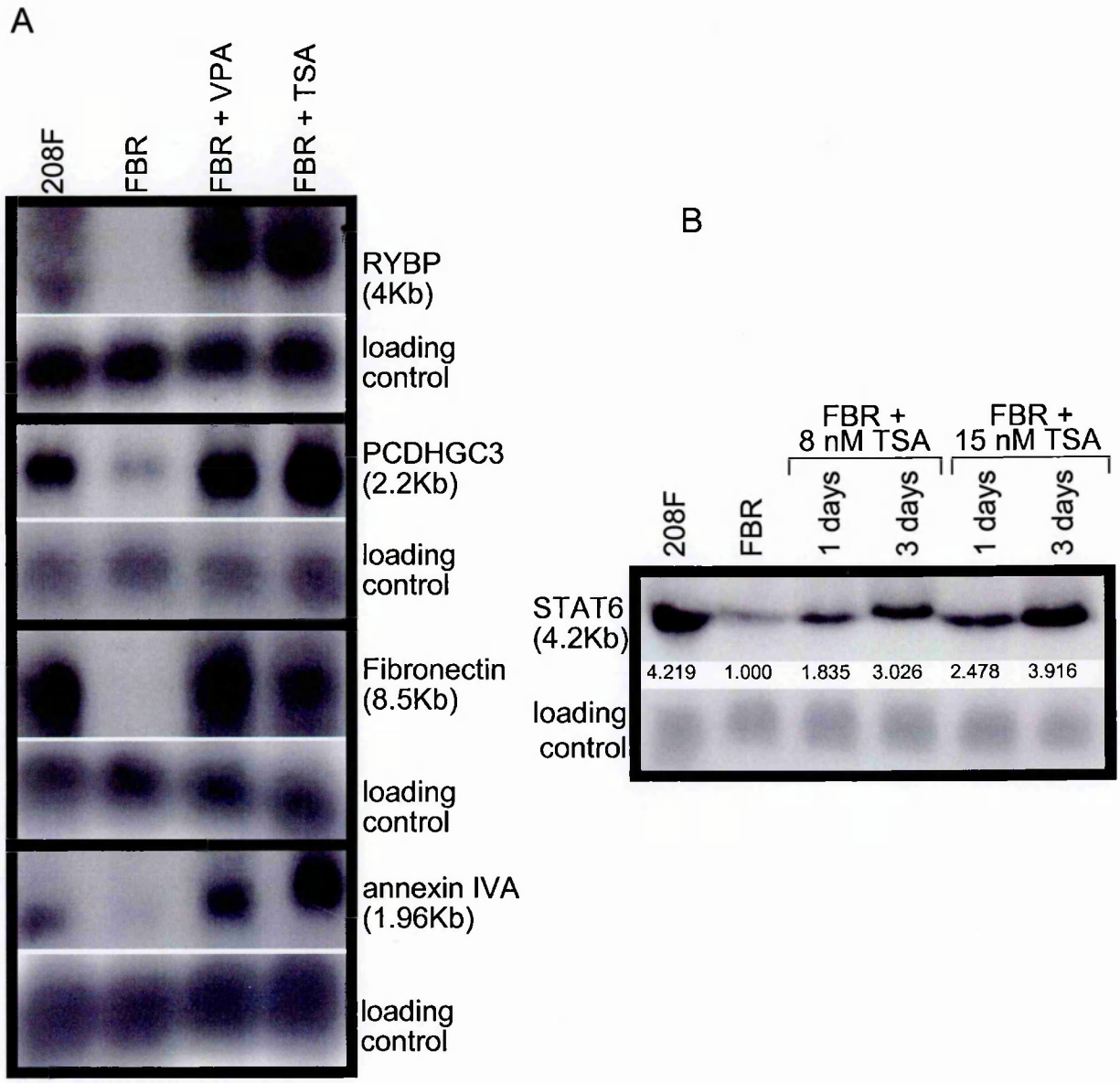

Figure 4.1

Northern blots showing:

A. The re-expression of RYBP, PCDHGC3, fibronectin and annexin IVA, in FBR cells treated with VPA (4 days, 25 $\mu g ml^{-1}$) or TSA (4 days, 8 nM).

B. The re-expression of STAT6 in response to TSA treatment is time and dose dependent. Values represent relative expression, in units of OD x mm^2, normalised to the loading control.

All loading controls are 7s rRNA.

Inhibition of HDAC activity does not facilitate re-expression of all genes down-regulated in v-Fos^{FBR}-transformed cells

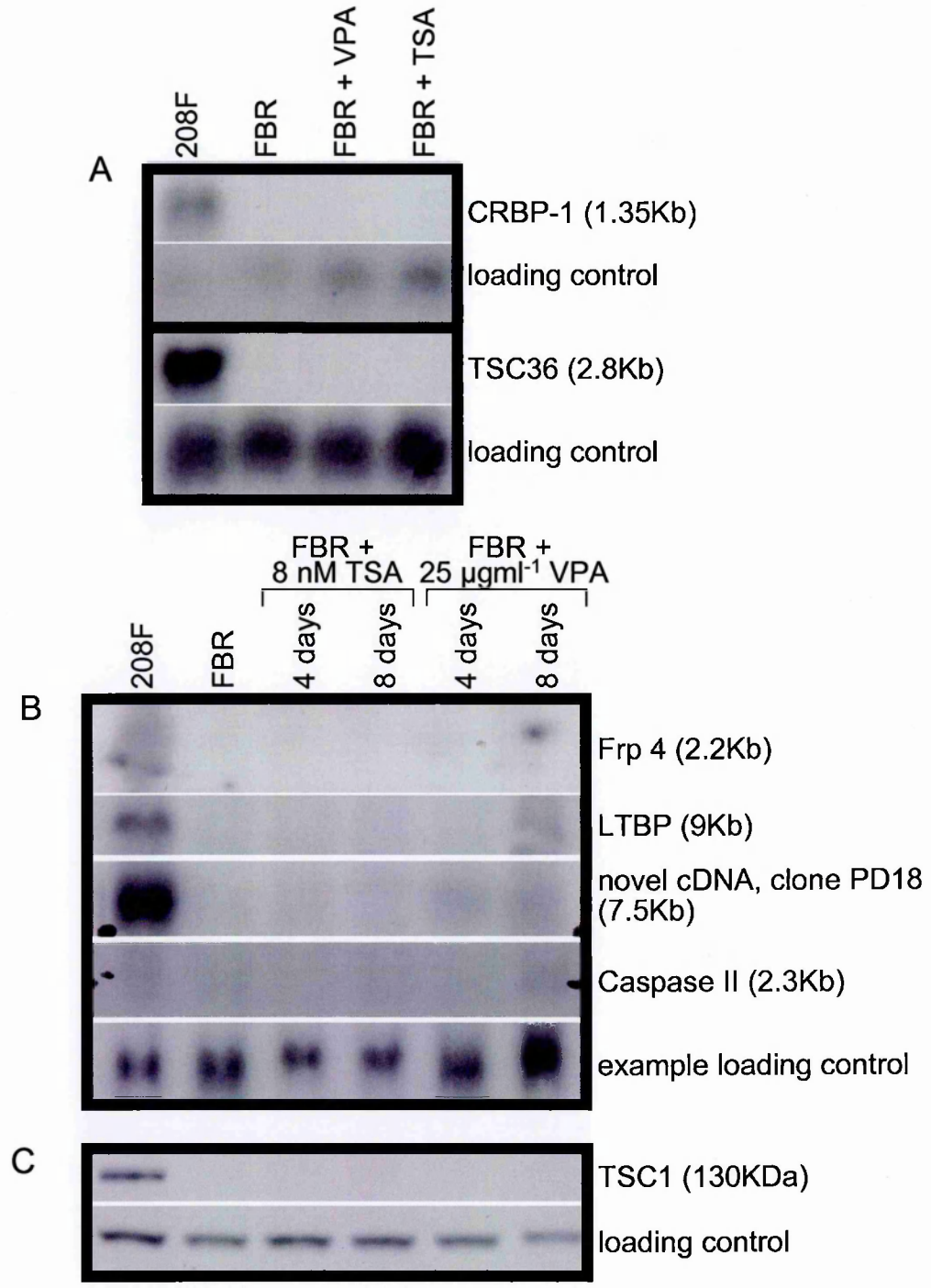

Figure 4.2

A. Northern blots showing CRBP-1 and TSC36 are not re-expressed in FBR cells when treated with VPA (4 days at 25 µgml^{-1}) or TSA (4 days at 8 nM). Loading controls are 7S rRNA.

B. Northern blots showing Frp 4, LTBP, caspase II, and the mRNA labelled with the novel cDNA probe, PD18, are not re-expressed in FBR cells when treated with 8 nM TSA or 25 µgml^{-1} VPA for 4 or 8 days. Example loading control is 7S rRNA.

C. Western blot showing TSC1 is not re-expressed in FBR cells treated with 8 nM TSA or 25 µgml^{-1} VPA for 4 or 8 days. Loading control is ERK2.

4.2 Ectopic re-expression of genes down-regulated in Fos-transformed cells

4.2.1 Introduction

We have shown that inhibition of HDACs inhibits the ability of FBR cells to invade and that inhibition of HDACs results in re-expression of down-regulated genes. We asked then, is invasion inhibited as a consequence of re-expression of these down-regulated genes? Is re-expression of these genes incompatible with invasion? To answer our question we ectopically re-expressed (individually) genes which are re-expressed as a consequence of HDAC inhibition, and asked whether invasion is inhibited.

4.2.2 Sub-cloning of RYBP, PCDHGC3 and STAT6, verification of sequence and molecular weight, and correct expression in cells

We chose three of the genes which we have shown to be re-expressed on inhibition of HDACs and investigated the effect of their individual ectopic re-expression in FBR cells. The genes were each cloned into the vector pEGFP-N1, which provides a 3' EGFP-tag, and introduced, individually, into FBR cells by nucleofection; an adaptation of the electroporation method, which delivers the vector directly to the nucleus. Having optomised the nucleofection protocol to achieve greater than 80% efficiency (data not shown) we were able to study transient, as well as, stable expression of these genes in FBR cells, which enabled us to discount any error arguably inherent in either system. Before expression in FBR cells, we confirmed the accuracy of the sequence of the cloned genes and of the gene/vector-junctions by DNA sequencing (carried out by BICR technology services) and demonstrated, by western analysis, the expression of a protein of the expected molecular weight, in Cos-7 cells (Figure 4.3A). Mouse endogenous RYBP is reported to be 32 KD and the untagged mouse cDNA to encode a protein of similar size (Garcia et al., 1999). We therefore expected, and were able to

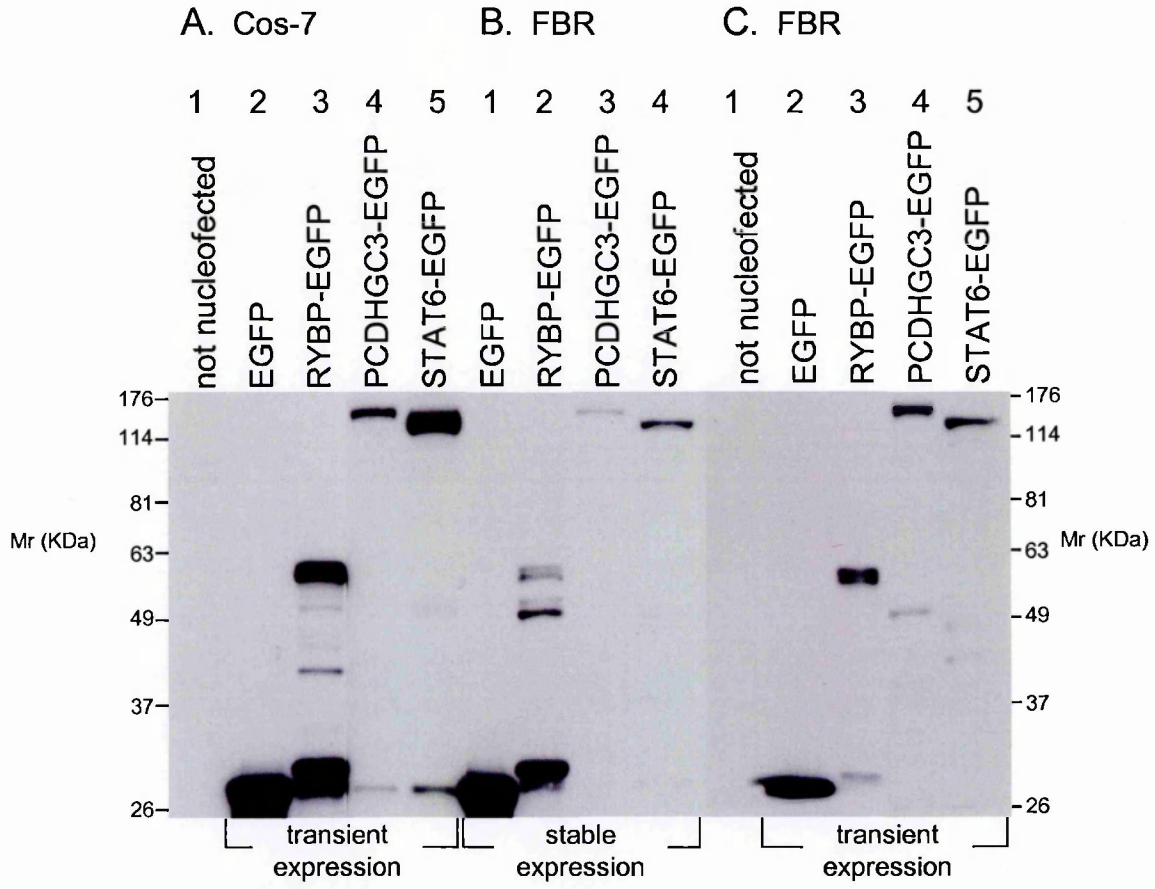

Figure 4.3

Western analysis of total cell lysates (25 µg per lane) using anti-EGFP mAb.

A. Transient expression in Cos-7 cells. Lane 1: un-transfected control. Lane 2: EGFP-only expressing control. Lanes 3-5: expression of 3'-EGFP-tagged-, RYBP, PCDHGC3 and STAT6, respectively.

B. Stable expression in FBR cells. Lane 1: EGFP-only expressing control. Lanes 2-4: expression of EGFP-tagged-, RYBP, PCDHGC3 and STAT6, respectively.

C. Transient expression in FBR cells. Lane 1: un-transfected control. Lane 2: EGFP-only expressing control. Lanes 3-5: expression of EGFP-tagged-, RYBP, PCDHGC3 and STAT6, respectively.

demonstrate, a protein of 59 KD (including the 27 KD EGFP-tag) transiently expressed in the Cos-7 cells. We showed the human, EGFP-tagged, PCDHGC3 cDNA to encode a protein of approximately 160 KD, again, allowing for the tag, the encoded protein should therefore, be 133 KD. Previously, it has been reported to encode a protein of "approximately" 150 KD (Sano et al., 1993) referring to a band between the, 97 and 200 KD molecular weight markers, which could equally be approximated to 133 KD. The murine STAT6 cDNA is reported to encode a major protein of 102 KD and a minor protein of 84 KD (Quelle et al., 1995), we would therefore expect a major band of 129 KD, and a minor band of 111 KD. This is indeed what we see in Cos-7 cells, although the minor band accounts for a very small proportion of the total.

The expression vectors were then introduced into FBR cells and the correct, both stable and transient, expression products confirmed by the same means (Figure 4.3B and C). Sizes were as expected, though the RYBP cDNA appears to encode a doublet at 59 KD, in both transients and stables, as well as a further doublet at 49 KD in stably expressing cells. One possible explanation is that this represents (at 59 KD) a post-translational modification and (at 49 KD) cleavage products of both larger bands, where a 10 KD peptide has been removed from the N-terminus of the protein.

4.2.3 Cellular localisation and distribution of re-expressed proteins

We then examined the spacial distribution and localisation of the ectopically expressed proteins in the FBR cells (Figure 4.4). EGFP is uniformly distributed within the cell. RYBP-EGFP is expressed only in the nucleus. PCDHGC3-EGFP is expressed primarily in the plasma membrane. Confirmation of the correct localisation is particularly important in the case of PCDHGC3 since it is a transmembrane protein

Localisation of ectopically re-expressed genes in v-Fos^{FBR}-transformed cells

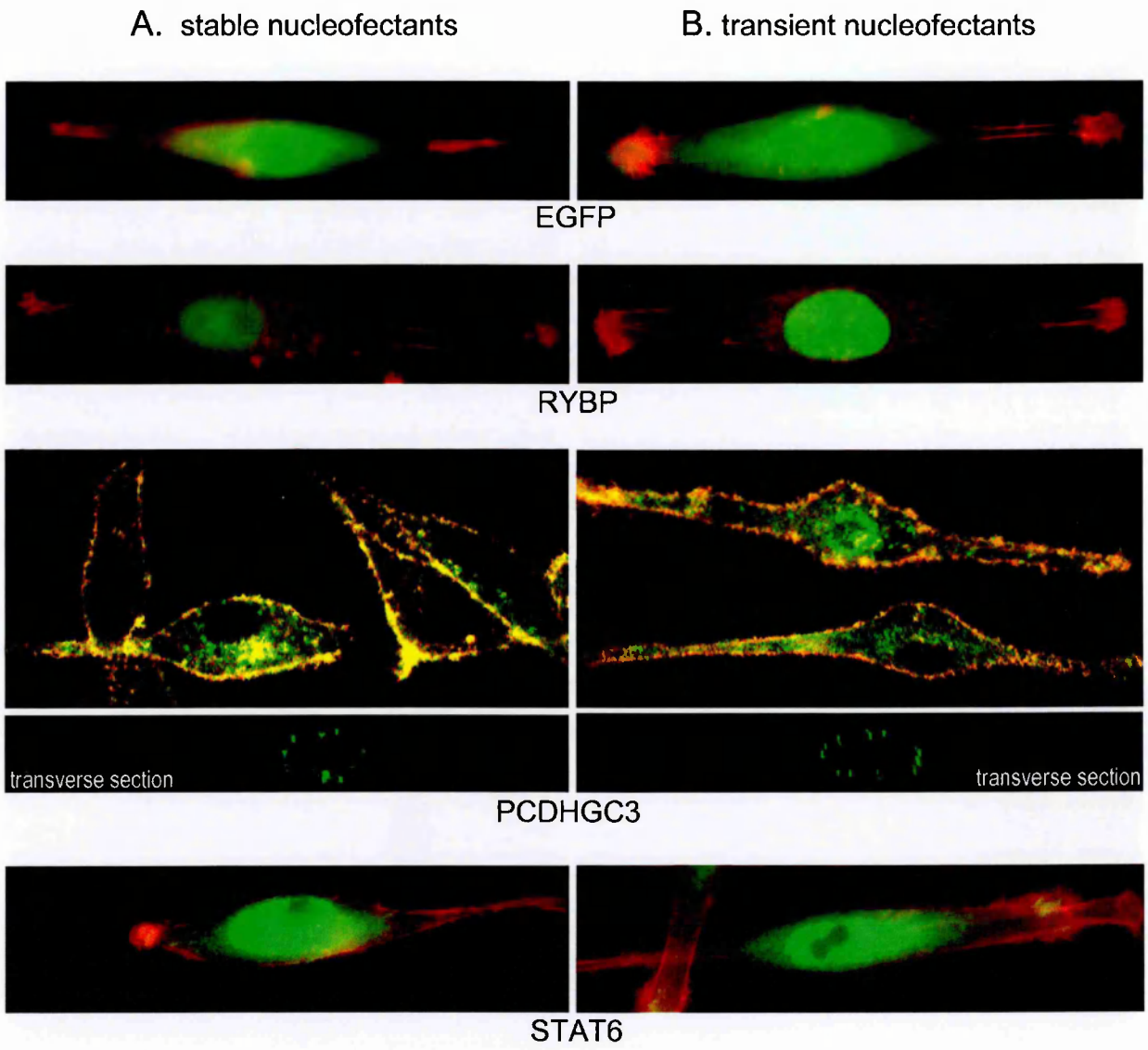

Figure 4.4

The localisation of ectopically expressed proteins in FBR cells.

A. Shows stable expression

B. Shows transient expression

Expressed proteins are EGFP-tagged, and therefore, green-fluorescent. F-actin is stained with TRITC-conjugated phalloidin and is, therefore, red-fluorescent.

PCDHGC3-expressing FBR cells are also shown in transverse section (F-actin not shown) further illustrating the localisation of the protein.

and its correct localisation may have been hindered by the presence of the EGFP-tag. It was for this reason that the tag was added in the 3' position since it is the N-terminus of the protein which has to traverse the plasma membrane. We also visualised the PCDHGC3-expressing FBRs (FP cells) in transverse section to more clearly define the distribution of PCDHGC3 in the membrane (Figure 4.4). STAT6-EGFP has an almost similar distribution to EGFP, however, STAT6-EGFP is considerably less bright, is excluded from the nucleoli, and can be seen more predominantly in the nucleus, consistent with its role as a transcription factor which shuttles between cytoplasm and nucleus. In addition, the fact that there is virtually no 27 KD band in western analysis of whole cell extracts from STAT6-EGFP-expressing (FS) cells (Figure 4.3B and C), confirms that the distribution pattern is not created as an artefact by cells within the population expressing only EGFP.

For all three proteins, in comparing transient versus stable transfectants there was no perceived difference in their distribution and localisation within the FBR cell.

4.2.4 Morphology and actin stress-fibres in FBR cells over-expressing RYBP, PCDHGC3 or STAT6

In FBR cells over-expressing RYBP (FR cells), PCDHGC3 or STAT6, we were unable to detect any change in morphology or in actin stress-fibre arrangement, as determined by TRITC-phalloidin staining (Figure 4.4). This was found to be the case for both transient and stable expression of the proteins in FBR cells.

4.2.5 Effect on invasion

We then assessed invasive ability, firstly of the *stable* transfectants expressing each of the transgenes. We found that in a three day inverse invasion assay (Section 2.2.7), both the parental FBR cells and FBR cells expressing only EGFP (FE cells) invaded

equally, and to the extent expected of FBR cells (Figure 4.5A). In contrast, FR, FP, and FS cell lines, showed markedly reduced invasion compared with these controls. FR cells in particular showed, on average, a 96% reduction in invasion, FP cells were approximately 92% reduced, whilst PS cells were the least inhibited, though still with a substantial overall reduction in invasion of 80%.

In similar experiments with FBR cells transiently expressing the cDNAs, cells were transferred to the invasion assay immediately following nucleofection and simultaneously (on each repetition of the experiment) were seeded, into the appropriate culture vessel, for fluorescent analysis by confocal microscopy (to confirm that 80% or more of the cells were expressing the protein, and with the expected distribution) and for western analysis (to confirm the correct size of expressed protein). The results from invasion assays of these transiently transfected cells (Figure 4.5B) were similar to those obtained for the equivalent stable cell lines, in that invasion was markedly inhibited in each case. The reduction in the transient transfectants was reduced to approximately 60%, and was similar for transient FR, FP and FS cells.

Since the expression of all three proteins (individually) appears to inhibit invasion, the question arises as to whether the effect we see is due to the expression of these protein *per se* or rather the non-specific by-product of the inappropriate and high level of expression of these proteins. For this reason, we carried out the following control experiments to validate our results.

4.2.6 Effect on proliferation

Firstly, we made a comparison of growth rates, which confirmed that exogenous expression of RYBP or PCDHGC3 or STAT6 does not affect the proliferation of the cells relative to the parental FBR cells or to the empty-vector-expressing control FBR

Re-expression of RYBP, PCDHGC3 or STAT6, inhibits invasion of v-Fos^{FBR}-transformed cells

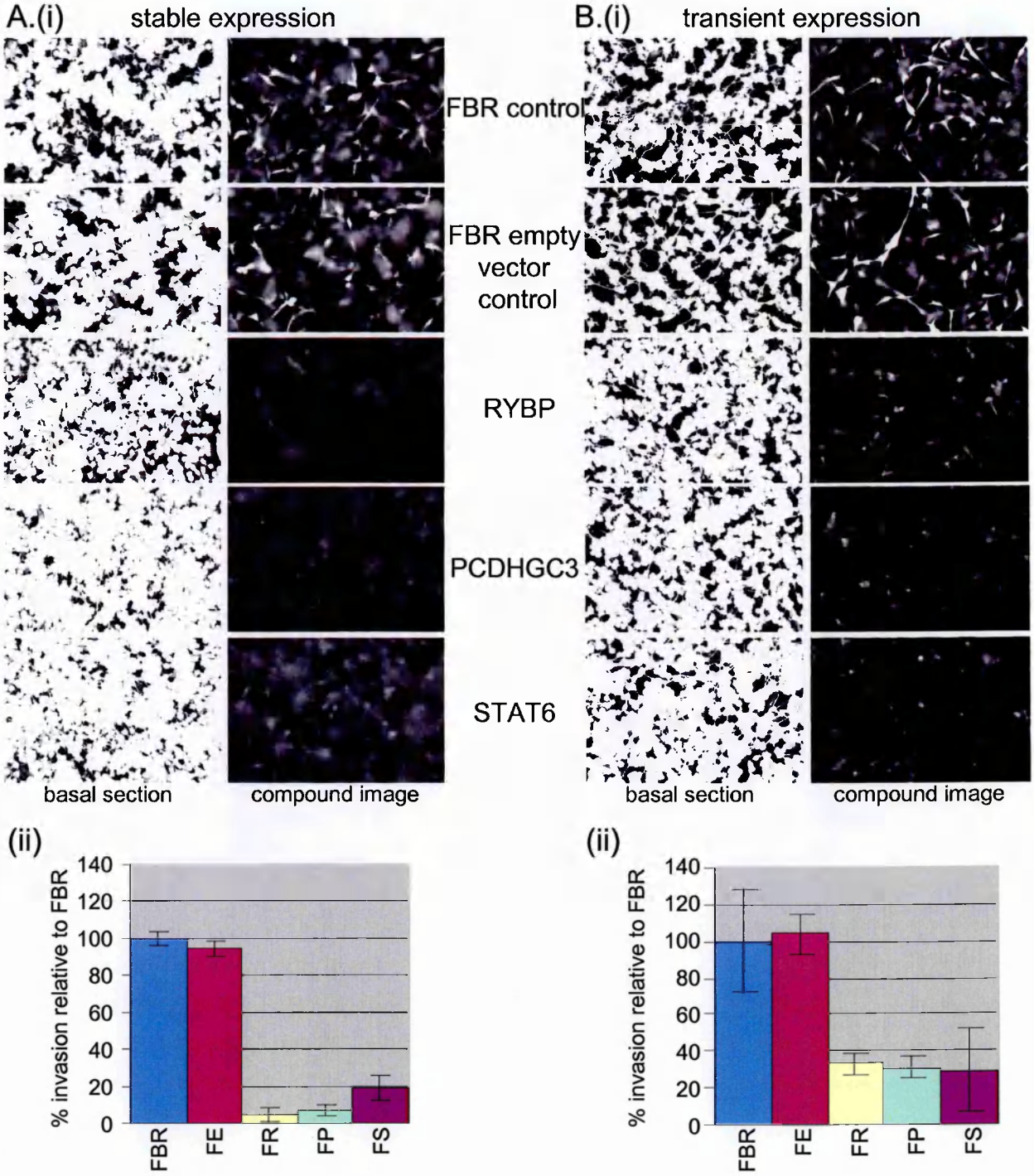

Figure 4.5

A. Stable expression of RYBP or PCDHGC3 or STAT6, inhibits the ability of FBR cells to invade relative to parental FBR cells or to EGFP-expressing FBR cells.

(i) Examples of images used to quantify the assay (Section 2.2.7). Basal sections show those cells which have remained on the filter and have, therefore, not invaded. The compound images show all cells which have travelled 9 μm or more into the Matrigel and are therefore invasive.

(ii) Histogram showing inhibition of invasion by RYBP or PCDHGC3 or STAT6, produced from the integrated quantitation of three separate assays with at least duplicate samples in each.

B. As in A. above, but with transient expression of RYBP or PCDHGC3 or STAT6 .

cells (Figure 4.6). Their rate of proliferation is, therefore, unaltered by the expression of these proteins. Moreover, the results obtained for stable and transient expressors are equivalent.

4.2.7 Effect on motility

To determine whether the cells are unable to invade because their motility is inhibited, we carried out wounding assays, and followed the rate of migration of the cells by time-lapse photography, as they moved to close a wound, this was done simultaneously for each cell population. For each assay the final time point was defined as that point immediately before cells from one side of the wound came in contact with those from the other side. We were able to demonstrate that ectopic expression of RYBP or PCDHGC3 or STAT6 has no effect on the motility of FBR cells (Figure 4.7); all cell lines were able to move to close a wound at a rate of approximately 32μmhr^{-1}.

4.2.8 Effect on chemotaxis

As with the HDAC inhibitor studies (Chapter 3), the possibility that the transfected cells are unable to invade due to impaired chemotaxis was investigated by analysis of the invasion assays. The migration of cells from the base of the filter, through the filter-pores to the upper surface is a measure of chemotaxis since it was previously shown in this laboratory that FBR cells will not migrate to the upper surface of the filter in the absence of Matrigel or serum (Hennigan et al., 1994; Lamb et al., 1997), i.e., without a chemoattractant. We found that the number of FBR cells migrating to the top of the filter is unaffected by the expression of RYBP, PCDHGC3 or STAT6 (Fig. 4.8), despite the marked effect we observe, on their migration into the Matrigel itself.

Re-expression of RYBP, PCDHGC3 or STAT6, in v-Fos^{FBR}-transformed cells does not affect their rate of proliferation

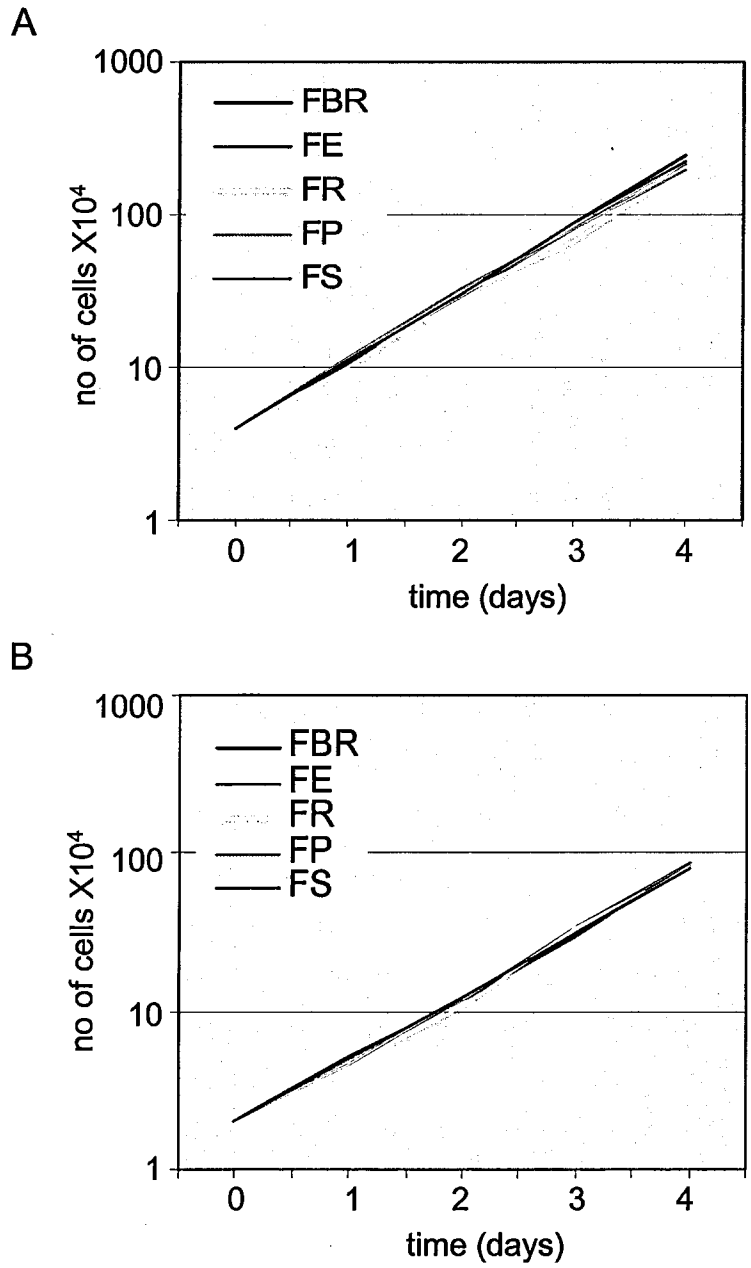

Figure 4.6

A. Growth rate of stable transfectants. Cells were seeded at 4 x 10^4 per well, at the same time as they were seeded in an invasion assay. Results depicted were derived from 4 separate wells per cell line per invasion assay.

There is no significant difference between the control, FBR and FE cells, compared with the experimental, FR, FP and FS cells.

B. Growth rate of transient transfectants. Cells were seeded at 2 x 10^4 per well, at the same time as they were seeded in an invasion assay. Results depicted were derived from 4 separate wells per cell line per invasion assay.

There is no significant difference between the control, FBR and FE cells, compared with the experimental FR, FP and FS cells. A lower number were seeded compared to the stable transfectants because cell numbers are limited by concentrations required for nucleofection.

Motility of FBR cells is unaffected by re-expression of down-regulated genes

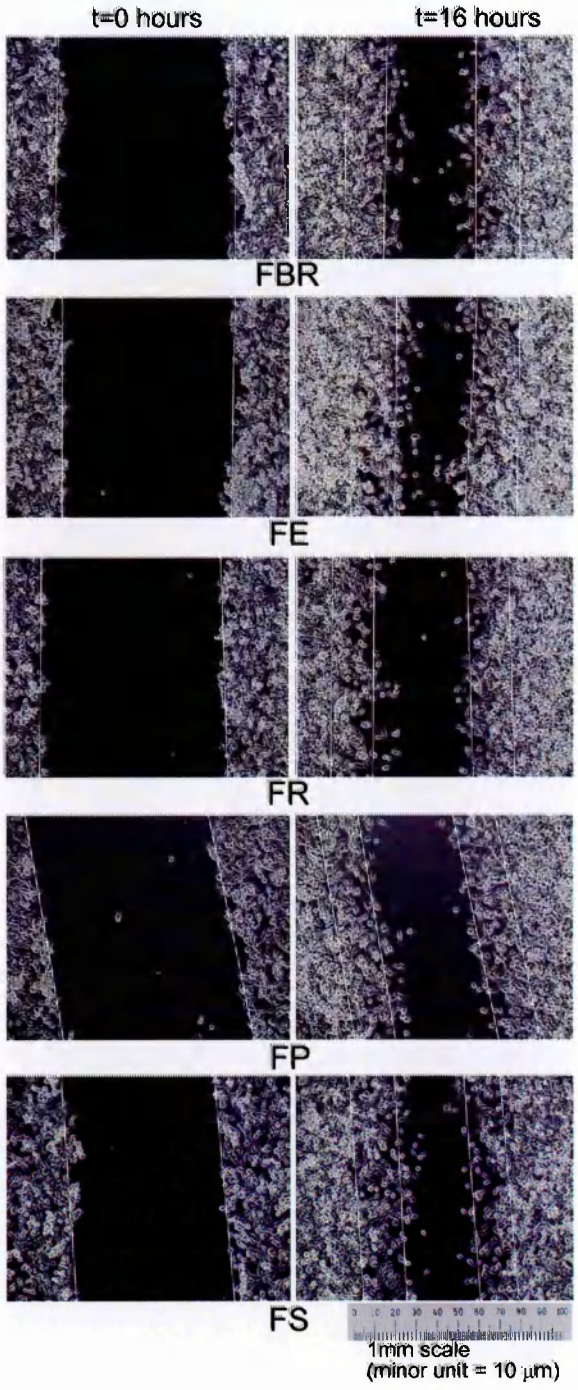

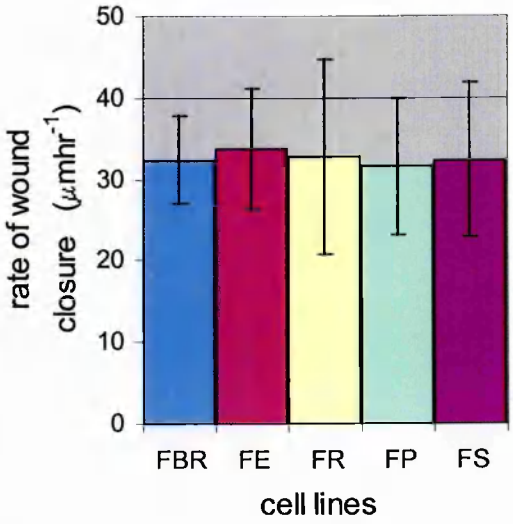

Figure 4.7

A. Example wounding assay with photographs taken from a time-lapse series. The left-hand column shows the wounds at t=0 and the right-hand column shows the wounds at t=16 hours. The scale bar shows that the initial wounds were on average 0.8 mm. White lines show the positions at which the measurements were taken. Photographs of each cell line were taken concurrently at each time point. Cells used were stable transfectants.

B. Graph showing the rate of wound closure (μm per hour) of each cell line (stable transfectants). Results depicted represent the average of 3 separate time-lapse experiments, with single samples in each.

Chemotaxis in FBR cells is unaffected by re-expression of down-regulated genes

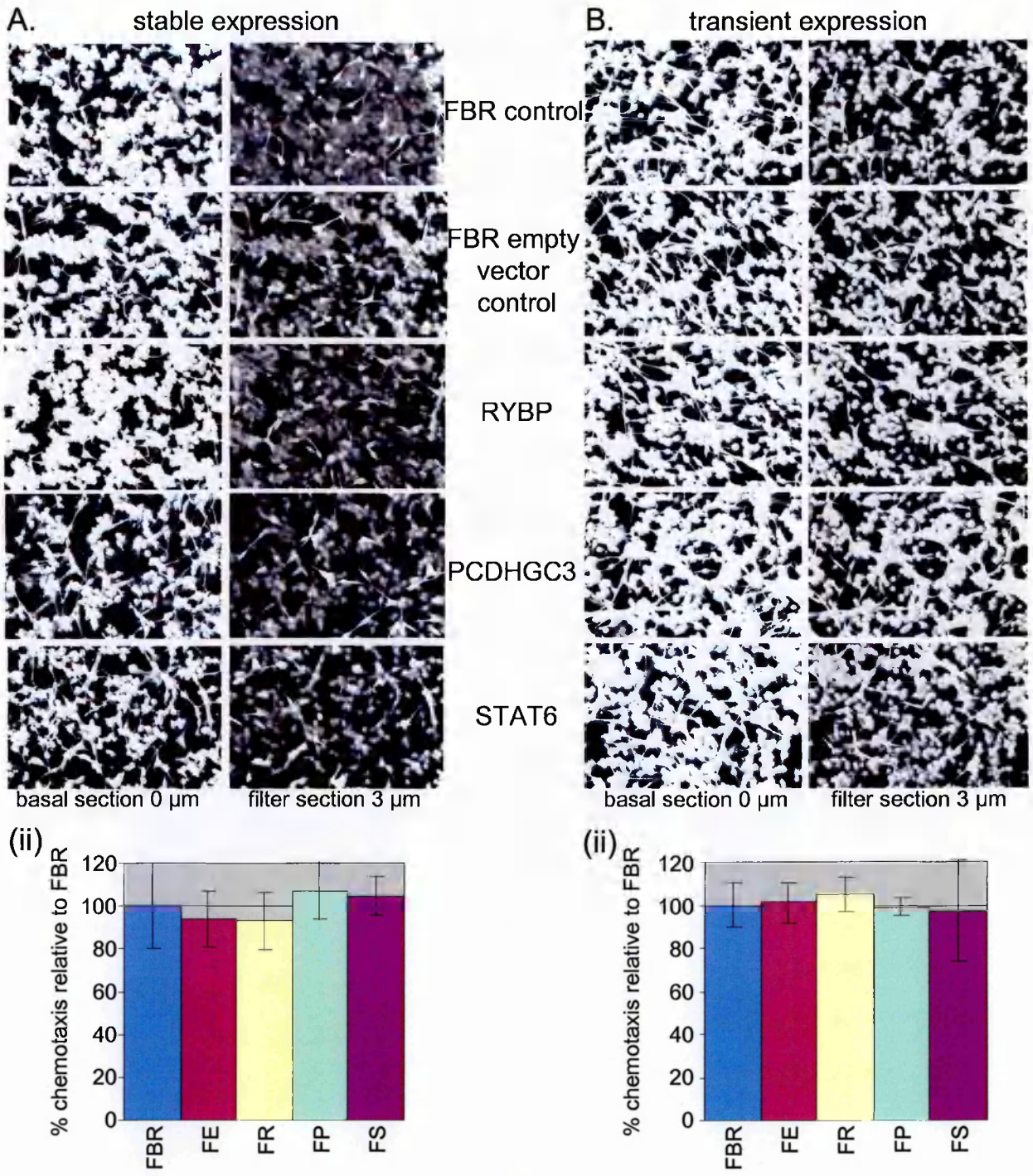

Figure 4.8

A.(i) Example sections used to quantify chemotaxis in FBR cells stably expressing RYBP or PCDHGC3 or STAT6 . The left-hand row shows those cells remaining on the underside of the filter and the right-hand row shows those cells which have moved through the filter pores to the upper surface of the filter. In quantitation a high background value must be subtracted to avoid bleed-through from the basal section to the filter section, affecting the result; also the chemotactic cells were counted by eye to verify and validated the computer quantitation.

(ii) Histograms showing that the chemotactic response in FBR cells stably expressing RYBP or PCDHGC3 or STAT6 is equivalent to that of parental FBR cells. Each graph is produced from the integrated quantitation of three separate assays with at least duplicate samples in each.

B. As in A. above, but with FBR cells which transiently express RYBP or PCDHGC3 or STAT6 .

4.3 Conclusions

We have shown that 5 out of 11 genes which are down-regulated in v-Fos^{FBR}-expressing cells, are re-expressed as a consequence of HDAC inhibition. When these genes are ectopically re-expressed, individually, in FBR cells, either transiently or stably, invasion is inhibited without affecting, proliferation, morphology, motility, chemotactic response, or filamentous actin arrangement.

Chapter 5

Strategies to modulate levels of HDAC4 in Fos-transformed cells

5.1 Introduction

In order to define the role of histone deacetylases in Fos-transformation we sought to modulate HDAC activity in both 208F and FBR cells, to determine the effect on their normal and transformed phenotypes. Theoretically, one might expect an increase in HDAC activity in 208F cells to move them to a more transformed phenotype and conversely a reduction in HDAC activity in FBR cells to revert some aspect of the transformed phenotype, as we have shown with HDAC inhibitor studies (Chapter 3). In addition, an increase in HDAC activity in FBR cells might be expected to reduce their response to HDAC inhibitors. This chapter describes the strategies we employed to modulate the activity of a single histone deacetylase, which we proposed to have a key role in Fos-transformation. Our candidate was HDAC4, primarily because, as we had shown, of the HDACs considered, it is the most substantially up-regulated in both v-Fos- and v-Ha-Ras-transformed cells (Figure 3.1E). This is significant because AP-1 is a downstream effector of Ras, and Ras is commonly mutated in human tumours, thus increasing the likelihood of the involvement of HDAC4 up-regulation in cancer itself. In addition, it was demonstrated that HDAC4 represses differentiation in myoblasts (Miska et al. 2001), supporting the idea that it has a role in transformation.

5.1.1 Nuclear levels of HDAC4

Since it is known that the activity of HDAC4 (and other class II HDACs) is controlled by active nuclear export (Section 1.3.6) it was necessary to determine the level of nuclear HDAC4 in 208F and FBR cells, to confirm that FBR cells do indeed have comparatively more enzyme with respect to nuclear levels, since increased total cellular HDAC4 need not reflect increased nuclear HDAC4. A western blot of nuclear extracts from both cell lines was used to confirm that there is approximately 3.8 times more nuclear HDAC4 in FBR cells compared to 208F cells (Figure 5.1).

FBR cells have an increased level of nuclear HDAC4 relative to 208F cells

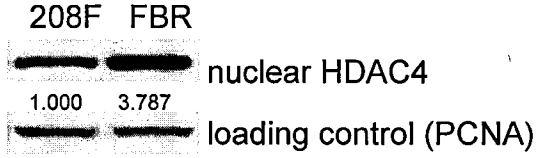

Figure 5.1

Western blot of nuclear extracts prepared from cell lysates, showing that the level of nuclear HDAC4 is approximately 3.8-fold increased in FBR cells compared to 208F cells. Values represent relative expression, in units of OD x mm^2, normalised to loading control.

5.1.2 Levels of HDAC4 in response to histone deacetylase inhibitors

We also determined the effect inhibitor treatment has on the level of endogenous HDAC4 expression, to confirm that HDAC4 inhibition is not accompanied by a compensatory increase in HDAC4. If this were the case, we could not conclude, without further investigation, that HDAC4 activity is actually inhibited. It was therefore, necessary to determine that this is not the case.

Western blots were performed on TSA- and VPA-treated FBR cells (Figure 5.2). It was found that treatment with up to 15nM TSA for 4 days has no effect on endogenous levels of HDAC4 (Figure 5.2A), likewise, treatment with up to 50 μgml^{-1} VPA for 4 days does not affect HDAC4 levels (Figure 5.2B). These results determined that, at the concentrations of inhibitor with which we treated FBR cells (12 nM TSA or 50 μgml^{-1} VPA) for 4 days, without affecting growth, their level of endogenous HDAC4 expression is unaffected.

Levels of HDAC4 in FBR cells in response to HDAC inhibitor treatment

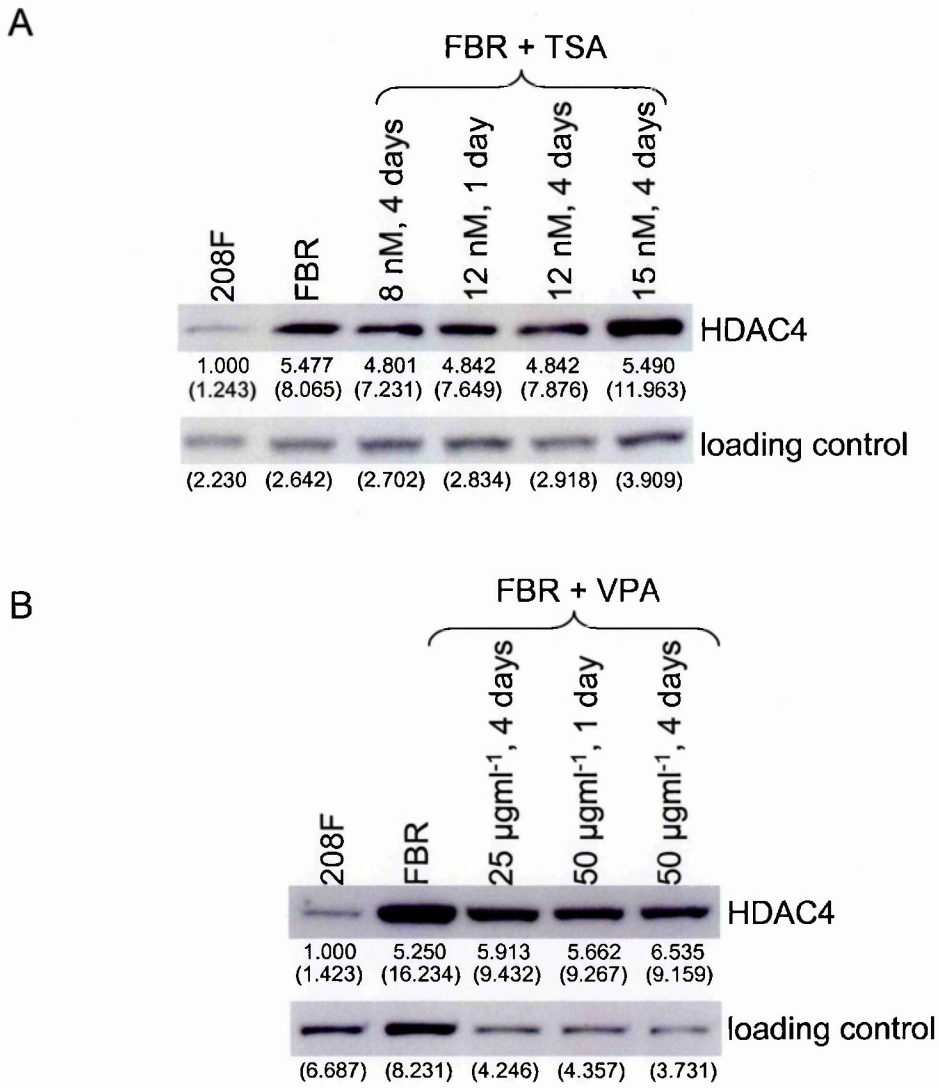

Figure 5.2

Western blots of whole cell lysates showing that:

A. Up to 15 nM TSA for 4 days does not affect the expression of endogenous HDAC4.

B. Up to 50 μgml^{-1} for 4 days does not affect the expression of endogenous HDAC4.

Loading controls are ERK2. Bracketed values are actual densitometric values, in units of OD x mm^2.

Values which are not in brackets represent relative expression, normalised to loading controls.

5.2 Over-expression of HDAC4 in both normal, and Fos-transformed, fibroblasts

5.2.1 Sub-cloning of HDAC4, verification of HDAC4 sequence, molecular weight and correct expression in cells

The wild type (wt) HDAC4 cDNA was cloned into the expression vector pEGFP-N1 (Section 2.2.9), which provides a C-terminal EGFP tag. The accuracy of the sequence of the cloned gene and of the gene/vector junctions was confirmed by DNA sequencing (Section 2.2.9.14). We noted a single base change in our cloned sequence compared to the Genbank sequence, which did not alter the predicted amino acid sequence, and was confirmed by later work (Section 5.3.2) to have been present in the original cDNA sequence. Then, by western analysis, we confirmed the expression of a protein of the correct expected molecular weight in Cos-7 cells, using both anti-EGFP and anti-HDAC4 antibodies (Figure 5.3A). HDAC4 has a predicted molecular weight of 109 KDa but runs in SDS-PAGE at 140 KDa, possibly due to post-translational modification (T. Kouzarides, personal communication). So, including an additional 27 KDa for the EGFP tag, we expected, and demonstrated, a protein with an approximate molecular weight of 167 KDa.

The vector, carrying HDAC4 cDNA, was transfected into both 208F and FBR cells, and those cells stably expressing the transgene were selected with G418. The populations were then FACS-sorted for EGFP-positive cells, as described (Section 2.2.10.2) to establish clonal 208F- and FBR-derived cell lines, stably expressing EGFP-tagged wild type HDAC4. Cell lines were chosen for further study on the basis of their high percentage of EGFP-positive cells, as determined by fluorescence microscopy, and the ease of detection of the ectopically expressed protein, by western analysis (Figure 5.3B).

Western analysis of ectopically expressed HDAC4-EGFP

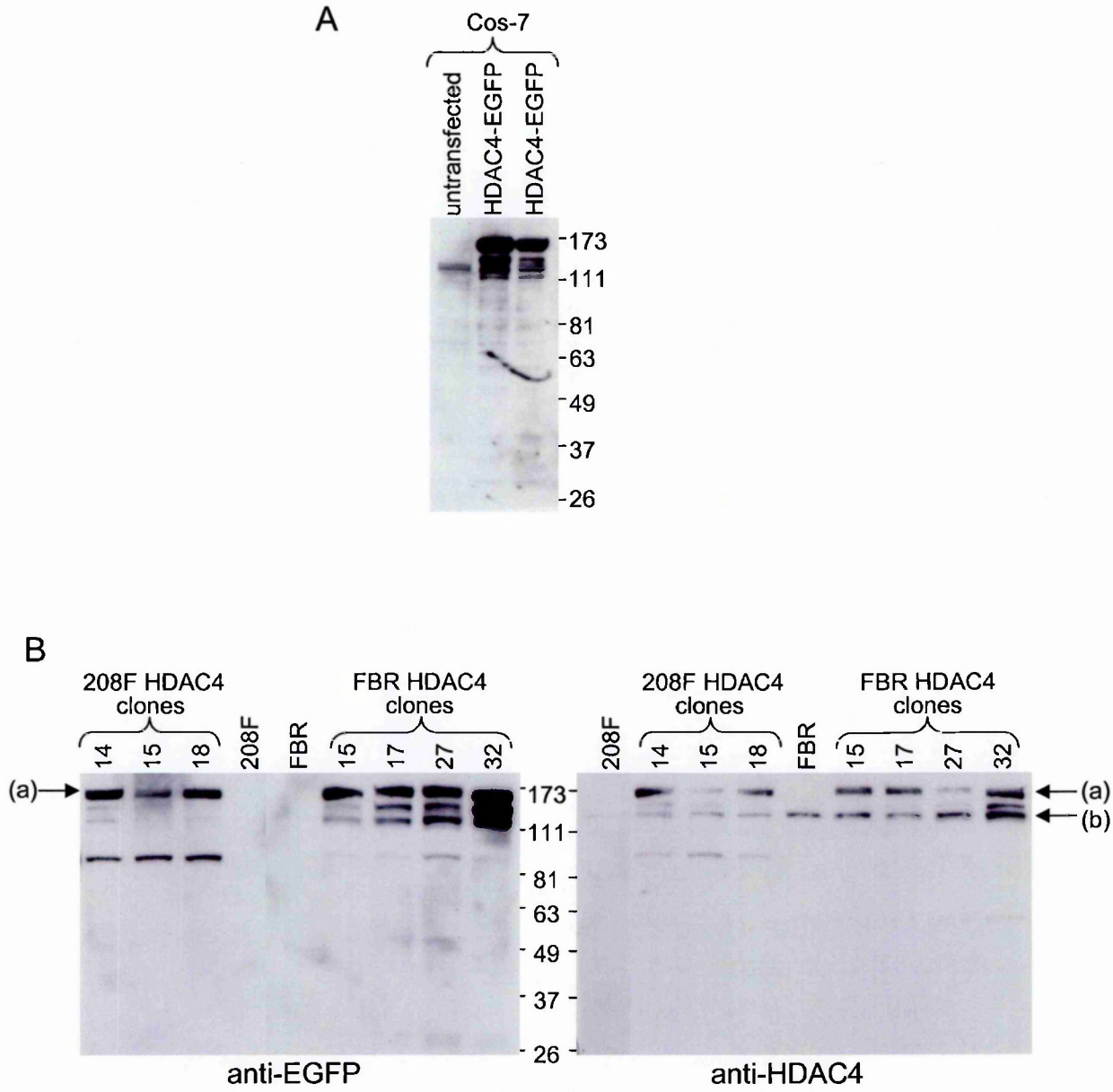

Figure 5.3

Western analyses of total cell lysates (25 μg per lane). Protein was detected using anti-EGFP or anti-HDAC4 antibodies, as indicated.

A. Transient expression in Cos-7 cells, confirming expression of a protein of the correct molecular weight.

B. Stable expression in selected FBR-cell-derived clones. Arrow (a) indicates EGFP-tagged HDAC4 and arrow (b) indicates endogenous HDAC4.

5.2.2 Cellular localisation and distribution of over-expressed HDAC4

Over-expressed HDAC4 was found mainly in the cytoplasm in both 208F and FBR cells, though a low level of the protein was also detectable in the nucleus (Figures 5.4 and 5.5). This was as expected, as studies have shown that the level of HDAC4 in the nucleus is controlled by an active transport mechanism by which the protein is exported from the nucleus (Section 1.3.6). In addition, to confirm that correct localisation had not been disrupted by the presence of the EGFP tag, we transiently transfected FBR cells with the myc-tagged HDAC4 (Miska et al. 2001) from which we had derived our EGFP-tagged HDAC4 expression construct. We found no difference in HDAC4 localisation with either tag (Figure 5.4A), which was as previously reported in a comparison of myc-tagged, and N-terminal GFP-tagged, HDAC4 (Miska et al. 2001). In addition, later experiments in which a mutated HDAC4 is expressed, also serve to demonstrate the normal localisation of wtHDAC4 (Figure 5.11B and section 5.4). The mutated HDAC4-EGFP cannot be phosphorylated and therefore cannot undergo nuclear export, however, the fact that it *does* locate to the nucleus demonstrates that the EGFP tag does not hinder nuclear localisation.

5.2.3 Over-expression of HDAC4 in 208F cells

As can be seen from the confocal microscope images (Figure 5.5), 208F cells that over-express HDAC4, have a mixed morphology: some are identical to parental 208F cells, whilst other cells have assumed a bipolar morphology. The majority of the cells, though, range in shape between these two extremes. It should be noted however, that we do not find cells which, like FBR cells, are without stress-fibres, although the stress-fibres seen in the bipolar cells run parallel with the long axis of the cell, which is what we find in FBRs treated with HDAC inhibitors, which remain bipolar, e.g., after 24

Localisation of ectopically expressed wtHDAC4 in FBR cells

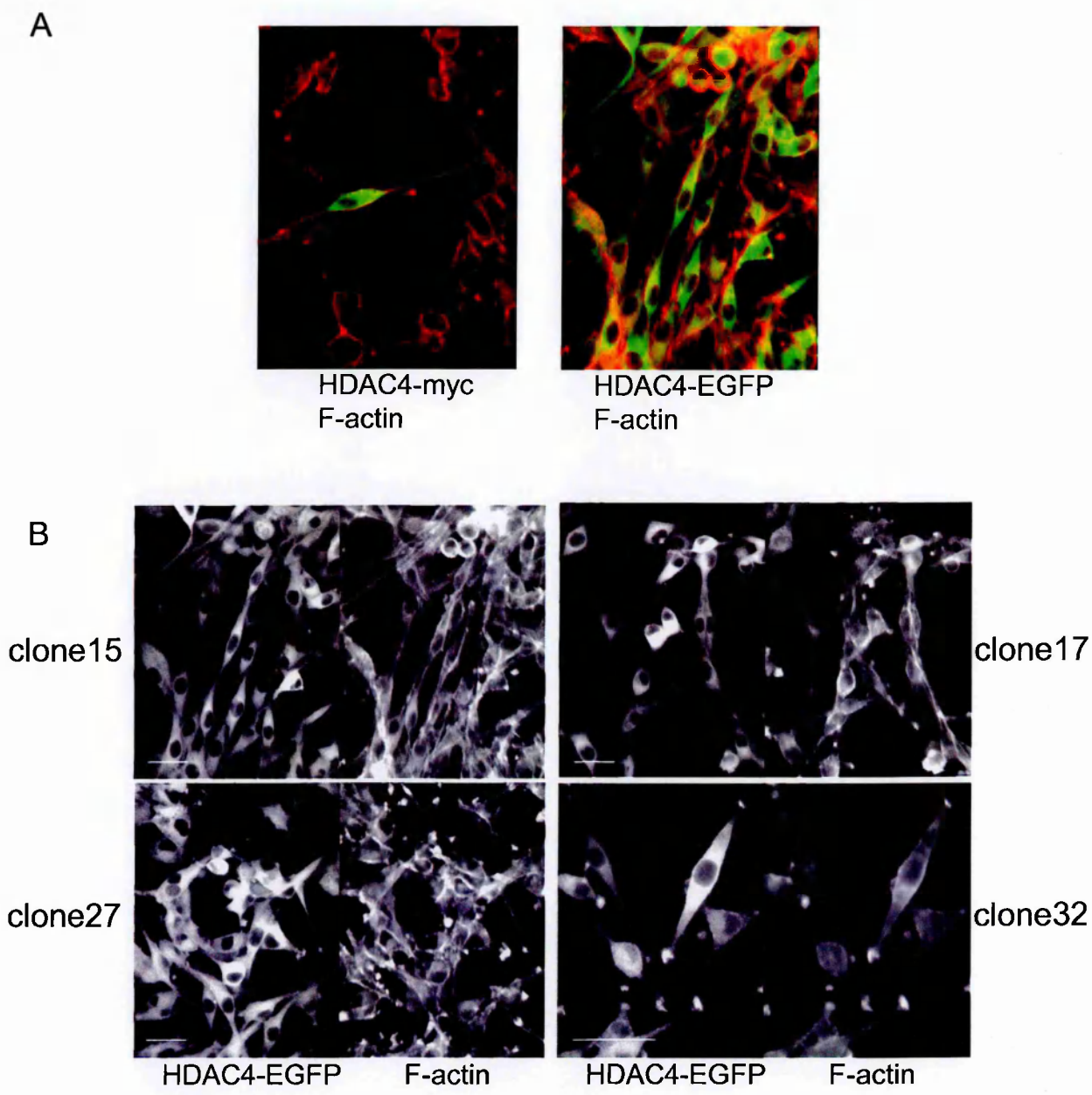

Figure 5.4

A. Confocal images showing a comparison of the distribution of ectopically expressed myc-tagged HDAC4 and ectopically expressed EGFP-tagged HDAC4, in FBR cells. Myc-tagged HDAC4 is visualised using mouse anti-myc antibodies hybridised to FITC-labelled anti-mouse antibodies, and is therefore green-fluorescent. EGFP is green fluorescent. In both cases, cells were counter-stained with TRITC-conjugated-phalloidin for F-actin which is red-fluorescent. HDAC4-myc is transiently expressed and HDAC4-EGFP is stably expressed. The distribution is the same in both myc- and EGFP-tagged proteins. B. Confocal images showing the distribution of HDAC4-EGFP, stably expressed in FBR cells. Cells were counter-stained with TRITC-phalloidin for F-actin. Results were similar for all clones.

Distribution of ectopically expressed HDAC4 in 208F cells

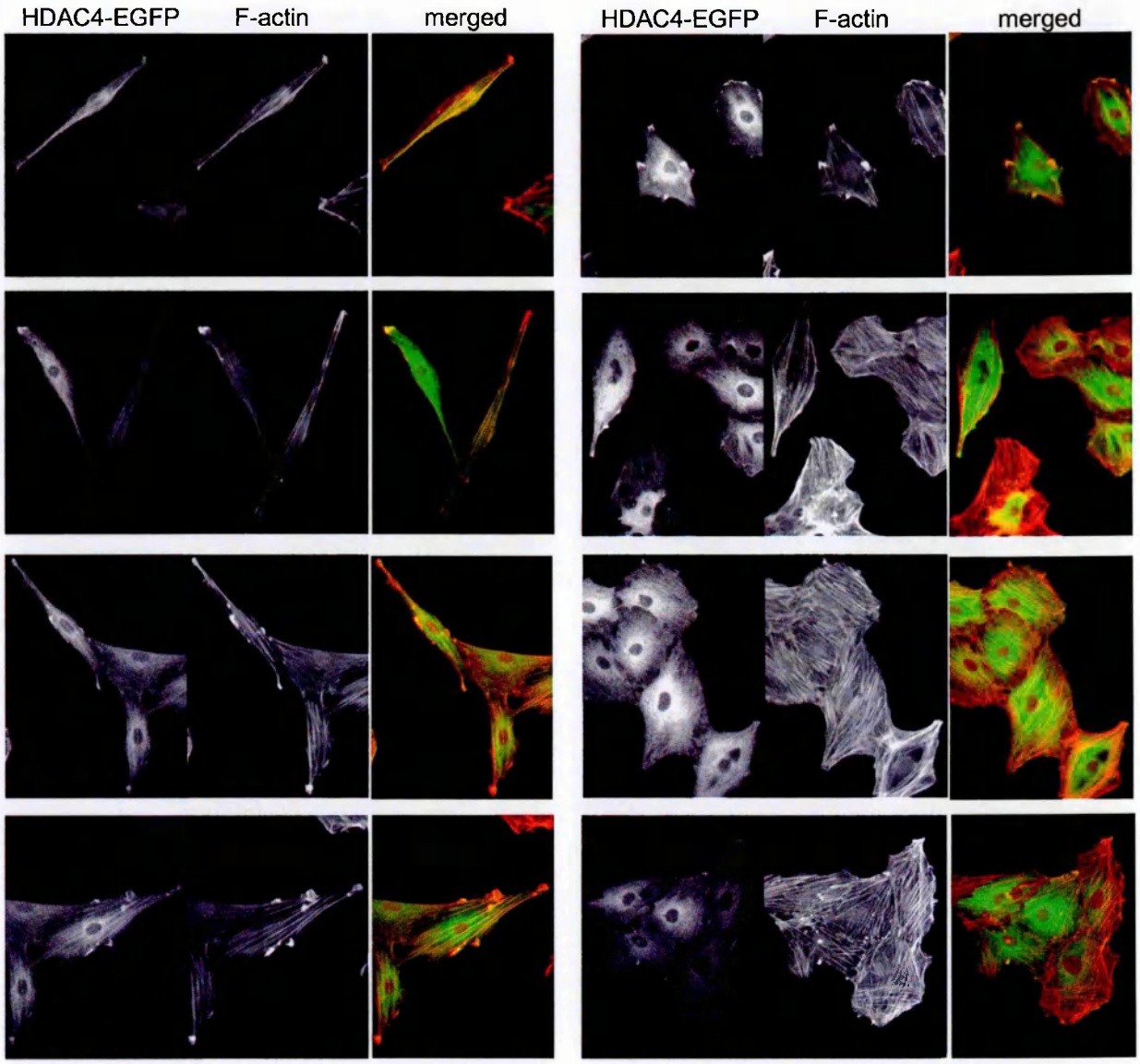

Figure 5.5

Confocal microscope images showing the distibution of HDAC4-EGFP (green fluorescence) in clones of 208F cells ectopically expressing HDAC4-EGFP. Cells were counter-stained with TRITC-phalloidin for F-actin (red fluorescence). The merged images are those shown in colour . Results were similar for all clones.

hrs VPA treatment at 25 μgml^{-1} (Figure 3.5). In quantitation of morphologies we used eight phase contrast images per clone; counting and classifying approximately 30 cells per image (Figure 5.6). It was not possible to sub-classify those cells with intermediate morphology without subjectivity; however, we determined that 26% of 208F cells over-expressing HDAC4 assume a bipolar morphology (Figure 5.6), whilst less than 2% remain similar to the parental phenotype. Consequently, the remaining 72% of cells showed a range of intermediate morphologies.

When the HDAC4-over-expressing 208F cells were assayed for invasion, however, none could be detected in any of the clones (data not shown), despite the move towards a more bipolar morphology. This is in keeping with our HDAC inhibitor studies (Chapter 3), where we have shown that morphology and ability to invade are separable characteristics in terms of HDAC activity.

5.2.4 Over-expression of HDAC4 in FBR cells

The morphology of FBR cells is unaffected by HDAC4 over-expression, nor is there any quantifiable effect on actin stress-fibres (Figure 5.4). In *in vitro* invasion assays we found that the HDAC4-expresssing FBR cells were not significantly more invasive than the EGFP-expressing control FBR cells (data not shown), however, what we did find in *in vitro* invasion assays was that although these cells are *not* more invasive than the control FBR cells, a higher concentration of TSA is required to achieve inhibition of their invasion (Figure 5.7), suggesting that the additional HDAC4 in these cells allows them to overcome the effects of the inhibitors. Inhibition of HDACs by inhibitors can be compensated for by HDAC4, suggesting that specifically HDAC4 is able to mediate invasion and therefore implying that the invasion of FBR cells is indeed, at least in part, a consequence of increased HDAC4 expression.

208F cells expressing HDAC4 have a more spindle-shaped morphology

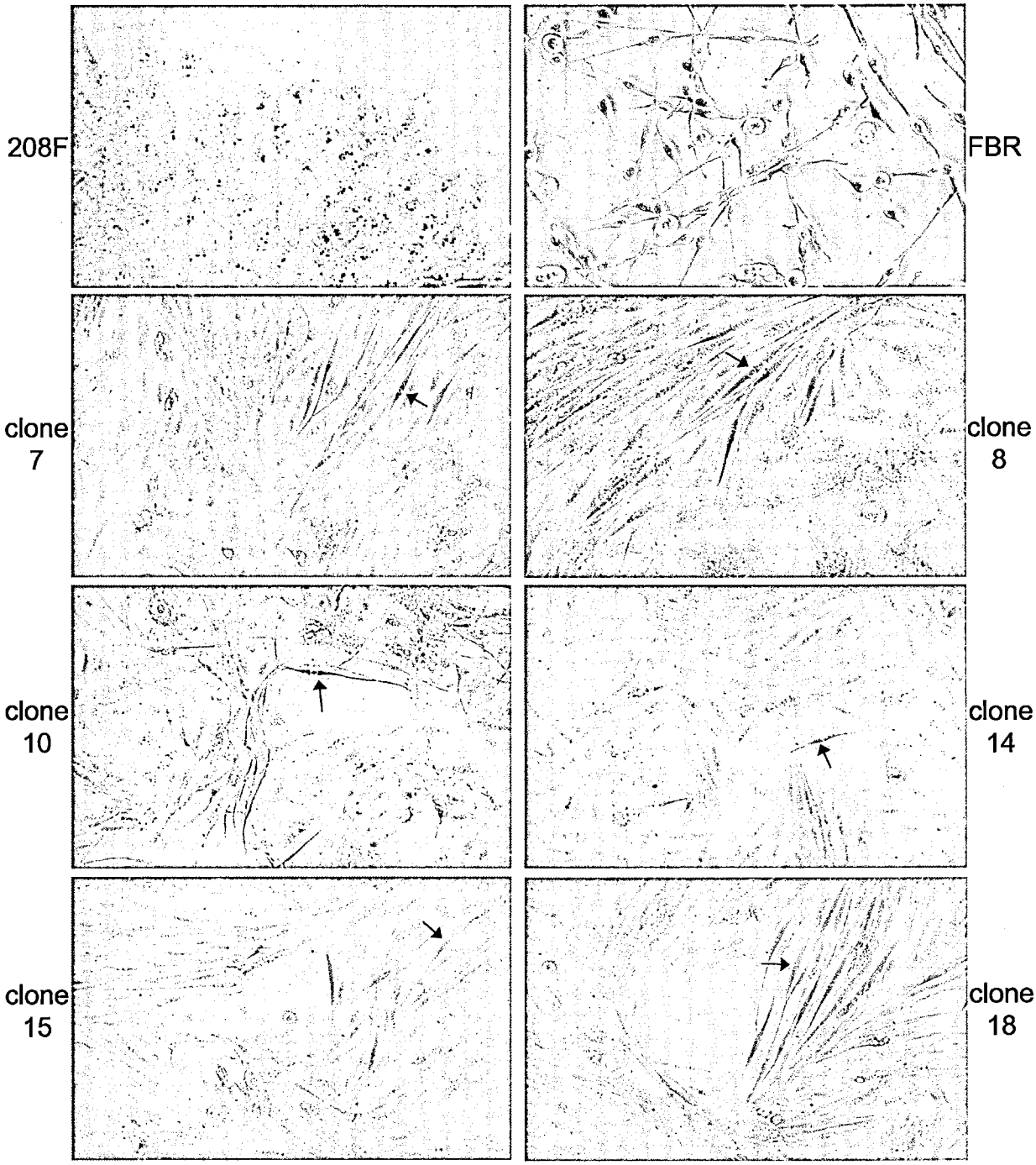

Figure 5.6

The morphology of 208F cells over-expressing wild type HDAC4 compared to that of the parental 208F cells and to FBR cells. 208F cells become more spindle-shaped when they over-express HDAC4. In quantitation, 26% of HDAC4-expressing cells were bipolar (indicated by arrows), 2% of cells resembled the parental 208F cells and the remaining 72% have an intermediate morphology. Each photograph is representative of the population as a whole.

FBR cells, over-expressing wild type HDAC4, are less sensitive to TSA-induced inhibition of invasion

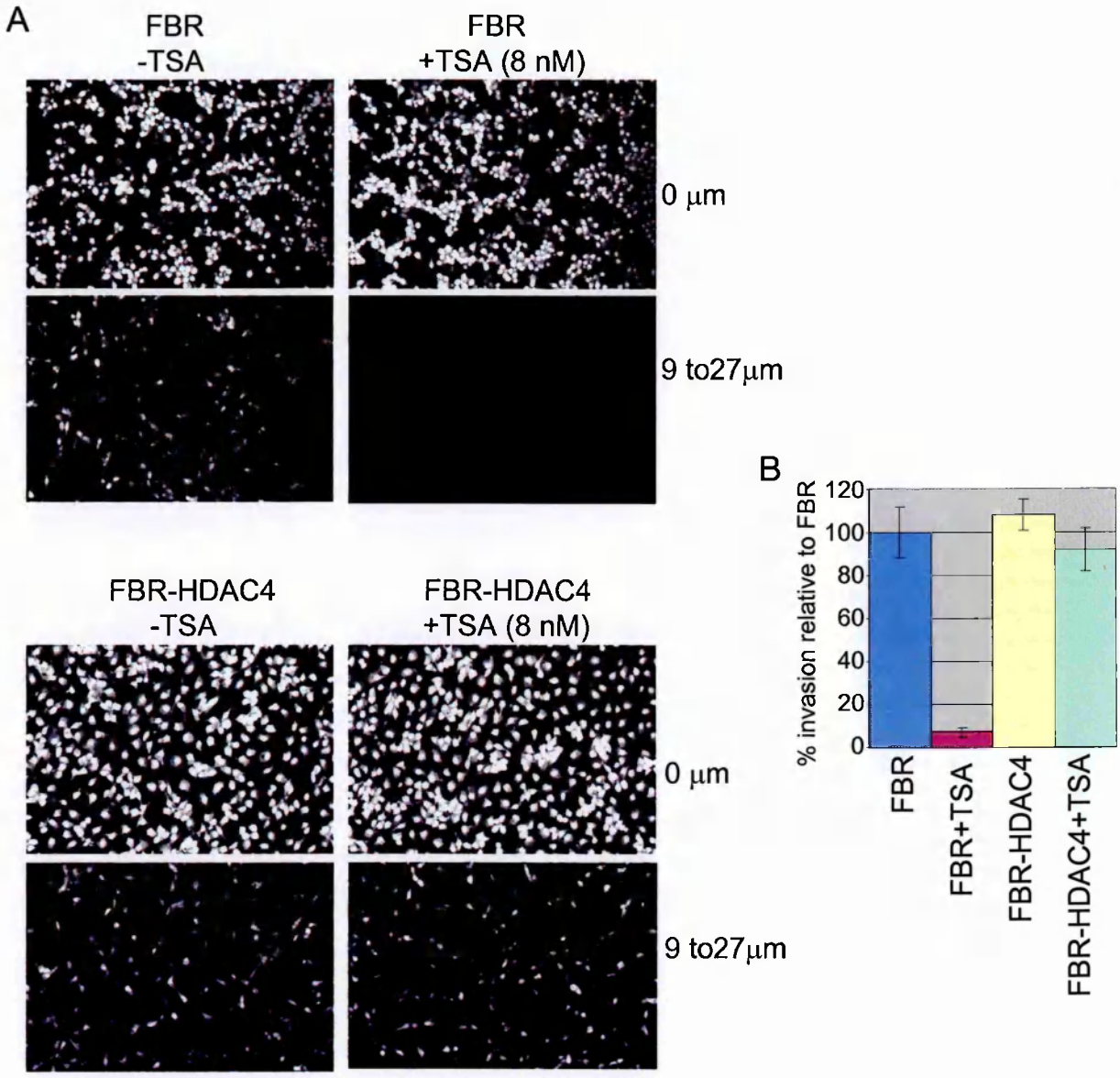

Figure 5.7

A. Example invasion assay showing that invasion of FBR cells is inhibited by 8 nM TSA, but that 8 nM TSA does not inhibit invasion in FBR cells over-expressing HDAC4. The upper assay shows the effect of 8 nM TSA on FBR cell invasion and the lower assay shows the effect of 8 nM TSA on invasion in FBR cells which have stable ectopic expression of HDAC4.

B. Histogram showing the combined quantitation of three invasion assays with duplicate samples, identical to that shown in A. TSA treatment is at 8 nM.

5.3 Expression of deacetylase-inactive forms (H803A and D840N) of HDAC4 in Fos-transformed cells

5.3.1 Introduction

With the intention of reducing the level of active HDAC4 in the cell we introduced, individually, by transfection, two deacetylase-inactive forms of HDAC4 (Miska et al. 1999). These genes each have a single point mutation in their catalytic site that has been shown to greatly reduce their deacetylase activity (Miska et al. 1999); they are termed HDAC4-H803A and HDAC4-D840N (Section 2.1.5.1). It was reported, in deacetylase assays of immunoprecipitated enzyme, that HDAC4-H803A had approximately 80% less activity than HDAC4 and HDAC4-D840N had approximately 70% less activity than HDAC4 (Miska et al. 1999). It was not known whether the inactive HDAC4 enzymes would act in a dominant-negative manner *in vivo*, however if this were the case we would hope to be able to demonstrate some indication of reversion of the transformed phenotype when they are expressed in FBR cells, such as re-appearance of actin stress-fibres or deceased invasion. Another possibility is that we would see an increased sensitivity to HDAC inhibitors, e.g., morphology would revert more quickly or at a lower concentration of inhibitor.

5.3.2 Sub-cloning of H803A and D840N, verification of sequence and molecular weight, and expression in FBR cells

The two point-mutated HDAC4 cDNAs; H803A and D840N (Miska et al. 1999), were each sub-cloned into the expression vector pEGFP-N1 (Section 2.2.9), again in the same manner as for the cloning of the wild-type gene. The accuracy of the sequence of the cloned genes and of the gene/vector junctions was confirmed by DNA sequencing (Section 2.2.9.14). Apart from the silent base change we had seen in the wild-type HDAC4 (Section 5.2.1), the only changes to the Genbank sequence resulted

from the engineered base substitutions, in each case. In H803A, the codon CAT for histidine, has been replaced with GCC for alanine; and in D840N, the codon GAC for aspartic acid, has been replaced with AAC for asparagine.

Western analysis confirmed the expression of a protein of the correct expected molecular weight in Cos-7 cells, using both anti-EGFP and anti-HDAC4 antibodies (Figure 5.8A). As previously discussed (Section 5.2.1) we would expect, and were able to demonstrate, a protein with a molecular weight of 167 KD. There are also three smaller molecular weight bands, which could perhaps represent less phosphorylated forms of the protein, and reflect the banding pattern we see for ectopically expressed wt HDAC4. We then transfected the vectors, carrying the cDNAs, into FBR cells. After G418 selection and FACS sorting, four stable populations were produced for each cDNA, that were distinct, in that they arose from four separate transfections, but (unlike the wtHDAC4-over-expressing populations) were not clonal (Section 2.2.10.2). We chose to move from clonal selection at this point to avoid the possibility that the response of a clone is not representative of the population as a whole. We had seen in previous experiments that clones sometimes differed slightly in morphology and in invasive ability, in addition a non-clonal population can be used in experiments more quickly (without the requirement to amplify cell numbers) after stable expression is established and we had seen previously that stable populations lose expression of the transgene with increasing time in culture.

Western analysis confirmed the expression of a protein of the correct molecular weight in FBR cells (Figure 5.8B). Using both anti-EGFP and anti-HDAC4 antibodies, we detected, as expected, a protein of approximately 167 KD. The anti-HDAC4-probed membrane also showed a protein band at 140 KD, representing the endogenous protein, also present in control FBR cells. Also detected in extracts from FBR cells

Expression of HDAC4-H803A and HDAC4-D840N proteins

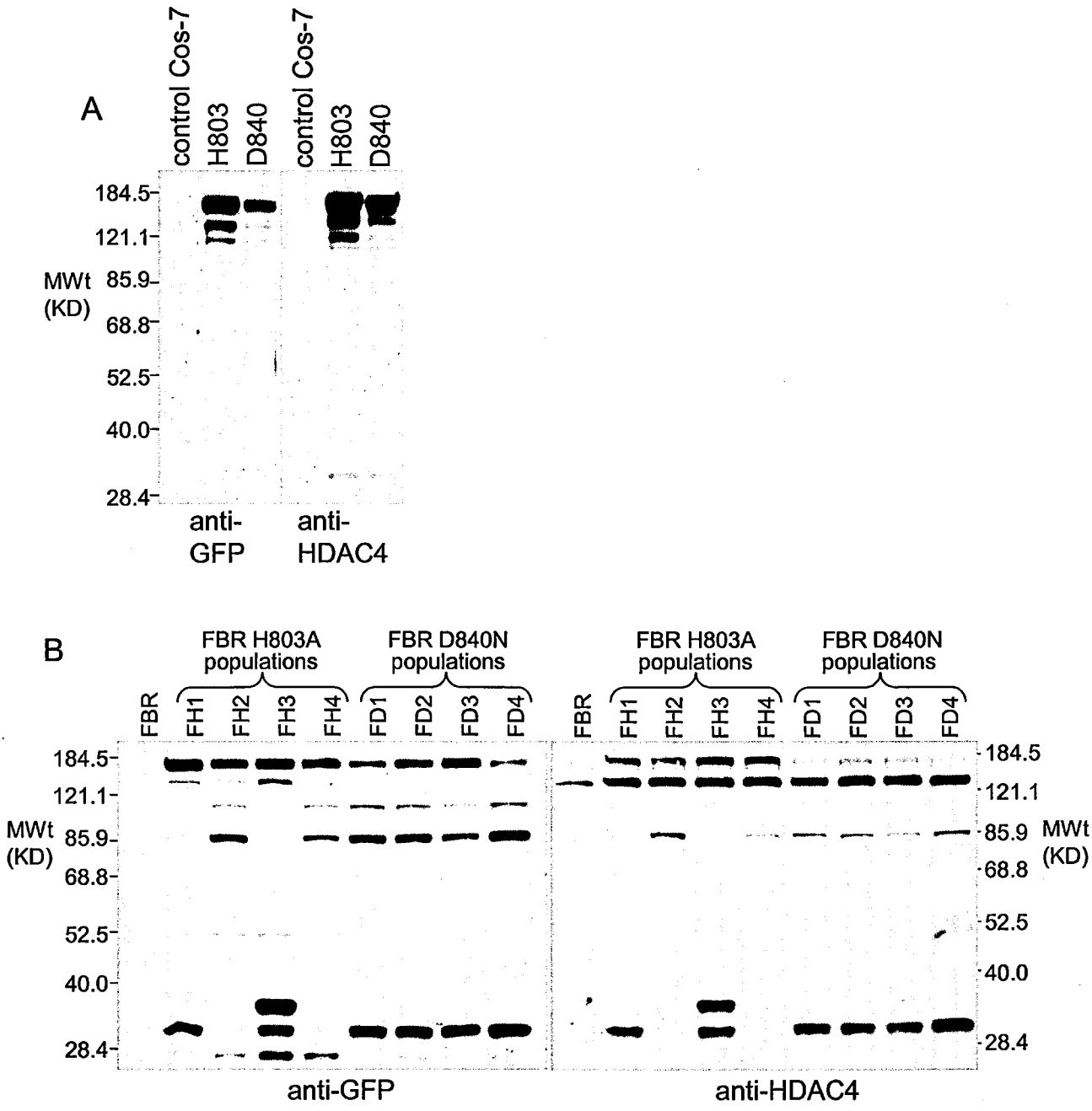

Figure 5.8

A. Western analysis of Cos-7 cells expressing deacetylase-inactive forms (H803A and D840N) of the HDAC4 gene.

B. Western analysis of FBR cells expressing deacetylase-inactive forms (H803A and D840N) of the HDAC4 gene. Populations 1-4 represent distinct, but non-clonal, populations of cells.

expressing deacetylase-inactive HDAC4-EGFP, were a number of extra lower bands, which are most likely products of degredation of the fusion protein, also detected by HDAC4 antibodies, since the immunogen for this antibody was the extreme C-terminus of HDAC4.

5.3.3 Localisation of H803A and D840N in FBR cells

Both deacetylase-inactive HDAC4 proteins localised, in FBR cells, in the same manner as their wild-type counter-part. The majority of the protein was in the cytoplasm, with a small, but clearly detectable proportion in the nucleus (Figure 5.9). We also counted 1.2% of cells which had either a uniform distribution over the whole cell, or an almost uniform distribution, but with a slight emphasis on the nucleus. This is in keeping with published studies, stating that in a small proportion of cells, HDAC4 does locate to the nucleus (Miska et al. 1999; Grozinger and Schreiber 2000; Wang et al. 2000), however, this distribution is similar to that we have observed for EGFP expressed alone, and is just as easily accounted for by the small protein (slightly larger than EGFP) seen by western analysis (Figure 5.8B) using both anti-EGFP and anti-HDAC4 antibodies, which could localise in a similar manner to EGFP.

5.3.4 Effect on morphology and actin stress fibres

We could not find any difference in the morphology of FBR cells over-expressing deacetylase-inactive HDAC4 compared to FBR cells, nor was there any increase in actin stress-fibres (Figure 5.9). Neither did we find an increased sensitivity to HDAC inhibitors, with regard to morphological reversion or re-appearance of stress-fibres (data not shown).

FBR cells with stable expression of HDAC4-H803A or HDAC4-D840N

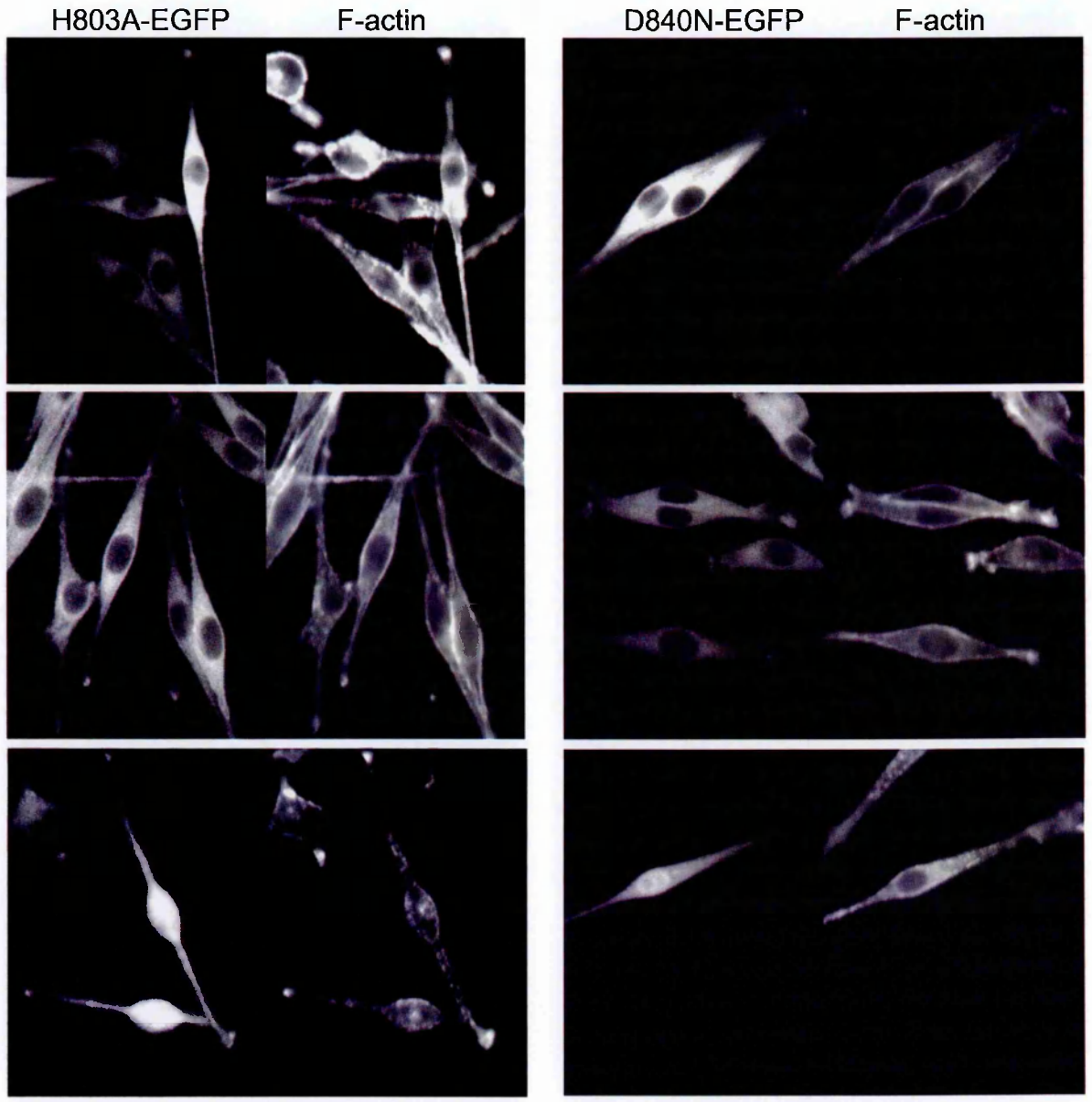

Figure 5.9

Examples of FBR cells with stable expression of either HDAC4-H803A or HDAC4-D840N. In each of the six double images, the left-hand panel shows the EGFP-tagged transgene (green fluorescent) and the right-hand panel shows F-actin which is stained with TRITC-phalloidin (red fluorescent). The third image in each column shows an example of the 1.2% of cells which had either a uniform distribution over the whole cell, or an almost uniform distribution but with a slight emphasis on the nucleus, as described in the text.

5.3.5 Effect on invasion

In *in vitro* invasion assays, the deacetylase inactive cells are, as anticipated, less invasive than FBR cells (Figure 5.10A, untreated cells, and 5.10B), which suggests a dominant-negative effect from the ectopically expressed gene and shows that HDAC4 is indeed required for the ability of the FBR cells to invade.

On treatment of the H803A- and D840N-expressing FBR cells with VPA, however, we found that the deacetylase inactive cells require a higher concentration of VPA to achieve a percentage inhibition of invasion equivalent to FBR cells (Figure 5.10). This is best seen in the 20μgml^{-1} VPA treatment (Figure 5.10A), where there are more invasive cells in FBR-HDAC4-D840N and in FBR-HDAC4-H803A, compared to FBR cells. This apparent resistance to inhibitor is probably best explained by binding of the inhibitor to the inactive enzyme, which, being in such excess, reduces the amount of inhibitor available for inhibition of endogenous HDACs. This could also be considered to be an explanation as to why wtHDAC4 over-expressing FBR cells are resistant to inhibition of invasion by HDAC inhibitors. In the case of wtHDAC4, however, the resistance to inhibitor is far more dramatic, which can be seen in a comparison of Figures 5.7A and 5.10A. It is therefore unlikely that this explanation would be sufficient. The fact that there is more *active* HDAC4 in these cells makes a significant difference to the level of resistance to inhibitors.

5.4 Over-expression of TMHDAC4, in both normal, and Fos-transformed fibroblasts

5.4.1 Introduction

It is known that the level of HDAC4 (and the other class II HDACs) in the nucleus is controlled by its export into the cytoplasm (Section 1.3.6). Since we found our over-

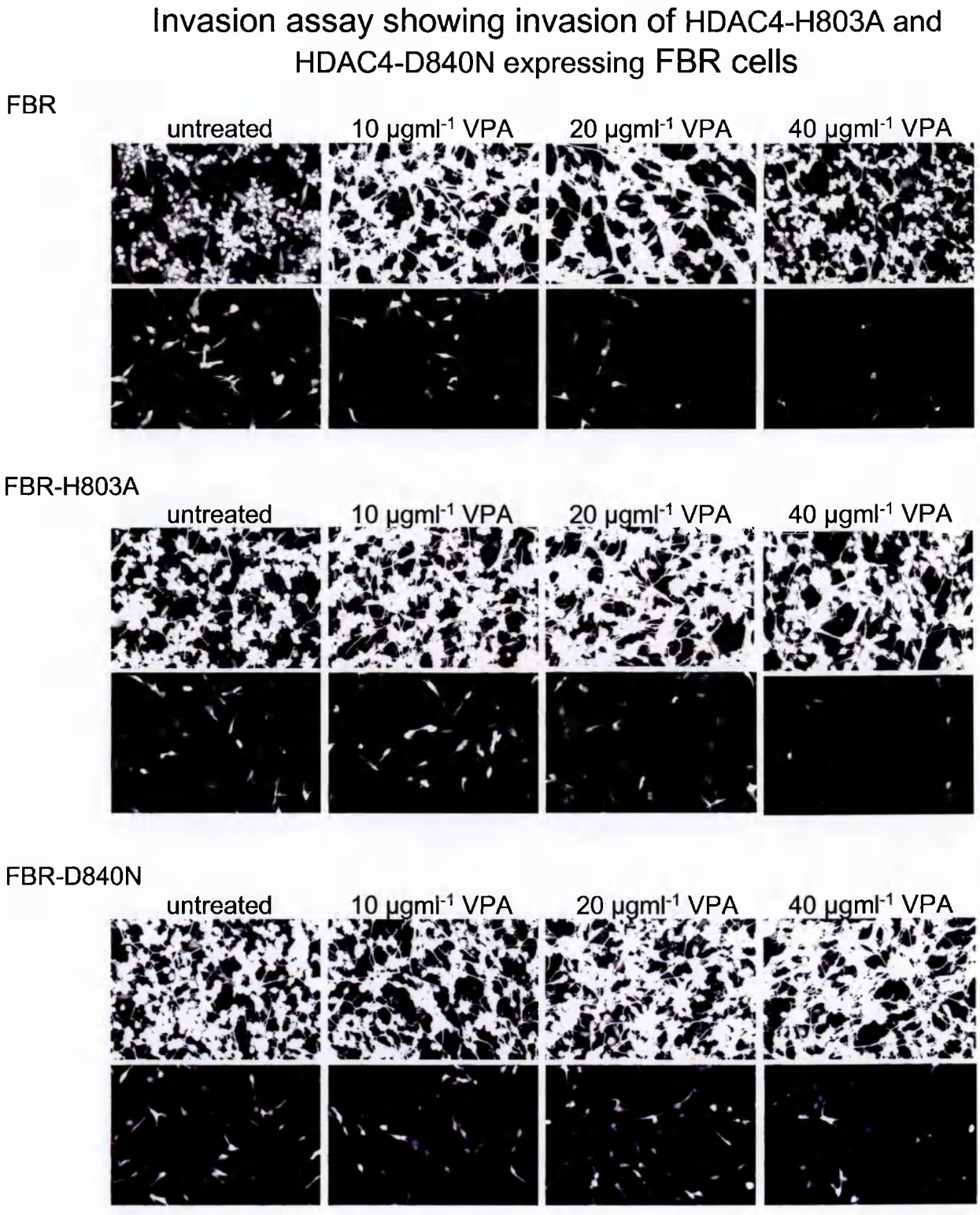

Figure 5.10A

Invasion assay showing that FBR cells expressing either HDAC4-H803A or HDAC4-D840N are less invasive than parental FBR cells. The assay also shows that FBR cells expressing deacetylase-inactive-HDAC4 are more resistant to the inhibition of invasion by VPA.

Invasion of HDAC4-H803A and HDAC4-D840N expressing FBR cells

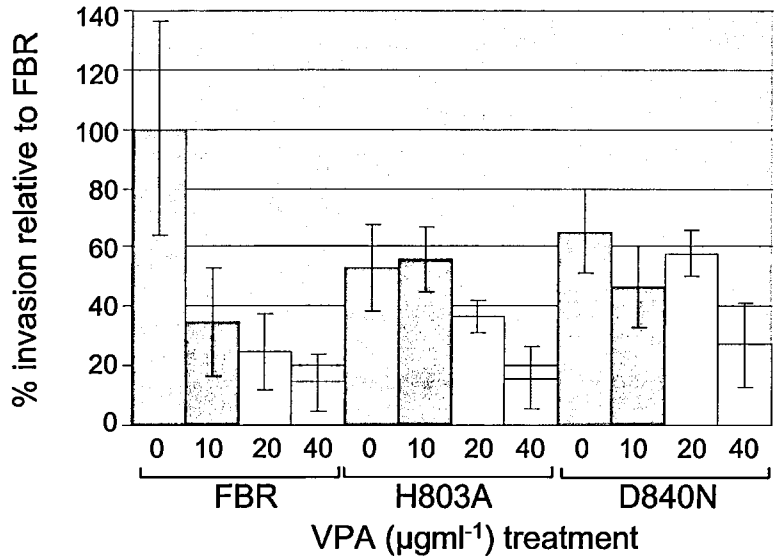

Figure 5.10B

Histogram showing the combined results of three invasion assays showing that FBR cells expressing either HDAC4-H803A or HDAC4-D840N are less invasive than parental FBR cells.
The assays also show that FBR cells expressing deacetylase-inactive-HDAC4 are more resistant to the inhibition of invasion by VPA.

expressed HDAC4 locates mainly to the cytoplasm of both 208F and FBR cells, we considered that this may be because the exogenous protein is being exported, so that although the cell over-expresses the protein, the level, active, in the nucleus is little affected. To address this possibility, we ectopically expressed a mutated form of HDAC4, that we have termed TMHDAC4, which has three serine residues replaced by alanines, and which, therefore, cannot be phosphorylated (Wang et al. 2000). The mechanism by which HDAC4 is exported requires its phosphorylation at these three serine residues. In this phosphorylated state 14-3-3β (and possibly ε) can bind to it, facilitating its nuclear export by complexing with the nuclear export receptor, CRM1 / exportin1.

5.4.2 Sub-cloning of TMHDAC4, verification of TMHDAC4 sequence and molecular weight, and its expression in cells

The sub-cloning of TMHDAC4 and the verification of its sequence was carried out exactly as described for wtHDAC4 (Sections 5.3.2 and 2.2.9) and TMHDAC4 was confirmed to have three point mutations relative to wild-type HDAC4. Sequencing showed these to be: T to G mutations at positions 736, 1399, and 1894, which change the codons from TCU, TCG and TCC, to GCU, GCG, and GCC respectively. Therefore our sub-cloned sequence differs from wild-type only in the three expected (Wang et al. 2000) serine-alanine substitutions.

Transfection into Cos-7 cells showed transient expression of a 167 KDa protein by western analysis (Figure 5.11A). In addition to this, we transiently expressed, in Cos-7 cells, TMHDAC4 which carries an N-terminal flag epitope, using the original vector (Wang et al. 2000) from which we had sub-cloned the TMHDAC4 gene, and demonstrated that a protein of approximately 140 KDa is expressed (Figure 5.11A).

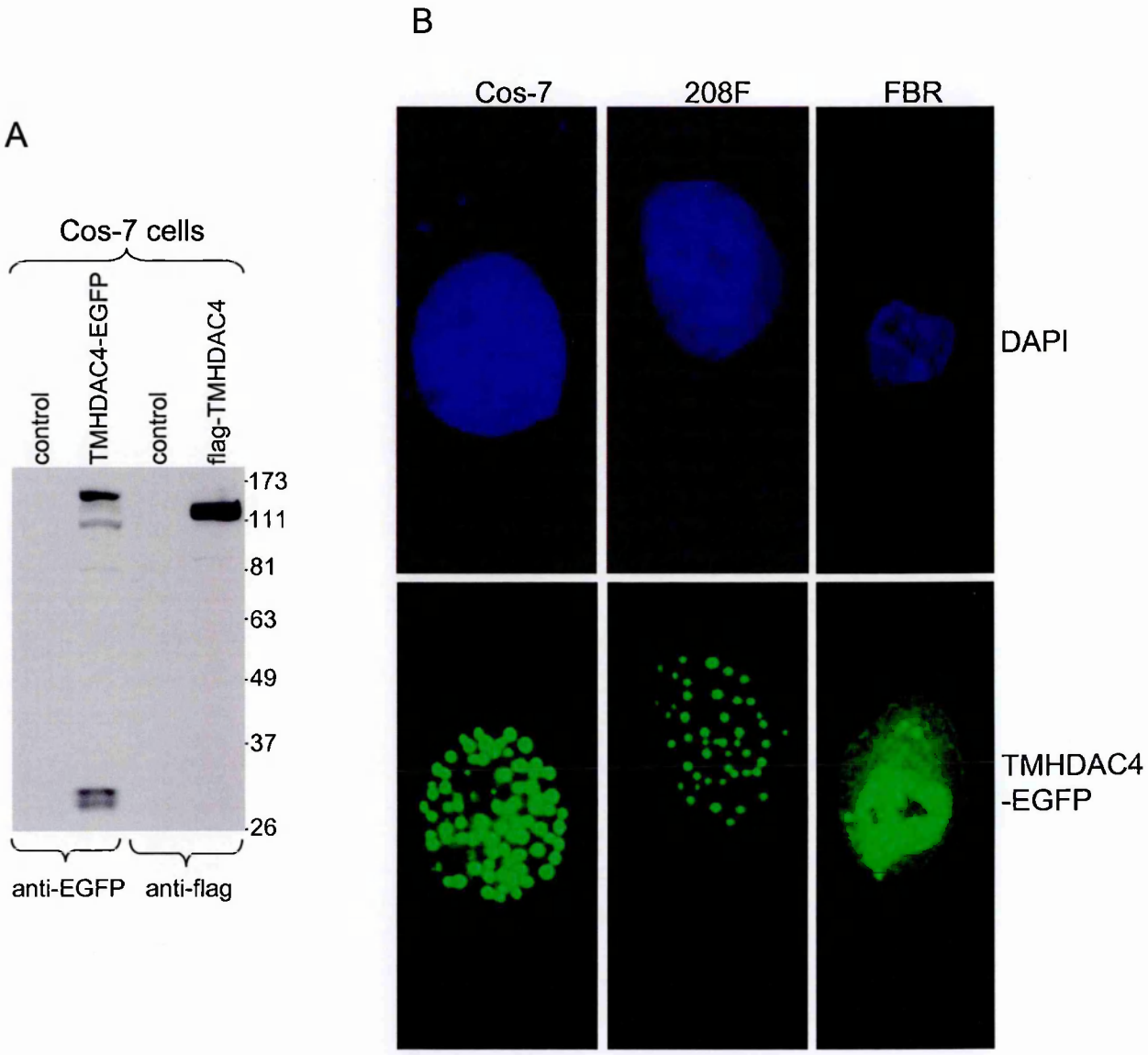

Figure 5.11

A. Western analysis of whole cell lysates of Cos-7 cells transiently expressing EGFP-tagged and myc-tagged TMHDAC4, detected using mouse anti-EGFP and mouse anti-flag antibodies respectively, hybridised to HRP-tagged anti-mouse antibodies in both cases.

B. Confocal microscope images of Cos-7, 208F or FBR cells, showing the localisation of transiently expressed TMHDAC4-EGFP to the nucleus. DAPI staining indicates the nucleus (blue fluorescence) and the EGFP tag shows the location of TMHDAC4 (green-fluorescence).

The difference between these expressed proteins is accounted for by the size of the EGFP-tag. Fluorescence microscopy of the transiently expressed TMHDAC4-EGFP showed the protein locates exclusively to the nucleus in 72% of cells (based on the classification of, an average of 25 cells, in each of 20 separate, random fields of view) a further 28% showed the protein in both nucleus and cytoplasm. The pattern of localisation in the nucleus is quite distinctive (Figure 5.11B) with a uniform distribution in discrete round dots. This pattern of localisation is now well documented, not only for HDACs (Miska et al. 1999; Wang et al. 2000) but also for other HDAC complex component proteins (Wu et al. 2001).

After confirmation of nuclear localisation, we attempted to create stable cell lines of FBR cells expressing either our TMHDAC4-EGFP or flag-TMHDAC4. Following transfection and G418 selection, TMHDAC4-EGFP-expressing cells were further selected, by FACS, for green fluorescence and pooled; and individual clones of G418-resistant, flag-TMHDAC4-expressing FBR cells were amplified. Unfortunately, the only cell populations derived, either did not express full-length protein, or in the one flag-TMHDAC4 clone which apparently *did*, expression was not in the nucleus. This suggests that TMHDAC4, is toxic to the cells. That is, when the cells are unable to control the nuclear HDAC4 levels by nuclear export, they are unable to reduce it to a level that can be tolerated. In the case of the clone which *did* express full length protein it is possible that this protein had acquired a mutation which allowed its nuclear export or prevented its nuclear import. Consequently, we did not proceed further with this approach.

5.5 Expression of CamKIV$_{1-313}$ and 14-3-3β in Fos-transformed cells

5.5.1 Introduction

As discussed previously (Section 1.3.6) it is thought that levels of nuclear HDAC4 and HDAC5 are controlled by the active transport of phosphorylated histone deacetylase across the nuclear membrane into the cytoplasm, thus reducing the level of HDAC4 and HDAC5 involved in transcriptional control. In myoblasts it was shown that the kinase which phosphorylates HDAC4 and HDAC5, is CamKIV and that it is, the transport protein, 14-3-3β which binds the phosphorylated deacetylase allowing it to be transported from the nucleus by CRM1 / exportin1 (Adachi and Yanagida 1989; Stade et al. 1997).

Based on this model we devised a strategy to reduce the nuclear HDAC4 levels in FBR cells, which would allow us to investigate the consequences of reduced transcriptional silencing by HDAC4, on the transformed phenotype. It was our intention then, to facilitate some form of reversion in the FBR cells, in particular to reduce their ability to invade, by expressing constitutively active CamKIV and over-expressing 14-3-3β (Tanji et al. 1994; Li et al. 1995) either independently, or simultaneously.

5.5.2 Sub-cloning of CamKIV$_{1-313}$ and 14-3-3β, verification of sequence and molecular weight, and expression in FBR cells

We acquired the cDNA of a constitutively active form of mouse CamKIV which is truncated at the C-terminus, and comprises only amino acids 1 to 313, therefore lacking its 3' regulatory region, termed CamKIV$_{1-313}$ (Sun et al. 1994). This cDNA was cloned into the expression vector, pEGFP-N1, which provides a C-terminal EGFP tag and confers G418 resistance. In addition CamKIV$_{1-313}$ was alternatively 3' myc-tagged using a PCR approach (Section 2.2.9) and cloned into the vector pLPCX2 which

confers puromycin resistance. The wild type 14-3-3β cDNA was cloned similarly, so that potentially we could create stable cell lines over-expressing either or both of these genes by puromycin and/or G418 selection plus FACS for green fluorescence. The accuracy of the sequence of the cloned genes and of the gene/vector junctions was confirmed by DNA sequencing (Section 2.2.9.14).

By western analysis, we confirmed the expression of proteins, with the correct expected molecular weight in Cos-7 cells, using both anti-EGFP and either anti-CamKIV or anti-14-3-3β antibodies (Figure 5.12A and B). This was done only with respect to the expression of those genes carried by the pEGFP-N1 vector, as only this vector carries the SV40 origin of replication necessary for amplification within Cos-7 cells. We confirmed the expression of a 59 KDa protein in the case of CamKIV and a protein of 56 KDa representing 14-3-3β. In the CamKIV blot the anti-EGFP antibody binds to a doublet at 30 KDa, which may be a degredation product of the full sized protein. In the 14-3-3β blots the lower band visualised by anti-EGFP is most likely a product of degredation of the fusion protein and the lower band visualised by anti-14-3-3β is endogenous 14-3-3β, present also in the control.

Using the pEGFP-N1 constructs, which we had confirmed correctly express $CamKIV_{1-313}$ and 14-3-3β, we attempted to create FBR cell lines with stable expression of these genes. We tried initially, to do this using a transfection method and latterly using nucleofection (Sections 2.2.10.2 and 2.2.10.5).

We were unable to create a population of FBR cells stably expressing constitutively active CamKIV. Cell death was particularly high in transfections, with dying cells showing extensive surface blebbing, characteristic of apoptosis. The populations we selected by G418 followed by FACS, expressed only two EGFP-tagged proteins of

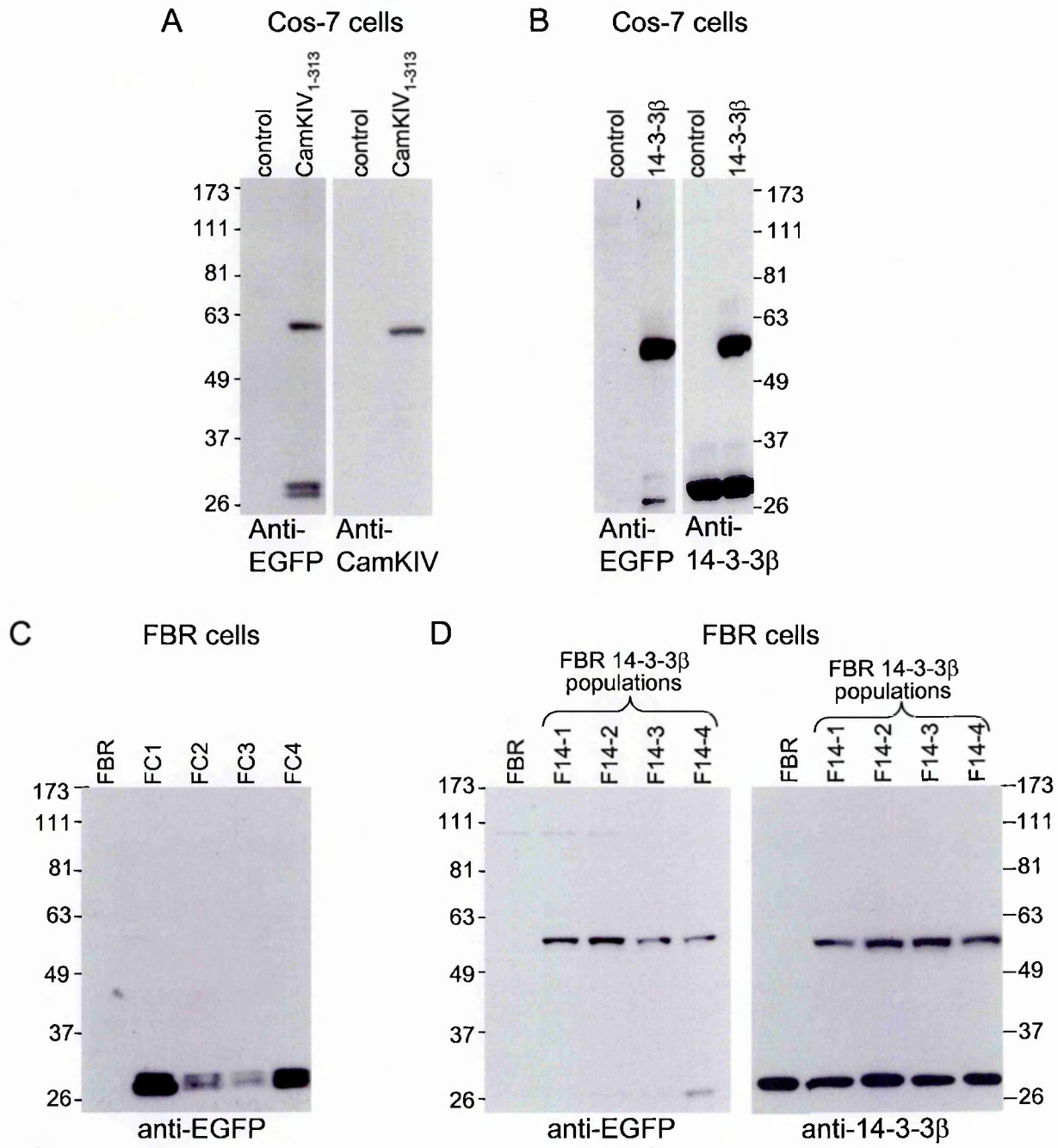

Figure 5.12

Western analysis of transfected cells.

A. Cos-7 cells transiently expressing CamKIV$_{1-313}$-EGFP, visualised using anti-EGFP (left) and anti-CamKIV (right) antibodies. EGFP-tagged CamKIV is, as expected, 59 KDa.

B. Cos-7 cells transiently expressing 14-3-3β, visualised using anti-EGFP (left) and anti-14-3-3β (right) antibodies; both showing expression of a protein of 56 KDa, as expected.

C. FBR cells which were expected to have stable expression of CamKIV$_{1-313}$-EGFP. Only a doublet band at 30 KDa is seen.

D. Four distinct, but non-clonal populations of FBR cells which have stable expression of 14-3-3β, visualised using anti-EGFP (left) and anti-14-3-3β (right) antibodies; all showing expression of a protein of 56 KDa, as expected. The anti-14-3-3β blot (right) also shows a lower 29 KDa band, corresponding to the endogenous protein.

approximately 30 KDa, as shown by western analysis (Figure 5.12C); and by fluorescence microscopy, the distribution of the ectopically expressed protein was consistent with that of EGFP (data not shown). The populations transfected with the pLPCX2 vector carrying myc-tagged $CamKIV_{1-313}$ gave no bands on western blot and no staining by immunofluorescence, with either anti-myc or anti-CamKIV antibodies (data not shown). We concluded that FBR cells are unable to tolerate constitutively active CamKIV, and that the enzyme is effectively toxic to them.

In contrast, our experiments showed that FBR cells easily accommodate over-expressed 14-3-3β-EGFP. In transfections there was negligible cell death as a consequence of its expression (data not shown), and western analysis showed the expression of a protein of 56 KDa, with either anti-EGFP or anti-14-3-3β antibodies, in each of four distinct, but non-clonal, populations (Figure 5.12D). Three of the four populations showed no bands other than the 56 KDa protein, using anti-EGFP antibody, and the only other band in the anti-14-3-3β-probed western blot corresponds to endogenous 14-3-3β. The cellular localisation of the expressed protein was consistent with a protein which shuttles between nucleus and cytoplasm and which remains bound to exported proteins in the cytoplasm preventing their re-entry into the nucleus. Expression is throughout the cell (though it is not consistently found in the ends of pseudopods) with less in the nucleus compared to the cytoplasm (Figure 5.13).

5.5.3 FBR cells stably over-expressing 14-3-3β: effect on morphology, actin stress-fibres and invasion, and response to TSA

As can be seen from the confocal images of 14-3-3β localisation in FBR cells (Figure 5.13), there is no apparent effect on the morphology or stress-fibre arrangement in 14-

FBR cells stably expressing 14-3-3β

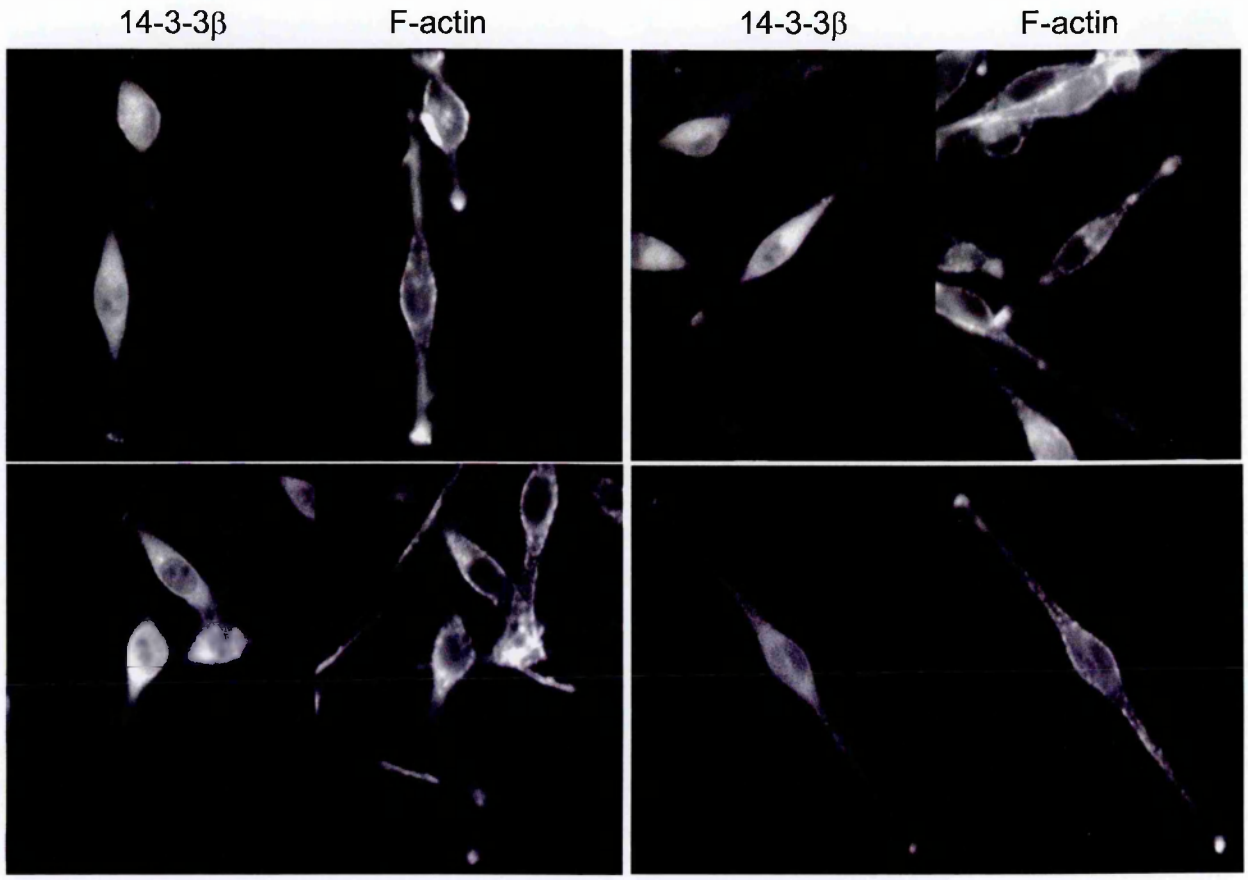

Figure 5.13

Confocal microscope images showing the distribution of ectopically expressed 14-3-3β-EGFP in FBR cells. In each of the four double images, the left-hand panel shows 14-3-3β-EGFP (green fluorescent) and the right-hand panel shows F-actin which is stained with TRITC-phalloidin (red fluorescent).

3-3β-EGFP over-expressing FBR cells (F14 cells). In *in vitro* invasion assays we could not detect any measured effect on the invasive ability of the cells (Figure 5.14A and B). We did find that there was slight variation between populations (though the variation was always within the error bars), however, when we pooled these, the resultant population was indistinguishable from FBR cells expressing EGFP. When treated with TSA, the F14 cells did not differ from FBR cells in their morphological response with respect to cell flattening and actin stress-fibre rearrangement (data not shown) either temporally or qualitatively. In invasion assays of TSA-treated cells, neither did we see any significant difference in inhibition of invasion, between the F14 populations and the two control populations of FBR or FBR expressing EGFP (Figure 5.14C).

5.5.4 Invasion assays with FBR cells co-expressing exogenous CamKIV$_{1\text{-}313}$, and 14-3-3β

We thought it is possible that there is no effect of expressing exogenous 14-3-3β because 14-3-3β can only export HDAC4, if HDAC4 is phosphorylated. It may therefore be necessary to express both 14-3-3β and CamKIV$_{1\text{-}313}$ simultaneously to facilitate nuclear export of HDAC4. Since we were unable to create stable CamKIV$_{1\text{-}313}$ expressing FBR cells, we transiently expressed CamKIV$_{1\text{-}313}$-myc in our F14 cells and used these in invasion assays, 24 hours post-nucleofection (Figure 5.15). In addition, we included in these assays FBR cells which were co-nucleofected with CamKIV$_{1\text{-}313}$-EGFP and 14-3-3β-myc. We found that transient CamKIV$_{1\text{-}313}$-EGFP or transient CamKIV$_{1\text{-}313}$-EGFP plus transient 14-3-3β-myc inhibited invasion of FBR cells by 100% and that CamKIV$_{1\text{-}313}$-myc expressed transiently in F14 cells inhibits invasion by 96% (Figure 5.15B).

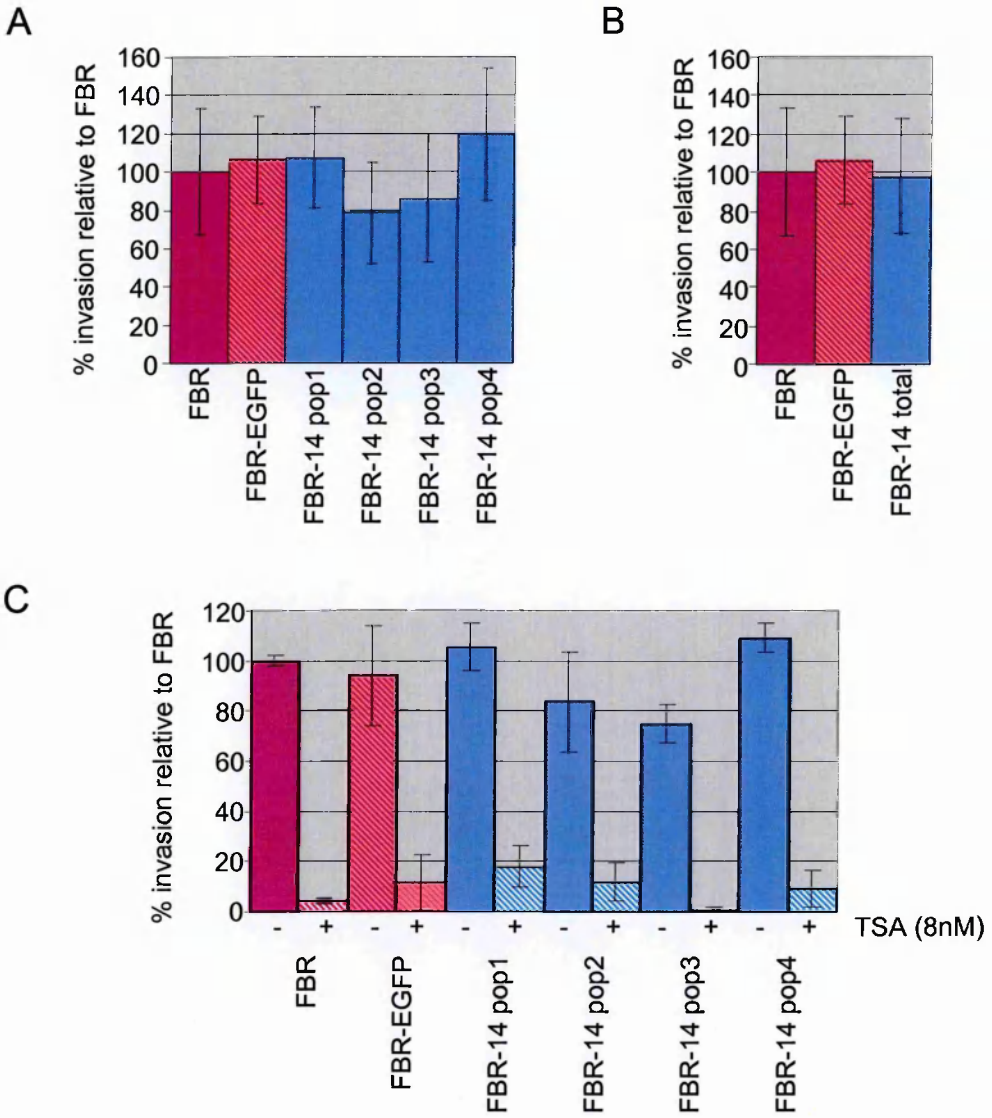

Figure 5.14

A. Histogram of the quantified results of two invasion assays, showing invasion in four distinct, but non-clonal, populations of 14-3-3β-expressing FBR cells.

B. Histogram of the quantified results of two invasion assays, showing the invasion in 14-3-3β-expressing FBR cells. In this case the separate populations, shown in A, have been pooled.

C. Invasion assay showing effect of TSA on four distinct, but non-clonal, populations of 14-3-3β-expressing FBR cells.

FBR cells expressing CamKIV$_{1-313}$, or CamKIV$_{1-313}$ and 14-3-3β, are not invasive

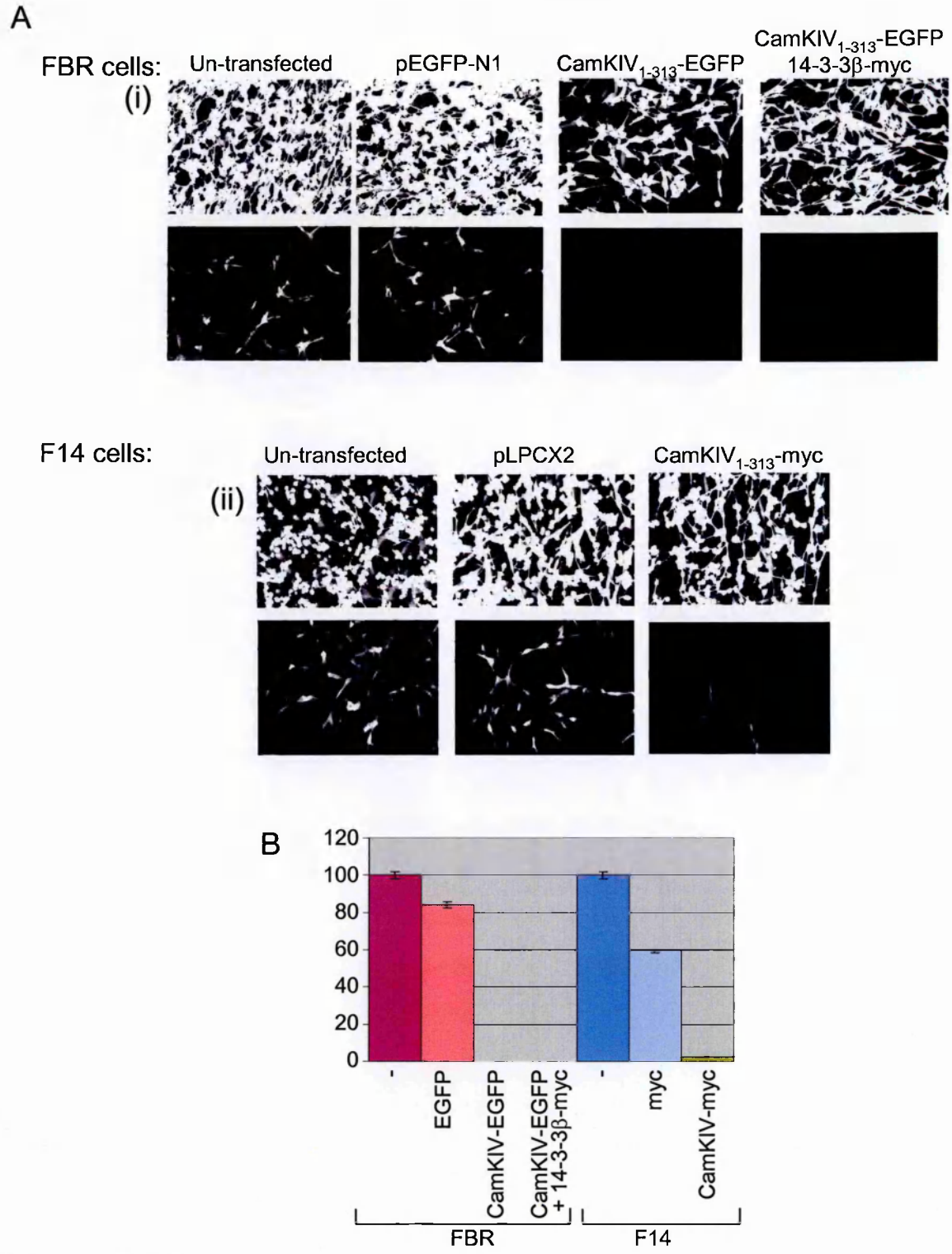

Figure 5.15

A. Invasion assay showing that:

(i) Invasion is inhibited in FBR cells transiently expressing CamKIV$_{1-313}$, or transiently co-expressing CamKIV$_{1-313}$ and 14-3-3β, compared to FBR cells or to FBR cells which transiently express EGFP.

(ii) Invasion is inhibited in F14 cells transiently expressing CamKIV$_{1-313}$, compared to F14 cells and to F14 cells transfected with the pLPCX2 vector.

B. Histogram depicting the quantified results of the invasion assay shown in A.

This experiment was performed only once as it was superseded by a larger experiment (Figure 5.16), Therefore, the error bars are small since they indicate only the error internal to the experiment, i.e., between samples rather than between experiments.

5.5.5 Invasion assays with FBR cells co-expressing exogenous CamKIV$_{1-313}$, 14-3-3β and/or TMHDAC4

If it is the case that invasion is inhibited by CamKIV$_{1-313}$ and 14-3-3β, or by CamKIV$_{1-313}$, because HDAC4 has been exported from the nucleus, then we thought it may be possible to rescue the non-invasive phenotype by expressing TMHDAC4 in these cells, since this protein cannot be phosphorylated to facilitate its export. Consequently we designed an invasion assay where FBR and F14 cells were co-nucleofected with various combinations of CamKIV$_{1-313}$, 14-3-3β and TMHDAC4 (Figure 5.16A and B). These experiments differed from those in the previous section, in that cells were transferred to the invasion assay immediately post-nucleofection.

We found that in FBR cells, when CamKIV$_{1-313}$ or TMHDAC4 are expressed individually (Figures 5.17 and 5.11 show confocal microscope images, demonstrating correct, expected localisation of CamKIV$_{1-313}$-EGFP or TMHDAC4-EGFP) they inhibit invasion by 83% and 91% respectively, however, when they are co-expressed, inhibition of invasion drops to 45%, thus the non-invasive phenotype of either protein is rescued by the expression of the other. Similarly, though more dramatically, we see this in F14 cells, where CamKIV$_{1-313}$ or TMHDAC4 inhibit invasion by 63% and 81% respectively, but when co-expressed there is no inhibition of invasion, indeed there appears to be an increase of 15% compared to F14 cells, though this differential is within error bars and is probably not be significant. Interestingly, when all three proteins are co-expressed in FBR cells invasion is inhibited by 73% yet when CamKIV$_{1-313}$ and TMHDAC4 are co-expressed in F14 cells (i.e., all three proteins are expressed, but in this case expression of 14-3-3β is stable) there is no inhibition of invasion.

FBR cells co-expressing TMHDAC4 and CamKIV$_{1-313}$ are invasive

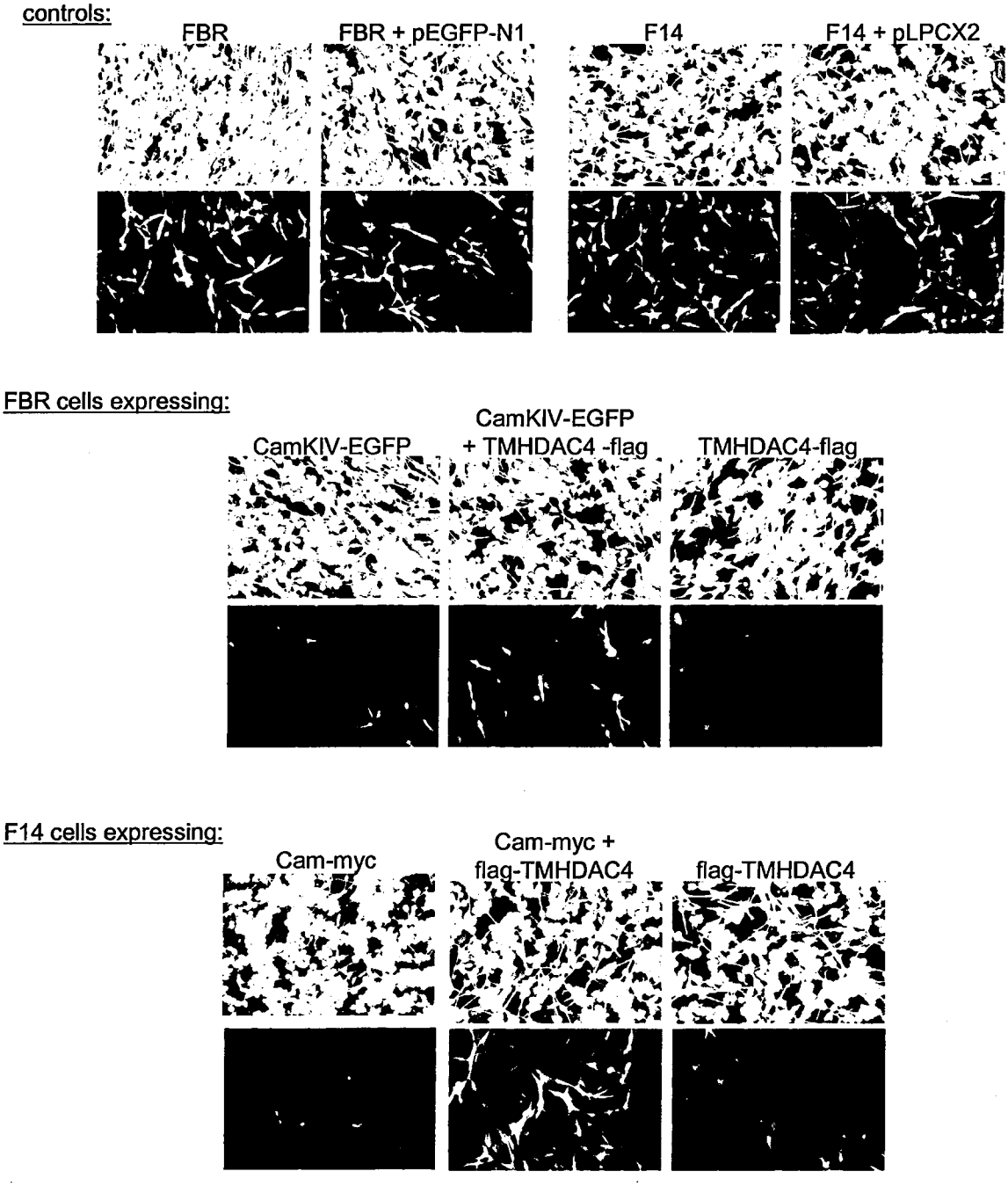

Figure 5.16A

Invasion assay showing that:

(i) FBR cells which transiently co-express CamKIV$_{1-313}$ and TMHDAC4 are invasive, in contrast to FBR cells which transiently express CamKIV$_{1-313}$ or which transiently express TMHDAC4, which are non-invasive.

(ii) F14 cells which transiently co-express CamKIV$_{1-313}$ and TMHDAC4 are invasive, in contrast to F14 cells which transiently express CamKIV$_{1-313}$ or which transiently express TMHDAC4, which are non-invasive.

FBR cells co-expressing TMHDAC4 and CamKIV$_{1-313}$ are invasive

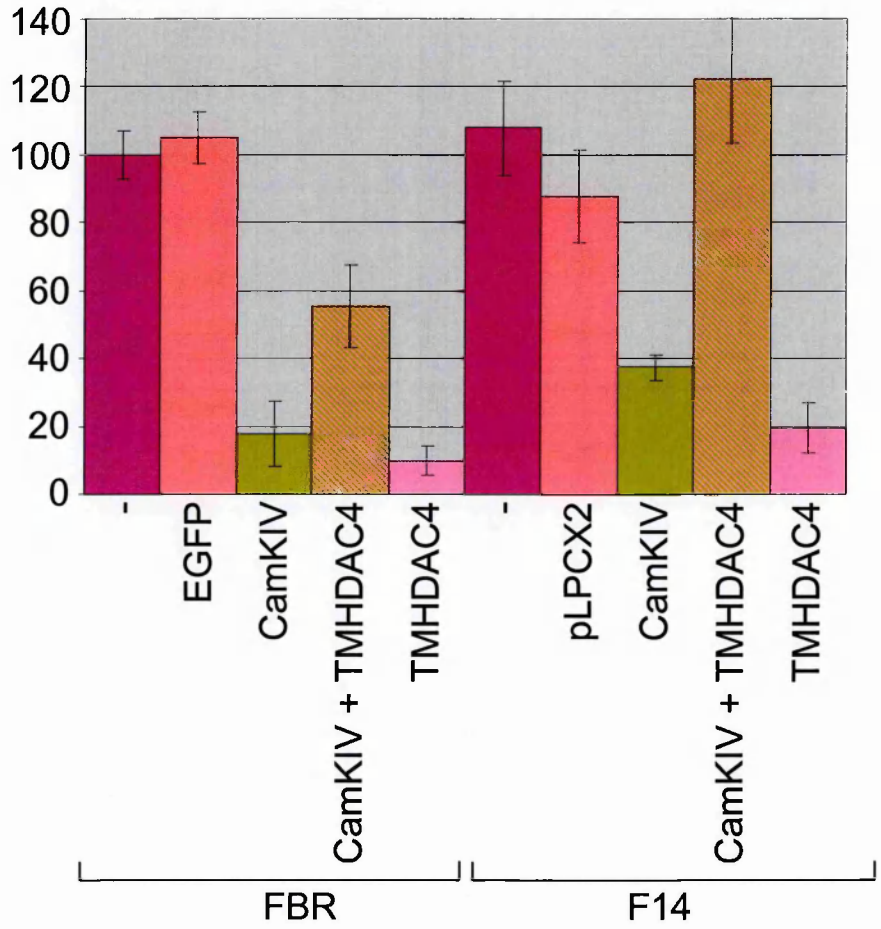

Figure 5.16B

Histogram depicting the quantified results of the invasion assays shown and described in A (Figure 5.16A). Quantification was of three identical assays, with duplicate samples in each.

FBR cells transiently expressing $CamKIV_{1-313}$

Figure 5.17

Confocal microscope images of nucleofected FBR cells used in invasion assays (Figure 5.16) , showing the distribution of transiently expressed $CamKIV_{1-313}$-EGFP in FBR cells. In each of the three double images, the left-hand panel shows $CamKIV_{1-313}$-EGFP (green fluorescent) and the right hand panel shows F-actin is stained with TRITC-phalloidin (red fluorescent). Images were captured 24 hours post-nucleofection. It is reported that wtCamKIV has a more uniform cellular distribution, but locates to the nucleus when activated (Lemrow et al. 2004). Constitutively active $CamKIV_{1-313}$, however, has been shown to locate to the nucleus (Lemrow et al. 2004).

5.6 Conclusions

In this chapter, we showed firstly, that over-expression of HDAC4 in FBR cells confers resistance to inhibition of invasion by HDAC inhibitors; and that over-expression of HDAC4 in 208F cells results in a morphological change, with cells becoming more bipolar in appearance. Secondly, we demonstrated that expression of deacetylase-inactive HDAC4 inhibits invasion in FBR cells. Finally, we showed that when individually expressed, $CamKIV_{1-313}$ and TMHDAC4, inhibit invasion in FBR cells, but when co-expressed, the non-invasive phenotype is rescued.

Many of the results described in this chapter, whilst interesting, remain preliminary. Although approaches taken were valid, we did not obtain results which, if further investigated, promised to yield data which would be easily interpreted and/or confirmed, and thus translated into publishable data. This being the necessary aim in today's scientific climate, we chose to leave these lines of research in order to concentrate on the more promising data described in chapters 3 and 4, which did ultimately prove fruitful (McGarry et al. 2004).

Chapter 6

Discussion

6.1 General Introduction

Work in this laboratory in recent years has been largely concerned with investigating the hypothesis that AP-1 regulates a multigenic invasion programme. This advocates that genes which are up-regulated by AP-1 are effectors of invasion and that genes which are down-regulated by AP-1 are suppressors of invasion. Generally, our strategy has been to *decrease* expression or function of genes which are *up*-regulated, by AP-1, in Fos-transformed cells; and conversely, to *increase* expression of genes which are *down*-regulated, by AP-1, in Fos-transformed cells, and, in both cases, to examine the consequences with respect to reversion of the transformed phenotype.

In the current study, we have shown that HDACs are up-regulated genes in v-Fos^{FBR}-transformed cells, and therefore, are proposed to be effectors of invasion. HDACs, however, function to down-regulate genes, so the consequence of their increased expression, is increased down-regulation of genes. Down-regulated genes are, by our hypothesis, invasion suppressors, thus their re-expression would suppress invasion. Consequently, we proposed that inhibition of HDACs (effectors of invasion) would result in the increased expression of down-regulated genes and in the inhibition of invasion. To establish a link between re-expression of down-regulated genes and inhibition of invasion, we re-expressed these HDAC-sensitive genes individually in FBR cells and assessed whether invasion is inhibited.

6.2 Studies with histone deacetylase inhibitors

6.2.1 Introduction

Initially we demonstrated that several histone deacetylases and functionally associated proteins are up-regulated in Fos-transformed fibroblasts relative to the parental non-transformed cells, leading us to consider the role of HDACs in the Fos-

transformed phenotype; thus, we investigated the consequences of their inhibition. The HDAC inhibitors we have used are both currently in clinical trials as anticancer agents. They are structurally distinct (Figures 1.8 and 1.9), which strengthens the validity of our results, making it is less likely that the phenotypic changes we see (similar for both inhibitors) are by mechanisms other than through the relief of HDAC-mediated transcriptional repression. The results from these studies of the effects of inhibitors on the Fos-transformed phenotype are summarised in Table 6.1 (below).

		Reverted morphology	Re-appearance of stress-fibres	Inhibition of:			
				motility	invasion	growth	chemotaxis
TSA (nM)	4	-	ND	-	+ 80%	-	-
	8	-	+	-	+ 90%	-	-
	12	+	+	+	+	-	ND
	20	+	+	+	+	+	ND
VPA (μgml^{-1})	25	-	+	-	+ 90%	-	-
	50	+	+	+	+ 95%	-	ND
	100	+	+	+	+	+	ND

Table 6.1
Summary of the effects of HDAC inhibitors on the Fos-transformed phenotype after treatment for 4 days. ND = not done.

6.2.2 Characteristics of Fos transformation are mediated by up-regulation of HDACs

Our results demonstrate that morphological transformation, lack of actin stress-fibres, increased motility, and ability to invade, as orchestrated by v-Fos^{FBR}, are mediated by the up-regulated expression of histone deacetylases, which are known to facilitate transcriptional repression of genes. We should perhaps bear in mind though, that transcriptional repression of a transcriptional repressor would result in the *up-regulation* of genes; or that the transcriptional repression of, say, a phosphatase could result in a higher proportion of phosphorylated, and therefore, *active* protein. So,

although we think of histone deacetylation in terms of gene silencing, the consequences of their increased expression may be more of a change in the balance of genes expressed; a shift in the steady-state.

6.2.3 Invasion can be inhibited without affecting morphology, motility, chemotaxis or proliferation

We have shown that proliferation of FBR cells is unaffected by ≤ 50 μgml^{-1} VPA or ≤ 12 nM TSA. The ability of Fos-transformed cells to invade is inhibited at concentrations of ≥ 25 μgml^{-1} VPA, or ≥ 4nM TSA, therefore, within the ranges, 25 to 50 μgml^{-1} VPA, and 4 to 12 nM TSA, we can inhibit invasion without affecting growth (Table 6.1). Moreover, at lower concentrations within these ranges invasion is inhibited without affecting transformed morphology or motility; nor is the chemotactic response diminished. This separates morphology, motility and chemotaxis from invasion, in terms of gene expression. Since HDAC inhibitors relieve the suppression of gene expression mediated by HDACs, it would suggest that very little re-expression of genes is required to inhibit invasion, in comparison with morphology / motility / chemotaxis, and therefore, that invasion is a very precisely orchestrated function, such that re-expression of down-regulated genes (or any slight disruption to the tightly defined balance of genes expressed) is incompatible with the phenotype. This has indeed proved to be the case, in our studies with the re-expression of genes down-regulated by Fos (Chapter 4; section 6.3).

6.2.4 HDAC inhibitor-induced morphological reversion is reversible

The phenotypic reversion we see in response to HDAC inhibition is reversible. By 4 days after the removal of inhibitor morphology has almost completely returned to bipolar. If the cells are passaged this happens more quickly. A plausible explanation

for this can be found using our data on the re-expression of genes in response to HDAC inhibition. One such re-expressed gene is fibronectin, which is secreted by the cell as part of the extracellular matrix. When HDAC inhibitor is removed from the culture, the fibronectin in the extracellular matrix will still be present. This could explain why, although the cells regain their bipolar morphology they retain what appear to be lateral points of attachment to the extracellular matrix along the pseudopod. These are most probably retraction fibres, where integrins in focal adhesions have not disengaged from their extracellular contacts. If the cells are passaged subsequent to removal of inhibitor the re-seeded cells do not have these "retraction fibres", probably because there is no fibronectin in the new vessel.

6.2.5 Inhibition of invasion correlates with formation of actin stress-fibres

From our data (Table 6.1), it appears that reversion of morphology correlates with inhibition of motility with respect to concentration of inhibitor required and therefore to a related gene-expression profile; whilst invasion correlates with a loss of actin stress-fibres. Reformation of F-actin, on inhibition of HDACs, shows that HDACs have a role in inhibition of F-actin formation, perhaps by the silencing of genes involved in its polymerisation. Surprisingly, we discovered that there is significant stress-fibre reformation within 24 hours of treatment with 25 μgml^{-1} VPA, which could provide an explanation as to why no preincubation with inhibitor is required to inhibit invasion in *in vitro* assay. This, however, assumes that stress-fibre reformation is required for inhibition of invasion, but when we have re-expressed genes down-regulated in FBR cells, we have shown that invasion is inhibited in the absence of stress-fibres (Sections 4.2.4 and 4.2.5), therefore this cannot be the case.

Stress-fibres reform in the absence of morphological reversion, this shows that the formation of stress-fibres is not sufficient to facilitate morphological reversion. It may

be that rearrangement of stress-fibres is required. In bipolar cells with stress-fibres the fibres run parallel to the long axis of the cell, however, on reversion of morphology the fibres tend to radiate from the centre of the cell (Figure 3.4). This differs from 208F cells in that their stress-fibres tend to have a more cross-wise appearance with bundles of fibres angled relative to one another. There is no further increase in the proportion of cells with stress-fibres when inhibitor concentration is increased, thus we have achieved the maximal quantitative effect at 25 μgml^{-1}. These results suggest that, like inhibition of invasion, little re-expression of genes is required to permit polymerisation, however, further re-expression is required to permit the re-arrangement of the polymerised actin. Thus, it is most probable that reversion of morphology correlates with the re-arrangement of stress-fibres rather than their formation.

It is perhaps also worthy of note here, that the reappearance of stress-fibres within 24 hours of inhibitor treatment, hints at the possibility of a cytoplasmic role for HDACs in this respect; perhaps inhibiting stress-fibre reformation by the direct deacetylation of a cytoplasmic protein, say for example, deacetylation of G-actin retains it in its monomeric state. Further experiments to determine exactly when, within the 24 hours, the stress-fibres reappear and whether this can occur in the absence of mRNA and protein synthesis, would determine whether a direct cytoplasmic role is likely.

6.2.6 EGF-stimulated invasion in non-transformed cells is inhibited by HDAC inhibition

Finally, in a supplementary experiment we also showed that TSA inhibits EGF-induced invasion of 208F cells. This is important in that it demonstrates that when AP-1 is up-regulated by a commonly occurring *in vivo* mechanism, inhibition of invasion is facilitated by HDAC inhibition. It answers the criticism that mutated Fos is not commonly found in tumours, and therefore that it cannot relate to the *in vivo* situation.

It is also for this reason that we included Ras-transformed cells in our survey of HDAC and related protein expression levels, in normal versus Fos-transformed cells, and why up-regulation of HDAC4 in Ras-transformation was a factor in its choice for further study (Section 5.2).

6.2.7 Conclusions

We conclude that, epigenetic repression of gene expression by up-regulated histone deacetylases plays a key role in the transformation of fibroblasts by v-Fos^{FBR}. When we inhibit the up-regulated histone deacetylases we inhibit invasion of the v-Fos-transformed cells, stress-fibres reform, transformed morphology reverts and motility is inhibited. At lower concentrations of HDAC inhibitors we inhibit invasion, and bring about reformation of actin stress-fibres, without affecting morphology, motility, or chemotaxis, separating these characteristics from invasion and stress-fibre reformation in terms of gene expression and suggesting that invasion is, in comparison, controlled by a very finely orchestrated programme of gene expression.

6.3 Genes down-regulated by histone deacetylation

6.3.1 Introduction

Previous work in this laboratory identified genes that are up- and down-regulated as a consequence of v-Fos^{FBR} expression (Johnston et al. 2000; Ozanne et al. 2000). Using HDAC inhibitors, we have demonstrated that HDAC activity is responsible for the down-regulation of several of these genes in Fos-transformed cells. In addition we have shown that not all genes down-regulated in FBR cells can be re-expressed as a consequence of HDAC inhibition. This shows that other factors are also required in the down-regulation of genes in FBR cells; probably primarily DNA methylation, as indicated by our finding that HDAC1, Sin3, SAP18, RbAp46 and MeCP2 are up-

regulated in FBR cells. These are all components of large protein complexes with deacetylase activity, which are recruited to DNA through methylated DNA binding proteins, thus methylation is required for targeting.

6.3.2 Histone deacetylases mediate suppression of genes down-regulated by v-Fos

Investigating the response to inhibition of histone deacetylases in terms of gene re-expression, we treated FBR cells with both TSA and VPA, which resulted in the increased expression of five out of eleven genes, to the levels observed in untransformed 208F cells; that is, the silencing of these genes by histone deacetylation (whether directly or indirectly) is relieved on treatment of FBR cells with histone deacetylase inhibitors. Three of the genes, STAT6, RYBP and PCDHGC3, when expressed individually in FBR cells, are potent inhibitors of invasion without any effect on cellular morphology, actin stress-fibres, motility, chemotaxis, or proliferation. This shows that it is not solely the re-expression of these genes, in response to HDAC inhibitors, which is responsible for reversion of transformed morphology, formation of stress-fibres or inhibition of motility; but that expression of any of one of these genes is incompatible only with invasion. Each gene then, is demonstrated to be a member of the, previously proposed, AP-1 regulated multigenic invasion programme (Johnston et al. 2000; Ozanne et al. 2000). By definition, each component of a programme (a single gene product) functions to achieve the aim of the programme. For down-regulated genes, their expression is inconsistent with invasion as we have demonstrated by their over-expression in FBR cells. The finding that HDAC inhibitors severely restrict invasion demonstrates that HDAC activity is a positive regulator of the multigenic invasion programme.

The inhibition of invasion that we have demonstrated when each of our genes is re-expressed, occurs both in FBR cells which transiently express the genes, and in FBR

cells, which stably express the genes. In transiently expressing cells, there is a sudden, high level of expression of the protein and the cell has little time to make adjustments; in stably expressing cells, the level of expression is lower and the cell has had several generations to re-establish the steady state of its expression profile, thus accommodating the gene. We have shown, therefore, that the inhibition of invasion cannot due to a long-term accommodation of the cell to expression of the repressed genes; nor can it be due to the cells reaction to a sudden high level of expression of the protein. Interestingly, invasion is more strongly inhibited when the genes are stably expressed, suggesting that when the cell has altered its steady-state of gene expression, as a consequence of the new protein, the impact on invasion is greater. It could be argued that this is closer to the *in vivo* situation as expression of any gene may have consequences in terms of gene-expression, particularly when the gene is a transcription factor like STAT6 or a transcription cofactor like RYBP. In the case of the transmembrane receptor, PCDHGC3, there could be, for example, intracellular signalling as a consequence of extracellular binding to the protocadherin, which results in gene expression changes.

6.3.3 Proteins, ectopically re-expressed in FBR cells

The mechanisms by which these genes inhibit invasion are not known, but it is probable that RYBP and STAT6 as transcription factors/cofactors inhibit invasion by altering gene expression. The targets of these genes in this context remain to be identified, but suggest that the v-Fos regulated multigenic invasion programme consists of a transcriptional cascade or network that controls the effectors and inhibitors of invasion.

RYBP, a transcription co-factor (Garcia et al. 1999), interacts with the transcription factors, YY1, E2F2, E2F3, E2F6 and the polycomb complex proteins, Ring1 and M33

(Garcia et al. 1999; Trimarchi et al. 2001; Schlisio et al. 2002), but does not bind DNA directly. Depending on the transcription factor to which it is bound, RYBP could function as a transcriptional repressor or activator. In the context of Fos-transformation its role awaits further investigation; however, it would seem less likely to be through interaction with E2F2 and E2F3, which stimulate expression of the cell cycle regulator Cdc6 (Schlisio et al. 2002), as the rate of cell cycle progression does not appear to be altered upon re-expression of RYBP, either by HDAC inhibitor treatment or by transgene. It may be that RYBP functions through interaction with the polycomb group proteins suppressing gene expression, however, since the role of E2F6 is not clearly defined, it could be a co-factor for E2F6, that is itself a component of the mammalian Bmi1-containing polycomb complex that functions to suppress gene expression (Trimarchi et al. 2001). There is of course the possibility that there are yet undiscovered transcription factors that RYBP interacts with.

STAT6, an interleukin (IL) -4 and IL-13-regulated transcription factor, is also down-regulated in FBR cells relative to 208F cells and its expression is returned to 208F levels following HDAC inhibition. The role of STAT6 in Fos-transformation may be related to role in activating transcription of tissue inhibitor of matrix metalloproteinase (TIMP) genes (Gatsios et al. 1996; Bugno et al. 1995) or in altering expression of extracellular matrix components such as type I collagen (McGaha et al. 2003; Buttner et al. 2004).

Re-expression of the cell-cell adhesion / recognition protein PCDHGC3 (formerly protocadherin-43 or PCDH2) may affect the way the cells interact. They may be able to make cell contacts where previously they could not, or it may be more difficult for them to break cell-cell contacts. If this is how inhibition of invasion occurs, one might also expect motility to be inhibited, which is not the case; though of course we could not predict how these cell-cell contacts will behave in a motility assay compared to an

invasion assay. Interestingly, mammalian E-cadherin has been shown to be a suppressor of cell migration and tumour invasion (Behrens et al. 1991; Chen and Obrink 1991; Frixen et al. 1991; Schipper et al. 1991; Fahraeus et al. 1992) and Drosophila *fat*, a cadherin-related protein, functions as tumour suppressor (Mahoney et al. 1991). The human homologue of *fat* has been shown to be expressed in fibroblasts (Matsuyoshi and Imamura 1997).

The finding that three HDAC-repressed genes *all* affect invasion without affecting proliferation or motility, strongly suggests that the invasion programme is precisely controlled to permit invasion and that genes are down-regulated as a consequence of activation of the invasion programme. In this context it is significant perhaps that the Fos-transformed cells have never been selected for invasiveness; rather it seems to be the consequence of a sustained increase in AP-1 activity that establishes the AP-1-regulated multigenic invasion programme.

6.3.4 Conclusions

From these experiments then we can conclude that, histone deacetylation alone, is sufficient to facilitate the silencing of at least a proportion of those genes, shown to be, down-regulated in Fos-transformation, and inhibition of histone deacetylase activity can relieve the silencing of such genes. The ectopic re-expression of some (RYBP, PCDHGC3, STAT6), if not all, of these silenced genes inhibits invasion; the inappropriate expression of any one of them then, is incompatible with the invasive phenotype. Although these cells have inhibited invasion they are unaffected in morphology, motility, chemotactic response, or rate of proliferation. That is, histone deacetylases are responsible for down-regulation of genes, the expression of which would be incompatible with invasion but not with transformed morphology, motility, chemotactic response, or rate of proliferation.

6.4 Strategies to modulate levels of HDAC4 in Fos-transformed cells

6.4.1 Introduction

To determine whether specifically, HDAC4 has a role in mediating transformation by v-Fos^{FBR}, we employed several strategies. To increase HDAC4 in both FBR and 208F cells we ectopically expressed wtHDAC4 (Section 5.2) or TMHDAC4 (Sections 5.4 and 5.5.5), and to decrease HDAC4 we ectopically expressed CamKIV$_{1-313}$, 14-3-3β (Section 5.5), or two forms of deacetylase-inactive HDAC4 (Section 5.3). One might expect an increase in HDAC4, in 208F cells, to confer some aspect of transformation; and in FBR cells, to provide resistance to the effects of HDAC inhibitors. Conversely, decreased HDAC4 in FBR cells may result in reversion of some aspect of the transformed phenotype.

6.4.2 Over-expression of wtHDAC4 in Fos-transformed fibroblasts

Our results showed that over-expression of HDAC4 in FBR cells has no effect on their ability to invade, though, significantly, they did become resistant to inhibition of invasion by HDAC inhibitors.

There are three main plausible explanations as to why an increase in HDAC4 does not increase invasion. Firstly, the level of HDAC4 may already be optimal for invasion. An increase in HDAC4 would result in increased transcriptional repression, and as previously discussed (Section 6.2.2), this would result in both decreases and increases, in genes expressed, and in activities of proteins. It would seem unlikely, since we are advocating that invasion is a very precisely controlled process, that this apparent disruption would favour increased invasion. Secondly, it is possible that, despite an increase in cellular HDAC4, the level in the nucleus remains unaffected due to a compensatory increase in nuclear export. Thirdly, it is equally possible that increased nuclear HDAC4 is ineffectual without a concomitant increase in proteins

which together form the HDAC4 transcriptional repression complex. These explanations are not mutually exclusive; in fact the true explanation could equally be a combination of all three.

We also showed that HDAC4-over-expressing FBR cells are resistant to inhibition of invasion by HDAC inhibitors; that a higher concentration of HDAC inhibitor is required in these cells, to achieve the equivalent percentage inhibition of invasion found in FBR cells. In terms of explanation, it may simply be that the increased HDAC4 binds inhibitor and effectively sequesters it, such that the level of HDAC inhibition is reduced in a general sense. It could also be the case that increased HDAC4 is able to compensate mechanistically for other HDACs which are inhibited; that there is redundancy in the HDACs in this situation. This would mean that HDAC4 is able to suppress gene expression such that invasion can occur. A more attractive scenario is that increased HDAC4 compensates, specifically for the HDAC4 which is inhibited. Here the conclusion would be that, in Fos-transformed cells, HDAC4 is a positive regulator of invasion, and our previous results suggest that it does this by down-regulating genes, the expression of which is incompatible with invasion.

6.4.3 Expression of wtHDAC4 in normal fibroblasts

208F cells have 9-fold less HDAC4 than FBR cells, and are non-invasive. One might expect that on ectopic expression of HDAC4, they would become invasive, but this is not the case. In chapter 5 we have shown that re-expression, in FBR cells, of any individual gene, normally down-regulated in FBR cells, inhibits their invasion (of those we tested). In addition, it was shown previously in this laboratory, that another gene that is down-regulated in FBR cells, TSC36, also inhibits invasion when re-expressed (Johnston et al. 2000; Ozanne et al. 2000). Thus unless increased HDAC4 in 208F cells is able to mediate the down-regulation of every gene which is down-regulated in

FBR cells, we would be unlikely to see an increase in invasion. In addition we also showed that not all genes down-regulated in FBR cells can be re-expressed as a consequence of HDAC inhibition. This shows that other events, such as DNA methylation, may also be required for the down-regulation of these genes, or that down-regulation also occurs by deacetylase-independent mechanism. Consequently, we could not expect an increase in HDAC expression to facilitate down-regulation of *all* genes, required to be down-regulated for invasion to occur. Of course, we should also consider that, as well as the requirement for down-regulation of invasion suppressors to facilitate invasion, there may also be the requirement for the up-regulation of genes which are effectors of invasion. Finally, an alternative possibility may be that other components, which are required to complex with HDAC4, are still lacking in HDAC4-over-expressing 208F cells, such that although HDAC4 is abundant, it is not sufficient to facilitate increased transcriptional repression required to permit invasion. Consequently, it is not surprising that HDAC4-over-expressing 208F cells are not invasive.

When we expressed wtHDAC4 in 208F cells, we partially transformed their morphology. As we have shown (Chapter 3 and 4) morphology and ability to invade are distinct in terms of gene profile (though they are clearly closely related). Again we can provide evidence to support this, in that populations of 208F cells over-expressing HDAC4 have a high proportion of bipolar cells, or of cells which have moved towards the bipolar phenotype, despite being non-invasive. Possibly HDAC4 has a role in the cytoplasm; a role which is relevant to the morphology of the cell but not to its ability to invade. This is not unprecedented since HDAC6 has been shown to have a cytoplasmic role, binding the dynein motors of tubulin, reportedly involved in regulating microtubule stability and function through deacetylation (Hubbert et al. 2002; Matsuyama et al. 2002; Zhang et al. 2003) and in the clearance of misfolded proteins

from the cytoplasm by dynein motors (Kawaguchi et al. 2003). In addition the NAD+-dependent, Sir2 class III deacetylase, has been shown to be a tubulin deacetylase (North et al. 2003).

6.4.4 Expression of deacetylase-inactive forms (H803A and D840N) of HDAC4 in Fos-transformed cells

Expression of deacetylase-inactive HDAC4 in FBR cells rendered them, up to 50% less invasive than control, EGFP-expressing, FBR cells, and perhaps surprisingly, conferred a slight resistance to inhibition of invasion by HDAC inhibitors.

To decrease invasion in FBR cells, deacetylase-inactive HDAC4 may be acting in a dominant-negative manner. There are three possible explanations as to how this may occur. Perhaps HDAC4-containing-complex formation cannot occur due to the change in stoichiometry. That is: a single complex which is normally A-HDAC4-B, becomes two incomplete complexes, A-H803A and H803A-B, thus suppression cannot occur. Were this the case however, it would seem unlikely that it would not also occur with wtHDAC4 over-expressed in FBR cells, which it does not. Another possibility is that, rather than disrupting the HDAC4 containing complex the deacetylase-inactive HDAC4 becomes part of the complex in the same way as would wtHDAC4, thus effectively sequestering it. Lastly, the mechanism by which the cell exports HDAC4 from the nucleus, may not distinguish between active and inactive enzyme, thus in maintaining the same nuclear level of HDAC4, it actually reduces HDAC4 nuclear activity, since a proportion of the remaining nuclear HDAC4 will be of the deacetylase-inactive form.

The data we generated in this experiment, was unusually variable between repetitions, which is reflected in the error bars generated. The variability in the data we collected could be a product of unstable dynamics of HDAC4 nuclear export in the deacetylase-

inactive HDAC4-expressing FBR cells, such that they are unable to achieve a comfortable equilibrium and constantly strive for maximal possible HDAC4 export. This may be less of a difficulty in wtHDAC4 over-expressing FBR cells if the high enzymatic activity plays a role in the mediation of increased nuclear export.

Deacetylase-inactive HDAC4-expressing FBR cells were slightly resistant to inhibition of invasion by HDAC inhibitors. The most likely explanation for this observation is simply that the deacetylase-inactive HDAC4 competes with endogenous HDACs for binding to the inhibitor, therefore, effectively sequestering it, and reducing inhibitor activity. One may think then, that this explanation could also be applied to the resistance to HDAC inhibitor observed in wtHDAC4 over-expressing FBR cells, however, there is a significant difference. The resistance to inhibition of invasion is slight in deacetylase-inactive HDAC4-expressing cells (Figure 5.10A), whereas, in wtHDAC4-expressing cells the resistance is greater than 90% on treatment with 8 nM TSA.

We considered the results from this section to be inconclusive in terms of explanation, and although many answerable questions arose, pursuing them was unlikely to yield worthwhile informative results in the timescale available.

6.4.5 Expression of TMHDAC4 in both normal, and Fos-transformed fibroblasts

By fluorescent microscopy we saw that HDAC4-EGFP and HDAC4-myc locate to the cytoplasm with low nuclear expression. Consequently, in further experiments we addressed the possibility that wtHDAC4 does not increase invasion simply because the cell exports all over-expressed HDAC4 from the nucleus. As previously described (Section 5.4.1), TMHDAC4 cannot be phosphorylated at sites required to facilitate its nuclear export. We were able to show that TMHDAC4-EGFP does indeed locate to the nucleus in cells transiently expressing the protein, however we were unable to

create stable cell lines of 208F or FBR expressing TMHDAC4-EGFP or TMHDAC4-flag and concluded that the protein is toxic to the cells, which agrees with the possibility that over-expressed HDAC4 is exported from the nucleus reducing nuclear activity to tolerated levels.

In studies with 208F and FBR cells transiently expressing TMHDAC4 we did not find these cells differed from parental cells, morphologically or in terms of actin stress-fibre arrangement. In invasion assays, FBR cells expressing TMHDAC4 were not invasive. If, as we believe, the level of HDAC4 in FBR cells is optimal for invasion, it is entirely expected that TMHDAC4-expressing FBR cells are non-invasive. In this case transcriptional repression by HDAC4 would be too high to mediate an invasion permissive gene profile. Of course alternatively, this could simply have been due to the toxicity of the protein, however, in invasion assays, discussed below (Section 6.4.7), where TMHDAC4 was transiently co-expressed with $CamKIV_{1-313}$ (which is able to phosphorylate endogenous HDAC4, thereby facilitating its nuclear export) we found that TMHDAC4 was able to rescue the non-invasive phenotype of $CamKIV_{1-313}$ expressing FBR cells.

6.4.6 Expression of $CamKIV_{1-313}$ or 14-3-3β in Fos-transformed cells

The purpose of expressing constitutively active CamKIV or 14-3-3β in FBR cells was, by facilitating HDAC4s nuclear export, to reduce the level of HDAC4 involved in transcriptional repression and, if HDAC4 has a role in transformation, particularly in invasion, we would expect reversion in some aspect of the transformed phenotype, specifically, in the ability to invade.

14-3-3β is a ubiquitous protein, and western analysis showed FBR cells have a high level of endogenous protein. Our experiments showed that FBR cells easily accommodate over-expressed 14-3-3β-EGFP. In transfections there was negligible

cell death as a consequence of its expression (data not shown). Its cellular localisation was as expected, however, there was no detectable effect on the proliferation (data not shown), morphology, actin stress-fibres or invasion, of FBR cells stably expressing the protein. In contrast, we were unable to create a population of FBR cells stably expressing constitutively active CamKIV. Cell death was particularly high in transfections, with cells showing extensive surface blebbing, characteristic of apoptosis (data not shown). Possible explanations are that 14-3-3β has almost no effect because it is already in excess; or that export of HDAC4 is not increased relative to that in FBR cells because HDAC4 is not more phosphorylated than it is in FBR cells, or perhaps an increase in other factors is also required to facilitate nuclear export. Constitutively active CamKIV, on the other hand, is most probably toxic to the cells; a likely scenario, since it is known to have multiple substrates unrelated to our study, the phosphorylation of which will have any number of unforeseen effects (Soderling 1999; Agell et al. 2002). This toxicity, however, rather than being general, may be specific to the export of HDAC4, in that the changes in gene expression as a consequence of decreased HDAC4 nuclear activity, are toxic. Alternatively, expression of $CamKIV_{1\text{-}313}$ may reduce the level of HDAC4 in the nucleus to the extent that the resultant changes in gene expression are incompatible with invasion, suggesting that HDAC4 is indeed required for the ability of FBR cells to invade.

6.4.7 Invasion assays with FBR cells co-expressing exogenous $CamKIV_{1\text{-}313}$, 14-3-3β, and/or TMHDAC4

FBR cells co-expressing $CamKIV_{1\text{-}313}$ and 14-3-3β are poorly invasive, as are FBR cells expressing TMHDAC4, however co-expressing $CamKIV_{1\text{-}313}$ with TMHDAC4 in FBR or F14 cells restores their ability to invade; in FBR cells to 55% of control cells and, dramatically, in F14 to ≥100% of control cells. We conclude that, although

CamKIV$_{1-313}$ mediates the nuclear export of HDAC4, it is unable to facilitate export of TMHDAC4 such that TMHDAC4 functionally replaces the exported wtHDAC4 in the nucleus, thus rescuing the invasive phenotype. In the case of non-invasive TMHDAC4-expressing cells, the level of HDAC4 (endogenous plus TMHDAC4) in the nucleus may be too high for invasion (or viability) to occur. Co-expression of CamKIV$_{1-313}$ and 14-3-3β along with TMHDAC4, however, decreases the level of nuclear HDAC4, by exporting the endogenous protein, thus invasion can occur. Why would the return to invasiveness be more dramatic in F14 cells? These cells stably express 14-3-3β and so have had several generations to make alterations in gene expression, to accommodate increased 14-3-3β expression. One might expect these changes to account for the difference in invasion we observe.

These results suggest that HDAC4 does have a role in the epigenetic silencing of genes incompatible with the invasive phenotype. Even if it is simply that expression of either CamKIV$_{1-313}$ or TMHDAC4 individually is toxic to the cells, the fact that one is no longer toxic in the presence of the other shows that this in itself is a specific response involving HDAC4, since the expression of one of these proteins is apparently incompatible with the normal functioning of the cell in the context of the gene expression profile of invasive cells.

6.4.8 Conclusions

The experiments carried out in this chapter were conceptually sound as evidenced by published studies. The TMHDAC4 approach has been used by several groups to force localisation of the transgene to the nucleus (Wang et al. 2000). Constitutively active CamKIV$_{1-313}$ was used to force nuclear localisation of wtHDAC4 (Miska et al. 2001) These studies, however, in looking at morphology and invasion with reference to Fos-transformation, yielded nothing concrete in terms of publishable results.

The main conclusions to this section, with regard to proving or disproving our hypothesis, that specifically, HDAC4 has a role in transformation by v-Fos, and in particular, is required for the ability of FBR cells to invade, are as follows. Firstly, we demonstrated that expression of HDAC4 in normal fibroblasts partially transforms their morphology. This tells us that probably, HDAC4 activity is necessary, but not sufficient to transform morphology. Secondly, we showed that expression of HDAC4 in v-Fos-transformed cells confers resistance to the inhibition of invasion by HDAC inhibitors, and thirdly, that expression of deacetylase-inactive HDAC4 in v-Fos-transformed cells inhibits invasion. From these we can conclude that probably, HDAC4 activity is necessary, but not sufficient to mediate invasion. These conclusions however, require confirmation, which would be best achieved using siRNA to HDAC4.

6.5 Summary of conclusions

Overall the work in this thesis demonstrates that:

1. HDACs are up-regulated in Fos-transformed cells.
2. HDAC activity is required for Fos-transformation, specifically invasion.
3. Individual aspects of transformation (bipolar morphology, increased motility, absence of stress-fibres) are controlled by specific groups of genes.
4. HDAC activity mediates down-regulation of genes in Fos-transformed cells.
5. Re-expression of down-regulated genes inhibits invasion in Fos-transformed cells.

In addition it is probable that:

6. HDAC4 activity is necessary but not sufficient for transformed morphology in fibroblasts.
7. HDAC4 activity is necessary but not sufficient to facilitate invasion in fibroblasts.

Chapter 7

Future Work

7.1 Introduction

Possible future work can be divided into two sections. There are the longer term aims which would further develop the project and are indeed new projects in themselves. Also, there are short term experiments designed to answer questions arising from the work presented in the preceding chapters. For the longer term, there are two, possibly three, main avenues of exploration which arise. Firstly, there is the question as to what are the mechanisms by which the genes, down-regulated in FBR cells (STAT6, RYBP and PCDHGC3), inhibit invasion when they are re-expressed? Secondly, we could ask, what are the larger scale changes in gene expression in response to HDAC inhibition? Thirdly, there is the question of a possible cytoplasmic role for HDACs in the mediation of cytoskeletal re-arrangement.

7.2 Short-term aims

For the short term, there are many experiments which could be done to substantiate our results and further develop our understanding of HDACs and HDAC-controlled gene expression in Fos-transformation. Perhaps the most obvious approach would be the use of small interfering RNA (siRNA) technology, to investigate the role of HDAC4 (or indeed other HDACs) in mediation of the transformed phenotype. We would be able to examine the consequences of decreasing the level of HDAC4 in FBR cells, with regard to reversion of their transformed characteristics, specifically invasion.

With regard to the role of HDAC4, perhaps an important question to ask may be: what is the level of expression of RYBP, PCDHGC3 and STAT6 in 208F cell lines which stably express HDAC4. This could be done by northern analysis of our stable cell lines of 208F cells expressing the HDAC4 transgene. It would help to determine whether the increased expression of HDAC4 in FBR cells is responsible for the down-regulation of these genes. In the complimentary experiment to this we could ask: given

that RYBP, STAT6 and PCDHGC3 are re-expressed in FBR cells, on treatment with VPA or TSA, does this re-expression still occur in our FBR cells which stably express HDAC4, upon inhibitor treatment. It is possible, since, as we have shown, these cells are resistant to inhibition of invasion by HDAC inhibitors, that they also do not re-express the genes that we have shown to be incompatible with invasion. This would further substantiate our conclusion that RYBP, STAT6 and PCDHGC3 are incompatible with invasion and that HDAC4 is capable of their suppression.

Of course, the direct interaction of HDAC4 with the promoter regions of the down-regulated genes (in FBR cells) could be determined by chromatin immunoprecipitation (ChIP) assay, though this would perhaps be a longer term aim.

7.3 Long-term aims

7.3.1 The role of STAT6, RYBP and PCDHGC3 in the inhibition of invasion

Perhaps the next step in this project would be to determine the mechanisms by which STAT6, RYBP and PCDHGC3 inhibit invasion. For the transcription factor STAT6, and the transcription co-factor RYBP, initial studies could use microarray technology to determine the gene changes which occur as a consequence of their ectopic expression in FBR cells. As already mentioned, ChIP assays could be used to determine the direct interaction of these transcriptional regulators with target genes. Those genes identified by these techniques would determine the future direction of the project. Studies with the cell-cell adhesion / recognition protein, PCDHGC3 would consider the role this protein has on cell interaction. We could reduce levels in 208F cells, or in HDAC inhibitor-treated FBR cells, and determine whether the cells become invasive. This could be done using siRNA to decrease expression of the protein in 208F cells. Alternatively we could add blocking antibody, which recognises the extracellular portion of the protein, to 208F cells in culture, to block cell-cell interaction;

or treat the cells with the extracellular portion of the protein itself, which may either block interaction, or if binding of this portion is required for intracellular signalling from the receptor, may result in the increased activity of the receptor.

7.3.2 Gene expression changes in response to HDAC inhibitors

The primary subject of this work is Fos. Since Fos is a transcription factor, our main concern must be gene expression changes as a result of increased AP-1 activity, and in this study as a consequence of, v-Fos-mediated, increased HDAC expression. To expand our limited study of genes re-expressed as a consequence of HDAC inhibition, we could use microarray technology. This was not done originally in our study because, at that time, rat microarrays were not as comprehensive as they are now. With microarrays we could determine which gene changes were common to VPA and TSA treatment, and of particular interest, we could determine which changes occurred at the different concentrations we have used to effect changes in the transformed phenotype. For example, as we have shown in FBR cells, treatment with 8nM TSA inhibits invasion but does not bring about morphological reversion, whereas treatment with 12nM TSA inhibits invasion *and* causes morphological reversion. A comparison of the gene changes occurring in each of these cases would yield genes which are specific to invasion. In addition we could carry out a time-course of gene expression changes, since as we have seen, for example, morphological reversion occurs over several days.

7.3.3 A cytoplasmic role for HDACs

Finally, it would be interesting to determine, whether HDACs have a cytoplasmic role in the re-formation of stress-fibres. As we have shown, in a time-course to track the re-appearance of stress-fibres in inhibitor treated FBR cells (Section 3.2.3), the stress-

fibres have reformed within 24 hours. If we were able to demonstrate that this re-appearance actually occurs quickly, say within 6 hours, and that it occurs in the absence of RNA or protein synthesis, then we would have evidence that a direct cytoplasmic role is likely. We could then investigate the possibility that HDACs deacetylate cytoskeletal proteins and inhibit the ability to form stress-fibres, or conversely, that acetylation of cytoskeletal proteins is required for stress-fibres formation.

References

References

Adachi, Y. and M. Yanagida. 1989. Higher order chromosome structure is affected by cold-sensitive mutations in a Schizosaccharomyces pombe gene crm1+ which encodes a 115 kD protein preferentially localized in the nucleus and its periphery. *J Cell Biol* **108**: 1195-207.

Afshar, G. and J.P. Murnane. 1999. Characterization of a human gene with sequence homology to Saccharomyces cerevisiae SIR2. *Gene* **234**: 161-8.

Agell, N., O. Bachs, N. Rocamora, and P. Villalonga. 2002. Modulation of the Ras/Raf/MEK/ERK pathway by Ca(2+), and calmodulin. *Cell Signal* **14**: 649-54.

Albini, A., A. Melchiori, L. Santi, L.A. Liotta, P.D. Brown, and W.G. Stetler-Stevenson. 1991. Tumor cell invasion inhibited by TIMP-2. *J Natl Cancer Inst* **83**: 775-9.

Andres, M.E., C. Burger, M.J. Peral-Rubio, E. Battaglioli, M.E. Anderson, J. Grimes, J. Dallman, N. Ballas, and G. Mandel. 1999. CoREST: a functional corepressor required for regulation of neural-specific gene expression. *Proc Natl Acad Sci USA* **96**: 9873-8.

Antequera, F. and A. Bird. 1993a. CpG islands. *Exs* **64**: 169-85.

Antequera, F. and A. Bird. 1993b. Number of CpG islands and genes in human and mouse. *Proc Natl Acad Sci USA* **90**: 11995-9.

Appleby, M.W., I.M. Greenfield, T. Crook, E.K. Parkinson, and M.A. Stanley. 1989. In vivo and in vitro effects of v-fos and EJ-Ha-ras oncogene expression in murine epidermal keratinocytes. *Oncogene* **4**: 1323-30.

Ayer, D.E., L. Kretzner, and R.N. Eisenman. 1993. Mad: a heterodimeric partner for Max that antagonizes Myc transcriptional activity. *Cell* **72**: 211-22.

Ayer, D.E., Q.A. Lawrence, and R.N. Eisenman. 1995. Mad-Max transcriptional repression is mediated by ternary complex formation with mammalian homologs of yeast repressor Sin3. *Cell* **80**: 767-76.

Bahassi, E.M., S. Karyala, C.R. Tomlinson, M.A. Sartor, M. Medvedovic, and R.F. Hennigan. 2004. Critical Regulation of Genes for Tumor Cell Migration by AP-1. Submitted.

Bailey, P., M. Downes, P. Lau, J. Harris, S.L. Chen, Y. Hamamori, V. Sartorelli, and G.E. Muscat. 1999. The nuclear receptor corepressor N-CoR regulates differentiation: N-CoR directly interacts with MyoD. *Mol Endocrinol* **13**: 1155-68.

Baker, A.H., S.J. George, A.B. Zaltsman, G. Murphy, and A.C. Newby. 1999. Inhibition of invasion and induction of apoptotic cell death of cancer cell lines by overexpression of TIMP-3. *Br J Cancer* **79**: 1347-55.Bakin, A.V. and T. Curran. 1999. Role of DNA 5-methylcytosine transferase in cell transformation by fos. *Science* **283**: 387-90.

Bar-Shira, A., J.H. Pinthus, U. Rozovsky, M. Goldstein, W.R. Sellers, Y. Yaron, Z. Eshhar, and A. Orr-Urtreger. 2002. Multiple genes in human 20q13 chromosomal region are involved in an advanced prostate cancer xenograft. *Cancer Res* **62**: 6803-7.

Barton, B.E., J.G. Karras, T.F. Murphy, A. Barton, and H.F. Huang. 2004. Signal transducer and activator of transcription 3 (STAT3) activation in prostate cancer: Direct STAT3 inhibition induces apoptosis in prostate cancer lines. *Mol Cancer Ther* **3**: 11-20.

Behrens, J., K.M. Weidner, U.H. Frixen, J.H. Schipper, M. Sachs, N. Arakaki, Y. Daikuhara, and W. Birchmeier. 1991. The role of E-cadherin and scatter factor in tumor invasion and cell motility. *Exs* **59**: 109-26.

Benekli, M., M.R. Baer, H. Baumann, and M. Wetzler. 2003. Signal transducer and activator of transcription proteins in leukemias. *Blood* **101**: 2940-54.

Bestor, T., A. Laudano, R. Mattaliano, and V. Ingram. 1988. Cloning and sequencing of a cDNA encoding DNA methyltransferase of mouse cells. The carboxyl-terminal domain of the mammalian enzymes is related to bacterial restriction methyltransferases. *J Mol Biol* **203**: 971-83.

Bradbury, J.M. and P.A. Edwards. 1988. Changes in in vitro growth behaviour of the mammary epithelial cell line NMuMG caused by the v-fos oncogene. *Int J Cancer* **42**: 923-9.

Brenner, D.A., M. O'Hara, P. Angel, M. Chojkier, and M. Karin. 1989. Prolonged activation of jun and collagenase genes by tumour necrosis factor-alpha. *Nature* **337**: 661-3.

Buggy, J.J., M.L. Sideris, P. Mak, D.D. Lorimer, B. McIntosh, and J.M. Clark. 2000. Cloning and characterization of a novel human histone deacetylase, HDAC8. *Biochem J* **350 Pt 1**: 199-205.

Bugno, M., L. Graeve, P. Gatsios, A. Koj, P.C. Heinrich, J. Travis, and T. Kordula. 1995. Identification of the interleukin-6/oncostatin M response element in the rat tissue inhibitor of metalloproteinases-1 (TIMP-1) promoter. *Nucleic Acids Res* **23**: 5041-7.

Buttner, C., A. Skupin, and E.P. Rieber. 2004. Transcriptional activation of the type I collagen genes COL1A1 and COL1A2 in fibroblasts by interleukin-4: analysis of the functional collagen promoter sequences. *J Cell Physiol* **198**: 248-58.

Cameron, E.E., K.E. Bachman, S. Myohanen, J.G. Herman, and S.B. Baylin. 1999. Synergy of demethylation and histone deacetylase inhibition in the re-expression of genes silenced in cancer. *Nat Genet* **21**: 103-7.

Carducci, M.A., J.B. Nelson, K.M. Chan-Tack, S.R. Ayyagari, W.H. Sweatt, P.A. Campbell, W.G. Nelson, and J.W. Simons. 1996. Phenylbutyrate induces apoptosis in human prostate cancer and is more potent than phenylacetate. *Clin Cancer Res* **2**: 379-87.

Carmen, A.A., S.E. Rundlett, and M. Grunstein. 1996. HDA1 and HDA3 are components of a yeast histone deacetylase (HDA) complex. *J Biol Chem* **271**: 15837-44.

Chen, W.C. and B. Obrink. 1991. Cell-cell contacts mediated by E-cadherin (uvomorulin) restrict invasive behavior of L-cells. *J Cell Biol* **114**: 319-27.

Chen, J.D. and R.M. Evans. 1995. A transcriptional co-repressor that interacts with nuclear hormone receptors. *Nature* **377**: 454-7.

Chen, R.H., P.C. Juo, T. Curran, and J. Blenis. 1996. Phosphorylation of c-Fos at the C-terminus enhances its transforming activity. *Oncogene* **12**: 1493-502.

Cheung, W.L., S.D. Briggs, and C.D. Allis. 2000. Acetylation and chromosomal functions. *Curr Opin Cell Biol* **12**: 326-33.

Dangond, F., D.A. Hafler, J.K. Tong, J. Randall, R. Kojima, N. Utku, and S.R. Gullans. 1998. Differential display cloning of a novel human histone deacetylase (HDAC3) cDNA from PHA-activated immune cells. *Biochem Biophys Res Commun* **242**: 648-52.

Decker, T. and P. Kovarik. 2000. Serine phosphorylation of STATs. *Oncogene* **19**: 2628-37.

Dequiedt, F., H. Kasler, W. Fischle, V. Kiermer, M. Weinstein, B.G. Herndier, and E. Verdin. 2003. HDAC7, a thymus-specific class II histone deacetylase, regulates Nur77 transcription and TCR-mediated apoptosis. *Immunity* **18**: 687-98.

Dhordain, P., R.J. Lin, S. Quief, D. Lantoine, J.P. Kerckaert, R.M. Evans, and O. Albagli. 1998. The LAZ3(BCL-6) oncoprotein recruits a SMRT/mSIN3A/histone deacetylase containing complex to mediate transcriptional repression. *Nucleic Acids Res* **26**: 4645-51.

Diatchenko, L., Y.F. Lau, A.P. Campbell, A. Chenchik, F. Moqadam, B. Huang, S. Lukyanov, K. Lukyanov, N. Gurskaya, E.D. Sverdlov, and P.D. Siebert. 1996. Suppression subtractive hybridization: a method for generating differentially regulated or tissue-specific cDNA probes and libraries. *Proc Natl Acad Sci USA* **93**: 6025-30.

Dong, Z., H.C. Crawford, V. Lavrovsky, D. Taub, R. Watts, L.M. Matrisian, and N.H. Colburn. 1997. A dominant negative mutant of jun blocking 12-O-tetradecanoylphorbol-13- acetate-induced invasion in mouse keratinocytes. *Mol Carcinog* **19**: 204-12.

Dressel, U., P.J. Bailey, S.C. Wang, M. Downes, R.M. Evans, and G.E. Muscat. 2001. A dynamic role for HDAC7 in MEF2-mediated muscle differentiation. *J Biol Chem* **276**: 17007-13.

Dunne, J., A.M. Hanby, R. Poulsom, T.A. Jones, D. Sheer, W.G. Chin, S.M. Da, Q. Zhao, P.C. Beverley, and M.J. Owen. 1995. Molecular cloning and tissue expression of FAT, the human homologue of the Drosophila fat gene that is located on chromosome 4q34-q35 and encodes a putative adhesion molecule. *Genomics* **30**: 207-23.

Eferl, R. and E. Wagner. 2003. AP-1: A double-edged sword in tumorigenesis. *Nature Reviews Cancer* **3**: 859-68.

Emiliani, S., W. Fischle, C. Van Lint, Y. Al-Abed, and E. Verdin. 1998. Characterization of a human RPD3 ortholog, HDAC3. *Proc Natl Acad Sci USA* **95**: 2795-800.

Erickson, P., J. Gao, K.S. Chang, T. Look, E. Whisenant, S. Raimondi, R. Lasher, J. Trujillo, J. Rowley, and H. Drabkin. 1992. Identification of breakpoints in t(8;21) acute myelogenous leukemia and isolation of a fusion transcript, AML1/ETO, with similarity to Drosophila segmentation gene, runt. *Blood* **80**: 1825-31.

Fahraeus, R., W. Chen, P. Trivedi, G. Klein, and B. Obrink. 1992. Decreased expression of E-cadherin and increased invasive capacity in EBV-LMP-transfected human epithelial and murine adenocarcinoma cells. *Int J Cancer* **52**: 834-8.

Finkel, M.P., B.O. Biskis, and P.B. Jinkins. 1966. Virus induction of osteosarcomas in mice. *Science* **151**: 698-701.

Finkel, M.P., C.A. Reilly, B.O. Biskis, and I.L. Greco. 1973. Bone Tumor Viruses. *Proceedings 24th Symposium of the Colston Research Society* **24**: 353-366.

Finnin, M.S., J.R. Donigian, A. Cohen, V.M. Richon, R.A. Rifkind, P.A. Marks, R. Breslow, and N.P. Pavletich. 1999. Structures of a histone deacetylase homologue bound to the TSA and SAHA inhibitors. *Nature* **401**: 188-93.

Fischle, W., F. Dequiedt, M. Fillion, M.J. Hendzel, W. Voelter, and E. Verdin. 2001. Human HDAC7 histone deacetylase activity is associated with HDAC3 in vivo. *J Biol Chem* **276**: 35826-35.

Fischle, W., S. Emiliani, M.J. Hendzel, T. Nagase, N. Nomura, W. Voelter, and E. Verdin. 1999. A new family of human histone deacetylases related to Saccharomyces cerevisiae HDA1p. *J Biol Chem* **274**: 11713-20.

Freier, K., S. Joos, C. Flechtenmacher, F. Devens, A. Benner, F.X. Bosch, P. Lichter, and C. Hofele. 2003. Tissue microarray analysis reveals site-specific prevalence of oncogene amplifications in head and neck squamous cell carcinoma. *Cancer Res* **63**: 1179-82.

Frixen, U.H., J. Behrens, M. Sachs, G. Eberle, B. Voss, A. Warda, D. Lochner, and W. Birchmeier. 1991. E-cadherin-mediated cell-cell adhesion prevents invasiveness of human carcinoma cells. *J Cell Biol* **113**: 173-85.

Frye, R.A. 1999. Characterization of five human cDNAs with homology to the yeast SIR2 gene: Sir2-like proteins (sirtuins) metabolize NAD and may have protein ADP-ribosyltransferase activity. *Biochem Biophys Res Commun* **260**: 273-9.

Fu, H., R.R. Subramanian, and S.C. Masters. 2000. 14-3-3 proteins: structure, function, and regulation [In Process Citation]. *Annu Rev Pharmacol Toxicol* **40**: 617-47.

Fuks, F., W.A. Burgers, A. Brehm, L. Hughes-Davies, and T. Kouzarides. 2000. DNA methyltransferase Dnmt1 associates with histone deacetylase activity. *Nat Genet* **24**: 88-91.

Gao, L., M.A. Cueto, F. Asselbergs, and P. Atadja. 2002. Cloning and functional characterization of HDAC11, a novel member of the human histone deacetylase family. *J Biol Chem* **277**: 25748-55.

Garcia, E., C. Marcos-Gutierrez, M. del Mar Lorente, J.C. Moreno, and M. Vidal. 1999. RYBP, a new repressor protein that interacts with components of the mammalian Polycomb complex, and with the transcription factor YY1. *EMBO J* **18**: 3404-18.

Gatsios, P., H.D. Haubeck, E. Van de Leur, W. Frisch, S.S. Apte, H. Greiling, P.C. Heinrich, and L. Graeve. 1996. Oncostatin M differentially regulates tissue inhibitors of metalloproteinases TIMP-1 and TIMP-3 gene expression in human synovial lining cells. *Eur J Biochem* **241**: 56-63.

Gottlicher, M., S. Minucci, P. Zhu, O.H. Kramer, A. Schimpf, S. Giavara, J.P. Sleeman, F. Lo Coco, C. Nervi, P.G. Pelicci, and T. Heinzel. 2001. Valproic acid defines a novel class of HDAC inhibitors inducing differentiation of transformed cells. *EMBO J* **20**: 6969-78.

Grignani, F., S. De Matteis, C. Nervi, L. Tomassoni, V. Gelmetti, M. Cioce, M. Fanelli, M. Ruthardt, F.F. Ferrara, I. Zamir, C. Seiser, M.A. Lazar, S. Minucci, and P.G. Pelicci. 1998. Fusion proteins of the retinoic acid receptor-alpha recruit histone deacetylase in promyelocytic leukaemia. *Nature* **391**: 815-8.

Grimes, J.A., S.J. Nielsen, E. Battaglioli, E.A. Miska, J.C. Speh, D.L. Berry, F. Atouf, B.C. Holdener, G. Mandel, and T. Kouzarides. 2000. The co-repressor mSin3A is a functional component of the REST-CoREST repressor complex. *J Biol Chem* **275**: 9461-7.

Grozinger, C.M., C.A. Hassig, and S.L. Schreiber. 1999. Three proteins define a class of human histone deacetylases related to yeast Hda1p. *Proc Natl Acad Sci USA* **96**: 4868-73.

Grozinger, C.M. and S.L. Schreiber. 2000. Regulation of histone deacetylase **4** and 5 and transcriptional activity by 14-3-3-dependent cellular localization. *Proc Natl Acad Sci USA* **97**: 7835-40.

Grunstein, M. 1997. Histone acetylation in chromatin structure and transcription. *Nature* **389**: 349-52.

Guardiola, A.R. and T.P. Yao. 2001. Molecular cloning and characterization of a novel histone deacetylase HDAC10. *J Biol Chem* **28**: 28.

Guarente, L. 2000. Sir2 links chromatin silencing, metabolism, and aging. *Genes Dev* **14**: 1021-6.

He, L.Z., F. Guidez, C. Tribioli, D. Peruzzi, M. Ruthardt, A. Zelent, and P.P. Pandolfi. 1998. Distinct interactions of PML-RARalpha and PLZF-RARalpha with co- repressors determine differential responses to RA in APL. *Nat Genet* **18**: 126-35.

Heinzel, T., R.M. Lavinsky, T.M. Mullen, M. Soderstrom, C.D. Laherty, J. Torchia, W.M. Yang, G. Brard, S.D. Ngo, J.R. Davie, E. Seto, R.N. Eisenman, D.W. Rose, C.K. Glass, and M.G. Rosenfeld. 1997. A complex containing N-CoR, mSin3 and histone deacetylase mediates transcriptional repression. *Nature* **387**: 43-8.

Hennigan, R.F., K.L. Hawker, and B.W. Ozanne. 1994. Fos-transformation activates genes associated with invasion. *Oncogene* **9**: 3591-600.

Hiebert, S.W., E.F. Reed-Inderbitzin, J. Amann, B. Irvin, K. Durst, and B. Linggi. 2003. The t(8;21) fusion protein contacts co-repressors and histone deacetylases to repress the transcription of the p14ARF tumor suppressor. *Blood Cells Mol Dis* **30**: 177-83.

Horie, S. and T. Suga. 1985. Enhancement of peroxisomal beta-oxidation in the liver of rats and mice treated with valproic acid. *Biochem Pharmacol* **34**: 1357-62.

Hu, E., Z. Chen, T. Fredrickson, Y. Zhu, R. Kirkpatrick, G.F. Zhang, K. Johanson, C.M. Sung, R. Liu, and J. Winkler. 2000. Cloning and characterization of a novel human class I histone deacetylase that functions as a transcription repressor. *J Biol Chem* **275**: 15254-64.

Hu, E., E. Mueller, S. Oliviero, V.E. Papaioannou, R. Johnson, and B.M. Spiegelman. 1994. Targeted disruption of the c-fos gene demonstrates c-fos-dependent and -independent pathways for gene expression stimulated by growth factors or oncogenes. *EMBO J* **13**: 3094-103.

Hubbert, C., A. Guardiola, R. Shao, Y. Kawaguchi, A. Ito, A. Nixon, M. Yoshida, X.F. Wang, and T.P. Yao. 2002. HDAC6 is a microtubule-associated deacetylase. *Nature* **417**: 455-8.

Imai, S., C.M. Armstrong, M. Kaeberlein, and L. Guarente. 2000. Transcriptional silencing and longevity protein Sir2 is an NAD- dependent histone deacetylase. *Nature* **403**: 795-800.

Iso, T., V. Sartorelli, C. Poizat, S. Iezzi, H.Y. Wu, G. Chung, L. Kedes, and Y. Hamamori. 2001. HERP, a novel heterodimer partner of HES/E(spl) in Notch signaling. *Mol Cell Biol* **21**: 6080-9.

Jenuwein, T., D. Muller, T. Curran, and R. Muller. 1985. Extended life span and tumorigenicity of nonestablished mouse connective tissue cells transformed by the fos oncogene of FBR-MuSV. *Cell* **41**: 629-37.

Johnston, I.M., H.J. Spence, J.N. Winnie, L. McGarry, J.K. Vass, L. Meagher, G. Stapleton, and B.W. Ozanne. 2000. Regulation of a multigenic invasion programme by the transcription factor, AP-1: re-expression of a down-regulated gene, TSC-36, inhibits invasion. *Oncogene* **19**: 5348-58.

Jones, K.A. and J.T. Kadonaga. 2000. Exploring the transcription-chromatin interface. *Genes Dev* **14**: 1992-6.

Jones, P.L., G.J. Veenstra, P.A. Wade, D. Vermaak, S.U. Kass, N. Landsberger, J. Strouboulis, and A.P. Wolffe. 1998. Methylated DNA and MeCP2 recruit histone deacetylase to repress transcription. *Nat Genet* **19**: 187-91.

Jooss, K.U. and R. Muller. 1995. Deregulation of genes encoding microfilament-associated proteins during Fos-induced morphological transformation. *Oncogene* **10**: 603-8.

Kakizawa, T., T. Miyamoto, K. Ichikawa, T. Takeda, S. Suzuki, J. Mori, M. Kumagai, K. Yamashita, and K. Hashizume. 2001. Silencing mediator for retinoid and thyroid hormone receptors interacts with octamer transcription factor-1 and acts as a transcriptional repressor. *J Biol Chem* **276**: 9720-5.

Kallenbach, S., S. Khantane, P. Carroll, O. Gayet, S. Alonso, C.E. Henderson, and K. Dudley. 2003. Changes in subcellular distribution of protocadherin gamma proteins accompany maturation of spinal neurons. *J Neurosci Res* **72**: 549-56.

Kao, H.Y., M. Downes, P. Ordentlich, and R.M. Evans. 2000. Isolation of a novel histone deacetylase reveals that class I and class II deacetylases promote SMRT-mediated repression. *Genes Dev* **14**: 55-66.

Kao, H.Y., C.H. Lee, A. Komarov, C.C. Han, and R.M. Evans. 2001. Isolation and characterization of mammalian HDAC10, a novel histone deacetylase. *J Biol Chem* **24**: 24.

Kawaguchi, Y., J.J. Kovacs, A. McLaurin, J.M. Vance, A. Ito, and T.P. Yao. 2003. The deacetylase HDAC6 regulates aggresome formation and cell viability in response to misfolded protein stress. *Cell* **115**: 727-38.

Kelly, W.K., O.A. O'Connor, and P.A. Marks. 2002. Histone deacetylase inhibitors: from target to clinical trials. *Expert Opin Investig Drugs* **11**: 1695-713.

Kerckaert, J.P., C. Deweindt, H. Tilly, S. Quief, G. Lecocq, and C. Bastard. 1993. LAZ3, a novel zinc-finger encoding gene, is disrupted by recurring chromosome 3q27 translocations in human lymphomas. *Nat Genet* **5**: 66-70.

Kerr, L.D., J.T. Holt, and L.M. Matrisian. 1988. Growth factors regulate transin gene expression by c-fos-dependent and c-fos-independent pathways. *Science* **242**: 1424-7.

Koipally, J., A. Renold, J. Kim, and K. Georgopoulos. 1999. Repression by Ikaros and Aiolos is mediated through histone deacetylase complexes. *EMBO J* **18**: 3090-100.

Kustikova, O., D. Kramerov, M. Grigorian, V. Berezin, E. Bock, E. Lukanidin, and E. Tulchinsky. 1998. Fra-1 induces morphological transformation and increases in vitro invasiveness and motility of epithelioid adenocarcinoma cells. *Mol Cell Biol* **18**: 7095-105.

Kwon, H.J., T. Owa, C.A. Hassig, J. Shimada, and S.L. Schreiber. 1998. Depudecin induces morphological reversion of transformed fibroblasts via the inhibition of histone deacetylase. *Proc Natl Acad Sci USA* **95**: 3356-61.

Laherty, C.D., W.M. Yang, J.M. Sun, J.R. Davie, E. Seto, and R.N. Eisenman. 1997. Histone deacetylases associated with the mSin3 corepressor mediate mad transcriptional repression. *Cell* **89**: 349-56.

Lamb, R.F., R.F. Hennigan, K. Turnbull, K.D. Katsanakis, E.D. MacKenzie, G.D. Birnie, and B.W. Ozanne. 1997a. AP-1-mediated invasion requires increased expression of the hyaluronan receptor CD44. *Mol Cell Biol* **17**: 963-76.

Lamb, R.F., B.W. Ozanne, C. Roy, L. McGarry, C. Stipp, P. Mangeat, and D.G. Jay. 1997b. Essential functions of ezrin in maintenance of cell shape and lamellipodial extension in normal and transformed fibroblasts. *Curr Biol* **7**: 682-8.

Lamph, W.W., P. Wamsley, P. Sassone-Corsi, and I.M. Verma. 1988. Induction of proto-oncogene JUN/AP-1 by serum and TPA. *Nature* **334**: 629-31.

Lee, J.D., R.J. Ulevitch, and J. Han. 1995. Primary structure of BMK1: a new mammalian map kinase. *Biochem Biophys Res Commun* **213**: 715-24.

Lee, M.S., J.H. Yang, Z. Salehi, P. Arnstein, L.S. Chen, G. Jay, and J.S. Rhim. 1993. Neoplastic transformation of a human keratinocyte cell line by the v- fos oncogene. *Oncogene* **8**: 387-93.

Lee, S.K., J.H. Kim, Y.C. Lee, J. Cheong, and J.W. Lee. 2000. Silencing mediator of retinoic acid and thyroid hormone receptors, as a novel transcriptional corepressor molecule of activating protein-1, nuclear factor-kappa B, and serum response factor. *J Biol Chem* **275**: 12470-4.

Lemrow, S.M., K.A. Anderson, J.D. Joseph, T.J. Ribar, P.K. Noeldner, and A.R. Means. 2004. Catalytic activity is required for calcium/calmodulin-dependent protein kinase IV to enter the nucleus. *J Biol Chem* **279**: 11664-71.

Lewis, J.D., R.R. Meehan, W.J. Henzel, I. Maurer-Fogy, P. Jeppesen, F. Klein, and A. Bird. 1992. Purification, sequence, and cellular localization of a novel chromosomal protein that binds to methylated DNA. *Cell* **69**: 905-14.

Li, S., P. Janosch, M. Tanji, G.C. Rosenfeld, J.C. Waymire, H. Mischak, W. Kolch, and J.M. Sedivy. 1995. Regulation of Raf-1 kinase activity by the 14-3-3 family of proteins. *EMBO J* **14**: 685-96.

Lin, R.J., L. Nagy, S. Inoue, W. Shao, W.H. Miller, Jr., and R.M. Evans. 1998. Role of the histone deacetylase complex in acute promyelocytic leukaemia. *Nature* **391**: 811-4.

Linggi, B., C. Muller-Tidow, L. van de Locht, M. Hu, J. Nip, H. Serve, W.E. Berdel, B. van der Reijden, D.E. Quelle, J.D. Rowley, J. Cleveland, J.H. Jansen, P.P. Pandolfi, and S.W. Hiebert. 2002. The t(8;21) fusion protein, AML1 ETO, specifically represses the transcription of the p14(ARF) tumor suppressor in acute myeloid leukemia. *Nat Med* **8**: 743-50.

Liu, L.T., H.C. Chang, L.C. Chiang, and W.C. Hung. 2003. Histone deacetylase inhibitor up-regulates RECK to inhibit MMP-2 activation and cancer cell invasion. *Cancer Res* **63**: 3069-72.

Lowry, O.H., N.J. Rosebrough, A.L. Farr, and R.J. Randall. 1951. *J Biol Chem* **193**: 265-275.

Luger, K., A.W. Mader, R.K. Richmond, D.F. Sargent, and T.J. Richmond. 1997. Crystal structure of the nucleosome core particle at 2.8 A resolution. *Nature* **389**: 251-60.

Luo, J., A.Y. Nikolaev, S. Imai, D. Chen, F. Su, A. Shiloh, L. Guarente, and W. Gu. 2001. Negative control of p53 by Sir2alpha promotes cell survival under stress. *Cell* **107**: 137-48.

Mahlknecht, U., D. Hoelzer, R. Bucala, and E. Verdin. 1999. Cloning and characterization of the murine histone deacetylase (HDAC3). *Biochem Biophys Res Commun* **263**: 482-90.

Mahoney, P.A., U. Weber, P. Onofrechuk, H. Biessmann, P.J. Bryant, and C.S. Goodman. 1991. The fat tumor suppressor gene in Drosophila encodes a novel member of the cadherin gene superfamily. *Cell* **67**: 853-68.

Malliri, A., M. Symons, R.F. Hennigan, A.F. Hurlstone, R.F. Lamb, T. Wheeler, and B.W. Ozanne. 1998. The transcription factor AP-1 is required for EGF-induced activation of rho-like GTPases, cytoskeletal rearrangements, motility, and in vitro invasion of A431 cells. *J Cell Biol* **143**: 1087-99.

Marks, P.A., T. Miller, and V.M. Richon. 2003. Histone deacetylases. *Curr Opin Pharmacol* **3**: 344-51.

Masui, T., R. Doi, T. Koshiba, K. Fujimoto, S. Tsuji, S. Nakajima, M. Koizumi, E. Toyoda, S. Tulachan, D. Ito, K. Kami, T. Mori, M. Wada, M. Noda, and M. Imamura. 2003. RECK Expression in Pancreatic Cancer: Its Correlation with Lower Invasiveness and Better Prognosis. *Clin Cancer Res* **9**: 1779-84.

Matsumoto, M., S. Matsutani, K. Sugita, H. Yoshida, F. Hayashi, Y. Terui, H. Nakai, N. Uotani, Y. Kawamura, K. Matsumoto, and et al. 1992. Depudecin: a novel compound inducing the flat phenotype of NIH3T3 cells doubly transformed by ras- and src-oncogene, produced by Alternaria brassicicola. *J Antibiot (Tokyo)* **45**: 879-85.

Matsuyama, A., T. Shimazu, Y. Sumida, A. Saito, Y. Yoshimatsu, D. Seigneurin-Berny, H. Osada, Y. Komatsu, N. Nishino, S. Khochbin, S. Horinouchi, and M. Yoshida. 2002. In vivo destabilization of dynamic microtubules by HDAC6-mediated deacetylation. *EMBO J* **21**: 6820-31.

Matsuyoshi, N. and S. Imamura. 1997. Multiple cadherins are expressed in human fibroblasts. *Biochem Biophys Res Commun* **235**: 355-8.

McGaha, T.L., M. Le, T. Kodera, C. Stoica, J. Zhu, W.E. Paul, and C.A. Bona. 2003. Molecular mechanisms of interleukin-4-induced up-regulation of type I collagen gene expression in murine fibroblasts. *Arthritis Rheum* **48**: 2275-84.

McGarry, L.C., J.N. Winnie, B.W. Ozanne. 2004. Invasion of v-Fos^{FBR}-transformed cells is dependent upon histone deacetylase activity and suppression of histone deacetylase regulated genes. *Oncogene* **23**: 5284-92.

McKinsey, T.A., C.L. Zhang, J. Lu, and E.N. Olson. 2000a. Signal-dependent nuclear export of a histone deacetylase regulates muscle differentiation. *Nature* **408**: 106-11.

McKinsey, T.A., C.L. Zhang, and E.N. Olson. 2000b. Activation of the myocyte enhancer factor-2 transcription factor by calcium/calmodulin-dependent protein kinase-stimulated binding of 14-3- 3 to histone deacetylase 5. *Proc Natl Acad Sci USA* **97**: 14400-5.

Mechta, F., D. Lallemand, C.M. Pfarr, and M. Yaniv. 1997. Transformation by ras modifies AP1 composition and activity. *Oncogene* **14**: 837-47.

Meehan, R.R., J.D. Lewis, and A.P. Bird. 1992. Characterization of MeCP2, a vertebrate DNA binding protein with affinity for methylated DNA. *Nucleic Acids Res* **20**: 5085-92.

Mikita, T., D. Campbell, P. Wu, K. Williamson, and U. Schindler. 1996. Requirements for interleukin-4-induced gene expression and functional characterization of Stat6. *Mol Cell Biol* **16**: 5811-20.

Mikita, T., C. Daniel, P. Wu, and U. Schindler. 1998. Mutational analysis of the STAT6 SH2 domain. *J Biol Chem* **273**: 17634-42.

Miller, A.D., I.M. Verma, and T. Curran. 1985. Deletion of the gag region from FBR murine osteosarcoma virus does not affect its enhanced transforming activity. *J Virol* **55**: 521-6.

Miska, E.A., C. Karlsson, E. Langley, S.J. Nielsen, J. Pines, and T. Kouzarides. 1999. HDAC4 deacetylase associates with and represses the MEF2 transcription factor. *EMBO J* **18**: 5099-107.

Miska, E.A., E. Langley, D. Wolf, C. Karlsson, J. Pines, and T. Kouzarides. 2001. Differential localization of HDAC4 orchestrates muscle differentiation. *Nucleic Acids Res* **29**: 3439-47.

Murphy, M., J. Ahn, K.K. Walker, W.H. Hoffman, R.M. Evans, A.J. Levine, and D.L. George. 1999. Transcriptional repression by wild-type p53 utilizes histone deacetylases, mediated by interaction with mSin3a. *Genes Dev* **13**: 2490-501.

Nakajima, H., P.K. Brindle, M. Handa, and J.N. Ihle. 2001. Functional interaction of STAT5 and nuclear receptor co-repressor SMRT: implications in negative regulation of STAT5-dependent transcription. *EMBO J* **20**: 6836-44.

Nan, X., H.H. Ng, C.A. Johnson, C.D. Laherty, B.M. Turner, R.N. Eisenman, and A. Bird. 1998. Transcriptional repression by the methyl-CpG-binding protein MeCP2 involves a histone deacetylase complex [see comments]. *Nature* **393**: 386-9.

Nau, H., R.S. Hauck, and K. Ehlers. 1991. Valproic acid-induced neural tube defects in mouse and human: aspects of chirality, alternative drug development, pharmacokinetics and possible mechanisms. *Pharmacol Toxicol* **69**: 310-21.

Newmark, H.L., J.R. Lupton, and C.W. Young. 1994. Butyrate as a differentiating agent: pharmacokinetics, analogues and current status. *Cancer Lett* **78**: 1-5.

Newmark, H.L. and C.W. Young. 1995. Butyrate and phenylacetate as differentiating agents: practical problems and opportunities. *J Cell Biochem Suppl* **22**: 247-53.

Ng, H.H. and A. Bird. 2000. Histone deacetylases: silencers for hire. *Trends Biochem Sci* **25**: 121-6.

Nomura, T., M.M. Khan, S.C. Kaul, H.D. Dong, R. Wadhwa, C. Colmenares, I. Kohno, and S. Ishii. 1999. Ski is a component of the histone deacetylase complex required for transcriptional repression by Mad and thyroid hormone receptor. *Genes Dev* **13**: 412-23.

North, B.J., B.L. Marshall, M.T. Borra, J.M. Denu, and E. Verdin. 2003. The human Sir2 ortholog, SIRT2, is an NAD+-dependent tubulin deacetylase. *Mol Cell* **11**: 437-44.

Obata, S., H. Sago, N. Mori, M. Davidson, T. St John, and S.T. Suzuki. 1998. A common protocadherin tail: multiple protocadherins share the same sequence in their cytoplasmic domains and are expressed in different regions of brain. *Cell Adhes Commun* **6**: 323-33.

Obata, S., H. Sago, N. Mori, J.M. Rochelle, M.F. Seldin, M. Davidson, T. St John, S. Taketani, and S.T. Suzuki. 1995. Protocadherin Pcdh2 shows properties similar to, but distinct from, those of classical cadherins. *J Cell Sci* **108 (Pt 12)**: 3765-73.

Ozawa, M., H. Baribault, and R. Kemler. 1989. The cytoplasmic domain of the cell adhesion molecule uvomorulin associates with three independent proteins structurally related in different species. *EMBO J* **8**: 1711-7.

Ozawa, M., M. Ringwald, and R. Kemler. 1990. Uvomorulin-catenin complex formation is regulated by a specific domain in the cytoplasmic region of the cell adhesion molecule. *Proc Natl Acad Sci U S A* **87**: 4246-50.

Ozawa, M. and R. Kemler. 1992. Molecular organization of the uvomorulin-catenin complex. *J Cell Biol* **116**: 989-96.

Papathoma, A.S., C. Petraki, A. Grigorakis, H. Papakonstantinou, V. Karavana, S. Stefanakis, F. Sotsiou, and A. Pintzas. 2000. Prognostic significance of matrix metalloproteinases 2 and 9 in bladder cancer. *Anticancer Res* **20**: 2009-13.

Papathoma, A.S., V. Zoumpourlis, A. Balmain, and A. Pintzas. 2001. Role of matrix metalloproteinase-9 in progression of mouse skin carcinogenesis. *Mol Carcinog* **31**: 74-82.

Parthun, M.R., J. Widom, and D.E. Gottschling. 1996. The major cytoplasmic histone acetyltransferase in yeast: links to chromatin replication and histone metabolism. *Cell* **87**: 85-94.

Peiro, G., J. Diebold, and U. Lohrs. 2002. CAS (cellular apoptosis susceptibility) gene expression in ovarian carcinoma: Correlation with 20q13.2 copy number and cyclin D1, p53, and Rb protein expression. *Am J Clin Pathol* **118**: 922-9.

Piechaczyk, M. and J.M. Blanchard. 1994. c-fos proto-oncogene regulation and function. *Crit Rev Oncol Hematol* **17**: 93-131.

Pilcher, B.K., J.A. Dumin, B.D. Sudbeck, S.M. Krane, H.G. Welgus, and W.C. Parks. 1997. The activity of collagenase-1 is required for keratinocyte migration on a type I collagen matrix. *J Cell Biol* **137**: 1445-57.

Quelle, F.W., K. Shimoda, W. Thierfelder, C. Fischer, A. Kim, S.M. Ruben, J.L. Cleveland, J.H. Pierce, A.D. Keegan, K. Nelms, and et al. 1995. Cloning of murine Stat6 and human Stat6, Stat proteins that are tyrosine phosphorylated in responses to IL-4 and IL-3 but are not required for mitogenesis. *Mol Cell Biol* **15**: 3336-43.

Razin, A. and A.D. Riggs. 1980. DNA methylation and gene function. *Science* **210**: 604-10.

Reichmann, E., H. Schwarz, E.M. Deiner, I. Leitner, M. Eilers, J. Berger, M. Busslinger, and H. Beug. 1992. Activation of an inducible c-FosER fusion protein causes loss of epithelial polarity and triggers epithelial-fibroblastoid cell conversion. *Cell* **71**: 1103-16.

Richon, V.M., S. Emiliani, E. Verdin, Y. Webb, R. Breslow, R.A. Rifkind, and P.A. Marks. 1998. A class of hybrid polar inducers of transformed cell differentiation inhibits histone deacetylases. *Proc Natl Acad Sci USA* **95**: 3003-7.

Rountree, M.R., K.E. Bachman, and S.B. Baylin. 2000. DNMT1 binds HDAC2 and a new co-repressor, DMAP1, to form a complex at replication foci. *Nat Genet* **25**: 269-77.

Rundlett, S.E., A.A. Carmen, R. Kobayashi, S. Bavykin, B.M. Turner, and M. Grunstein. 1996. HDA1 and RPD3 are members of distinct yeast histone deacetylase complexes that regulate silencing and transcription. *Proc Natl Acad Sci USA* **93**: 14503-8.

Rundlett, S.E., A.A. Carmen, N. Suka, B.M. Turner, and M. Grunstein. 1998. Transcriptional repression by UME6 involves deacetylation of lysine 5 of histone H4 by RPD3. *Nature* **392**: 831-5.

Saez, E., S.E. Rutberg, E. Mueller, H. Oppenheim, J. Smoluk, S.H. Yuspa, and B.M. Spiegelman. 1995. c-fos is required for malignant progression of skin tumors. *Cell* **82**: 721-32.

Saleh, M., I. Rambaldi, X.J. Yang, and M.S. Featherstone. 2000. Cell signaling switches HOX-PBX complexes from repressors to activators of transcription mediated by histone deacetylases and histone acetyltransferases. *Mol Cell Biol* **20**: 8623-33.

Sambrook, J., E.F. Fritsch, and T. Maniatis. 1989. *Molecular Cloning. A laboratory manual.* Cold Spring Harbour Laboratory Press.

Sanger, F., G.M. Air, B.G. Barrell, N.L. Brown, A.R. Coulson, C.A. Fiddes, C.A. Hutchison, P.M. Slocombe, and M. Smith. 1977. Nucliotide sequence of bacteriophage phi X174 DNA. *Nature* **265**: 687-95.

Sano, K., H. Tanihara, R.L. Heimark, S. Obata, M. Davidson, T. St John, S. Taketani, and S. Suzuki. 1993. Protocadherins: a large family of cadherin-related molecules in central nervous system. *EMBO J* **12**: 2249-56.

Sato, H., M. Kita, and M. Seiki. 1993. v-Src activates the expression of 92-kDa type IV collagenase gene through the AP-1 site and the GT box homologous to retinoblastoma control elements. A mechanism regulating gene expression independent of that by inflammatory cytokines. *J Biol Chem* **268**: 23460-8.

Sawa, C., T. Yoshikawa, F. Matsuda-Suzuki, S. Delehouzee, M. Goto, H. Watanabe, J. Sawada, K. Kataoka, and H. Handa. 2002. YEAF1/RYBP and YAF-2 are functionally distinct members of a cofactor family for the YY1 and E4TF1/hGABP transcription factors. *J Biol Chem* **277**: 22484-90.

Schipper, J.H., U.H. Frixen, J. Behrens, A. Unger, K. Jahnke, and W. Birchmeier. 1991. E-cadherin expression in squamous cell carcinomas of head and neck: inverse correlation with tumor dedifferentiation and lymph node metastasis. *Cancer Res* **51**: 6328-37.

Schlisio, S., T. Halperin, M. Vidal, and J.R. Nevins. 2002. Interaction of YY1 with E2Fs, mediated by RYBP, provides a mechanism for specificity of E2F function. *EMBO J* **21**: 5775-86.

Schonthal, A., P. Herrlich, H.J. Rahmsdorf, and H. Ponta. 1988. Requirement for fos gene expression in the transcriptional activation of collagenase by other oncogenes and phorbol esters. *Cell* **54**: 325-34.

Scott, L.A., J.K. Vass, E.K. Parkinson, D.A.F. Gillespie, J.N. Winnie, and B.W. Ozanne. 2004. Invasion of normal human fibroblasts induced by v-Fos is independent of proliferation, immortalization and the tumor suppressors $p16^{INK4a}$ and p53. *Mol Cell Biol* **24**: 1540-59.

Shimoda, K., J. van Deursen, M.Y. Sangster, S.R. Sarawar, R.T. Carson, R.A. Tripp, C. Chu, F.W. Quelle, T. Nosaka, D.A. Vignali, P.C. Doherty, G. Grosveld, W.E. Paul, and J.N. Ihle. 1996. Lack of IL-4-induced Th2 response and IgE class switching in mice with disrupted Stat6 gene. *Nature* **380**: 630-3.

Soderling, T.R. 1999. The Ca-calmodulin-dependent protein kinase cascade. *Trends Biochem Sci* **24**: 232-6.

Sparrow, D.B., E.A. Miska, E. Langley, S. Reynaud-Deonauth, S. Kotecha, N. Towers, G. Spohr, T. Kouzarides, and T.J. Mohun. 1999. MEF-2 function is modified by a novel co-repressor, MITR. *EMBO J* **18**: 5085-98.

Spence, H.J., I. Johnston, K. Ewart, S.J. Buchanan, U. Fitzgerald, and B.W. Ozanne. 2000. Krp1, a novel kelch related protein that is involved in pseudopod elongation in transformed cells. *Oncogene* **19**: 1266-76.

Stade, K., C.S. Ford, C. Guthrie, and K. Weis. 1997. Exportin 1 (Crm1p) is an essential nuclear export factor. *Cell* **90**: 1041-50.

Stephanou, A. and D.S. Latchman. 2003. STAT-1: a novel regulator of apoptosis. *Int J Exp Pathol* **84**: 239-44.

Sugita, K., H. Yoshida, M. Matsumoto, and S. Matsutani. 1992. A novel compound, depudecin, induces production of transformation to the flat phenotype of NIH3T3 cells transformed by ras-oncogene. *Biochem Biophys Res Commun* **182**: 379-87.

Sun, P., H. Enslen, P.S. Myung, and R.A. Maurer. 1994. Differential activation of CREB by Ca2+/calmodulin-dependent protein kinases type II and type IV involves phosphorylation of a site that negatively regulates activity. *Genes Dev* **8**: 2527-39.

Suzuki, S.T. 2000. Recent progress in protocadherin research. *Exp Cell Res* **261**: 13-8.

Takami, Y. and T. Nakayama. 2000. N-terminal region, C-terminal region, nuclear export signal, and deacetylation activity of histone deacetylase-3 are essential for the viability of the DT40 chicken B cell line. *J Biol Chem* **275**: 16191-201.

Takeda, K., T. Tanaka, W. Shi, M. Matsumoto, M. Minami, S. Kashiwamura, K. Nakanishi, N. Yoshida, T. Kishimoto, and S. Akira. 1996. Essential role of Stat6 in IL-4 signalling. *Nature* **380**: 627-30.

Tanji, M., R. Horwitz, G. Rosenfeld, and J.C. Waymire. 1994. Activation of protein kinase C by purified bovine brain 14-3-3: comparison with tyrosine hydroxylase activation. *J Neurochem* **63**: 1908-16.

Taunton, J., C.A. Hassig, and S.L. Schreiber. 1996. A mammalian histone deacetylase related to the yeast transcriptional regulator Rpd3p. *Science* **272**: 408-11.

Terasawa, K., K. Okazaki, and E. Nishida. 2003. Regulation of c-Fos and Fra-1 by the MEK5-ERK5 pathway. *Genes Cells* **8**: 263-73.

Tong, J.K., C.A. Hassig, G.R. Schnitzler, R.E. Kingston, and S.L. Schreiber. 1998. Chromatin deacetylation by an ATP-dependent nucleosome remodelling complex. *Nature* **395**: 917-21.

Townsend, P.A., T.M. Scarabelli, S.M. Davidson, R.A. Knight, D.S. Latchman, and A. Stephanou. 2004. STAT-1 interacts with p53 to enhance DNA damage-induced apoptosis. *J Biol Chem* **279**: 5811-20.

Trimarchi, J.M., B. Fairchild, J. Wen, and J.A. Lees. 2001. The E2F6 transcription factor is a component of the mammalian Bmi1-containing polycomb complex. *Proc Natl Acad Sci USA* **98**: 1519-24.

Tsuji, N., M. Kobayashi, K. Nagashima, Y. Wakisaka, and K. Koizumi. 1976. A new antifungal antibiotic, trichostatin. *J Antibiot (Tokyo)* **29**: 1-6.

Underhill, C., M.S. Qutob, S.P. Yee, and J. Torchia. 2000. A novel nuclear receptor corepressor complex, N-CoR, contains components of the mammalian SWI/SNF complex and the corepressor KAP-1. *J Biol Chem* **275**: 40463-70.

Valente, P., G. Fassina, A. Melchiori, L. Masiello, M. Cilli, A. Vacca, M. Onisto, L. Santi, W.G. Stetler-Stevenson, and A. Albini. 1998. TIMP-2 over-expression reduces invasion and angiogenesis and protects B16F10 melanoma cells from apoptosis. *Int J Cancer* **75**: 246-53.

Valge-Archer, V.E., J. de Villiers, A.J. Sinskey, and A. Rao. 1990. Transformation of T lymphocytes by the v-fos oncogene. *J Immunol* **145**: 4355-64.

Van Beveren, C., S. Enami, T. Curran, and I.M. Verma. 1984. FBR murine osteosarcoma virus. II. Nucleotide sequence of the provirus reveals that the genome contains sequences acquired from two cellular genes. *Virology* **135**: 229-43.

Van den Wyngaert, I., W. de Vries, A. Kremer, J. Neefs, P. Verhasselt, W.H. Luyten, and S.U. Kass. 2000. Cloning and characterization of human histone deacetylase 8. *FEBS Lett* **478**: 77-83.

van Holde, K.E. 1988. *Chromatin*. Springer, New York.

van Straaten, F., R. Muller, T. Curran, C. Van Beveren, and I.M. Verma. 1983. Complete nucleotide sequence of a human c-onc gene: deduced amino acid sequence of the human c-fos protein. *Proc Natl Acad Sci USA* **80**: 3183-7.

Vaziri, H., S.K. Dessain, E. Ng Eaton, S.I. Imai, R.A. Frye, T.K. Pandita, L. Guarente, and R.A. Weinberg. 2001. hSIR2(SIRT1) functions as an NAD-dependent p53 deacetylase. *Cell* **107**: 149-59.

Verdel, A., S. Curtet, M.P. Brocard, S. Rousseaux, C. Lemercier, M. Yoshida, and S. Khochbin. 2000. Active maintenance of mHDA2/mHDAC6 histone-deacetylase in the cytoplasm. *Curr Biol* **10**: 747-9.

Verdel, A. and S. Khochbin. 1999. Identification of a new family of higher eukaryotic histone deacetylases. Coordinate expression of differentiation-dependent chromatin modifiers. *J Biol Chem* **274**: 2440-5.

Verreault, A., P.D. Kaufman, R. Kobayashi, and B. Stillman. 1996. Nucleosome assembly by a complex of CAF-1 and acetylated histones H3/H4. *Cell* **87**: 95-104.

Vial, E. and C.J. Marshall. 2003. Elevated ERK-MAP kinase activity protects the FOS family member FRA-1 against proteasomal degradation in colon carcinoma cells. *J Cell Sci* **116**: 4957-63.

Vidal, M. and R.F. Gaber. 1991. RPD3 encodes a second factor required to achieve maximum positive and negative transcriptional states in Saccharomyces cerevisiae. *Mol Cell Biol* **11**: 6317-27.

Vorhees, C.V., K.D. Acuff-Smith, W.P. Weisenburger, D.R. Minck, J.S. Berry, K.D. Setchell, and H. Nau. 1991. Lack of teratogenicity of trans-2-ene-valproic acid compared to valproic acid in rats. *Teratology* **43**: 583-90.

Wang, A.H., N.R. Bertos, M. Vezmar, N. Pelletier, M. Crosato, H.H. Heng, J. Th'ng, J. Han, and X.J. Yang. 1999. HDAC4, a human histone deacetylase related to yeast HDA1, is a transcriptional corepressor. *Mol Cell Biol* **19**: 7816-27.

Wang, A.H., M.J. Kruhlak, J. Wu, N.R. Bertos, M. Vezmar, B.I. Posner, D.P. Bazett-Jones, and X.J. Yang. 2000. Regulation of histone deacetylase 4 by binding of 14-3-3 proteins. *Mol Cell Biol* **20**: 6904-12.

Wang, J., T. Hoshino, R.L. Redner, S. Kajigaya, and J.M. Liu. 1998. ETO, fusion partner in t(8;21) acute myeloid leukemia, represses transcription by interaction with the human N-CoR/mSin3/HDAC1 complex. *Proc Natl Acad Sci USA* **95**: 10860-5.

Wang, M., Y.E. Liu, J. Greene, S. Sheng, A. Fuchs, E.M. Rosen, and Y.E. Shi. 1997. Inhibition of tumor growth and metastasis of human breast cancer cells transfected with tissue inhibitor of metalloproteinase 4. *Oncogene* **14**: 2767-74.

Warrell, R.P., Jr., L.Z. He, V. Richon, E. Calleja, and P.P. Pandolfi. 1998. Therapeutic targeting of transcription in acute promyelocytic leukemia by use of an inhibitor of histone deacetylase. *J Natl Cancer Inst* **90**: 1621-5.

Weiss, M.M., A.M. Snijders, E.J. Kuipers, B. Ylstra, D. Pinkel, S.G. Meuwissen, P.J. van Diest, D.G. Albertson, and G.A. Meijer. 2003. Determination of amplicon

boundaries at 20q13.2 in tissue samples of human gastric adenocarcinomas by high-resolution microarray comparative genomic hybridization. *J Pathol* **200**: 320-6.

Werling, U., S. Siehler, M. Litfin, H. Nau, and M. Gottlicher. 2001. Induction of differentiation in F9 cells and activation of peroxisome proliferator-activated receptor delta by valproic acid and its teratogenic derivatives. *Mol Pharmacol* **59**: 1269-76.

Westermarck, J. and V.M. Kahari. 1999. Regulation of matrix metalloproteinase expression in tumor invasion. *Faseb J* **13**: 781-92.

Wolffe, A.P. 1998. *Post-translational modification of core histones.* Academic Press, San Diego.

Wolffe, A.P. and D. Guschin. 2000. Review: chromatin structural features and targets that regulate transcription. *J Struct Biol* **129**: 102-22.

Workman, J.L. and R.E. Kingston. 1998. Alteration of nucleosome structure as a mechanism of transcriptional regulation. *Annu Rev Biochem* **67**: 545-79.

Wu, C. 1997. Chromatin remodeling and the control of gene expression. *J Biol Chem* **272**: 28171-4.

Wu, X., H. Li, E.J. Park, and J.D. Chen. 2001. SMRTE inhibits MEF2C transcriptional activation by targeting HDAC4 and 5 to nuclear domains. *J Biol Chem* **276**: 24177-85.

Xu, L., R.M. Lavinsky, J.S. Dasen, S.E. Flynn, E.M. McInerney, T.M. Mullen, T. Heinzel, D. Szeto, E. Korzus, R. Kurokawa, A.K. Aggarwal, D.W. Rose, C.K. Glass, and M.G. Rosenfeld. 1998. Signal-specific co-activator domain requirements for Pit-1 activation. *Nature* **395**: 301-6.

Xue, Y., J. Wong, G.T. Moreno, M.K. Young, J. Cote, and W. Wang. 1998. NURD, a novel complex with both ATP-dependent chromatin-remodeling and histone deacetylase activities. *Mol Cell* **2**: 851-61.

Yamashita, Y., M. Shimada, N. Harimoto, T. Rikimaru, K. Shirabe, S. Tanaka, and K. Sugimachi. 2003. Histone deacetylase inhibitor trichostatin A induces cell-cycle arrest/apoptosis and hepatocyte differentiation in human hepatoma cells. *Int J Cancer* **103**: 572-6.

Yang, W.M., C. Inouye, Y. Zeng, D. Bearss, and E. Seto. 1996. Transcriptional repression by YY1 is mediated by interaction with a mammalian homolog of the yeast global regulator RPD3. *Proc Natl Acad Sci USA* **93**: 12845-50.

Yang, W.M., Y.L. Yao, J.M. Sun, J.R. Davie, and E. Seto. 1997. Isolation and characterization of cDNAs corresponding to an additional member of the human histone deacetylase gene family. *J Biol Chem* **272**: 28001-7.

Yang, W.M., S.C. Tsai, Y.D. Wen, G. Fejer, and E. Seto. 2002. Functional domains of histone deacetylase-3. *J Biol Chem* **277**: 9447-54.

Yoder, J.A., N.S. Soman, G.L. Verdine, and T.H. Bestor. 1997. DNA (cytosine-5)-methyltransferases in mouse cells and tissues. Studies with a mechanism-based probe. *J Mol Biol* **270**: 385-95.

Yoshida, M., S. Nomura, and T. Beppu. 1987. Effects of trichostatins on differentiation of murine erythroleukemia cells. *Cancer Res* **47**: 3688-91.

Yoshida, M., M. Kijima, M. Akita, and T. Beppu. 1990. Potent and specific inhibition of mammalian histone deacetylase both in vivo and in vitro by trichostatin A. *J Biol Chem* **265**: 17174-9.

You, A., J.K. Tong, C.M. Grozinger, and S.L. Schreiber. 2001. CoREST is an integral component of the CoREST- human histone deacetylase complex. *Proc Natl Acad Sci USA* **98**: 1454-8.

Yu, F., J. Thiesen, and W.H. Stratling. 2000. Histone deacetylase-independent transcriptional repression by methyl-CpG-binding protein 2. *Nucleic Acids Res* **28**: 2201-6.

Zhang, Y., R. Iratni, H. Erdjument-Bromage, P. Tempst, and D. Reinberg. 1997. Histone deacetylases and SAP18, a novel polypeptide, are components of a human Sin3 complex. *Cell* **89**: 357-64.

Zhang, Y., G. LeRoy, H.P. Seelig, W.S. Lane, and D. Reinberg. 1998. The dermatomyositis-specific autoantigen Mi2 is a component of a complex containing histone deacetylase and nucleosome remodeling activities. *Cell* **95**: 279-89.

Zhang, Y., H.H. Ng, H. Erdjument-Bromage, P. Tempst, A. Bird, and D. Reinberg. 1999. Analysis of the NuRD subunits reveals a histone deacetylase core complex and a connection with DNA methylation. *Genes Dev* **13**: 1924-35.

Zhang, Y., N. Li, C. Caron, G. Matthias, D. Hess, S. Khochbin, and P. Matthias. 2003. HDAC-6 interacts with and deacetylates tubulin and microtubules in vivo. *EMBO J* **22**: 1168-79.

Zhou, G., Z.Q. Bao, and J.E. Dixon. 1995. Components of a new human protein kinase signal transduction pathway. *J Biol Chem* **270**: 12665-9.

Zhou, X., V.M. Richon, R.A. Rifkind, and P.A. Marks. 2000. Identification of a transcriptional repressor related to the noncatalytic domain of histone deacetylases 4 and 5. *Proc Natl Acad Sci USA* **97**: 1056-61.

Zhou, S. and S.D. Hayward. 2001a. Nuclear localization of CBF1 is regulated by interactions with the SMRT corepressor complex. *Mol Cell Biol* **21**: 6222-32.

Zhou, X., P.A. Marks, R.A. Rifkind, and V.M. Richon. 2001b. Cloning and characterization of a histone deacetylase, HDAC9. *Proc Natl Acad Sci USA* **98**: 10572-7.